Author:
Houghton, Benjamin

Title:
Developing regulatable lentiviral vectors for the treatment of nerve injuries and Parkinson's disease

Developing regulatable lentiviral vectors for the treatment of nerve injuries and Parkinson's disease

Ben Houghton

A thesis submitted to the University of Bristol in accordance with the requirements for a reward of degree of Doctor of Philosophy in the Faculty of Medicine and Dentistry

School of Clinical Sciences **2012**

Abstract

Gene therapy is a promising approach for the treatment of diseases of the central nervous system. However, there is an unmet need for systems to regulate the levels of therapeutic transgenes. In this study, we investigate recently described destabilisation domain technology - novel regulatory systems that may offer advantages over existing methodologies. The destabilisation domain (DD) paradigm is composed of a conditionally stabilised protein domain that can be genetically fused to any protein of interest. Upon translation of this fusion partner in cells, the unstable DD targets the fusion protein to be degraded by the proteasome. The fusion protein is rescued by the presence of a ligand that stabilises the DD, forming a rapid, reversible and tunable regulatory system. We utilised two different forms of DD to create regulatable vectors suitable for use *in vitro* - to test the ability of the system to regulate fluorescent reporter proteins in cell lines and primary cultured neurons - and *in vivo.* After choosing the most favourable DD, we developed the technology to regulate levels of therapeutic genes suitable for the treatment of spinal cord injury (the nuclear receptor retinoic acid receptor β2) and Parkinson's disease (the novel neurotrophic factor CDNF (conserved dopamine neurotrophic factor)). We found we could use the regulatable vector systems to provide dose-dependent gene expression in vitro, and long-term gene expression *in vivo* by oral administration of the stabilising ligand, with minimal levels of transgenes in the absence of the ligand. We suggest that with further optimisation, DD regulatory technology may provide an

efficacious methodology to regulate levels of proteins in the central nervous system.

Author's declaration

I declare that the work in this dissertation was carried out in accordance with the regulations of the University of Bristol. The work is original, except where indicated by special reference in the text and no part of the dissertation has been submitted for any other academic award. Any views expressed in the dissertation are those of the author.

Signed……

Date…….....

Table of Contents

List of Figures

List of tables

Chapter 1 Introduction

1.1 Gene therapy

Gene therapy, as its name suggests, is the use of genetic material such as DNA or RNA as a pharmaceutical drug to treat disease. The basic concept of gene therapy is to introduce genetic material into individuals' cells to supplement, replace or correct genetic defects so as to rectify conditions arising from genetic disease. The first approved gene therapy experiment in humans took place in 1990, where a four-year old girl was treated for ADA-SCID (adenosine deaminase deficient severe combined immunodeficiency); the effects were temporary but successful (Blaese et al., 1995) Since then, gene therapy clinical trials have been conducted for a number of different diseases, for example various forms of severe combined immunodeficiency disease (SCID), leukaemia, retinal diseases and Parkinson's disease. In the last five years, clinical successes that have been reported, for example in retinal diseases (reviewed by Ali, 2012), have revived interest in gene therapy and this area of research continues to be hotly pursued by scientists.

Efficient gene transfer continues to represent one of the largest obstacles limiting the success of gene therapy. Many clinical trials are now using viral vectors to transfer DNA into cells as viruses are exceedingly well adapted for this purpose, as they must enter cells as part of their replicative life cycle. Viral particles are nanoscale-sized objects, usually sheltering their nucleic acid genome within a protective protein shell that mediates entry into cells. The most commonly used viral vectors have been created by modifying retroviruses (RV), adeno viruses (AdV), adeno-associated virus (AAV), lentiviruses (LV) and herpes simplex

virus (HSV). These vectors vary in their suitability to different therapeutic situations.

1.1.1 Retroviral vectors

The retroviral genome of gammaretroviruses such as Moloney-murine leukaemia virus (MoMLV) is 9-11kb long and when integrated (provirus form) consist of two identical 400-700bp sequences called long terminal repeats (LTRs) flanking three essential genes: *gag*, *pol*, *env*. The remainder of the genome contains four other genes necessary for completing the viral life cycle (Miller, 1992). When constructing vectors, these five genes must remain in the genome, while the *gag pol* and *env* can be removed and replaced with a therapeutic gene of interest (GOI). GOI expression will be driven by the promoters residing in the 5'LTR, or by CMV/LTR hybrid promoters. Removing *gag pol* and *env* from the vectors blocks the ability of the virus to replicate once it has invaded the host cell, therefore making them safer for use in humans. However, to enable production of infectious vector particles *gag pol* and *env* must be provided in trans by using a cell line expressing the three proteins (Miller, 1990). In this way, the particles will contain all the necessary machinery to invade cells. Once inside host cells, reverse transcriptase (present in the virion) converts the mRNA to DNA, before the proviral DNA is integrated into the host genome by integrase, also present in the virion.

Initial safety issues stemmed from recombination events between the vector construct and the packaging constructs, resulting in the generation of replication competent particles. To combat this, the *gag/pol* and *env* were divided into

separate constructs in the packaging cells. The risk that vector mobilisation will be mediated by endogenous retroviruses in the target cells prompted the development of self-inactivating vectors. In these vectors, LTR mediated transcription is prevented, and completely replaced with separate promoters (Yu et al., 1986).

After initial successes in treating diseases such as severe combined immunodeficiency (SCID) (Cavazzana-Calvo et al., 2000) (Aiuti et al., 2002) (Ott et al., 2006), a series of events marred these discoveries, such as the death of a patient (Hacein-Bey-Abina et al., 2003) and the development of leukaemia in others (Yu et al., 1986; Miller, 1990; 1992; Blaese et al., 1995; Buckley, 2002; Hacein-Bey-Abina et al., 2003; Kohn et al., 2003; McCormack and Rabbitts, 2004; Ali, 2012) due to activation of oncogenes by the retroviral promoters. Since this time, retroviral based vectors have been much less considered, partly because of these insertional mutagenesis problems. A further major limitation of retroviral vectors is their inability to transduce non-dividing cells, reducing their use for gene therapy in the central nervous system (CNS).

1.1.2 Lentiviral vectors

Unlike retroviruses, lentiviruses have the ability to cross the nuclear membrane and can therefore transduce non-dividing cells. Like retroviruses they integrate into the host genome to provide stable, long-term expression, while producing only a minimal immune response. The first lentiviral vectors were developed from human immune deficiency virus-1 (HIV-1).

In addition to *gag pol* and *env*, HIV-1 also contains an extra set of six accessory genes that are essential for the viral life cycle. Through the development of three different generations of vectors (Zufferey et al., 1997; Dull et al., 1998; Cavazzana-Calvo et al., 2000; Naldini, 2001; Aiuti et al., 2002; Hacein-Bey-Abina et al., 2003; Ott et al., 2006), these genes have been removed, in the interest of improving safety (Sinn et al., 2005). Third generation vectors require only three of the original nine viral genes, which are provided in trans and split between four separate plasmids which must be cotransfected into packaging cells to yield functional vectors. The first plasmid corresponds to the self-inactivating therapeutic gene transfer vector, in which the GOI, promoter and polyadenylation signal reside. A strong promoter outside the LTRs (long terminal repeats) in the packaging cells drives transcription of this construct, while the LTRs themselves are attenuated such that they cannot trigger transcription of provirus after integration or form functional virus if a wild type HIV infection arises. The central poly purine tract/central termination sequence (cPPT/CTS - part of pol gene) remains, as this increases viral titres by enhancing reverse transcriptase and pre-integration complex nuclear transport (Follenzi et al., 2000; Zennou et al., 2000). An RRE (*rev* responsive element) is also included. A second plasmid provides *gag* and *pol* genes, while a third provides *rev* (to ensure efficient nuclear export of full-length of vector mRNA into cytosol by binding RRE) and a fourth provides the coat protein, usually the broad spectrum vesicular stomatitis virus G protein (VSV-G), although the tropism can be modified by pseudotyping the virus with different coat proteins (Watson et al., 2002). For example, using Rabies-G coat protein will enable to the vector to retrogradely transduce neurons, while VSV-G will not (Cronin et

al., 2005). This ability means that lentiviral vectors can be applied into muscle and transduce nerve terminals in the periphery, before being retrogradely transported to the cell bodies and provide long term expression once integrated. This approach is being investigated for motor neuron disease (Azzouz et al., 2004a).

Vectors derived from viruses that are non-pathogenic to humans, such as simian immunodeficiency virus (SIV), feline immunodeficiency virus (FIV) and equine infectious anaemia virus (EIAV) provide a means of working with vectors that may have improved safety profiles (Sinn et al., 2005; Valori et al., 2008). Indeed, EIAV vectors are being used in clinical trials to deliver a dopamine replacement strategy in Parkinson's patients (Azzouz et al., 2002). Acute immune responses to lentiviral vectors are weak or non existent in primates (Kordower et al., 2000) and even animals that have been primed to have an adaptive immune response by pre-injection of viral capsid proteins do react when encountering them again (Follenzi et al., 2000), suggesting that these vectors are particularly non-immunogenic.

With low immunogenicity, genome integration, large cloning capacity and the ability to modulate their transduction properties by pseudotyping, lentiviral vectors offer an attractive tool for delivering genes to the CNS.

1.1.3 Adenovirus (AdV) vectors.

Adenoviral vectors were one of the first vector systems used for gene delivery to the CNS. The wild-type AdV is a pathogen of humans, causing a range of ailments from the respiratory system disease to gastroenteritis and conjunctivitis.

However, the tropism of AdV for the respiratory system and conjunctiva is mainly due to the mode of transmission of the virus; indeed, the CAR (coxsackie adenovirus receptor) that mediates viral entry to cells is ubiquitously expressed and the virus can enter both diving and non-dividing cells (Law and Davidson, 2005; Cohen et al., 2012). More than 50 serotypes of AdV have been isolated and classified into 6 groups. Most gene therapy vectors are derived from serotypes 2 and 5; both belong to group C of the family. The viral genome is 36kb of double stranded DNA, consisting of early transcriptional units (that become activated upon cell infection), delayed early transcriptional units and one major late transcription unit, all flanked by two identical 103bp inverted terminal repeats (ITRs). The first generation of viruses was created by deleting certain early transcriptional units and replacing them with a therapeutic gene of interest (GOI), including a promoter and polyadenylation signal (reviewed by Danthinne and Imperiale, 2000). However, expression of remaining viral proteins resulted in a strong immune response to cells transduced by these vectors (Hermens and Verhaagen, 1997; Thomas et al., 2000; Watson et al., 2002; Azzouz et al., 2004a; Cronin et al., 2005), and led to the death of one patient in a clinical trial when AdV vectors were applied to the liver (Batshaw et al., 1999; Lehrman, 1999). To try to combat these issues, in the second generation vectors more of the early transcriptional units were removed, but this did not abrogate the immune response and resulted in lower GOI expression (Wang and Finer, 1996). Third generation (‘gutless’) vectors are characterized by the near complete removal of the AdV genome, only the ITRs and DNA packaging signal (ψ) are retained (Kochanek et al., 1996; Parks et al., 1996). Production of these vectors is entirely reliant on the producing cells expressing

all the necessary proteins in trans. They are relatively easy to design and produce high titre preparations. The removal of viral genes has given these vectors a large maximum cloning capacity of approximately 30kb. As the immune response to cells that have been transduced is lowered, gene expression from these vectors *in vivo* is observed over much longer periods (Barcia et al., 2007). Although the capsid proteins themselves initiate an immune response (Kafri et al., 1998; Follenzi et al., 2000; Kordower et al., 2000; McCaffrey et al., 2008), reports suggest that these vectors can be used safely in the brain at low titres . In addition, pseudotyping capsid proteins with different AdV serotypes may decrease the immune response further (Nayak and Herzog, 2010). While the broad tropism of AdV vectors may be of use in many situations, a clinical setting may require more control over the cells that express the vectors. For this purpose, capsid engineering and cell specific promoters have been used to target viral expression (Coughlan et al., 2010).

The potential risks of immunogenicity perhaps explain why these vectors have been mostly implemented in situations where an immune response would not deleterious to the therapy. For example AdV based treatments of glioma have entered clinical trials (reviewed by Danthinne and Imperiale, 2000; Gwendalyn D King, 2005; Mohyeldin and Chiocca, 2012).

1.1.4 Adeno-associated virus (AAV) vectors

AAV is a non-pathogenic single stranded DNA virus that can transduce both dividing and non-dividing cells. Over 100 AAV variants have been isolated in primates alone and new serotypes are being continuously discovered. They have

not been associated with disease in humans, yet more than 80% of adults over 20 show an antibody response to AAV, proving they have encountered the virus (Erles et al., 1999).

All of the serotypes that have been extensively characterized (at least AAV1-AAV12) thus far share very similar structure, size and genetic organisation, only differing in the proteins that form the viral capsid, which determines the receptor selectivity of the virus (Wu et al., 2006). Of these, AAV2 is the most studied serotype and formed the basis of the development of AAV vectors. The receptors that different AAV serotype capsids bind are all widely expressed. Pseudotyping AAV2 vectors with different capsids extends the tropism of the virus to permissive organs (including neurons, photoreceptors). However, transduction of cell types that are resistant to AAV2 gene transfer (such as endothelial cells and fibroblasts) will not be improved. AAV2 viruses enter cells by clathrin-mediated endocytosis, escaping the early endosome and translocating to a perinuclear location. After shedding their capsid proteins in the nucleus, second strand synthesis is mediated by endogenous DNA repair mechanisms to form a double stranded DNA molecule required for gene expression (Ferrari et al., 1996). The wild type virus genome consists of two structural genes Rep and Cap, responsible for replication and capsidation respectively. These genes are flanked by two non-coding 145nt inverted terminal repeats (ITRs). An internal complementary stretch in the first 125nt of the ITR forms a T-shaped hairpin structure. Viral expression of the Rep gene in the host allows site-specific integration into the AAVS1 locus human chromosome 19 (Kotin et al., 1992). In the creation of an AAV vector, all viral genes have been removed except the ITR

sequences, creating a 4.7kb cloning capacity (Ferrari et al., 1997). To produce viral particles, Rep and Cap genes must be provided in trans, along with other adenovirus helper genes in the producing cells (Mezzina and Merten, 2011). Therefore, without the rep gene expressed in host cells, the viral genome forms episodic concatamers, with some random integration events (Wang and Finer, 1996; Tenenbaum et al., 2003; Smith, 2008). A limitation of AAV vectors lies in the small packaging capacity. However, the formation of genomic concatamers by head-to-tail recombination of the ITRs has been exploited as a means to increase capacity. This method requires co-transduction of cells with two different AAV particles that have the genomic load split between them (Nakai et al., 2000; Duan et al., 2002). Expression will only occur after recombination and the efficiency is often reduced. Once transduced with AAV vectors, cells *in vivo* have been seen to express GOI for the entire lifetime of rodents.

As AAV vectors do not express viral proteins, immune reactions to transduced cells are not evident although, similar to adenoviruses, the immune system can react to the capsid proteins (Mingozzi and A High, 2011). However, versatility provided by the range of tropisms of AAV serotypes can be used to improve efficiency and pattern of transduction in the specific regions in the CNS. For example, while AAV2 has a tropism for neurons in the brain (Bartlett et al., 1998), it binds heparin sulphate proteoglycan (HSPGs – cell surface receptor for AAV2) present in the extracellular matrix (Paterna et al., 2004; Broekman et al., 2006; McFarland et al., 2009), limiting its ability to diffuse away from the infusion site. AAV1, 5, 7 and 8 show greater diffusion through the parenchyma as they do not bind HSPGs. Astrocytes are preferentially transduced by AAV4 in

the subventricular zone (Liu et al., 2005), AAV5 transduces astrocytes and neurons in the striatum (Coughlan et al., 2010) (reviewed by Burger et al., 2005) while, in the cortex, AAV1 led to the most efficient transduction of corticospinal tract (CST) neurons (Hutson et al., 2011). Further to the isolated serotypes, studies are recombining capsid proteins, inserting DNA, and directing evolution to improve their characteristics even further (reviewed by Erles et al., 1999; Asokan et al., 2012; Bartel et al., 2012). AAV vectors are becoming one of the most utilised gene therapy vectors for use in the CNS (McCown, 2005) with phase I trials targeting diseases such as Alzheimer's disease, Canavan's disease and phase II clinical trials underway for Parkinson's disease (Weinberg et al., 2012).

1.1.5 Herpes simplex virus-based (HSV) vectors

HSV is a naturally neurotropic human virus that can transduce both dividing and non-dividing cells and can establish latency. This means that the viral genome remains episomal in the cell nucleus for the lifetime of the host organism. Wild type HSV also has a lytic life cycle, which results in viral replication and cell death.

There are three types of HSV vectors: attenuated, replication-deficient, and amplicon vectors. Attenuated vectors can replicate in rapidly dividing cells, but have had certain genes removed required for replication in non-dividing cells. However, several studies have shown these vectors do replicate after inoculation into the brain (Frampton et al., 2005), suggesting that these vectors are perhaps best suited towards oncolytic therapy of cancer (Harrow et al., 2004).

Replication defective vectors lack more genes that render them unable to replicate in neurons. There is a phase I clinical underway using them to treat pain (Wolfe et al., 2009). Amplicon vectors (or helper-dependent vectors) have had nearly all viral elements removed to give a 150kb cloning capacity. The amplicon consists of the GOI cassette, a minimal HSV replication (ori) and cleavage/packaging (pac) genes. To produce the particles, the amplicon is either co-transfected with sets of partially overlapping cosmids, or a single bacterial artificial chromosome, as a source of the viral proteins required to package the DNA into particles (Kotin et al., 1992). The potential of HSV vectors to deliver large genetic loads long term is appealing, yet the relative complexity and lack of understanding of the HSV genome hampers wider utilisation of this system.

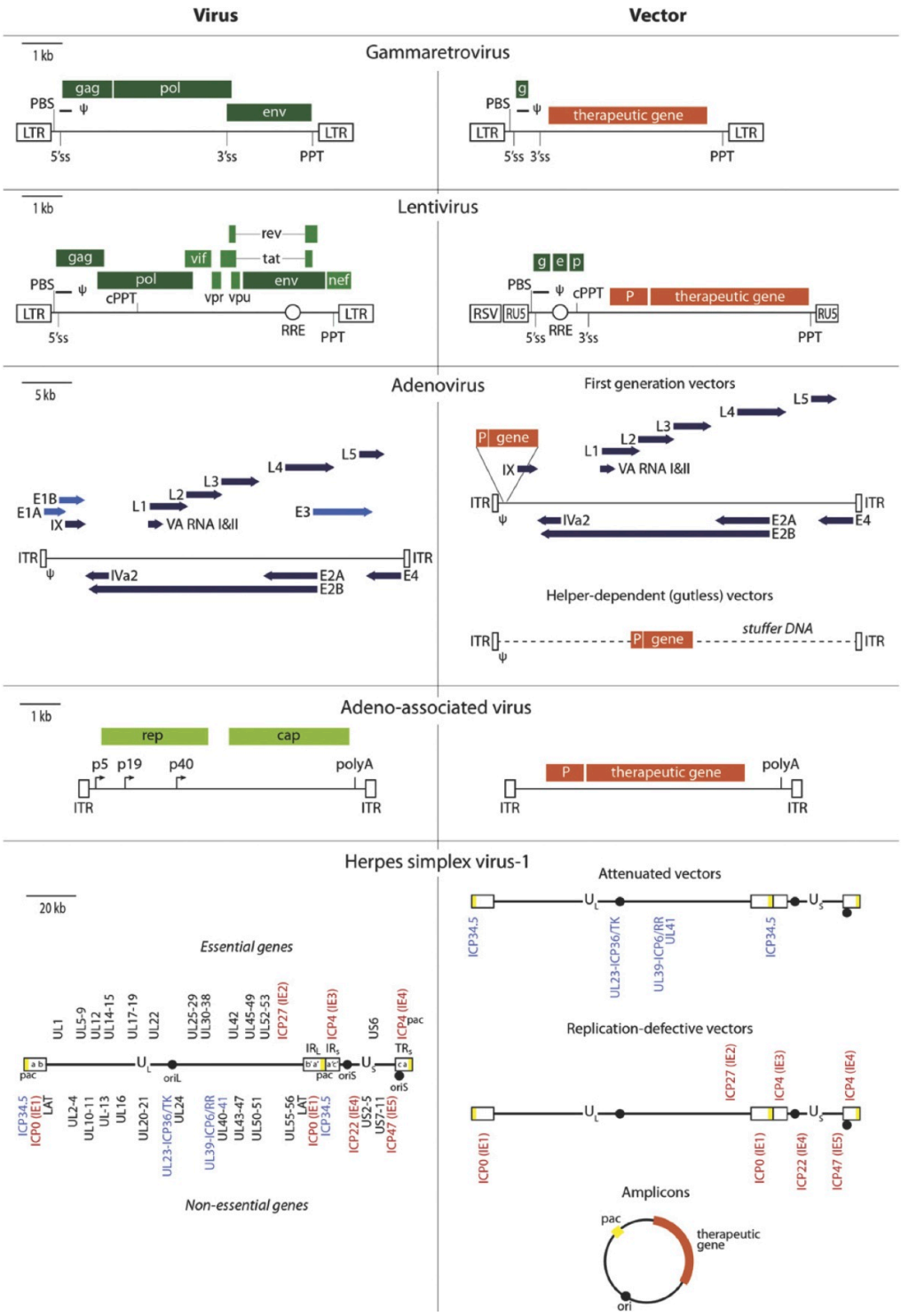

Figure 1-1 A chart to show the development of vectors from viruses
Adapted from Giacca et al., 2012

1.2 Regulation of gene therapy vectors

Gene therapy offers many advantages for treating neurological disorders; not least its ability to induce long-term, high level expression of therapeutic genes in the CNS. Often, studies using viral vectors use powerful constitutive promoters, to ensure that the therapeutic GOI is expressed a high enough levels to cause an effect (Ramezani et al., 2000). For example preclinical studies in Parkinson's disease have noted a relationship between vector dose and enzyme function or behavioural improvements (Ferrari et al., 1997; Forsayeth et al., 2006).

However, it is often the case that prolonged or high levels of proteins can lead to problems. For example, striatal overexpression of glial derived neurotrophic factor (GDNF) can lead to GDNF release and aberrant fibre sprouting at downstream striatal targets in an animal model of PD (Georgievska et al., 2002). Systemic administration of ciliary neurotrophic factor (CNTF) or brain derived neurotrophic factor (BDNF) led to substantial weight loss and anorexia in humans (Pelleymounter et al., 1995; Anon, 1996). It may also be necessary to tune the level of therapy. For example, aromatic L-amino acid decarboxylase (AADC) therapy for Parkinson's disease has the potential to increase L-DOPA induced dyskinesias in patients if too high a dose is received (Cress, 2008). As Parkinson's disease is progressive, the level of therapy required may change. An ideal viral vector would therefore direct transgene expression as long as the therapeutic protein is needed at the level that is required, for as long as the therapeutic protein improves disease symptoms.

Many approaches have been attempted to regulate the levels of proteins being produced. Here we will focus on systems that are of use in the context of vector mediated gene therapy, rather than controlling the levels of endogenously produced proteins (from genes). Many of these systems rely on a pharmacological ligand to bring about activation or inactivation of the system. To be suitable for clinical use, a pharmacological regulated system should ideally fulfil the following criteria. The ligand should be an "on switch", so that it activates the system that has been inactivated until such time that it is required. This is preferable to systems that are activated until "turned off" by a ligand, as this will require prolonged exposure to the drug to silence the system. Furthermore, the induction kinetics will rely on the rate of clearance of the drug, which may take longer than is desirable. It is necessary that the regulation is tightly controlled, so that there is minimal activation when the transgene is not wanted. It must facilitate rapid transition between the on and off state, in a reversible manner, such that precise temporal regulation can be repeatedly achieved, to potentially coincide with therapeutic windows. There should be a dose-dependent increase in the levels of target gene upon induction of the system so levels of therapy can be tuned to individual patients. The ligand should be specific to the regulatory system and not cause off target effects, yet also be able to penetrate into tissues. In order to be safe, the system must not promote immunogenic responses and be compatible with prolonged therapeutic use. Furthermore, the system must be applicable to as wide a range of cells types as possible so it can be used to regulate different genes in as many tissues or organs as may be required. It must also be a simple as possible, to avoid using multiple genetic manipulations. Even when the system does not require a

pharmacological ligand, many of these goals are desirable. Many regulatory systems have been developed and some have already been tested *in vivo*, although none have as yet been implemented in the clinic, indicating the difficulty in meeting these criteria.

1.2.1 TetOn/TetOFF systems

Tetracycline (Tet) regulated systems are based on the *E. coli* TN10 Tet resistance operon, comprised of the Tet operator (TetO) DNA sequence and the Tet repressor protein (TetR) (Wissmann et al., 1986). When Tet (or its derivative Doxycycline (Dox)) binds to the TetR protein, the change in conformation prevents it from binding to the operator sequence, allowing gene transcription. When the drug is removed this is reversible and the TetR can once again bind and block transcription. These components were developed into a regulatory system by Gossen and Bujard (Gossen and Bujard, 1992) Seven repeats of the TetO (called TRE – Tet responsive elements) were fused upstream of a minimal CMV promoter (that has low intrinsic activity) upstream of a gene of interest. TetR was fused to the eukaryotic VP16 transactivation domain to produce the tTA (Tet-controlled transcriptional activator), operational under its own promoter and polyadenylation signals autonomous from the TRE cassette. In the presence of Dox, the tTA cannot bind to the TRE and the gene of interest is silenced. However, when Dox is removed tTA can binds to the TRE, resulting in the expression of the gene of interest. The functionality of this system has been proven in the CNS *in vivo* (Harding et al., 1998). However, this approach has limitations. It is only suitable for situations when the system will be required to be activated for long periods, as silencing gene expression will require chronic

administration of Dox. Furthermore, the kinetics of activation of the system is largely dependent on the clearance of Dox.

In a bid to provide a more useful system from these initial findings, four further Tet regulated systems have been developed: TetON, TetKRAB, TetONcombined and Autoregulatory loop-based TetON-TetOFF.

TetON was developed by randomly mutating the TetR to form rTetR. Four mutations led to a reversal in the binding properties of the TetR such that in the presence of Dox, the rTetR bound to the TRE (Gossen et al., 1995). By fusing the VP16 transactivator to the rTetR (to form rtTA), gene expression could be induced by the addition of Dox. The kinetics of activation were more rapid than the TetOFF system (Gossen et al., 1995; Kistner et al., 1996) and this system has been investigated in non-human primates (Favre et al., 2002). However, this system also had limitations. The VP16 domain was found to exhibit some affinity for the TRE in the absence of Dox, leading to low levels of gene expression in the off state (Goverdhana et al., 2005). Furthermore, high levels of Dox were needed for maximal activation, prompting concerns that these levels could not easily be reached in the brain. To combat these concerns, Urlinger and colleagues induced further mutations to rtTA. Several mutants were tested and rtTA2-M2 was found to have lower basal activation and improved sensitivity to Dox (Urlinger et al., 2000; Lamartina et al., 2002; Mingozzi and A High, 2011). It is this form of TetON that has now been studied in non human primates (Latta-Mahieu et al., 2002; Chenuaud, 2004; Stieger et al., 2006). However, immunological responses to cells expressing the rtTA have been reported (Favre

et al., 2002; Latta-Mahieu et al., 2002; Chenuaud, 2004; Liu et al., 2005; Guiner et al., 2007).

TetON-KRAB was a different approach aimed at lowering the immunogenicity of the viral protein VP16 transactivator. KRAB (Krupple-Associated Box) domains (Bellefroid et al., 1991) were isolated from zinc finger proteins Kox1 (Deuschle et al., 1995) or Kid-1 (Witzgall et al., 1994a; 1994b; Hutson et al., 2011). These transrepressive domains (Margolin et al., 1994) are known to inhibit RNA polymerases up to 3kb away from the zinc finger binding site (Deuschle et al., 1995). Fusion to TetR formed TetR-KRAB also known as tTS (Deuschle et al., 1995), or tTS^{Kid} (Freundlieb et al., 1999). In this system, the minimal CMV promoter used for the original TetOn system was replaced with a constitutive active CMV promoter downstream of the TRE. Thus, in the absence of Dox, tTS binds to TRE and inhibits the CMV promoter. This system reportedly lowered basal activity(Freundlieb et al., 1999), yet the maximal expression levels were effected in some cases (Lamartina et al., 2003; Gardaneh and O'Malley, 2004; McCown, 2005). There are few reports of this system being explored further *in vivo*.

Bujard and colleagues continued to improve the system by co-expressing rtTA and tTS from a bicistronic expression cassette, separated by an internal ribosome entry (IRES) site. In the absence of Dox, tTS binds TRE and silences gene expression, yet in the presence of Dox the tTS will be released, allowing rtTA can bind to bind TRE leading to increased maximal activation (Baron and Bujard, 2000; Lamartina et al., 2003; Harrow et al., 2004; Weinberg et al.,

2012). This system has been used in several *in vivo* studies (including in the CNS (Xiong et al., 2006; Chen et al., 2008; Wolfe et al., 2009)), yet the clinical application is likely to be delayed due safety concerns relating to the expression of three foreign proteins.

Another strategy to reduce the immunogenic response and decrease background activation is to limit the production of these proteins to the time at which Dox is supplied by placing both rtTA and transgene - separated by an IRES fragment - under the control of a Tet-inducible promoter, which is simply the TRE coupled to a minimal CMV (Strathdee et al., 1999; Gould et al., 2000; Markusic, 2005). Very low levels of the rtTA are produced in the absence of Dox, so there is very tight regulation over the transgene. However, there is enough produced such that when Dox is supplied, the rtTA can bind to the TRE and transactivate the cassette. The induction of this system is delayed, as the rtTA must first reach sufficient levels to fully activate the TRE. These system have been studies *in vivo* in the CNS (reviewed by Stieger et al., 2009), however, immunogenic responses have again been seen with these constructs (Markusic et al., 2010).

As a ligand to regulate gene expression, Dox satisfies many of the aforementioned criteria. It has been used as a treatment for infectious diseases for many years and is thus well characterized. It is almost 100% bioavailable after oral administration (compared to intravenous administration) and penetrates tissues effectively, including the brain. Long-term administration has lead to renal toxicity and photosensitivity and a decrease in bone growth rate in youngsters (Agwuh and MacGowan, 2006). The possibility of raising antibiotic

resistance through excessive use of Dox may be solved by using 4-epidoxycycline, a metabolite of Dox that does not have antibiotic activity (Eger et al., 2004).

Underlying problems that hinder the use of Tet regulated systems are those relating to the basal leakiness exhibited by the rtTA-M2 transactivator (Georgievska et al., 2004a; Wakeman et al., 2011), and conflicting reports regarding the immunogenic responses to this chimeric bacteria/viral protein system (Wissmann et al., 1986; Gossen and Bujard, 1992; Gossen et al., 1995; Harding et al., 1998; Favre et al., 2002; Latta-Mahieu et al., 2002; Chenuaud, 2004; Ginhoux et al., 2004; Guiner et al., 2007; Cress, 2008; Han et al., 2010). Recent attempts have been made to reduce the immunogenicity of the rtTA (Zaldumbide et al., 2010), while others have increased the sensitivity of rtTA to Dox, implying a lower dose would be required to achieve maximal expression (Favre et al., 2002; Zhou et al., 2006). While further development of this system is required before entering the clinic, it is the most established method for regulating levels of gene therapy agents.

1.2.2 Ecdysone

Ecdysone is a steroid hormone that triggers moulting and metamorphosis in insects by stimulating the ecdysone receptor (EcR). Functional EcR is a non-covalent hetero-dimeric receptor with the insect ultraspiracle protein (USP), which together bind ecdysone response elements (EREs) in DNA to activate gene transcription (Yao et al., 1992; 1993; Goverdhana et al., 2005; reviewed by Riddiford et al., 2000). No and colleagues developed an inducible system (No et

al., 1996) by creating a novel transactivator form of the truncated EcR fused to transactivational domains of the glutocorticoid receptor and VP16 (VgEcR). This domain therefore responds to ecdysone, but has enhanced transcriptional activity. Human retinoic X receptor (RXR) was used as a dimerization partner in replacement of the USP (Thomas et al., 1993). Co-expression of VgEcR and RXR in cells containing an improved ERE (E/GRE) allowed induction of transgenes when ecdysone was applied, but tight regulation implies that the system is not induced by endogenous mammalian nuclear hormone receptors. A direct comparison of ecdysone to tetracycline regulated systems available at the time indicated that ecdysone had lower basal expression, greater inducibilty and more rapid induction kinetics (No et al., 1996). This system has been modified for use in lentiviral vector technology, such that all components are contained in a single expression cassette (Galimi et al., 2005). A hybrid *Drosphila*/*Bombyx* (Suhr et al., 1998) EcR was developed that does not require RXR (Hoppe et al., 2000), simplifying the system and reducing potential risks associated with overexpressing a protein involved in endogenous signalling pathways.

This system was further improved by the development of potent activating ligands. Plants produce phytoecdysones as a defence against feeding insects, leading to abnormal moulting (Kubo and Klocke, 1983) and muristerone A (murA) had been isolated from seeds of a plant (*Ipomoea calonyction*) (Canonica et al., 1972). Growing interest in the system required more readily available ligands, such as ponasterone A (PonA, from *Pomoea calonyction*) (Saez et al., 2000) among many others. As steroid hormone analogues they have good pharmacological properties (Bellefroid et al., 1991; Deuschle et al., 1995;

Bathori et al., 2008; Lapenna et al., 2009), and appear to be non-toxic (Spencer et al., 1993).

The system has been used in animal models (Margolin et al., 1994; Albanese et al., 2000; Niikura et al., 2000) including gene therapy in neurons (Deuschle et al., 1995; Ma et al., 2010), however, there has been no move into preclinical models in primates. As hormones, the activating ligand may have off-target effects in cells and this needs to be fully elucidated. Furthermore, because these molecules may be present in humans through consumption of crop plants (Deuschle et al., 1995; Freundlieb et al., 1999; 1999; Dinan et al., 2001; Dinan and Lafont, 2006), unwanted activation of the system may occur in a clinical setting. Similarly to the tet-systems, the chimeric EcRs still incorporate elements of viral proteins, which could lead to immunogenic responses.

1.2.3 Cre/LoxP

The Cre/LoxP system is one of the most well known methods to conditionally control a transgenic protein. In this system, the gene of interest is flanked by motifs recognized by a DNA recombinase "Cre". When the recombinase makes contact with the DNA motifs the DNA is rearranged. The Cre-LoxP site specific recombinase was originally found in the P1 bacteriophage (Sternberg and Hamilton, 1981). The Cre recombinase binds to the 34bp LoxP DNA motif comprised of two 13bp inverted repeat regions separated by 8bp (Hoess et al., 1982). Depending on the relative orientation of the motifs, the result will either be a reversal of the flanked DNA, or the removal of a DNA minicircle (Abremski et al., 1983; Hamilton and Abremski, 1984). This tool can be used to

produce deletions (Ramirez-Solis et al., 1995; Dolan et al., 2011), gene replacements (Hanks et al., 1995), insertions (Sauer and Henderson, 1990), or by flanking a stop codon it could be used as a conditional activator (Lakso et al., 1992). The system was later developed to induce transient gene expression and conditional knockouts in mice (Lakso et al., 1992; Orban et al., 1992; Ramirez-Solis et al., 1995). In order for tissue specific DNA alterations to occur, Cre driven by tissue specific promoters is typically used in double transgenic mice (Gu et al., 1994). While the Cre/LoxP system has been used extensively in this field of transgenics, it is very limited in the context of gene therapy. Once the LoxP-flanked gene of interest is delivered to cells, silencing the gene would require the unlikely event of all the cells that had been transduced in the first instance to be transduced a second time. Also, the requirement of a second delivery of vector is disadvantageous. Attempts to remedy this shortcoming have been attempted by creating inducible forms of Cre, such that they can be delivered at the same time of the therapeutic gene and activated through the use of small molecules.

Metzger and colleagues fused the ligand-binding domain of the oestrogen receptor (Metzger et al., 1995) to yield a constitutively expressed hybrid Cre-ER that is sequestered by heat shock proteins in the cytosol of cells in the absence of activating ligand. When 4-hydroxytamoxifen is supplied to cells, the hybrid Cre is released and can mediate recombination evens in the nucleus. The system was updated by using a mutated ER ligand-binding domain (forming Cre-ER^{T}). Validation in living mice (Feil et al., 1996), suggests that nearly 100% recombination occurs within 3 days of tamoxifen administration in some cell

types (Brocard et al., 1997). Other forms of regulatable Cre have also been developed by hybridizing the ligand binding domain of progesterone receptor activated by synthetic molecule RU486 (Kellendonk et al., 1996). Despite these and many on going improvements, this system still does not fulfil many of the criteria desirable to regulate gene therapy agents, such as dose-dependency, rapidity and especially reversibility. While the brief requirement for tamoxifen means it can even be used in pregnant mice (Danielian et al., 1998), some studies indicate incomplete or ligand independent recombination (Schwenk et al., 1998; Kellendonk et al., 1999) and there are reports of toxicity by Cre (Hameyer et al., 2007; Thanos et al., 2012). More recent developments using Cre/LoxP such as the Brainbow project indicate its power as a investigative tool (Livet et al., 2007), yet do not increase its suitability to clinical applications.

1.2.4 Regulation by affecting protein function

Protein function can also be conditionally controlled at the level of translated proteins. In these systems, the proteins are usually constitutively expressed and whether a protein will have an effect is mediated by controlling its location, degradation, or ability to fold correctly. Traditionally, small molecules have been used to target specific proteins. These must be screened and individually tested for safety and therefore do not have a general applicability. Furthermore, cross-reactivity can affect one or several off target proteins (Davies et al., 2000; Bain et al., 2003).

1.2.4.1 Destabilisation domain technology

Another method of creating a regulatable system that can be applied to many proteins is to create a fusion protein that can be conditionally altered. Varshavsky and colleagues discovered that the half life of a protein depends, in part, on its N-terminal residue (Bachmair et al., 1986; Bachmair and Varshavsky, 1989). Szostak and colleagues developed this idea to discover that a N-terminal fusion of a small peptide could confer instability onto a protein of interest (Park et al., 1992). However, this "degron" did not offer conditional control and gave a similar outcome to that of a genetic knock out. Varshavsky used this approach to develop a mutant dihydrofolate reductase (DHFR) that could be temporally regulated by temperature (Dohmen et al., 1994). An N-terminally fused arginine (to form Arg-DHFR) residue resulted in a temperature sensitive (TS) mutant that was maintained in cells growing at 23^{o}C, but degraded at 37^{o}C. Fusing this to other proteins conferred the phenotype onto them (Dohmen et al., 1994; Kanemaki et al., 2003), meaning that the Arg-DHFR could be used to produce TS mutants without searching for TS mutations. While this temperature sensitive regulation is of no use for *in vivo* studies, it was an interesting proof of concept that it is possible to target many different GOIs to be degraded by fusing one conditionally regulated protein to it. The next development was to find a fusion protein that could be conditionally regulated by a small molecule. This breakthrough came when it was fortuitously discovered that a mutated domain of the mTOR (mammalian target of rapamycin) protein named FRB* (FKBP-rapamycin binding domain) was unstable until it was bound and stabilized by a rapamycin analogue MaRap (Liberles et al., 1997). Furthermore, proteins fused to FRB* were also degraded

and rescued in response to MaRap in living mice (Stankunas et al., 2003; 2007). While this system provided dose dependent stabilization of a protein of interest, the stabilising ligand MaRap made this system unsuitable for wide spread adoption, as it is difficult to formulate, expensive and exhibits poor pharmacokinetics *in vivo* (Bayle et al., 2006).

However, it acted as a proof of principle that a conditionally stabilized fusion protein partner can be used to regulate a protein of interest. Recognising the potential of this approach, Wandless and colleagues set out to develop an improved system, by engineering a protein specifically to be unstable ("destabilisation domain") and allowing fusion partners to be destabilised until stabilized by a ligand.

The studies that had revealed the FRB*-MaRap protein ligand pair had been focused on other aspects of the ternary complex formed between rapamycin, FRB and FKBP12 (FK506-binding protein, 12kDa, hereafter FKBP). In light of these studies, they selected the FKBP protein to develop into a destabilisation domain, as it had already been investigated as a fusion partner, and a range of high affinity ligands had already been developed (Yang et al., 2000; Pollock and Clackson, 2002). They created a library of mutants of the FKBP protein fused to fluorescent reporter protein and screened it to find individual mutations that were stabilized by the synthetic ligand for FKBP (SLF) (Banaszynski et al., 2006). They isolated mutants that conferred dose dependent regulation of the fusion partner, with low basal expression levels in the absence of ligand and rapid, reversible induced expression in the presence of ligand.

To avoid targeting the endogenous FKBP, they used a F36V mutant of FKBP. This form has a cavity that ligands bearing a "bump" can bind with over 1000 fold selectivity. Small modifications of SLF yielded the novel ligand Shield1 with improved stabilising effects and better cell permeability. (Maynard-Smith et al., 2007). Similar ligands tested in humans had not provoked undesired side effects (Iuliucci et al., 2001).

This group have since tested the ability of the system to regulate several different classes of proteins by fusing the DD to the N-terminus of proteins: including GTPases (Rac1, RhoA, Cdc42), Kinases (GSK-3b), and cell cycle regulatory proteins (Securin, p21); and the C-terminus of proteins: a transcription factor (CREB), small GTPases (Arf6 and Arl7) and a transmembrane protein (CD8a) (Banaszynski et al., 2006). This range of protein sizes, folds, function and cellular localization indicated the versatility of the system. To test the system *in vivo*, they xenographed living mice with cells expressing a destabilisation domain-luciferase fusion protein. Administration of Shield1 caused dose dependent accumulation of luciferase activity in the tumours (Banaszynski et al., 2008). One other study has used this system in mice to regulate malonyl-CoA decarboxylase (Rodriguez and Wolfgang, 2012). It has also been implemented extensively when studying parasite proteins. Shield1 regulated proteins have been studied in *Plasmodium* (Balabaskaran Nina et al., 2011; Farrell et al., 2012), *Trypanosome* (Ma et al., 2012), *Apicomplexa* (Brooks et al., 2010; Limenitakis and Soldati-Favre, 2011), and *Leshmania* (Madeira da Silva et al., 2009); reviewed by de Azevedo et al., 2012).

While the FKBP-Shield1 system proves that a destabilisation domain can be engineered in this way, this system is of little use in the CNS, as Shield1 is predicted to have poor pharmacokinetic properties across the blood brain barrier. Recognising this, Wandless and colleagues have subsequently developed two further destabilisation domains, the first derived from the *E. coli* DHFR (Iwamoto et al., 2010), and the second from the estrogen receptors (Miyazaki et al., 2012).

The DHFR system is stabilized by trimethoprim, a widely available molecule that has excellent pharmacokinetic properties. Trimethoprim is readily absorbed from the gut and penetrates the blood brain barrier (BBB), meaning that this system can be used in the CNS. There are few publications using this relatively new system and none investigating its potential to conditionally regulate proteins in the CNS.

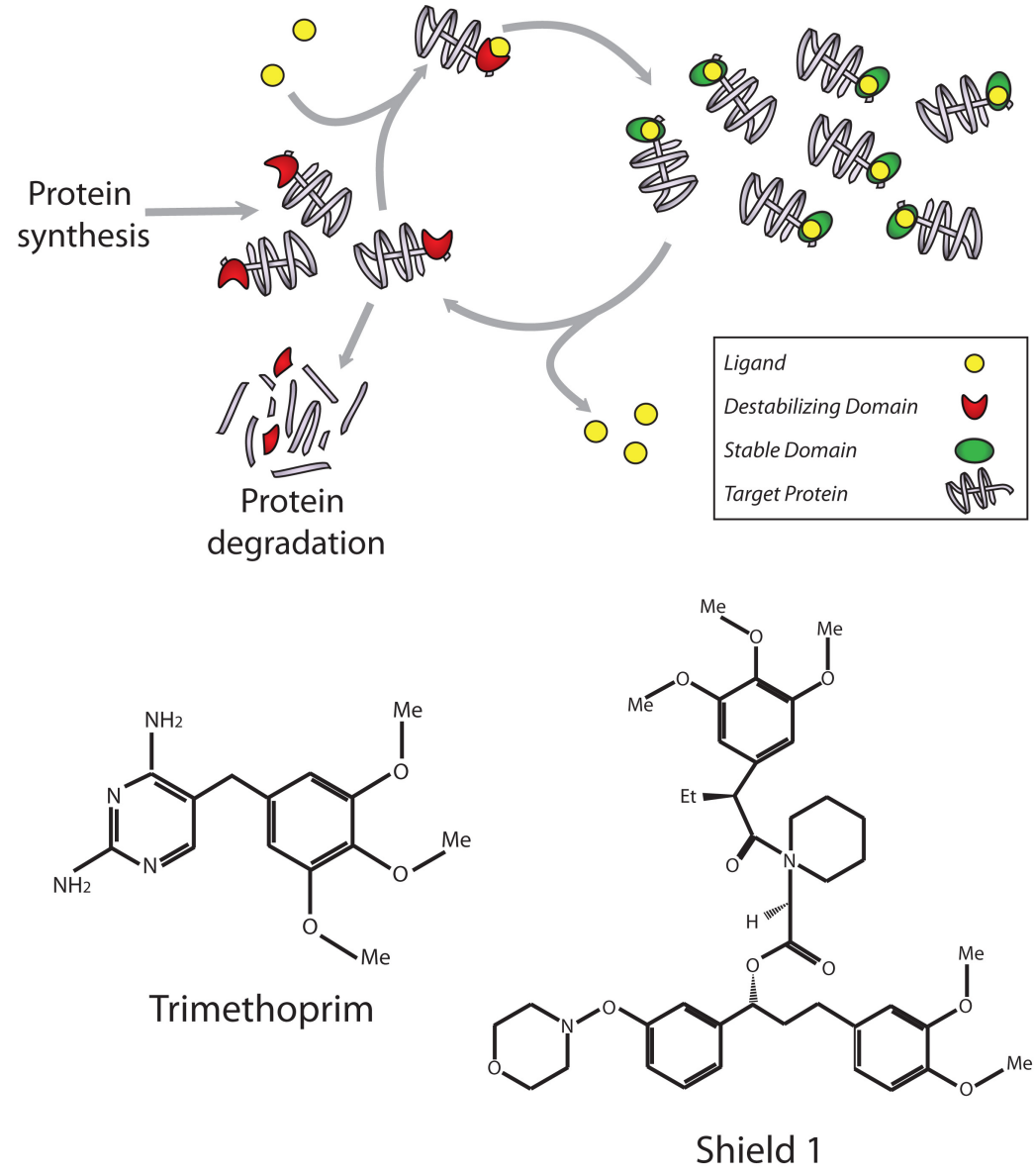

Figure 1-2 Illustration of the destabilisation domain technology, stabilising ligands and configurations in fusion proteins

1.2.4.2 SURF

The Muir group recently developed SURF (split ubiquitin for the rescue of function) technology (Pratt et al., 2007). In this system, the protein of interest is

fused to the C-terminal half of ubiquitin and FRB that targets the fusion to the proteasome. The N-terminal half of ubiquitin is fused to FKBP. In the presence of rapamycin, the FKBP and FRB are brought together, allowing the split ubiquitin to refold into a function molecule. The advantage of this system is that the FRB-FKBP-Rapamycin is then removed by endogenous deubiquitinating enzymes, releasing the protein of interest unhindered by other protein moieties.

1.2.4.3 PROTACs

Another system that uses endogenous proteolytic pathways to target proteins for degradation is the Protac (proteolysis-targeting chimeric protein) system, developed by the Deshiaes laboratory (Sakamoto et al., 2001). Protacs are heterobifunctional cell permeable molecules that contain a ligand that recognizes the target protein, yet also specifically bind to a specific ubiquitin ligase (Schneekloth et al., 2004). Therefore, these molecules bring the E3 ligase into proximity with the target protein and the resulting polyubiquitination tags it for degradation. This approach has been validated with several endogenously expressed proteins including methionine aminopeptidase-2 and the aryl hydrocarbon receptor (Sakamoto et al., 2001; Lee et al., 2007; Rodriguez and Wolfgang, 2012). Although this could be extended to protein expressed in gene therapy vectors, the system is limited by the fact that a binding ligand (usually a peptide) for the protein of interest must be developed. However, Protacs do offer a broader range of application than small molecule inhibitor systems that must functionally inhibit an enzymatic site to cause an effect, particularly as a greater proportion of proteins do not have enzymatic activity (Arakaki et al., 2006).

However, the lack of understanding of the proteasome system means this method is some way from clinical application (Long et al., 2012).

1.3 CNS diseases that have been targeted by gene therapy approaches

The central nervous system presents a unique challenge to gene therapy approaches as it is physically enclosed by a skeletal system and the blood brain barrier (BBB). Therefore, the routes of access to the CNS are limited to direct injection of gene therapy vectors into the parenchyma or direct delivery to cerebrospinal fluid (CSF) through injection into lateral ventricles or into the intrathecal space. Some examples of gene therapy approaches that have been applied to specific CNS diseases include motor neuron disease, Alzheimer's disease, Huntington's disease, spinal cord injury and Parkinson's disease, and these will be discussed briefly below.

1.3.1 Motor neuron disease

Motor neuron disease is characterized by progressive motor neuron dysfunction and death, leading to muscular weakness and wasting. The two most common examples of motor neuron diseases are amyotrophic lateral sclerosis (ALS) and spinal muscular atrophy (SMA). Approximately 10% of ALS cases are familial (fALS) and recently a number of genes have been found to be associated with fALS. Gene therapy approaches for ALS have centered on delivery of growth factors such as insulin growth factor-1 (IGF-1) (Kaspar et al., 2003; Dodge et al., 2010) and vascular endothelial growth factor (VEGF) (Azzouz et al., 2004b; Dodge et al., 2010), and RNAi-based silencing of mutant SOD1 alleles in transgenic ALS mouse models (Ralph et al., 2005; Raoul et al., 2005; Xia et al., 2006). In most cases, these studies have extended the lifespan of the transgenic

mice, but have not prevented disease progression completely. SMA is an autosomal recessive disease caused by loss of function of the "survival of motor neuron" gene *SMN1,* which leads to degeneration of motor neurons and infant mortality. Gene therapy strategies that have been tested experimentally include using AAV9 to deliver SMN1 cDNA to the spinal cord in a mouse model of SMA (Foust et al., 2010; Dominguez et al., 2011) or using EIAV-based lentiviral vectors to deliver SMN2 to spinal cord motor neurons following vector injection into muscles of neonatal SMA mice (Azzouz et al., 2004a).

1.3.2 Alzheimer's disease

Alzheimer's disease (AD) is a neurodegenerative disorder characterized by severe memory loss and cognitive impairment following the loss of basal forebrain cholinergic neurons. One strategy to prevent further cholinergic neuron loss is to supply neurotrophic factors such as nerve growth factor (NGF) via retrovirus-transduced fibroblast grafts in lesioned rodents and aged non-human primates In an initial phase I clinical trial of ex vivo NGF gene therapy, no detrimental side effects were observed at 22 months post-engraftment and the rate of cognitive decline slowed (Tuszynski et al., 2005). More recently, Ceregene are conducting phase I and phase II clinical trials using an AAV vector express NGF.

1.3.3 Huntington's disease

Huntington's disease is caused by progressive death in specific collections of striatal neurons and cortical degeneration, leading to lack of muscle coordination, cognitive decline and psychiatric illness. It is caused by an over-

expanded polyglutamine (CAG) tract in exon 1 of the huntingtin gene, *htt*. To date there are no effective cures for Huntington's disease. Examples of gene therapy approaches that have been tested in mouse models of Huntington's disease include using AAV vectors to deliver brain derived neurotrophic factor (BDNF) (Gharami et al., 2008; Kells et al., 2008), adenoviral vectors and lentiviral vectors to deliver ciliary derived neurotrophic factor (CNTF) (Mittoux et al., 2002; Zala et al., 2004), AAV vectors to deliver GDNF (McBride et al., 2003; 2006) and neurturin (Ramaswamy et al., 2009), as well as RNAi approaches to knock down huntingtin proteins (Harper et al., 2005; Boudreau et al., 2009; Drouet et al., 2009). While RNAi approaches remain an attractive option in HD therapy (where the cause of the disease is completely genetic), the studies that have been described thus far decrease expression of both wild-type and mutant huntingtin proteins, and the effects of decreased htt expression on normal cellular function is unclear. Researchers are therefore currently pursuing strategies of allele-specific targeting in which only mHtt expression would be down-regulated and this may be a promising approach in the future for treating HD.

1.3.4 Parkinson's disease

Parkinson's disease is a chronic, neurodegenerative disorder characterised by shaking, rigidity, slowness of movement and difficulty with walking, due to the loss of dopaminergic neurons in the substantia nigra. To date a large number of gene therapy approaches to target this disease has been tested in experimental models; the success of these studies have resulted in several preclinical trials that are currently being conducted in this patient group. The etiology of Parkinson's

disease and gene therapy strategies will be described in more detail in Section 1.5.

1.3.5 Spinal cord injury

Traumatic nerve injuries such as spinal cord injury can produce devastating and long-lasting effects in patients, with symptoms ranging from loss of sensation, paralysis, chronic pain, incontinence and loss of sexual function. Currently there are limited effective treatments for spinal cord injury. Recent breakthroughs in spinal cord research have increased our understanding of the problems underlying adult nerve regeneration and have facilitated the development of experimental therapies for spinal cord injury. These will be described in more detail in the next section.

1.4 Spinal cord injury

1.4.1 Pathophysiology of spinal cord injury

Primary spinal cord injury (SCI) describes the initial traumatic events that can results from contusion, compression, penetration or maceration of the spinal cord. The immediate events that occur after injury include necrotic cell death of neural and endothelial cell tissue and rupturing of blood vessels leading to ischemia around the injury site (Dumont et al., 2001). Secondary SCI describes the physiological changes that occur in the cord after the initial primary injury event. Within a few hours after injury, there is an immunological response to SCI. Endothelial cells within the damaged tissue release chemo attractants recruiting neutrophils and macrophages to the site of damage. They release oxidative and proteolytic enzymes that can lead to damage of spared tissue (Taoka et al., 1997), while also releasing pro-inflammatory cytokines that exacerbate inflammation by triggering leukocyte invasion (Jones et al., 2005). Both neutrophils and macrophages phagocytose debris which can help to clear the site of debris, but also leads to reactive oxygen species being released (Carlson et al., 1998; Satake et al., 2000)

Glutamate, the major excitatory neurotransmitter of the CNS (Gasic and Hollmann, 1992), is also released at the site of injury, leading to excitotoxic effects (Xu et al., 2005) (McAdoo et al., 1999). Neurons and oligodendrocytes are particularly susceptible to excitotoxicity as they express a full range of glutamate receptors (McTigue, 2008). Excitotoxicity initiates a cascade of events that results in the generation of reactive molecules that kill neurons through a

variety of mechanisms, including inactivation of membrane sodium channels, inhibition of Na^+-K^+ ATPase activity, direct inhibition of mitochondrial respiratory chain enzymes, and other modifications to key proteins (Dawson and Dawson, 1996; Dumont et al., 2001). Furthermore, lipid peroxidation leads to breakdown of cell membrane and mitochondria dysfunction (Sullivan et al., 2007) and contributes to calcium influx causing damaging changes in cell physiology and cell necrosis (Schanne et al., 1979; Xiong et al., 2007).

Many of the proteins and molecules released either by immune cells or from excitotoxicity can trigger apoptosis of neighbouring cells, contributing to further loss of neurons, oligodendrocytes and microglia (Crowe et al., 1997; Liu et al., 1997; Shuman et al., 1997; Beattie et al., 2000). Chronic loss of oligodendrocytes from the spinal cord leads to demyelination of spared neurons, slowing or blocking the electrical transmission ability of these neurons (Guest et al., 2005; McTigue, 2008). Furthermore, demyelinated neurons are more vulnerable to attack by the hostile environment in the lesion, leading to further cell death (Oyinbo, 2011).

These processes result in the formation of a cavity, surrounded by a progressive glial scar. Initially the scar is formed from myelin and oligodendrocytic debris, and some spared oligodendrocytes (Perry and Gordon, 1991). Activated microglia and macrophages begin to remove this debris and the site is still permissive to axon growth (Fawcett and Asher, 1999). However, as the scar progresses it leads to the deposition of molecules that inhibit axonal regrowth. Invading immune cells and oligodendrocyte precursors express surface markers

NG2 – an inhibitory chondroitinase sulphate proteoglycan (CSPG) (Jones et al., 2002). Non-CNS cells such as fibroblasts and Schwann cells also migrate to the lesion site (Grimpe and Silver, 2002) . Over time the scar becomes a predominantly astrocytic mesh held together by many tight junctions and gap junctions (Fawcett and Asher, 1999). Astrocytes also produce CSPGs (Lemons et al., 1999; Jones et al., 2003) meaning the scar forms a physical and chemical barrier to neurite outgrowth and regeneration.

1.4.2 Current cellular approaches for treating spinal cord injury

After spinal cord injury (SCI), the severe loss of cells (including neurons and oligodendrocytes) at the lesion site and the formation of the glial scar results in permanent barrier through which spared axons cannot regenerate to recover spinal cord function. Cell-based therapy has been touted as a promising avenue for SCI therapy, as cellular interventions can bridge the cavities with in the lesion, replace cells that have been lost, or provide a more permissive environment to axon regeneration.

Unlike the CNS, the PNS has regenerative properties in the adult. To try to exploit this, peripheral nerve grafts have been used in the injured spinal cord to encourage regeneration. Although regeneration from supraspinal axons was not seen when used alone (Richardson et al., 1980); when used in combination with other therapies such as anti-inflammatory drugs, vertebral wiring and fibrin glue, axons were observed to regenerate down the spinal cord, through and beyond grafts in rodents (Cheng et al., 1996; Lee et al., 2004). However when this approach was test in nonhuman primates, no functional recovery was detected (Levi et al., 2002). There has been very limited experimentation of this idea in humans and the outcomes have been inconclusive (Cheng et al., 2004; Steeves et al., 2004).

Olfactory ensheathing cells (OECs) have been hailed as a promising cellular therapy for SCI, due to reported successes in rats and non-human primate studies. OECs are glial cells derived from the embryonic and adult olfactory bulb or mucosa and support growth of olfactory neurons in adults. The use of

OECs in SCI was tested in human phase I clinical trials, many of which have reported success (reviewed by Radtke et al., 2008). These results should be viewed with caution as the lab-to-lab variation in cell biopsy and cell preparation, the lack of international standards for safety and efficacy and incomplete understanding of how OECs can contribute to axonal regeneration suggests that more research in this area is warranted before this strategy is implemented in the clinic.

The embryonic and fetal CNS can regenerate after injury and when fetal spinal cords were transplanted into the damaged adult cord, researchers observed some functional recovery, but the regenerating axons did not penetrate beyond the transplant border (Jakeman and Reier, 1991) (Bregman et al., 1997). Furthermore, ethical and resource limitations restrict the wider application of this therapy.

Progress in the field of neural stem cells has made it possible to expand neural progenitor cells (NPCs) obtained from a small amount of fetal tissue or embryonic stem cells as floating cell aggregates called neurospheres (Reynolds and Weiss, 1992). When NPCs were transplanted into rat models of SCI, they were observed to differentiate into neurons, astrocytes and oligodendrocytes accompanied by function recovery (McDonald et al., 1999; Ogawa et al., 2002). Human neural stem cells have also been shown to promote functional recovery in mouse and primate models of SCI (Cummings et al., 2005; Iwanami et al., 2005) and clinical trials are underway (reviewed by Sandner et al., 2012). Human embryonic stem cells that have been pre-differentiated into

oligodendrocyte progenitor cells demonstrated tremendous efficacy in a rat model of cervical spinal cord injury (Keirstead et al., 2005) and this led to a Geron-funded phase I trial to test these cells in thoracic spinal cord injuries, however the trial was halted due to financial reasons. More recently, Lu and colleagues grafted neural stem cells into fibrin matrices containing growth factor cocktails into spinal cord lesions and showed axonal extension over remarkable distances (Lu et al., 2012).

For many of these cell-based therapies, chronic immuno-suppression is often required in order stop immune-rejection of the transplanted cells. Induced pluripotent stem cells (iPSCs), derived from the cells of patients using four reprogramming factors (Takahashi and Yamanaka, 2006) should abrogate this need and reduce ethical concerns. Neural stems derived from iPSCs were initially tested in a mouse model of SCI (Tsuji et al., 2010) and functional recovery was observed, although the tumourogenicity of these cells was an important factor to consider. Neurospheres generated from human iPSC have been generated and tested in a mouse model, and have shown to form functional synapses (Nori et al., 2011). However, the safety and immunogenicity generated by these cells is not fully understood (Miura et al., 2009; Gore et al., 2011; Zhao et al., 2011b).

Other sources of stem cells that can be utilised for SCI therapy include cells derived from adult bone marrow. Bone marrow contains several different populations of stems cells, including haematopoietic stem cells (HSCs) and bone marrow stromal cells (BMSCs). Both have been seen to improve functional

recovery in mouse models of SCI (Wu et al., 2003; Koshizuka et al., 2004; Koda et al., 2005). Clinical trials of BMSCs are on going and the clinical efficacy is as yet unknown (reviewed by Wilcox et al., 2012). Neural stem cells can also been harvested from adult CNS. Active NSCs are found in the dentate gyrus of the hippocampus and the subventricular zone (SVZ). They have been shown to self renew and be multipotent after transplantation into the CNS. *In vivo*, adult mouse brain SVZ-derived NSCs were able to elicit functional recovery in a rat model of SCI when transplanted within a therapeutic window after injury, but not a chronic model of SCI (Karimi-Abdolrezaee et al., 2006). Other studies with neural stem cells from the spinal cord give mixed results (reviewed by Tetzlaff et al., 2011).

1.4.3 Molecular therapies for spinal cord injury

In the past decade, there has been significant breakthroughs in understanding why injured nerves, particularly that of the adult mammalian CNS, fail to regrow after injury. One main reason is the hostile environment in the spinal cord that is generated by the injury and significant progress has been made to identify the factors that contribute to this inhospitable environment. Another reason for regenerative failure is the poor intrinsic growth potential of the injured nerves. This section will aim to briefly describe some examples of experimental therapies have been targeted at neutralising the inhibitory growth environment of the lesion site or to increase the intrinsic growth potential of injured neurons, thus providing a snapshot of the strategies that are currently being explored to develop clinical medicines for spinal cord injury.

1.4.3.1 Chondroitinase.

CSPGs built up during secondary SCI become a long lasting inhibitory boundary that has been shown to hinder regenerative growth and synaptogenesis (reviewed by Silver and Miller, 2004). CSPGs consist of a core protein with one or more covalently attached chondroitin sulphate glycosaminoglycan (CS-GAG) side chains, which are important for the biological function of the CSPGs. Administration of the bacterial enzyme chondroitinase ABC can degrade the CS-GAG from CSPG molecules (Yamagata et al., 1968) reducing their inhibitory effect. Lemons and colleagues first demonstrated that ChABC applied to contusion-injured rats could degrade CSPGs *in vivo* (Lemons et al., 1999), indicating the therapeutic potential of ChABC. Studies assessing the regeneration, functional connectivity, locomotion and proprioception of injured

rats revealed that ChABC promoted functional repair and regeneration (Bradbury et al., 2002). Subsequent studies have indicated ChABC is polyfaceted in promoting repair, including regeneration of lesioned axons, sprouting and enhanced connectivity of intact remaining pathways, and neuroprotection of injured neurons (reviewed by Bradbury and Carter, 2011). Currently, ChABC therapy requires infusion of protein directly into the spinal cord. A gene therapy would have advantages, such as a long lasting effect with a single injection, while lowering the risk of further trauma and infection. Secretion of bacterial ChABC from mammalian cells is hindered by glycosylation events, so Muir and colleagues created ChABC mutants that retained enzymatic activity, but allowed the protein to be fully secreted when overexpressed form a lentiviral vector (Muir et al., 2010). These vectors are now being tested in a rat model of spinal cord injury. While there was no test of behavioural recovery at this stage, injection to either the CST neurons in the sensory motor complex or the spinal cord directly lead beneficial effects similar to those seen by direct infusion of ChABC protein (Zhao et al., 2011a)

A number of studies have investigated the possibility of combining ChABC treatment with other interventions that target different challenges for repair. For example, combining ChABC administration with peripheral nerve graft implantation gave increased regeneration (Yick et al., 2000) and ChABC infusion at the interface of a Schwann cell bridge enhanced re-growth into host tissue (Chau et al., 2004).

1.4.3.2 Anti-Nogo therapeutics

In the normal CNS, myelin plays a critical role in solidifying connections established in development but in the adult mammal, myelin-derived molecules are critical inhibitors of axonal growth/regeneration after SCI. The main myelin-derived inhibitors present at the lesion site are Nogo (a component of central myelin), myelin-associated glycoprotein (MAG) and oligodendrocyte myelin glycoprotein (OMgp). All three signal through a common Nogo receptor complex consisting of NgR, low-affinity neurotrophin receptor p75, LINGO-1 and TAJ/TROY. Upon activation, the complex activates the GTPase RhoA which subsequently recruits Rho kinase and activates downstream events to remodel the actin cytoskeleton to inhibit regeneration (reviewed by Zörner and Schwab, 2010). Following the identification of Nogo-A as a potent inhibitor, Schwab and colleagues demonstrated that neutralization of Nogo-A with antibodies (IN-1) increased functional regeneration of injured CNS neurons (Schnell and Schwab, 1990). Since this study, new anti-Nogo-A antibodies such as 11C7 and 7B12, the NgR blocking peptide NEP1–40, soluble NgR-Fc and Lingo-Fc fusion proteins have been developed and tested in animal models (reviewed by Zörner and Schwab, 2010).

1.4.3.3 Increasing the intrinsic growth potential of injured spinal cord neurons

In addition to identifying the inhibitors that present a major obstacle to axon regeneration in the injured CNS, researchers have also attempted to uncover factors that can promote intrinsic growth pathways within injured spinal cord neurons. For example, cAMP has been shown to induce axonal sprouting of cultured neurons *in vitro* and of injured adult rat spinal sensory neurons *in vivo*

when prophylactically applied (Neumann et al., 2002; Qiu et al., 2002). Researchers have also used peripheral nerve injury models to identify neuron-intrinsic regeneration-associated genes (RAGs) that play a role in axon regeneration. A number of these RAGs include transcription factors such as Atf3, c-Jun, Stat3 and Sox11 and it has been proposed that transcription factor hubs may potentially coordinate the regenerative response via a regeneration-associated gene network (reviewed by van Kesteren et al., 2011). Indeed, gene transfer of transcription factors such as CREB (cAMP response element binding protein) (Gao et al., 2004), ATF3 (activating transcription factor 3) (Seijffers et al., 2006), or RARβ2 (retinoic acid receptor β2) (Wong et al., 2006; Yip et al., 2006) has been shown to enhance axonal outgrowth. The study of RARβ2 in nerve injury models will be described in more detail in Chapter 5.

1.4.4 Combinatorial approaches to treating spinal cord injury

It is becoming increasingly clear that given the complexity of obstacles to axonal regeneration following spinal cord injury, it is quite likely that combinatorial approaches that address both the intrinsic and extrinsic cues will be the best strategy forward to achieve axonal growth sufficient for robust functional recovery after spinal cord injury. Gene therapy can provide a means of achieving one or more of these goals. An example of such a combinatorial approach is the use of sciatic nerve conditioning lesion, mesenchymal stem cells and NT-3 expressing lentiviral vector to facilitate successful bridging regeneration of adult CNS axons following dorsal column transection at the C3 level (Kadoya et al., 2009). Indeed, gene transfer to provide neurotrophic factors such as NT-3 and BDNF in combination with cell grafts (to bridge the lesion site) have been

explored in a large variety of animal models of axon injury (reviewed by Franz et al., 2012).

1.5 Parkinson's disease

Parkinson's disease (PD) is a neurodegenerative disease characterised by the progressive loss of dopaminergic neurons in the substantia nigra pars compacta (SNPC) and the presence of intraneuronal proteinaceous cytoplasmic inclusions, called Lewy bodies. As striatal dopamine is lowered, motor deficits symptomatic of PD emerge, namely rigidity, tremor, brady-kinesia, gait impairment and postural instability (Forno, 1996). The cause of PD is unknown in the majority of cases: only 10% of cases can be directly linked to genetic mutations. Environmental factors, or combinations of environment and genetic susceptibility are proposed to play a role in sporadic cases. Though as yet poorly understood, the death of dopaminergic neurons has been linked to mitochondrial dysfunction, oxidative stress, neuro-inflammation and insufficient proteasomal protein degradation (Dauer and Przedborski, 2003; Hirsch and Hunot, 2009)

The current standard treatment for PD is based on restoration of striatal dopamine (DA) neurotransmission by supplying the DA precursor L-3,4-dihydroxyphenylalanine (L-DOPA) through oral medication to provide relief from motor symptoms. In the early stages of PD this approach is very effective, but declines in efficiency as the disease progresses. Many patients develop side effects such as dyskinesias and hallucinations, which can limit the dose of L-DOPA that can be tolerated (Obeso et al., 2000). Therefore the search continues for an alternative treatment that requires only a single administration to safely provide symptomatic relief, halting or even reversing the progression of the disease.

1.5.1 Models of Parkinson's disease

In order to study Parkinson's disease, several pre-clinical models have been developed that replicate aspects of the pathology seen in human patients. These can be broadly divided in two categories: neurotoxic and genetic models. Of the neurotoxic models, the most widely used are the rodent 6-hydroxydopamine (6OHDA) lesion model and the 1-methyl-4-phenyl-1,2,3,6-tetrahydropyridine (MPTP) non-human primate model.

The 6OHDA model has been developed for the study of PD since the late 1960s (Ungerstedt, 1968). In the brain, 6OHDA is preferentially taken up by the dopamine transporter expressed by the DA cells projecting from cell bodies residing in the SNPC (Luthman et al., 1989). In the cytosol, 6OHDA generates reactive oxygen species leading to oxidative stress related cytotoxicity (Saner and Thoenen, 1971; Graham, 1978). 6OHDA does not cross the BBB so it must be delivered directly into the brain, usually at either the SNPC, the striatum or medial forebrain bundle (MFBB). Injection of 6OHDA to the SNPC or MFBB leads to significant and rapid degeneration of DA neurons and striatal terminals within days (Faull and Laverty, 1969; Jeon et al., 1995). In contrast, and potentially indicating a more relevant model of PD, striatal injection of 6OHDA produces a slower, progressive, partial lesion of DA neurons in the SNPC (Sauer and Oertel, 1994; Kirik et al., 1998).

This model has a major advantage in that it can be used to produce quantifiable asymmetric rotation behaviour in unilaterally lesioned animals. Subsequent to lesion, this behaviour is triggered by the injection of either dopamine receptor

agonists (such as apomorphine) or dopamine releasing compounds (such as amphetamine). The number of rotations, due to the imbalance of striatal dopamine signalling between lesioned and non-lesioned hemispheres, correlates with the magnitude of the SNPC lesion and DA neuron loss. (Ungerstedt, 1968; Ungerstedt and Arbuthnott, 1970). A disadvantage is that the 6OHDA model does not produce proteinaceous aggregates or Lewy bodies. Despite this, the model has been extensively utilized as a preclinical model for screening the efficacy of novel treatments for PD.

The MPTP model was developed from the accidental finding that drug users unintentionally using drugs contaminated with MPTP, developed severe symptoms similar to those of PD patients (Langston et al., 1983). Indeed, their motor deficits were successfully treated with L-DOPA, suggesting a common underlying pathology, and postmortem studies confirmed the loss of the nigrostriatal pathway in these patients (Davis et al., 1979; Langston et al., 1999). Although this pathology can be applied to many higher mammals, it is perhaps best represented in the non-human primate MPTP model that has become the gold standard of pre-clinical testing.

MPTP toxicity arises from its metabolite MPP+, produced by astrocyte and released in the vicinity of DA neurons. Upon accumulation in DA neurons, MPP+ inhibits complex 1 of the mitochondrial electron transport chain, leading to ATP depletion and increased oxidative stress (Nicklas et al., 1985; Mizuno et al., 1987). The neurotoxic effect of the nigrostriatal system and behavioural evaluations of motor deficits have been well characterized, and it has even been

suggested that Lewy bodies may be formed in primates using this model (Fornai et al., 2005).

1.5.2 Genetic models of Parkinson's disease

The first gene to be linked to familial PD is α-synuclein. α-Synuclein is a small (140 amino acids) but abundant neuronal protein that is particularly enriched in pre-synaptic terminals. Three missense mutations (A53T, A30P and E46K) cause dominantly inherited PD (Gasser, 2009; Lees et al., 2009). Furthermore, simple duplication or triplication of α-synuclein itself is sufficient to cause PD, suggesting that the level of expression of α-synuclein is a critical determinant of PD progression (Singleton et al., 2003; Singleton, 2005). A number of animal models of α-synuclein induced neurodegeneration have been generated; these include transgenic mice overexpressing wild-type A53T or A30P α-synuclein under the control of Thy1 or PrP promoters (reviewed by Dawson et al., 2010) or more recently, AAV-mediated overexpression of human α-synuclein in rats (Decressac et al., 2011). Interestingly, GDNF did not exert any neurotrophic factor effects in the latter PD model, as opposed to positive results described in previous studies involving the more commonly used neurotoxin models of PD. The difference in these results raises the importance of testing experimental therapies in both chemical and genetic preclinical models of PD.

The increasing number of genetic associations that have been identified with PD have also led to the development of other genetic models of PD. These include transgenic mice overexpressing leucine rich repeat kinase 2 (LRRK2) and mice

that are deficient for Parkin, DJ-1, phosphatase and tensin homolog (PTEN)-induced novel kinase 1 (PINK1) (reviewed by Dawson et al., 2010).

1.5.3 Gene therapy and Parkinson's disease.

Gene therapy is a promising approach for the treatment of Parkinson's disease for several reasons. It does not require indwelling hardware, yet therapeutic factors can be consistently delivered directly into the required area, abrogating dose fluctuations and the requirement for agents to pass the blood-brain-barrier (BBB). There are several therapeutic genes that have entered clinical trials, briefly discussed below.

1.5.3.1 Glutamic decarboxylase (GAD)

In PD, the subthalamic nucleus (SN) become disinhibited due to decreased GABA input leading to excessive activation, potentially giving rise to the symptoms of PD. Delivering GAD (glutamic decarboxylase, a catalyst for the inhibitory GABA) to the SNPC using AAV2 vectors is an approach to restore normal function. Indeed, in phase I clinical trials, improvements in motor function were seen without any observable adverse side effects (Kaplitt et al., 2007; LeWitt et al., 2011). However, this approach is not neuroprotective or restorative, nor does it address PD symptoms outside of motor circuitry.

1.5.3.2 Aromatic L-amino acid decarboxylase (AADC)

Aromatic L-amino acid decarboxylase (AADC) is an enzyme involved in the dopamine synthesis pathway, converting L-DOPA (L-3,4-dihydroxyphenylalanine) to dopamine. Levels of AADC activity, mRNA and protein have been found to be lower in the postmortem brains of PD patients

(Lloyd et al., 1975; Nagatsu and Sawada, 2007), potentially contributing to the need for increased frequency and dosage of levodopa in advanced stages of PD. By re-introducing AADC using AAV vectors, local conversion of levodopa to dopamine can be increased; meaning the dose of levodopa can be lowered to reduce side effects. Pre-clinical data in rats (Leff et al., 1999) and primates (Bankiewicz et al., 2006) indicated long term expression of AADC lead to increased striatal DA levels. Two phase I trials have been carried out (Muramatsu et al., 2010; Mittermeyer et al., 2012), and although improvement in motor function have been observed, side effects experienced by some patients indicate that more investigation is needed to determine the safety and clinical relevance of this approach.

1.5.3.3 AADC, GTP-cyclohydrolase-1 (GCH-1) and tyrosine hydroxylase (TH)

These enzymes are all members of the dopamine synthesis pathway. Tyrosine hydroxylase (TH) catalyses the synthesis of L-DOPA from L-tyrosine, which is then converted to dopamine by AACD. GTP cyclohydrolase 1 (GCH1) is the late limiting enzyme in the formation of tetrahydrobiopterin (BH4), an essential cofactor for TH (Kumer and Vrana, 1996; Elsworth and Roth, 1997) that is also reduced in PD (Nagatsu and Ichinose, 1997). Re-introducing these genes into the striatum can increase dopamine production at the site of injection; yet avoid excessive production in areas where dopamine is not depleted. Furthermore, the continuous production of dopamine, compared to pulsatile levodopa, may prevent levodopa-induced dyskinesia (Olanow and Obeso, 2000).

Pre-clinical studies co-transducing three individual AAV vectors expressing these enzymes in rat and primate models of PD (Shen et al., 2000; Muramatsu et al., 2002) decreased motor deficits. Tricistronic EIAV vector expressing these genes was also successful in preclinical studies (Azzouz et al., 2002; Jarraya et al., 2009) and dose escalation studies are underway, so far indicating reduction of motor deficits in patients.

1.5.4 Neurotrophic factors for Parkinson's disease

The strategies discussed so far aim to treat the symptoms of PD. A further reaching strategy is to delay symptoms by providing protection to, or even stimulating restoration of SNPC neurons, by providing additional trophic support.

1.5.4.1 Glial derived neurotrophic factor (GDNF)

Interest in using GDNF (Glial derived neurotrophic factor) as a potential therapy for PD stems from *in vitro* studies, where it was found that embryonic ventral mesencephalon (VM) DA cell survival was increased in the presence of GDNF (Lin et al., 1993). Subsequent studies revealed the potent dopaminotrophic effects of GDNF protein infusions that lead to both neuroprotection and neurorestoration in animal models (Gash et al., 1996; Shults et al., 1996; Björklund et al., 1997; Rosenblad et al., 1998; 1999). However, studies reported that improvements in symptoms were lost after cessation of treatment (Zhang et al., 1997), suggesting chronic infusion of GDNF is required. However, long term direct infusion of GDNF into the brain can lead to problems, including complications associated with the chronically implanted infusion device (Kirik

et al., 2004). Gene therapy offers an alternative method to supply specific regions of the brain with GDNF long term. Indeed, in many studies, this approach was efficacious using AD, AAV and lentiviral vectors (reviewed by Hong et al., 2008). However, some reported a decrease in TH levels and aberrant neuronal sprouting, raising concerns about the long-term high levels of delivery (Georgievska et al., 2002; 2004b). Furthermore, GDNF fails to exert neuroprotection in a α-synuclein rat model of Parkinson's disease, indicating GDNF may not be able to modulate metabolic cell death due to abnormal protein aggregation (Bianco et al., 2004; Decressac et al., 2011). Clinical trials using GDNF have focused on the infusion of protein rather than gene therapy approaches. Results of these trials have given mixed results. PD symptoms were not reduced in two trials delivering GDNF to the ventricles (Kordower et al., 1999; Nutt et al., 2003) and while one reported improvements following Intraputamenal delivery (Gill et al., 2003; Patel et al., 2005), further studies have failed to validate these findings (Lang et al., 2006).

1.5.4.2 Neurturin

Neurturin is a neurotrophic factor in the GDNF family (Kotzbauer et al., 1996) and has been shown to enhance the survival of dopaminergic neurons both *in vitro* and in rodent (Horger et al., 1998; Rosenblad et al., 2000; Oiwa et al., 2002) and non-human primate models of PD (Li et al., 2003; Kordower et al., 2006). Furthermore, there have been indications that it can aid restoration of DA neurons in rodent lesion models (Oiwa et al., 2002). In the preclinical studies, AAV2-Neuturin vectors were injected into the striatum of non humans primates, resulting in an increase of neurturin in the striatum and SNPC, along with an

increase in tyrosine hydroxylase in DA neurons (Herzog et al., 2007; 2008). In phase I clinical trial, there were no adverse effects and measures of motor function showed improvement (Marks et al., 2008). However, in a phase II double blind randomized clinical trial, analysis 12 months post injection of vector showed there was no difference in motor function between treated and sham operated groups. Subsequent analysis suggested that although neurturin was being adequately expressed a the site of injection (putamen), it was not transferred back to the SNPC (Bartus et al., 2011). This indicated that further trials were required, including an additional intranigral injection of vector, which are now underway.

1.5.4.3 Conserved dopamine neurotrophic factor and Mesenchymal astrocyte derived neurotrophic factor (CDNF/MANF)

CDNF and MANF are members of the novel family of neurotrophic factors (Lindholm et al., 2007). *In vitro* studies revealed that MANF could promote the survival of DA neurons in ventral midbrain (VM) cultures (Petrova et al., 2003). Subsequently, MANF protected DA and there was a reduction in rotation behaviour in the 6OHDA model of PD (Voutilainen et al., 2009). Similar benefits have been seen with CDNF, where a single pre-treatment with CDNF protein prevented 6OHDA-induced degeneration of DA neurons. (Lindholm et al., 2007) Furthermore, chronic administration starting two weeks post-lesion inhibited the 6OHDA induced loss if DA neurons in the SNPC, and TH fibres in the striatum (Voutilainen et al., 2011).

1.6 Aims and Objectives

Gene therapy is a powerful tool for delivering therapeutic factors into the CNS. However, there is an unmet need for systems to regulate the levels of transgenes in a clinical setting. Existing methodologies for regulating gene therapy agents have disadvantages that make them unsuitable for the clinic, so novel regulatory systems are of interest.

Destabilisation domain (DD) technology, developed by the Wandless laboratory at Stanford University, is a novel approach that is receiving considerable interest. This technology is composed of a protein domain engineered to be unstable until stabilised by a ligand. When fused to a protein of interest, the conditional stability of the domain is conferred to the fusion partner.

In this study, we will assess two different DD technologies to determine which is best suited to regulating the levels of therapeutic genes in the CNS. We will begin this process by attempting to regulate levels of reporter proteins (such as green fluorescent protein (GFP) and luciferase) delivered using viral vectors to cell lines and primary cultured neurons. After testing and identifying the constructs that yield the most efficacious results, we will proceed to test the ability of the vectors to regulate reporter genes *in vivo.*

Next, we will determine if this regulatory system is able to regulate genes that may of interest in the treatment of nerve injuries or Parkinson's disease.

Retinoic acid receptor β2 (RARβ2) has been shown to mediate pro-regenerative retinoic acid outgrowth programs in neurons. When delivered to the sensorimotor cortex in rat models of SCI, the increased sprouting of new projections correlated with a reduction in motor deficits, suggesting it may have potential as a therapy for spinal cord injury. We will develop a regulatable RARβ2 vector and test it *in vitro* to determine if the appropriate downstream pathways can be stimulated in DRG neurons to encourage neurite outgrowth. We will then determine the efficacy of the vector *in vivo*, in a rat model of SCI.

CDNF has recently been identified as a potential candidate for protecting and restoring dopaminergic neurons of the substantia nigra pars compacta (SNPC) that are lost in Parkinson's disease. Here we will investigate a gene therapy approach to deliver a regulatable form of CDNF to the SNPC. After preliminary testing of the vector *in vitro*, we will implement it in a rat model of Parkinson's disease.

Overall, we aim to add to the modest body of evidence so far collected on destabilisation domain systems, to help predict if these systems could be of clinical relevance in the future.

Chapter 2 Methods

2.1 DNA manipulation techniques

2.1.1 Polymerase chain reaction (PCR)

Double stranded DNA fragments were produced using the Fast start high fidelity PCR kit (Roche). The reaction conditions were the following:

High fidelity PCR

	AMOUNT	*SUPPLIER*
Template	***20-40ng***	
Forward primer (10µM)	***1µl***	*MWG operon*
Reverse primer (10µM)	***1µl***	*MWG operon*
10X Reaction Buffer (+Mg^{2+})	***2.5µl***	*Roche*
10mM dNTPs	***4µl***	*Invitrogen*
DMSO	***2µl***	*Roche*
Taq	***0.5µl***	*Roche*
ddH_2O	***Up to 25µl***	*Sigma*

2min at 95ºC	
30s at 95ºC	***X 40 cycles***
30s at 55-65ºC*	
60s at 72ºC	
10min at 72ºC	

Figure 2-1 High fidelity PCR using Fast start high fidelity PCR kit (Roche)
*Cloning PCR primers were typically run on a gradient of annealing temperatures between 55-65°C.

PCR products were typically separated by electrophoresis on a 1% agarose gel at 75V. Annealing temperature was changed to match specific primer pairs, usually between 55 and 65ºC.

2.1.2 Agarose gel electrophoresis

DNA fragments were separated and purified using agarose gel electrophoresis. Electrophoresis-grade agarose (Invitrogen) was dissolved in 1x TAE (40mM tris-acetate, 1mM EDTA) by boiling briefly in a microwave oven. Once the agarose solution (usually 1% [w/v]) had cooled, ethidium bromide (EtBr) was

added (final concentration of 0.5μg/ml), before the mix was poured into a suitably sized casting tray with an appropriate comb. Once the gel had set, it was submerged into 1x TAE buffer in a horizontal gel electrophoresis tank (Jencons). Prior to loading, the DNA sample was mixed with 0.2 volumes of a 6x DNA loading buffer (Invitrogen). Appropriately sized molecular weight markers were run alongside the samples (e.g. the '1kb DNA ladder' (NEB)). The gel was run at a constant voltage of between 5–10V/cm for sufficient time to allow the different DNA bands the separate. The bands were visualised using a ultra-violet illumination source (Ultra-Violet Products, Cambridge, UK) and images captured using a Gel-Doc image capture system (Bio-Rad, Hercules, CA, USA).

2.1.3 DNA extraction from agarose gels

To extract DNA from gel, the band was excised from the gel using a scalpel. The QIAquick gel extraction kit (QIAGEN) was used to extract the DNA from the gel according to the manufacturer's instructions. Briefly, 3 volumes of buffer QG were added to 1 volume of gel and dissolved at 50ºC. Isopropanol (1 gel volume) was added to the tube and mixed and the resulting sample loaded onto a QIAquick column and centrifuged at 17,900 RCF for 1 minute. The flow-through was discarded and 750μl buffer PE was added to the column and centrifuged at 17,900 RCF for 1 minute. Again, the flow through was discarded and the column was centrifuged again for 1 minute to remove residual PE. DNA was eluted in 30-50μl ddH_2O.

2.1.4 Quantification of DNA

DNA was quantified using agarose gel electrophoresis and the intensity of the sample band was compared with the intensity of bands of known concentration from the molecular marker (1KB ladder, NEB). In addition, DNA concentration may be determined using spectrophotometry. The 260/280 ratio used to determine the quality of the sample, with ratios in the range of 1.8-2.1 considered high quality DNA.

2.1.5 Desphosphorylation of DNA fragments

Prior to ligation, vector backbones were dephosphorylated to prevent self-ligation of the cut ends (thus reducing empty vector clones) using the Rapid DNA Dephosphorylation kit (Roche). rAPid Alkaline Phosphatase Buffer (10x - Roche) was diluted to 1x in DNA sample and 1µl (1U) Rapid Alkaline Phosphatase (Roche) was added after making a total reaction volume of 20µl with ddH_2O. The sample was incubated for 10 minutes (5' overhangs) or 30 minutes (3' extensions) at 37ºC before heat inactivating the enzyme at 75ºC for 2 minutes.

2.1.6 Ligation of DNA fragments

Vector and insert DNA were ligated together using the Rapid DNA Ligation Kit (Roche) according to the manufacturer's protocol. Briefly, 5x DNA dilution Buffer was diluted to 1x in a total reaction volume of 10µl containing DNA fragments (200ng total) and ddH_2O. To calculate the volumes of DNA required to give either a 3:1 or 5:1 ratio between insert DNA and vector DNA, the following equation was used:

$$mass_{insert} = \frac{length_{insert}}{length_{vector}} \times mass_{vector} \times Ratio$$

After mixing, 10µl of 2x DNA Ligation Buffer was added and mixed, before the addition of 1µl (5U) of T4 DNA Ligase. The reaction was allowed to proceed for 5 minutes at room temperature before transformation into chemically competent *Escherichia coli.*

2.1.7 Transformation of chemically competent Escherichia coli

Escherichia coli strains DH5α or Stbl3 (Invitrogen) were used for all transformations. DH5α cells were used for all cloning until such time as the DNA was required for lentivirus production, at which point Stbl3 cells were used. All transformations were performed according to the manufacturer's instructions, using aseptic techniques. Briefly, between 1-10ng of DNA was added to 50µl cells thawed on ice (without vortexing). The cells were incubated on ice for 30 minutes prior to heat shock at 42ºC for 20 seconds (DH5α) or 45 seconds (Stbl3). The tube was incubated on ice for 2 minutes and then 950 µl LB media (25g/L LB-Broth Miller (Fisher), 1mM NaOH) (DH5α) or 250µl SOC medium (Invitrogen) - Stbl3) was added to the cells. Cells were incubated for 1 hour at 37^{o}C with shaking before plating on onto pre-warmed LB agar plates (25g/L LB-Broth Miller (Fisher), 1mM NaOH, 1.5% agar [w/v], 1mM NaOH) containing the appropriate antibiotic. Cells were either plated directly (20-200µl of incubated cells), or briefly centrifuged (2000 RCF) before resuspension in 20µl media, depending on the expected efficiency of the ligation reaction. LB agar plates contained either 100µg/ml ampicillin (Sigma) for pRRL series plasmids, or 50µg/ml kanamycin (Sigma) for pONYK series plasmids. Plates

were incubated overnight at 37ºC and colony growth examined the following day.

2.1.8 Small scale preparation of plasmid DNA

Single bacterial colonies were picked from agar plates using a sterile pipette tip. The tip was dropped into 5ml LB broth (25g/L LB-Broth Miller (Fisher), 1mM NaOH) containing appropriate antibiotic selection, and incubated at 37˚C with shaking for 12-16 hours. 1-2ml of the bacterial broth was transferred into a microcentrifuge tube and centrifuged at 5000 RCF for 2 minutes. The supernatant was discarded and the cell pellet was processed using the QIAprep miniprep kit (QIAGEN). The cell pellet was resuspended in 250 µl buffer P1 and then 250 µl lysis buffer P2 added to the cells. The tube was inverted to mix the contents. Buffer N3 (350 µl) was added to the tube and inverted to neutralise the lysis reaction. The tube was centrifuged at 17,900 RCF for 10 minutes at room temperature and the resulting supernatant transferred to a QIAprep spin column. The spin column was centrifuged for 1 minute and then washed by adding 500µl buffer PB and centrifuging again for another minute. The flow-through was discarded and a further wash step was carried out by the addition of 750µl buffer PE. The column was centrifuged for 1 minute, the flow-through discarded and the column was centrifuged again for 1 minute. Purified DNA was eluted in 30-50µl ddH_2O.

2.1.9 Confirmation of ligation by restriction enzyme digest

To evaluate whether the ligation of the insert into the vector backbone had been successful, DNA was restriction digested with appropriate restriction enzymes

using the appropriate reaction buffer for a minimum of 3 hours at 37˚C. Digested DNA was electrophoresed on a 1% agarose gel and bands visualised under UV light.

2.1.10 DNA sequencing

Plasmid DNA obtained in either small or large scale preparations were sent for sequencing to Value Read Tube Sequencing service at Eurofins Genetic Service London (Ltd.), or the Single Run Sequencing Service at GATC Biotech, Germany, or the SpeedREAD service at Sourcebioscience (Oxford). Sequencing primers were selected to allow maximal coverage of a newly inserted DNA fragment (Table 2-1). ClustalW online software was used to compare the desired sequence to that obtained from sequencing (http://www.ebi.ac.uk/Tools/clustalw2/).

Primer Name	*Primer Sequence (5'-3')*
CMV 3' forward	*ATCCACGCTGTTTTGACCTC*
WPRE 5' reverse	*GGCATTAAAGCAGCGTATCC*

Table 2-1 Sequencing primers
CMV 3' forward binds to the 3' end of the CMV promoter and extends downstream into genes of interest. WPRE 5' reverse bid and the 5' of WPRE and extends upstream into genes that precede the WPRE. By using either or both of these primers, transgenes can be fully sequenced provided they are not longer than 1400kb.

2.1.11 Large scale preparation of plasmid DNA

The double-caesium chloride (CsCl) density gradient technique was used to purify large quantities of DNA of high enough purity for transfection reactions. Confluent bacterial cultures (1ml) were used to inoculate 500ml LB broth

containing appropriate antibiotics (usually 100µg/ml ampicillin), and incubated at 37ºC with shaking for 12-16 hours. Cell suspensions were centrifuged at 3,434 RCF for 20 minutes at room temperature. The supernatant was discarded and the pellet was resuspended in 18ml Solution 1 (25mM Tris-HCl pH8.0, 10mM EDTA pH8.0, 50mM glucose). Following resuspension, 2ml Lysozyme solution (1% lysozyme [w/v] (Sigma), 10mM Tris pH8) was added along with 40ml Solution 2 (0.2M NaOH; 1% [w/v] SDS) and incubated for no longer than 10 minutes at room temperature. Ice cold Solution 3 (5M potassium acetate; 11.5% glacial acetic acid) was then added and mixed by inversion 6 times. The lysate was then incubated for 10 minutes on ice before centrifugation at 3,434 RCF for 20 minutes at 4˚C. The supernatant was filtered through Whatman filter paper to remove protein contamination, before the addition of 0.6 volumes isopropanol. The solution was left at room temperature for at least 10 minutes before centrifugation at 4,020 RCF for 20 minutes at room temperature. The supernatant was discarded and the pellet air dried, before re suspension in 3 ml TE buffer (10mM Tris pH 8, 1mM EDTA pH 8) followed by purification in a caesium chloride (CsCl) gradient centrifugation.

An equal amount of CsCl [w/v] was added to the DNA followed by ethidium bromide (EtBr) (200µg/ml final concentration) before centrifugation at 12,000 RCF for 10 minutes at room temperature. The supernatant was transferred into an OptiSeal Ultracentrifuge tube (Beckman) and topped up with TE/CsCl solution (1:1) prior to centrifugation at 400,670 RCF (NVT65 Rota, Optimal LE-80K Ultracentrifuge, Beckman Coulter) for 12-16 hours at 20ºC. The resulting DNA band was excised and placed into a fresh OptiSeal Ultracentrifuge tube

taking care not to carry over any 'nicked' DNA (visible as a smaller band higher up in the tube). Again, the volume was topped up using TE/CsCl and centrifuged for 400,670 RCF for 6 hours. The DNA band was excised and EtBr removed using butanol saturated with H_2O. CsCl was removed from DNA by adding 10ml ddH_2O followed by 45ml 100% ethanol and incubating at 4˚C for 20 minutes. DNA was centrifuged at 12,000 RCF for 20 minutes at 4˚C. The supernatant was discarded and the pellet washed in 70% ethanol (200µl) prior to centrifugation for 5 minutes at 12,000 RCF. The pellet was dried using suction and resuspended in ddH_2O.

2.1.12 Transfection of HEK293T cells with plasmid

To test DNA constructs before lentivirus production, plasmids were transfected into human embryonic kidney cells, bearing the large T antigen of SV40 virus (HEK293T) cells. Cells were plated at 75,000 cells/well in a 12 well plate in 1ml of DMEM culture medium 24 hours prior to transfection. 1µg of DNA was transfected in each well using Fugene6 transfection reagent (Roche). Reaction ratio was 1µg DNA: 3.6µl Fugene6. Briefly, for one well, 3.6µl Fugene6 reagent was added to 36.4µl serum free medium (DMEM with no supplements), mixed well and incubated for 5 minutes at room temperature. DNA was then added and mixed thoroughly before incubation at room temperature for 30 minutes. The media volume on the cells was reduced to 0.5ml before addition of DNA/Fugene6 mix. After 3 hours, wells were topped up with 1ml DMEM and incubated for a further three days, before harvesting for analysis via flow cytometry or Western blot.

2.2 Lentivirus production and titration

2.2.1 Generation and amplification of recombinant lentiviral vectors

$8x10^6$ low passage (<40) HEK293T cells were plated into $15cm^2$ plates (12 plates required per virus for concentrated preparations, 3 for unconcentrated) in 20ml medium (DMEM supplemented with 10% FBS (Sigma), 2mM L-glutamine, 100 units/ml penicillin 100µg/ml streptomycin and 1x MEM non-essential amino acids (Sigma)) before incubation at 37˚C in a humidified atmosphere containing 5% carbon dioxide and 20% oxygen for 24 hours.

Cells were co-transfected with the genome plasmid (10µg), pMDLgp-RRE (gag/pol, 10µg), pMD2-VSV-G (Env, 3.4µg) and pRSV-Rev (2µg). Briefly, DNA added to a sterile polypropylene container and made up to 1125µl with ddH_2O. 140µl 2M Calcium chloride was added to the DNA solution and mixed. 1125µl Hepes-buffered saline (HBS; 50mM HEPES, 280mM NaCl, 1.5mM Na_2HPO_4) was added to the DNA drop wise with mixing and the solution left to incubate at room temperature for 30 minutes. Transfection mix (2.4ml/plate) was added evenly to the cells and plates were returned to the incubator.

	1x	***3.5x***	***12.5x***
genome	*10µg*	*30µg*	*125µg*
gag/pol	*10µg*	*30µg*	*125µg*
env	*3.4µg*	*11.9µg*	*42.5µg*
rev	*2µg*	*7µg*	*25µg*
H_2O	*up to 1.125ml*	*up to 3.938ml*	*up to 14.063ml*
2 M $CaCl_2$	*140µl*	*490µl*	*1.75ml*
HBS (added drop-wise)	*1.125ml*	*3.938ml*	*14.063ml*

Table 2-2 Scale up of transfection reactions
Reaction mixture required for one, three or twelve 15cm^2 plates. Three plates were used for unconcentrated preparations, 12 plates for concentrated preparations.

Table 2-2 shows how the reactions mixture is scaled up for multiple pates. The following morning, all media was replaced with fresh medium containing 10mM sodium butyrate (NaBu). Medium was harvested 6 hours later and replaced with 16ml fresh medium (no NaBu). Cells were returned to the incubator and the harvested medium was stored at 4^{o}C for concentrated preparations. For unconcentrated preparations this harvest was discarded.

The following morning the rest of the medium was harvested and pooled together with the first harvest. Culture plates were discarded at this point. Harvested medium was centrifuged for 5 minutes at 1200 RCF (Megafuge-20R; Heraeus Sepatech) before the supernatant was filtered through a 0.45µm filter unit (Nalgene) using a vacuum pump. The cell-free supernatant was stored at -20^{o}C if an unconcentrated preparation. For concentrated preparations, the supernatant was centrifuged at 6337 RCF (SLA 3000 rotor - Sorvall Evolution RC) overnight at 4˚C. To further concentrate the viral particle suspension, the resulting pellet was resuspended in 5ml of ice-cold PBS and transferred into a 14ml thin-wall polyallomer tube (Beckman-Coulter) and centrifuged at 70952

RCF (SW40 Ti ultra-Rotor, Beckman) for 90 min. The supernatant was discarded and pellets left to drain for several minutes. 100µl of TSSM buffer (20mM tromethamine (Sigma), 100mM NaCl (Melford), 10g/L sucrose (Sigma) and 10g/L D-mannitol (Sigma)) was added to the pellet and left on ice for 2 hours. The pellet was then resuspended by gently pipetting and the final resuspension volume was adjusted to 192µl with TSSM (this corresponds to a 2000x concentration of the original culture medium). Concentrated viral preparations were aliquoted and stored at -80ºC.

2.2.2 Lentiviral titering by fluorescent activated cell sorting (FACS)

HEK293T cells were seeded at a density of 7.5 x 10^4 cells/well in a 12 well plate and incubated overnight. The following day, cells were transduced with the lentiviral vectors in serial dilution (1 x 10^{-3} - 1 x 10^{-6}) in a total volume 500µl. An untransduced control was also included. Cells were returned to the incubator and the media topped up to a total volume of 1.5ml 5-6 hours later. Cells were counted in one representative well at the time of transduction, in order to subsequently calculate the titre. Cells were harvested after a further 72 hours. To titre lentiviral vectors expressing GFP fused to a destabilisation domain, media was exchanged for 1ml DMEM containing either 500nM Shield1 (FKBP12-based DD) or 50µM Trimethoprim (DHFR-based DD) 24 hours prior to harvesting for FACS analysis (Method 2.3). After recording the percentage of GFP positive cells, the titre was calculated using the formula:

$$\frac{TU}{ml} \equiv \frac{1}{n} \sum_{\substack{i=3 \\ \forall\, \%GFP^{+} \in [5\text{-}60]}}^{i=6} \frac{\left(\begin{matrix}\%\ GFP^{+} \\ cells\end{matrix}\right)_i x \left(\begin{matrix}Total \\ number \\ of\ cells\end{matrix}\right) x 100}{0.5\ ml\ x\ 10^{-i}}$$

Transduced Volume

Viral preparation dilution factor

2.2.3 Titering of Lentivirus by Taqman

Taqman QPCR was performed to determine the titre of non-GFP expressing lentiviruses by analysing the number of HIV integration sites. HEK293T cells were plated at a density of 7.5 x 10^{-4} cells per well of a 12 well plate and transduced with lentivirus at a dilution of 1:250 and 1:1000. As a control, a lentivirus with a known biological titre was also transduced at concentrations of 1:250 and 1:1000. Cells were passaged 1:5 every 3 days for 12 days and genomic DNA was extracted using a wizard DNA extraction kit (Promega), following manufacturers instructions. PCR reactions were set up in triplicate: 12.5µl Taqman 2x master mix, 1µl HIV Forward primer, 1µl HIV Reverse primer, 1µl Probe, 100ng genomic DNA, and ddH2O up to 25µl.

2.3 Fluorescent activated cell sorting (FACS)

To harvest cells for FACS, media was aspirated and the cells gently washed with PBS. After aspirating the PBS, 200µl trypsin/EDTA was added to the cells and incubated at 37ºC for 5 minutes. Once cells detached from the plate, the trypsin was neutralised by adding 800µl complete DMEM medium, while simultaneously triturating the cells to break up clumps. Cells were held on ice until ready for analysis using the FACS machine (FACSCalibur, Becton Dickenson). Using Cellquest Pro software, the population of single whole cells was gated using side and forward scatter measurements. Further gating of this population according to the fluorescence of the cells allowed determination of the percentage of GFP positive cells and the mean fluorescent intensity.

2.4 Western Blot

2.4.1 Protein extraction from cultured cell lines

Cell culture medium was aspirated and cells washed once with ice cold PBS. Cells were lysed in 100µl RIPA buffer per well (50mM Tris-HCL pH 7.4, 150mM NaCl, 1% Triton X-100, 1% sodium deoxycholate, 0.1% sodium dodecyl sulphate (SDS) supplemented with protease inhibitors (Complete Mini (1 tablet per 10ml RIPA buffer) (Roche)). Cells were scraped from the surface of the well to ensure complete removal, before homogenisation with a needle and syringe in an Eppendorf tube. Lysates were incubated on ice for 20 minutes and then centrifuged at 17,900 RCF for 20 minutes at 4˚C. The pellet was discarded and protein concentration of supernatant was determined using the BCA Protein Assay kit (Pierce) according to the manufacturer's protocol (see *2.4.2*). Cell lysates were stored at -20ºC or -80ºC for long-term storage.

2.4.2 BCA Protein Assay

BCA assay (Pierce) was performed according to the manufacturers protocol. Briefly, protein standards were prepared by diluting 2mg/ml bovine serum albumin to concentrations ranging from 2000µg/ml to 25µg/ml. Protein samples from cell lines were typically diluted 1:5 before assay, samples from primary cell cultures were used neat. BCA working reagent is prepared by diluting BCA Reagent B 1:50 into BCA reagent A. Samples and standards were added to a 96 well plate (5µl) before adding BCA Working Reagent (95µl), and incubating at 37ºC until purple colouration had sufficiently developed (approximately 30 minutes). Plate was read in a plate reader at a wavelength between 540-590nm.

2.4.3 SDS polyacrylamide gel electrophoresis (SDS-PAGE)

PAGE gels (10-12%) were prepared using Mini Protean II apparatus (Bio-Rad). A 4% stacking gel was cast on top of the running gel. Prior to loading, cell lysates were boiled for 5 minutes in 2x reducing sample buffer (100mM Tris-HCl pH6.8, 200mM dithiothreitol (Sigma), 4% [w/v] SDS, 0.3% [w/v] bromophenol blue (Sigma), 20% [v/v] glycerol (Melford)). Samples were loaded onto the gel along with standard protein markers (Precision Rainbow markers, Biorad) and run in tris-glycine buffer (25mM Tris; 250mM glycine; 0.5% [w/v] SDS) at 100v until proteins had migrated sufficiently through the gel.

Components	***8%***	***10%***	***12%***
H_2O	*9.3ml*	*7.9ml*	*6.6ml*
30% acrylamide mix	*5.3ml*	*6.7ml*	*8.0ml*
1.5M Tris pH8.8	*5.0ml*	*5.0ml*	*5.0ml*
10% SDS	*0.2ml*	*0.2ml*	*0.2ml*
10% ammonium persulphate	*0.2ml*	*0.2ml*	*0.2ml*
TEMED	*0.012ml*	*0.008ml*	*0.008ml*

Table 2-3 Solutions for preparing resolving gels for Tris-glycine SDS-Polyacrylamide gel electrophoresis
Total volume is suitable for casting two resolving gels at the indicated percentage of acrylamide.

Components	***Volume***
H_2O	*5.5ml*
30% arcylamide mix	*1.3ml*
1.0M Tris p6.8	*1.0ml*
10% SDS	*0.08ml*
10% ammonium persulphate	*0.08ml*
TEMED	*0.008ml*

Table 2-4 Solutions for preparing stacking gels for Tris-glycine SDS-Polyacrylamide gel Electrophoresis
Total volume is suitable for casting two stacking gels.

2.4.4 Transfer of proteins onto polyvinylidene difluoride (PVDF) membrane

Proteins were transferred onto PVDF membrane using a wet trans-blot cell (Bio-Rad). Two pieces of thick filter paper (Biorad) were soaked in transfer buffer (150mM glycine; 20mM Tris Base, 0.038% SDS, 20% methanol). The PVDF membrane was briefly soaked in methanol to activate it and rinsed in transfer buffer prior to transfer. The transfer 'sandwich' was assembled: filter paper, PVDF membrane, gel, filter paper. Sufficient transfer buffer was used to wet the transfer sandwich. The transfer was performed for 90 minutes at 220Amps.

2.4.5 Immunodetection of proteins

Following protein transfer, membrane was blocked 5% milk powder (Marvell)/PBS for at least 1 hour at room temperature with gentle agitation. The membrane was incubated in primary antibody (1:1000 anti-GFP raised in mouse (Roche)) diluted in 5% milk powder/PBS, overnight at 4˚C with gentle agitation. The next day the membrane was washed 3 x 10 minutes in PBS-T (1xPBS; 0.01% Tween20) before being incubated in horseradish peroxidase (HRP)-conjugated secondary antibody (typically anti-mouse (Roche) at 1:5000 dilution in 5% milk powder/PBS) for at least 1 hour at room temperature with gentle agitation. The membrane was washed again for 3 x 10 minutes in PBS-T before protein detection.

2.4.6 Enhanced chemiluminescence (ECL) detection of bound antibodies

Bound antibody was detected using ECL Western Blotting Detection Reagent (Amersham) Autoradiograph film (Amersham) was exposed to the membrane and developed using a Kodak film processor.

2.4.7 Quantification of proteins

Western blots were scanned and the density of bands quantified using ImageJ software. Data from ImageJ was then normalised for protein loading, by dividing the density of each band of GOI/treament by the density of corresponding bands of a protein loading control. α-tubulin was used as a loading control in all Western blots, probed on the same membrane, by stripping other antibodies and reprobing using an anti-α-tubulin antibody. α-tubulin was used as a loading control due to its abundance in cells, ease of detection with highly specific antibodies and unchanging expression profile in response to treatments used in similar experiments already optimised in our laboratory.

2.5 HEK293T cell culture

2.5.1 Cell culture technique

All cell culture techniques were performed using sterile tissue culture conditions in a category 2 laminar flow hood.

2.5.2 General maintenance of HEK293T cultured cell line

HEK293 cells were maintained in Dubecco's Modified Eagle medium (DMEM, Sigma) supplemented with 10% foetal bovine serum (FBS, Sigma), 2mM L-glutamine, 100units/ml penicillin and 100μg/ml streptomycin. Cells were incubated at 37˚C in a humidified atmosphere containing 5% carbon dioxide (CO_2).

Cells were sub-cultured once they reached around 70-80% confluence. Briefly, after aspirating the culture medium cells were washed with phosphate buffered

saline (PBS, Gibco). Following aspiration of PBS, ~1-3ml trypsin/EDTA (500µg/mL trypsin; 200µg/mL EDTA in PBS, Sigma) was added and incubated at 37˚C for approximately 2 minutes. Cells were detached from the flask by gentle rocking and topped up to 10ml using the appropriate pre-warmed culture medium before triturating to break up clumped cells. 1ml of cell suspension was placed into a fresh culture flask containing fresh medium. A haemocytometer was used to count the remaining cells if required.

2.5.3 Transduction of HEK293T cells with lentiviral vectors

HEK293T cells were seeded at a density of 7.5 x 10^4 cells/well in a 12 well plate and incubated overnight. The following day, cells were transduced with the lentiviral vectors (usually at MOI1) in a total volume 500µl. An untransduced control was also included. Cells were returned to the incubator and the media topped up to a total volume of 1.5ml 5-6 hours later. Typically on day 5, photomicrographs were taken prior to harvesting for Western blot analysis or cells were fixed using 4% paraformaldehyde in preparation for immunocytochemistry.

2.6 E18 rat cortical neuron culture

2.6.1 Preparation of plates

Poly-D-Lysine solution (0.1 mg/ml (Sigma)) was added to each well of a 24-well plate (Nunc), followed by incubation at room temperature for at least 4 hours, or at 4^{o}C over night. The solution was then removed and wells washed three times with sterile ddH_20, for 15 minutes per wash. After the final wash,

the water was removed and the plates left open to dry in laminar flow hood for at least 1 hour.

2.6.2 Dissection of cortex

This method is an adaptation of the hippocampal culture methods of Brewer et al (Brewer et al., 1993;Brewer, 1997). All surgical instruments were cleaned and sterilised by autoclave. Pregnant Wistar rats at E18 gestation were obtained from the central animal facility (University of Bristol). The animal was swabbed with 100% ethanol and the embryos removed into a 90mm petri dish containing 5ml Hanks Balanced Salt Solution without calcium and magnesium (HBSS, Gibco). Foetal heads were removed, washed in HBSS and the dissection performed under a MZ6 dissection microscope (Leica, Switzerland) with a K1500 electronic light source (Schott, USA). The skin and soft bone tissue were removed using forceps and the brain transferred into another dish containing 10ml fresh HBSS. Next the cerebellum was removed and the two brain hemispheres separated. Each hemisphere was placed on its side to enable removal of the thalamus, followed by the complete removal of the meninges. Finally the cortex was dissected out and placed into fresh HBSS medium on ice.

2.6.3 Trituration and plating of cortical neurons

Once the cortex had been collected they were cut into smaller pieces using the fine forceps before being placed in 5ml of HBSS medium containing 0.05% (w/v) trypsin (Sigma) and incubated for 20 minutes at 37^{o}C. The cortex were then washed three times in HBSS and triturated with a flame-polished Pasteur pipette in 1ml of Cortical Neuron plating medium (Neurobasal medium (Gibco)

supplemented with 2% (v/v) B-27 supplement (Gibco), 0.5mM L-glutamine, 100U/ml Penicillin and 0.1mg/ml Streptomycin, 25uM Glutamic acid). Following trituration, additional plating medium was added to the cell suspension so that cells were plated at a density of 100,000 cells per 500µl aliquots.

2.6.4 Culture maintenance and transduction

After three days *in vitro*, one third of the volume of medium in each well was removed and replaced with fresh feeding medium (Neurobasal medium supplemented with 2% (v/v) B-27, 100U/ml Penicillin and 0.1mg/ml Streptomycin). Two days later (5 days in culture), cells were transduced with lentivirus (MOI2). To increase the efficiency of transduction, one third of the media was removed prior to addition of virus. After incubation in the reduced media volume for at least 6 hours, the deficit was filled with fresh media. Media was changed (as above) after a subsequent two days, followed by media changes every three days. If appropriate, the final feed (day 12) contained stabilising ligands (Shield1, trimethoprim) at a range of dilutions, in triplicate. On day 15, photomicrographs were taken prior to harvesting for Western blot analysis or fixed using 4% paraformaldehyde in preparation for immunocytochemistry.

2.7 In vivo

2.7.1 Animals, housing and licence

Adult male Wistar rats weighing between 250-275g were obtained from either B&K Universal or Charles River, and kept for a minimum of one week to acclimatize before surgery. All animal work was performed under the license numbers: PIL: 30/8693 and PPL: 30/2537. All procedures were carried out using sterile instruments, drapes, gloves and solutions in accordance with the Animals (Scientific Procedures) Act 1986.

2.7.2 Stereotactic surgery

Animals were anaesthetised with a mixture of 1mg/Kg medetomidine (*Dormitor,* Pfizer) and 75mg/Kg ketamine (*Vetalar*, Pfizer) by IP injection. Confirmation of anaesthesia was obtained by footpad pinch test, before shaving the site of incision and placing the animal into a stereotactic frame. After cutting through skin using a scalpel and retracting to the skin to facilitate localisation of bregma, holes were drilled at the appropriate stereotactic coordinates relative to bregma, according to the brain atlas of Paxinos and Watson. A Hamilton 700 series syringe and 33G gauge-15mm needle was loaded with 2µl (plus a surplus) of concentrated vector preparation. Vectors were typically infused at rate of 0.2µl/min and the needle left in place for 5 minutes afterwards. At the end of procedure, the wound was closed using absorbable sutures and the animal recovered by subcutaneous administration of 0.2mg/Kg atipamezole (*Antisedan*, Pfizer). Additional post-operative analgesia was not used in these studies in accordance with techniques in project licence PPL 30/2537 indicating that

ketamine has analgesic properties that persist after surgery. In experiments modelling either Parkinson's disease or spinal cord injury *in vivo*, it has to be noted that the trauma to the tissues of rats is substantial and that in future work we would seek to administer additional post-operative analgesia. This would

2.7.3 Transcardial perfusions and brain harvesting

Animals were terminally anaesthetised with 150mg/Kg pentobarbital (*Euthatal*, Merial animal Health Ltd). Adequate anaesthesia was determined by footpad pinch test. After cessation of breathing, an incision was made through the sternum and the heart exposed by retracting the rib cage retracted. After removal of pericardium, blunted needle (19 gauge for rats) was introduced into the left ventricle and clamped in place using a pair of mosquito-haemostats. The right atrium was pierced to allow the drainage of the perfusate. PBS-Heparin (1U/ml, Sigma) was injected using a peristaltic pump 200ml at a rate of 40ml/min were used for rats. This was followed by perfusion with 4% [w/v] PFA, again, 200ml at 40ml/min for rats. The animals were then decapitated, the brains harvested, and post-fixed in 4% [w/v] PFA overnight, before being transferred into a 30% [w/v] sucrose solution until sectioning.

2.8 Sectioning tissue

2.8.1 Brain harvesting and section using cryostat

After perfusion fixing the animal firstly with Heparin-0.9% Saline, then 4% Paraformaldehyde (PFA) (pH7-7.4), the brain was harvested, and post-fixed for 24 hours in 4% PFA. It was then transferred to a 30% sucrose solution for three

days, or until the brain sank in the tube. Brains were then mounted into OCT mounting matrix (Thermo) and frozen to -20°C in a Leica CM190 cryostat for cutting typically 40μm sections. Sections were kept free floating in PBS until immunohistochemical staining and mounted onto glass coverslips in Fluorosave (Calbiochem).

2.8.2 Spinal cord sectioning using a vibratome

After perfusion fixing the animal firstly with Heparin-0.9% Saline, then 4% Paraformaldehyde (PFA) (pH7-7.4), the brain was harvested, and post-fixed for 24 hours in 4% PFA. It was then transferred to a 30% sucrose solution for three days. 10% gelatin (Sigma) was warmed until melted, then cooled to 40°C. In a shallow tray, sections of cord were submerged into the gelatin and left to set. The cord could then be cut out incorporating a border of gelatin and mounted into a vibratome. 40μm sections were harvested into PBS and stored at 4°C.

2.9 Immunohistochemistry

2.9.1 Immunofluorescent staining of brain sections

Sections were washed three times in 0.1% TritonX-100/PBS, before blocking against non-specific binding using 10% normal goat serum (NGS) in 0.1% TritonX-100/PBS for 1 hour at room temperature. Primary antibodies were added in a volume of 500μl 10% NGS/0.1% TritonX-100/PBS, and incubated at 4°C over night. Sections were washed 3x with PBS (5min per wash) before adding secondary antibodies diluted in PBS and incubating for 2-4 hours at room

temperature in the dark. After washing 3x in PBS (5 minutes per wash) sections were mounted on glass slides using Fluorosave (Calbiochem). Slides were kept at 4°C in the dark.

2.9.2 DAB staining of brain sections

Brain sections were transferred into staining pots and washed as described in method 2.9.1. Blocking, incubation with primary antibodies and washes were also as method 2.9.1, but were performed using TBS (100mM Tris-HCl (Melford); 154mM NaCl (Melford)) instead of PBS as the presence of phosphate groups can inhibit the activity of HRP. After binding primary antibody, sections were incubated with a biotinylated secondary antibody diluted (typically 1:400) in 500µl of TBS-0.1%Tx100 containing 5% [v/v] serum, 1% [w/v] BSA. Sections were blocked on a horizontal rocker at 10rpm (Stuart Scientific), 4ºC, overnight. The following day, sections were washed with TBS-0.1%Tx100 3 times and treated with HRP-conjugated avidin (ABC-Kit, Vector Labs) following manufacturer recommendations. Briefly, 0.5% [v/v] "Solution A" and 0.5% [v/v] "Solution B" were pre-mixed in 500µl of TBS and placed on ice for 30min, then added to the pots and incubated on a horizontal rocker at 10rpm, 4ºC, for 2h. ABC-solution was then washed twice with TBS and once with TNS (Tris non-saline buffer, 100mM, Melford). The HRP-substrate 3-3'-diaminobenzidine (DAB Substrate Kit for peroxidase, Vector Laboratories) was prepared following manufacturer's instructions. Briefly, 2 drops of *buffer solution* were added to 5ml of ddH_2O and mixed, followed by 4 drops of *DAB solution* and 2 drops of *H_2O_2 solution*. 750µl of this mixture were added to each pot and incubated on a horizontal shaker at 40rpm at room temperature until a

suitable staining developed (usually between 5 to 10 minutes). The sections were then washed once in ddH_2O and kept in TBS at 4ºC until mounting.

Antibodies used in immunostaining

Antibody	***Species***	***Supplier***	***Typical dilution***
Anti-βIII tubulin	*Mouse*	*Roche*	*1:1000*
Anti-CDNF	*Rabbit*	*ProSciInc*	*1:500*
Anti-ChickenALEXA488	*Goat*	*Invitrogen*	*1:500*
Anti-GFAP	*Rabbit*	*Dako*	*1:1000*
Anti-GFP	*Chicken*	*Roche*	*1:1000*
Anti-Mouse-Cy3	*Goat*	*Jackson Labs*	*1:500*
Anti-MouseALEXA660	*Goat*	*Invitrogen*	*1:400*
Anti-MouseBiotinylated	*Goat*	*Vector*	*1:400*
Anti-NeuN	*Mouse*	*Chemicon*	*1:500*
Anti-PKCγ	*Rabbit*	*Santa Cruz*	*1:500*
Anti-RabbitALEXA405	*Goat*	*Invitrogen*	*1:400*
Anti-RabbitALEXA568	*Goat*	*Invitrogen*	*1:500*
Anti-RabbitBiotinylated	*Goat*	*Vector*	*1:400*
Anti-RARβ2	*Rabbit*	*Santa Cruz*	*1:50*
Anti-TH	*Mouse*	*Covance*	*1:600*

Table 2-5 Antibodies used in immunostaining

Chapter 3 FKBP12 Destabilisation Domain

3.1 Introduction

Destabilization domain technology comprises a small, inherently unstable domain that confers instability to any protein it is fused to. The destabilization domain (DD) utilized in this chapter has been developed from the 107-residue FKBP12 protein (FK506-binding protein, 12kDa, hereafter FKBP) and is stabilized by the ligand Shield1. In humans, the FKPB protein is an abundant cytosolic protein that acts as the intracellular receptor for the immunosuppressive drugs FK506 and rapamycin. It was chosen for development into a DD as it has been widely studied by the Wandless Lab and others, often in the context of fusion proteins. Furthermore, a range of high affinity binding ligands were already available (Yang et al., 2000; Pollock and Clackson, 2002). To combat the potential issue of off target effects via interaction with endogenous FKBP, they utilised an FKBP-F36V mutant. This mutation forms a cavity in the ligand binding domain, enabling ligands bearing a "bump" to bind with over 1000 fold increased selectivity to the mutant over the wild type protein (Clackson et al., 1998; Yang et al., 2000). Promisingly, undesired responses to highly similar ligands had not been seen in cultured cells, animals, or humans (Iuliucci et al., 2001).

To create a destabilization domain, FKBP-F36V was further mutated using an error-prone PCR strategy (Banaszynski et al., 2006). A library was formed by cloning the random mutants in frame upstream of the yellow fluorescent protein (YFP) reporter gene. After transducing the library into cells using a retroviral delivery system, it was screened using flow cytometry to select mutants that

were destabilising to YFP in the absence of ligand, yet also stabilising in the presence of ligand (Banaszynski et al., 2006). Initially the ligand SLF* (Synthetic ligand for FKBP) was used, before a range of SLF* derivatives were synthesised (Maynard-Smith et al., 2007) revealing the cell permeable Shield1 to be most effective at stabilising the fusion proteins. Genomic DNA was extracted to enable identification of potential clones. Further testing revealed the FKBP-F36V/L106P clone to be most destabilising to YFP, yet rescued to high levels by Shield1. To ensure that the system could be applied to other genes of interest (GOI), such as proteins that have a cellular function, the system was tested on a range of classes of proteins, including GTPases, kinases, and cell cycle regulatory proteins (Banaszynski et al., 2006).

DD fusion proteins produced in the absence of stabilising ligands are thought to be degraded by the proteasome, due to the presentation of the unfolded domain. Cells expressing DD-YFP fusions in the presence of Shield1 before treatment with proteasome inhibitors Lactacystin (Maynard-Smith et al., 2007) and MG132 (Banaszynski et al., 2006) failed to degrade the fusions when Shield1 was withdrawn. Furthermore, a destabilized green fluorescent protein reporter (DD-zsGFP) colocalised with subunits of the proteasome in the absence of Shield1 (Leong et al., 2012). Most recently, ubiquitin chains have been found associated with DD within minutes after withdrawal of Shield1 from cells (Egeler et al., 2011).

At the time of our study, the authors had investigated the DD system in living mice, firstly observing the conditional expression of a luciferase reporter in pre-

transduced xenografted cancer cells, when Shield1 was supplied intravenously. Secondly, the tumour burden of cancerous xenografts expressing destabilised Interleukin-2 could be conditionally reduced in the presence of Shield1 (Banaszynski et al., 2008). There were no studies investigating the use of the DD system in the central nervous system (CNS) and as such we undertook to test this system in the CNS.

In this chapter, we will describe our design of DD/GOI fusion cassettes. These constructs are formed of the DD fused to the N- or C-terminus of GFP, separable using unique restriction sites to facilitate exchange of GOIs. Initially we will test the ability of the Shield1 to regulate the levels of GFP in cells transduced with lentiviral vectors bearing these constructs. To ensure that the system is versatile, and also to investigate the kinetics of the system, we will clone a luciferase reporter to replace GFP. If these studies are efficacious, we will then attempt to use these vectors to regulate the levels of reporter genes in the CNS of living rats.

3.2 Methods

3.2.1 Restriction site optimised destabilisation domain construct design

Two DD GOI fusion constructs were designed. One contained the destabilisation domain at the N-terminus of GFP (DD-GFP) and the other at the C-terminus (GFP-DD). In order to facilitate exchange of reporter (GFP) genes for other genes of interest and insertion of the cassette into two different lentiviral vector backbones while maintaining a very similar genetic construction, restriction enzyme sites were chosen with care to be unique in both the cassette and the parental plasmids. The parental EIAV (equine infectious anaemia virus) based vector plasmid was pONYK-CMV-GFP and the parental HIV (human immunodeficiency virus) based vector plasmid was pRRL-CMV-GFP (both obtained from Oxford Biomedica Plc. Oxford, UK).

In both parental plasmids, there was a unique *AgeI* site upstream of GFP. Down stream, *SalI* and *KpnI* were unique to the pRRL and pONYK plasmids, respectively. Neither pRRL nor pONYK (or DD/GFP cassette) contained an *NheI* or *PspOMI* site, meaning that these sites could be implemented in the boundary between the GOI and DD. Selecting unique enzyme sites in this way will facilitate exchange of the GOI, as only one digestion/ligation cycle is required for directional cloning of new GOIs. The DD/GFP constructs were supplied in a pMA plasmid by GeneArt gene synthesis services (Germany) (Figure 3-1 and Figure 3-2). After transforming into *E. coli*, DNA was harvested from an overnight culture via maxi prep (Method 2.1).

DD-GFP

accggtgccaccatgggagtgcaggtggaaaccatctccccaggagacgggcgcaccttccccaagcgcggccagacctgtgtggtgcactacaccgggatgcttgaagatggaaagaaag
tcgattcctcccgggacagaaacaagccctttaagtttatgctaggcaagcaggaggtgatccgaggctgggaagaaggggttgcccagatgagtgtgggtcagagagccaaactgactat
atctccagattatgcctatggtgccactgggcacccaggcatcatcccaccacatgccactctcgtcttcgatgtggagcttctaaaaccggaaggggcccctcgtgagcaagggcgaggag
ctgttcaccggggtggtgcccatcctggtcgagctggacggcgacgtaaacggccacaagttcagcgtgtccggcgagggcgagggcgatgccacctacggcaagctgaccctgaagttca
tctgcaccaccggcaagctgcccgtgccctggcccaccctcgtgaccaccctgacctacggcgtgcagtgcttcagccgctaccccgaccacatgaagcagcacgacttcttcaagtccgc
catgcccgaaggctacgtccaggagcgcaccatcttcttcaaggacgacggcaactacaagacccgcgccgaggtgaagttcgagggcgacaccctggtgaaccgcatcgagctgaagggc
atcgacttcaaggaggacggcaacatcctggggcacaagctggagtacaactacaacagccacaacgtctatatcatggccgacaagcagaagaacggcatcaaggtgaacttcaagatcc
gccacaacatcgaggacggcagcgtgcagctcgccgaccactaccagcagaacaccccccatcggcgacggccccgtgctgctgcccgacaaccactacctgagcacccagtccgccctgag
caaagaccccaacgagaagcgcgatcacatggtcctgctggagttcgtgaccgccgccgggatcactctcggcatggacgagctgtacaagtaaggtaccgtcgac

GFP-DD

accggtgccaccatggtgtccaagggcgaggaactgttcaccggcgtggtgcccatcctggtggagctggacggcgacgtgaacggccacaagttcagcgtgtctggcgagggcgaaggcg
acgccacctacggcaagctgaccctgaagttcatctgcaccaccggcaagctgcctgtgccttggcctaccctggtgaccaccctgacctacggcgtgcagtgcttcagcagataccccga
ccacatgaagcagcacgacttttcaagagcgccatgcccgagggctacgtgcaggaacggaccatcttcttcaaggacgacggcaactacaagaccagagccgaagtgaagttcgagggc
gacacactggtgaaccggatcgagctgaagggcatcgacttcaaagaggacggcaatatcctgggccacaagctggaatacaactacaacagccacaacgtgtacatcatggccgacaagc
agaaaaacggcatcaaagtgaacttcaagatccggcacaacatcgaggacggcagcgtgcagctggccgaccactaccagcagaacaccccccatcggcgacggacctgtgctgctgcccga
caaccactacctgagcacccagagcgccctgagcaaggaccccaacgagaagcgggaccacatggtgctgctggaattcgtgaccgccgctggcatcaccctgggcatggacgagctgtac
aaggctagcggagtgcaggtggagacaatcagccctggcgacggcagaacctttccccaagcggggccagacctgtgtggtgcactacaccggcatgctggaagatggcaagaaggtggaca
gcagccgggaccggaacaagcccttcaagttcatgctgggcaagcaggaagtgatccggggctgggaagagggcgtggctcagatgtctgtgggccagcgggccaagctgaccatcagccc
cgattacgcctacggcgccacaggccaccctggcatcatcccacctcacgccaccctggtgttcgacgtggagctgctgaagcccgagtgaggtaccgtcgac

Figure 3-1 Sequence of DD-GFP and GFP-DD cassettes
Restriction enzyme sites are indicted by red nucleotides (*AgeI*, accggt; *PspOMI*, gggccc; *NheI*, gctagc; *KpnI*, ggtacc; *SalI*, gtcgac). Blue nucleotides code for the destabilisation domain. Green nucleotides code for GFP. Black nucleotides indicate either the Kozak sequence (gccacc) or nucleotides required to mention translation frame (tc).

3.2.2 Cloning DD constructs into pRRL and pONYK lentiviral genomes

pONYK and pRRL backbones were prepared by digestion with restriction enzymes *AgeI* and *KpnI*, or *AgeI* and *SalI* respectively. The DD/GFP inserts were prepared by digestion with appropriate enzyme pair for the destination backbone. Digestions (1ug DNA, 2µl 10X Buffer, 1µl Enzyme, up to 20µl Water) were incubated at 37^{o}C for a minimum of 2 hours, before purifying correct band via gel electrophoresis (Method 2.1.2). After desphosphorylation of the backbone, ligation, transformation and plating bacteria, individual colonies were picked, grown overnight at 37^{o}C so DNA could be harvested by miniprep and sequenced to confirm DNA sequence. Subsequently, larger volumes of high quality DNA were prepared by maxiprep and CsCl gradient purification.

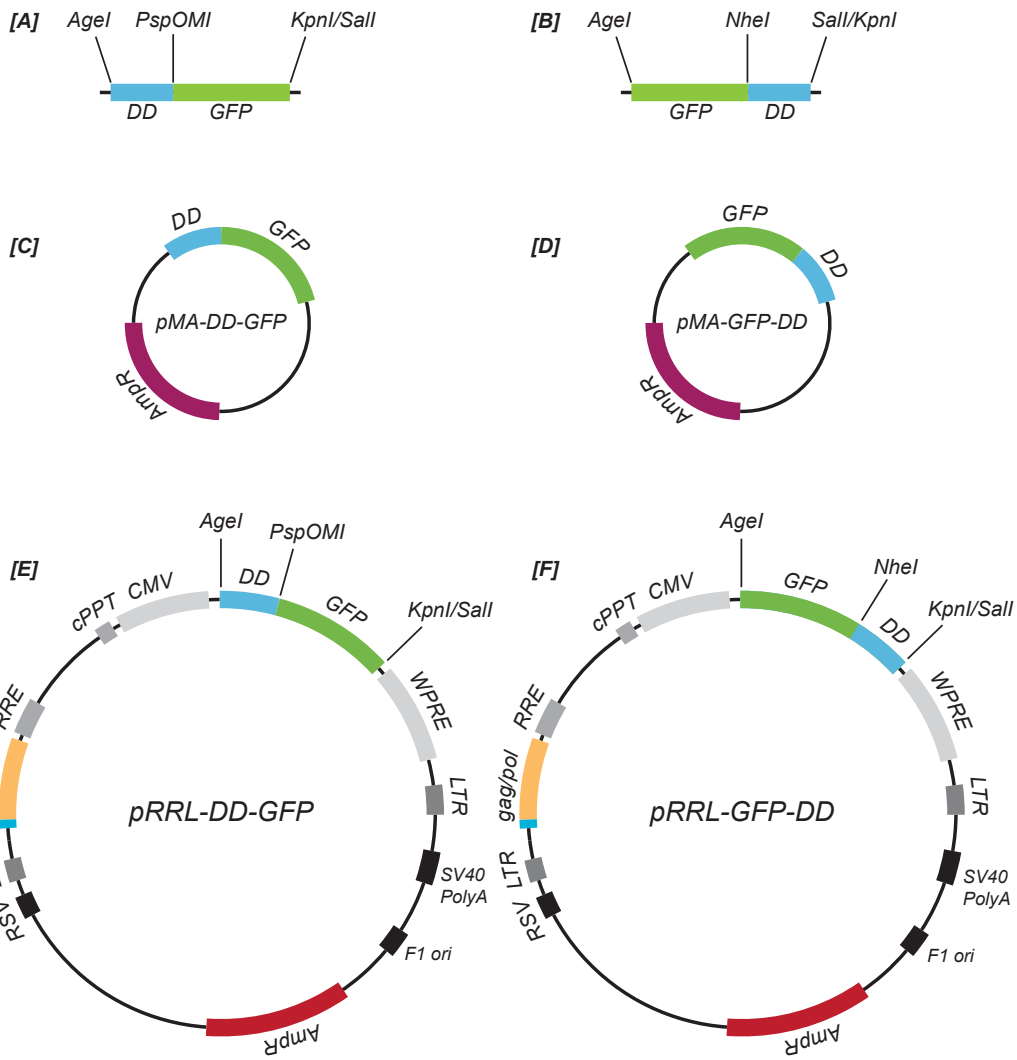

Figure 3-2 Design and cloning strategy for producing lentiviral genome plasmids containing DD/GFP cassettes
[A/B] Schematic of the location of restriction sites selected for DD-GFP and GFP-DD respectively. *AgeI* and *KpnI/SalI* allow insertion into lentiviral genome plasmids, but can be used in conjunction with *PspOMI* or *NheI* to exchange GFP for other GOI. ***[C/D]*** pMA plasmids containing DD/GFP cassettes supplied by GeneArt. ***[E/F]*** After restriction digest of pMA and parental pRRL or pONYK plasmids with appropriate enzyme pairs, lentiviral genome plasmid and DD/GFP cassette were ligated.

3.2.2.1 PCR amplification of Luciferase

PCR was performed as described (Method 2.1.1) using the primers listed in Table 3-1 and the template pRRL-CMV-Luciferase.

Primer Name	Primer Sequence (5'-3')
DD-Luciferase forward	TAGCATGGGCCCTC**GAAGACGCCAAAAACATA** (PspOMI)
DD-Luciferase reverse	TATAATGTCGACGGTACC**TCACTCGAGCAATTTGG** (SalI)
Luciferase-DD forward	TAGCATACCGGT**GCCACCATGGAAGACGCC** (AgeI)
Luciferase-DD reverse	CGGCCTGCTAGC**CTCGAGCAATTTGGACT** (NheI)

Table 3-1 Primers designed for the amplification of luciferase from pRRL-CMV-Luciferase
Annotated sequences indicate RE sites, while sequences shown in bold represent regions of template complementarity.

3.2.2.2 Cloning pRRL-DD-Luciferase and pRRL-Luciferase-DD

PCR products were separated in a 1% agarose gel, the correct band was excised and DNA recovered (Methods 2.1). Backbone plasmid pRRL-DD-GFP and luciferase (to be N-terminally tagged) were digested with the REs *PspOMI*/*SalI*; pRRL-GFP-DD and luciferase (to be C-terminally tagged) with the *AgeI*/*NheI* pair. After agarose gel electrophoresis, band excision and DNA recovery, products were quantified and backbone-insert pairs ligated, transformed and sequenced.

3.2.3 Lentiviral production, titration and use

Lentiviral vectors were produced and titred (Method 2.2). In all *in vitro* experiments in this chapter, vectors were used at MOI1. HEK293T cells and E18 rat cortical neurons seeded and transduced (Methods 2.5.3 and 2.6.4 respectively). Shield1 (Clontech) is purchased at 1mM and diluted to a range of doses usually below 1μM.

3.2.4 Stereotactic injection of HIV-DD-GFP and HIV-GFP into the CNS of adult rats

In all *in vivo* experiments in this chapter, adult male Wistar rats (250-300g) received 2µl of vector via stereotactic injection (0.2µl/min infusion rate) into the striatum at the coordinate (AP/ML/DV relative to bregma) 0/±3.5/-4.75 (Method 2.7). HIV-DD-GFP was infused into the left hemispheres; HIV-GFP control was infused into the right hemisphere. Titres: CMV-DD-GFP, $7.43x10^8$tfu/ml; CMV-GFP, $1.64x10^9$tfu/ml. Titres were not matched for *in vivo* experiments.

3.2.5 Injection of Shield1 to the striatum and ventricles

Vector was allowed to transduce for three weeks before injecting 2µl of the stabilising ligand Shield1, diluted to an appropriate concentration in 0.9% Saline, at a rate of 0.2µl/minute, either into the striatum, using the above co-ordinate, or into the ventricles, at the co-ordinate (AP/ML/DV relative to bregma) -0.8/1.5/-3.9, on the left side (the side with DD-GFP). 0.9% saline was infused into the same coordinates on the right hand side.

The animals were euthanized 24 hours later and brains were harvested after perfusion fixation using 4% paraformaldehyde. After cryoprotection 30% sucrose, the brains were sectioned to 40µm in a cryostat and kept free floating in PBS until immunohistological staining (Method 2.9 and Table 2-5 for details of antibodies).

3.3 Result

3.3.1 Designing an optimized cassette to express DD-GOI in lentiviral vectors

Published literature suggested that the domain had regulatory properties when fused to either the N or C terminus of the gene of interest (GOI). Two constructs (DD-GOI and GOI-DD) were therefore designed. Design of the constructs began by looking for conveniently located single cutting restriction enzyme (RE) sites in the parental lentiviral genome plasmids (pRRL-CMV-GFP and pONYK-CMV-GFP. Any REs that cut within the DD sequence or GOIs (GFP, Luciferase or RARβ2) were discounted (See methods for full details). The completed constructs comprised a GFP gene with one construct bearing the DD fused to the N-terminus of GFP, and the other construct bearing DD fused to the C-terminus fusion of GFP. DD-GFP and GFP-DD were synthesised by GeneArt and delivered in a minimal pMA plasmid. After digestion with appropriate RE enzymes, the DD/GFP cassette could be ligated into either a pRRL or pONYK series plasmid that had been digested with the same enzyme pair. This resulted in the plasmids pONY-DD-GFP and pONY-GFP-DD, pRRL-DD-GFP, and pRRL-GFP-DD.

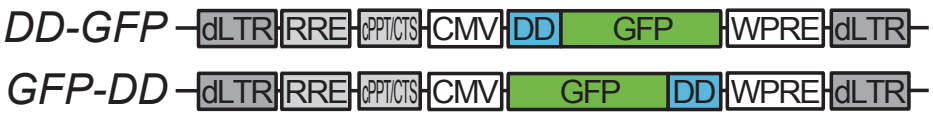

Figure 3-3 Schematic diagram of the viral insert of DD-GFP and GFP-DD

3.3.2 HEK293T cells transduced with EIAV DD-GFP or EIAV GFP-DD accumulate GFP in the presence of Shield1

To begin initial assessments of the regulatable system, unconcentrated EIAV-based lentiviral vector preparations of pONYK-DD-GFP, pONYK-GFP-DD and pONYK-GFP (control) were produced, and used to stably transduce individual populations of HEK293T cells. A range of Shield1 concentrations ranging from 0 to 5μM was applied in duplicate to the transduced cells for 48 hours prior to FACS analysis (Figure 3-4 *[A]*). GFP production from both DD-GFP and GFP-DD constructs, as indicated by mean fluorescence, was dependent on the dose of Shield1 supplied. Mean fluorescence from the GFP protein was observed to increase with increasing Shield1 concentrations. Shield1 did not affect the fluorescence of an untagged GFP control.

To confirm these findings and evaluate the system further, HEK293T cells transduced with the three constructs were subjected to Shield1 concentrations of an optimised range – 0, 1, 10, 100, 200, 500, 1000nM – in triplicate, 48 hours prior to microscopy and FACS analysis. Again, GFP fluorescence dose-dependently increased with increasing Shield1 concentration (Figure 3-4 *[B/C/D/E]*). FACS data indicated that cells expressing either DD-GFP or GFP-DD showed a 30- or 4-fold greater amount of GFP respectively in the presence of 500nM Shield1, compared to untreated cells. Western blotting of cell lysates from each treatment group showed that the increase in fluorescence is due to an increase in the amount of GFP protein present in the cells. This technique also suggested that the N-terminally tagged GFP exhibited less basal activity, as there was no detectable GFP protein present from 0 to 10nM of Shield1. The C-

terminally tagged GFP construct showed a 22-fold increase in fluorescence with the 500nM dose of Shield1 in Western blot analysis. Furthermore, it was clear the basal expression of the C-terminally tagged system was higher than that of the N-terminally tagged construct.

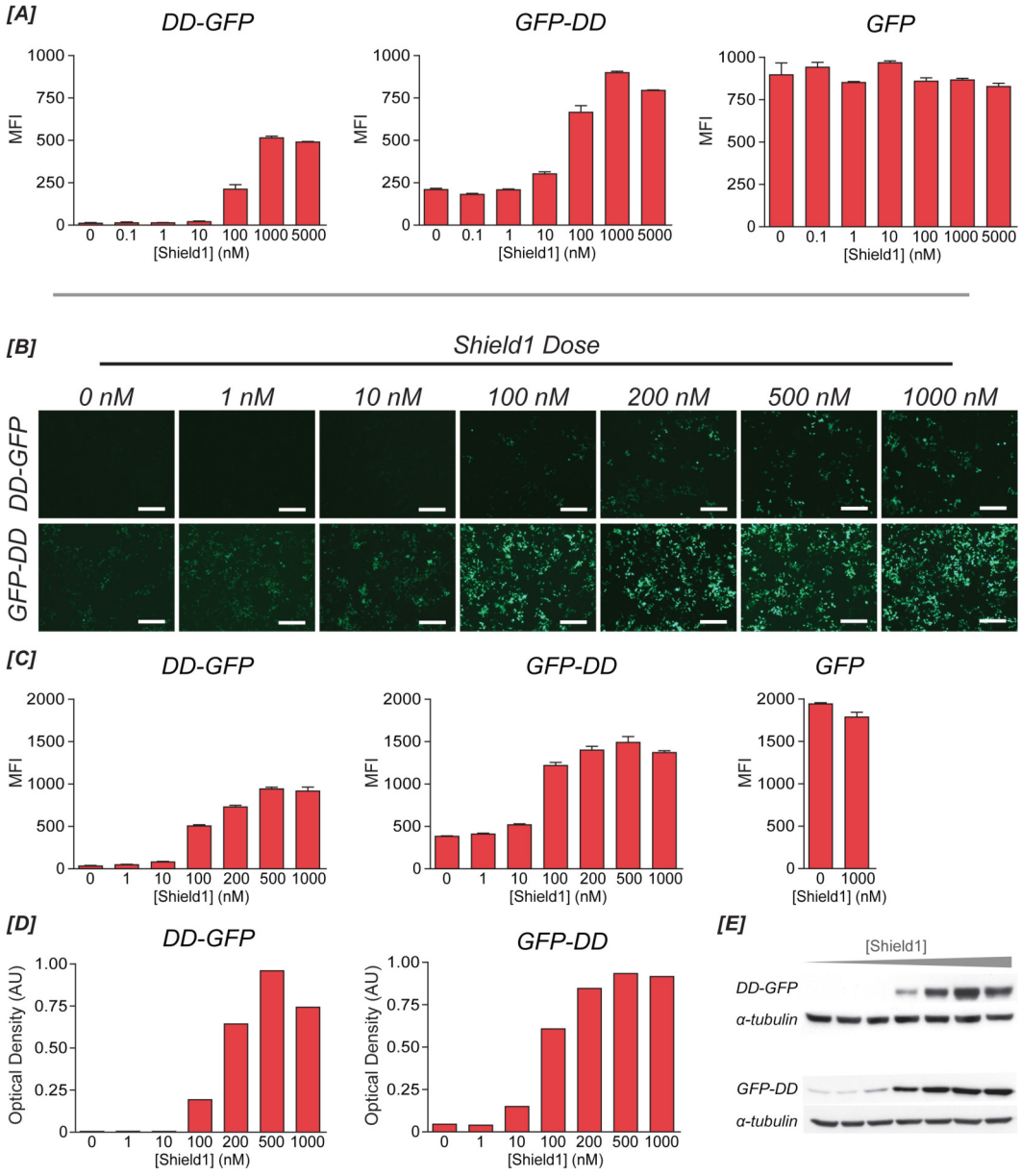

Figure 3-4 HEK293T cells transduced using EIAV vector of DD-GFP, GFP-DD or GFP control, treated with Shield1

[A] HEK293T cells transduced with EIAV lentiviral vectors expressing DD-GFP, GFP-DD or GFP control, were treated with a range of Shield1 doses 48h before FACS analysis (n=2). ***[B/C/D/E]*** Following the same procedure, a different range of Shield1 doses were applied 48h before imaging ***[B]*** (Scale bar=400μm) and ***[C]*** FACS analysis. ***[D/E]*** Triplicate samples were pooled for Western blot analysis. Blots were probed with anti-GFP primary antibody, and α-tubulin as a loading control. ***[D]*** Densitometry was performed using ImageJ software. ***[E]*** Shield1 doses (left to right): 0, 1, 10, 100, 200, 500 and 1000nM.

3.3.3 HEK293T cells transduced with HIV-DD-GFP or HIV-GFP-DD show dose dependent accumulation of GFP to Shield1

To determine if the destabilisation domain system is comparable between different lentiviral vector delivery systems, a similar experiment was performed with HIV vectors produced from using pRRL-DD-GFP, pRRL-GFP-DD and pRRL-GFP plasmids. The results obtained were similar to those obtained with the EIAV lentiviral vector constructs. FACS analysis indicated that there was a 37 fold greater amount of GFP produced by the DD-GFP construct, and 4 fold greater amounts by the GFP-DD construct, when treated with 500nM Shield1, compared to untreated cells (Figure 3-5). When the samples were analysed by Western blot, the DD-GFP construct again showed very tight regulation, with basal levels of GFP being 234 fold lower than that of cells treated with 500nM Shield1, although this much larger range of induction may be due to variations in the α-tubulin loading control. This variation has not been seen in other experiments using Shield1, suggesting that this is most likely due to experimental error, not Shield1 affecting the levels of α-tubulin in high concentrations.

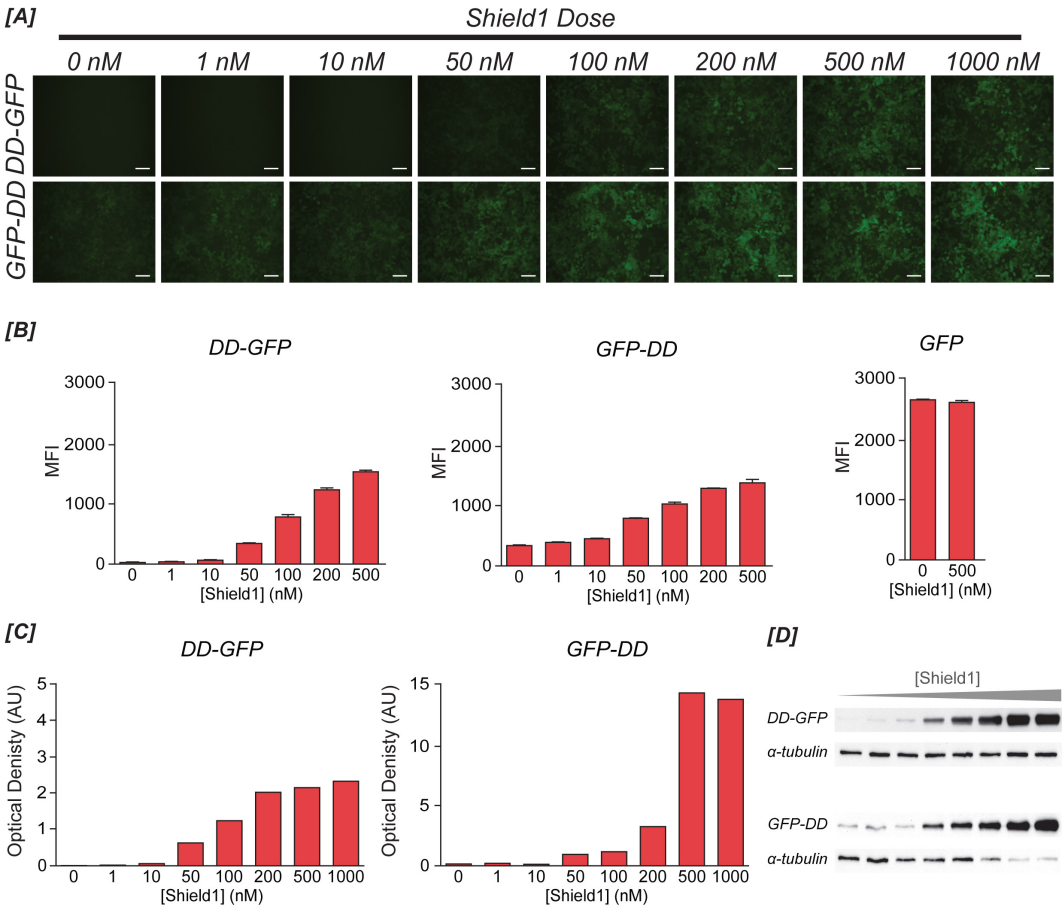

Figure 3-5 HEK293T cells transduced using unconcentrated HIV vector of DD-GFP, GFP-DD or GFP control, treated with Shield1.
[A] HEK293T cells transduced with unconcentrated HIV vector of DD-GFP, GFP-DD, or GPF, exposed to a range of Shield1 concentrations. Scale bar=200μm. ***[B]*** FACS analysis of imaged cells (n=3). MFI=mean fluorescent intensity. ***[C/D]*** Triplicate samples were pooled for Western blot analysis. ***[D]*** Blots were probed with anti-GFP primary antibody and subsequently α-tubulin as a loading control. ***[C]*** Densitometry was performed using ImageJ software. ***[D]*** Shield1 doses (left to right): 0, 1, 10, 50, 100, 200 and 500nM.

3.3.4 Concentration of HIV vector preparations does not affect regulation

In vivo experiments require the use of a concentrated preparation of lentiviral vector. To test if the destabilisation system would be affected by the concentration process (involving several spin steps, and possible concentration of contaminating factors from cell culture) a further replicate of the experiment described above was performed by transducing HEK293T cells with concentrated HIV virus preparations of pRRL-DD-GFP, pRRL-GFP-DD and pRRL-GFP. FACS data and Western blot analysis for the DD-GFP construct

indicated a 44-fold and 19-fold increase in the amount of GFP respectively, upon exposure to 500nM Shield1 (Figure 3-6). Both FACS and western blot analysis indicated a 5-fold induction for the GFP-DD construct.

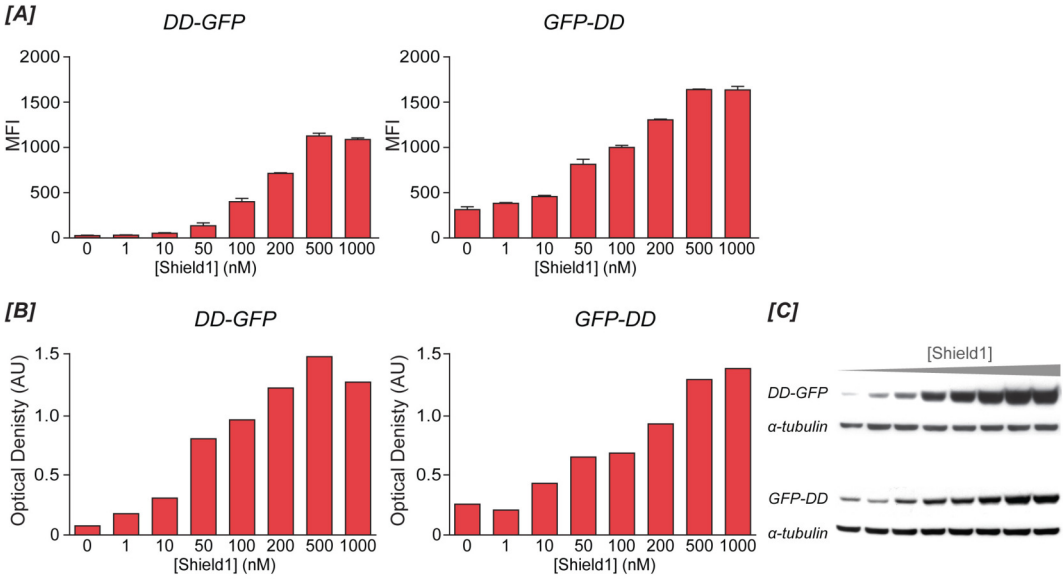

Figure 3-6 HEK293T cells transduced using a concentrated preparation of HIV vector of either DD-GFP or GFP-DD, treated with Shield1.
[A] HEK293T cells transduced with concentrated HIV vector of DD-GFP, GFP-DD, or GPF, exposed to a range of Shield1 concentrations. FACS analysis of cells (n=3). MFI=mean fluorescent intensity. ***[B/C]*** Triplicate samples were pooled for Western blot analysis. ***[C]*** Blots were probed with anti-GFP primary antibody, and α-tubulin as a loading control. ***[B]*** Densitometry was performed using ImageJ software. ***[C]*** Shield1 doses (left to right): 0, 1, 10, 50, 100, 200, 500 and 1000nM. Approximate molecular weight: DD-GFP, 39kDa; GFP-DD, 39kDa; α-tubulin, 50kDa.

3.3.5 E18 rat cortical neurons transduced with HIV vectors of DD-GFP and GFP-DD show dose dependent regulation

To determine the efficacy of the system in a neuronal cell type, E18 rat cortical neurons were transduced using concentrated HIV viral vector preparations of pRRL-DD-GFP, pRRL-GFP-DD and pRRL-GFP. A range of Shield1 concentrations was applied in triplicate to the transduced cells – 0, 1, 10, 100, 500nM – prior to imaging. Subsequently, the triplicate wells were pooled, a protein extraction performed, and analysed in Western blot. Again, there was no detectable GFP in cells overexpressing the DD-GFP construct at in the presence

of 0, 1, or 10nM Shield1, while ample GFP in cells treated with 100 and 500nM, suggesting tight regulation (Figure 3-7).

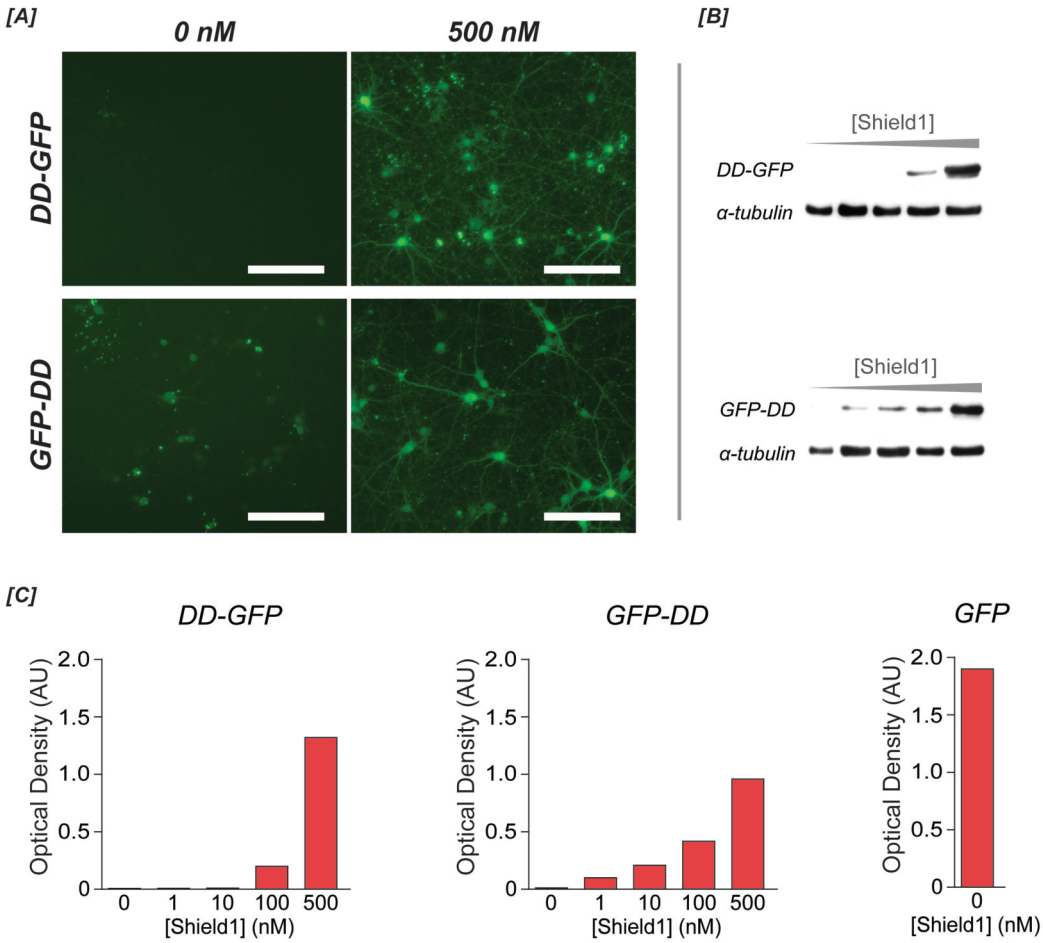

Figure 3-7 E18 rat cortical neurons transduced with HIV vector of either DD-GFP or GFP-DD, treated with Shield1.
[A] E18 cortical rat neurons cultured for a total of 18 days after transduction with (MOI10) HIV vector containing pRRL-CMV-DD-GFP, pRRL-CMV-GFP-DD and pRRL-CMV-GFP. Fed at day 15 with media containing a range of Shield1 dilutions (n=3). ***[B/C]*** After imaging (representative wells shown, n=3), triplicate samples were pooled for Western blot, probed with anti-GFP primary antibody. ***[B]*** Shield1 doses (left to right): 0, 1, 10, 100 and 500nM. Approximate molecular weight: DD-GFP, 39kDa; GFP-DD, 39kDa; α-tubulin, 50kDa. ***[C]*** Densitometry was performed using ImageJ software.

3.3.6 Cloning destabilised luciferase vectors for transduction of HEK293T cells: Dose response to Shield1 and Shield1 over a time course

A destabilised luciferase construct was made for two reasons. First, to test that the regulatory characteristics exhibited by the DD-GFP construct can be applied to other GOI. Second, to facilitate studies on the kinetics of the activation and

inactivation of the system. The much shorter half life of luciferase (approximately 3 hours (Kafri et al., 1998),) compared to that of GFP (26 hours (Corish and Taylor-Smith, 1999) may mean that a destabilised luciferase reporter will better reflect changes in levels of activation of the system (Wang et al., 2002). Thus, the firefly luciferase reporter gene was cloned to replace the GFP reporter. PCR primers (Table 3-1) were designed to amplify the Luciferase gene from the parental plasmid (pRRL-CMV-Luciferase-WPRE) such that the stop codon, or the transcription start sequence (ATG) was removed, to enable formation of the DD-Luciferase and Luciferase-DD fusion proteins, respectively. Unconcentrated preparations of HIV lentivirus containing pRRL-DD-Luciferase and pRRL-Luciferase-DD were produced and used to transduce HEK293T cells. Shield1 was applied at a range of concentrations 48 hours prior to cell lysis in preparation for luminometry. In both DD-Luciferase and Luciferase-DD transduced cells, there was a dose dependent increase in Luciferase activity with increasing Shield1 concentration (Figure 3-8 *[A/B]*), becoming significant with a minium dose of 100nM (Dunnetts posthoc test). A desirable characteristic of a regulatory system is rapidity. To test the time taken to reach maximal induction levels, Shield1 was applied to cells transduced with the DD-Luciferase construct over a time course before harvesting for luminometry (Figure 3-8 *[C]*). Luciferase activity was significantly increased within the forth hour of Shield addition (Dunnetts posthoc test), and reached maximal levels within 24 hours after Shield addition, with no significant increase observed after this time.

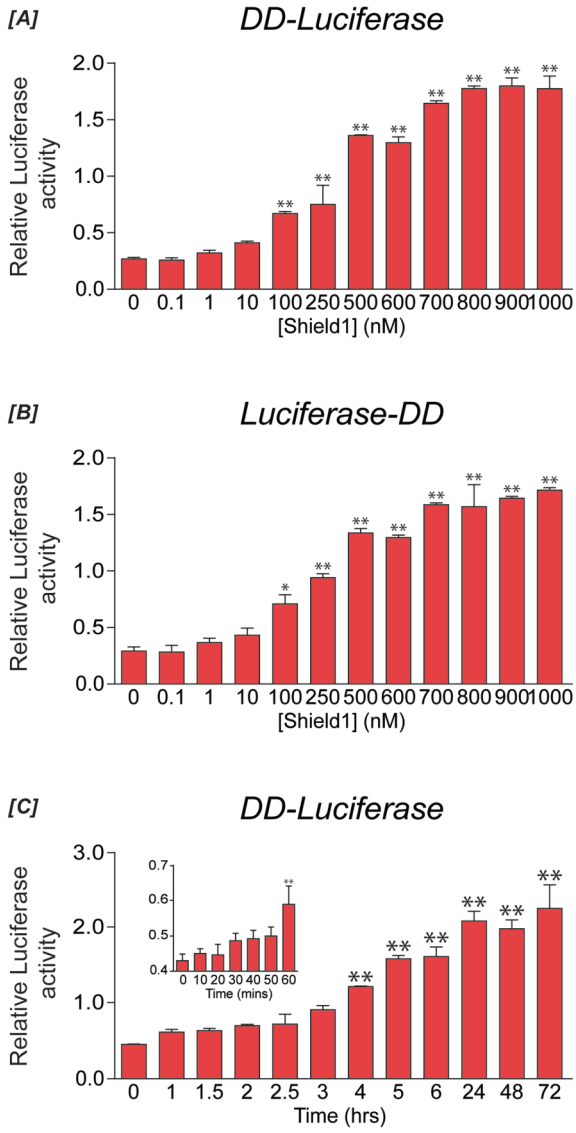

Figure 3-8 HEK293T cells expressing DD-Luciferase or Luciferase-DD - Dose response and time course ***[A/B]*** HEK293T cells transduced with concentrated HIV vector of DD-Luciferase or Luciferase-DD, exposed to a range of Shield1 concentrations 48h before harvesting (n=4). After cells lysis, a luciferase assay was performed. ***[A]*** Luciferase activity increases with Shield1 dose: One way ANOVA: *** $p<0.0001$, ($f=71.23$, $R^2=0.9703$); Stars indicate Dunnett posthoc test: 0vs100nM, ** $p<0.01$, ($q=3.712$). ***[B]*** Luciferase activity increases with Shield1 dose: One way ANOVA: *** $p<0.0001$, ($f=49.44$, $R^2=0.9577$); Stars indicate Dunnett posthoc test: 0vs100nM, * $p<0.05$, ($q=3.596$); 0vs250nM, ** $p<0.01$, ($q=5.603$) ***[C]*** HEK293T cells transduced with concentrated HIV vector of DD-Luciferase were treated with Shield1 over a time course before harvesting (n=4). After cell lysis, a luciferase assay was performed. Luciferase activity increases after Shield1 addition: One way ANOVA: *** $p<0.0001$, ($f=23.78$, $R^2=0.879$); Stars indicate Dunnett posthoc test: 0vs4hrs ** $p<0.01$, ($q=4.065$). *[Inset]* One way ANOVA * $p=0.0237$, ($f=3.129$, $R^2=0.4720$); Stars indicate Dunnett posthoc test: 0vs60mins, ** $p<0.01$, ($q=3.760$).

3.3.7 Evaluation of the DD system to the central nervous system of adult rats

From the experiments we have performed so far, the DD-GFP construct has consistently exhibited lower basal accumulation of GFP in cells that have not

been treated with Shield1, thus suggesting that this is the best candidate for use *in vivo*. To test the efficacy of the system *in vivo*, concentrated preparations of pRRL-DD-GFP and pRRL-GFP were injected stereotactically into the left and right striatum of rats respectively and incubated for 3 weeks before stereotactic administration of Shield1. Shield1 was injected into either the striatum at 500nM or the lateral ventricle at 500nM on the left side of the brain 24 hours before harvesting. The right hemisphere received a mock treatment of saline. After sectioning and immunohistochemical analysis, animals that received striatal and ventricular delivery of Shield1 had only very weakly GFP positive cells in the left striatum (DD-GFP) that co-stained for the neural marker (NeuN) (Figure 3-9). In fact, expression was not considerably greater than animals that had received a mock treatment, where there were also low levels of GFP expression in areas surrounding the infusion needle tract. In contrast, the right striatum had considerably more GFP expression due to the constitutively expressing GFP vector. Dose response experiments (Figure 3-4) indicate that when the system is fully activated, DD-GFP levels approach that of a constitutive GFP reporter, therefore suggesting that the system was not being activated to its maximum potential. To investigate further, animals receiving the same virus injection regimen received a one hundred times higher dose (50μM) of Shield1 into the ventricles. Again, only very weak expression was observed in areas surrounding DD-GFP infusion needle tract (Figure 3-9).

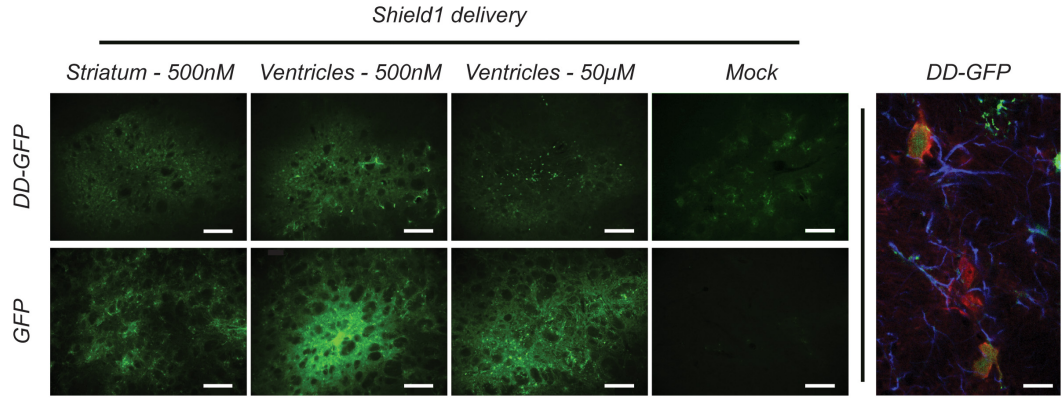

Figure 3-9 HIV DD-GFP vector transducing neurons in adult rat brain
Stereotactic injections of concentrated HIV constructs of pRRL-CMV-DD-GFP (LHS) and pRRL-CMV-GFP (RHS) to the striatum of rat brain were performed three weeks before injection of either 2μl of 500nM Shield1 solution to striatum (n=2), 2μl of 50μM Shield1 solution to striatum (n=3), or 2μl of 50μM Shield1 solution to the ventricles (n=2), on the LHS. A vehicle (Mock) treatment of 0.9% NaCl was also included (n=1). Brain were harvested 24 hours later and prepared for cryosection to 40μm slices. Scale bar=200μm. **GFP**. *[Right-hand confocal image]*. Close up of neurons transduced with DD-GFP vector. **GFP**/**NeuN**/**GFAP**. Scale bar=10μm.

3.3.8 Administration of Shield1 via permanent cannulation of the lateral ventricles

The pharmacokinetic properties of Shield1 in the brain are unknown. Following injection of Shield1 into the striatum/ventricles, the ligand can potentially be washed away from the transduced area and DD-GFP expression may return to minimal basal levels. For longer term stabilisation of GFP expression we sought to deliver Shield1 to the brain over a longer time course using cannulas that were implanted into the lateral ventricles. Animals received stereotactic injections of vector as before. At the time of vector injection, a guide cannula was permanently implanted into both right and left lateral ventricles. At three weeks post implantation, Shield1 was administered through an infusion cannula twice a day for three days, before being harvested 6 hours after the final infusion. Immunohistochemistry did not indicate a build up of GFP in the striatum of rats (data not shown).

3.3.9 HEK293T cells transduced with DD-GFP accumulate GFP in the absence of Shield1 at high MOI

It was thought that the weakly GFP positive cells in mock treated could be due to high basal expression caused as a result from some cells receiving a higher number of vector copies than others, producing much more fusion protein, thereby overloading the degradation machinery and leading to accumulation of the protein. Cells surround the needle tract would be more likely to come into contact with more viral particles, explaining why the weakly GFP expressing cells were found in this area. To test this idea *in vitro*, HEK293T cells were transduced at a range of MOIs with the same DD-GFP vector preparation used for the *in vivo* experiments. At high MOIs (above 5), GFP can be seen accumulating the in the cells in the absence of Shield1 (Figure 3-10).

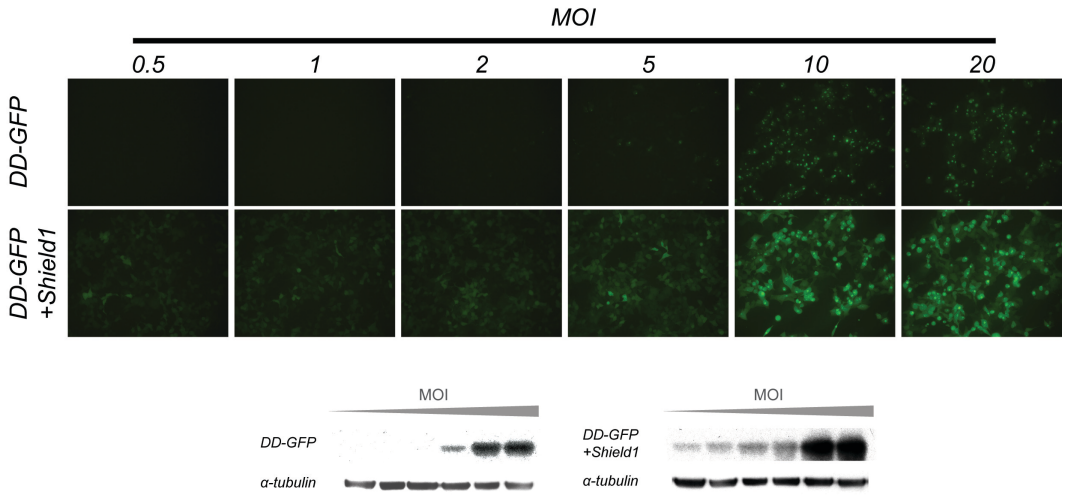

Figure 3-10 HEK293T cells transduced with HIV vector of DD-GFP at a range of MOI
HEK293T cells were transduced over a range of MOI using concentrated HIV vector of DD-GFP, and either mock treated, or treated with Shield1 48 hours before imaging and harvesting for Western blot. MOIs for western blot (left to right): 0.5, 1, 2, 5, 10, and 20. Approximate molecular weight: DD-GFP, 39kDa; α-tubulin, 50kDa.

3.4 Discussion

These results show that it is possible to design and construct lentiviral vectors that tightly and dose-dependently regulate the expression of a GOI *in vitro* using the DD technology.

The DD was originally isolated via a screen of random mutants cloned at the N-terminus of YFP (Banaszynski et al., 2006). C-terminal fusions also exhibited destabilizing characteristics and this arrangement may be useful for situations where an N-terminal fusion would be non viable, indicating the importance of testing both construct designs with each new GOI. In dose response experiments the DD system displayed dose dependent levels of induction between 0-100nM Shield1. Similar dose responsiveness has been reported by others (Dolan et al., 2011; Skafte-Pedersen et al., 2012). In our hands the DD-GFP construct exhibited preferential characteristics such as a higher maximal level of induction and lower basal accumulation.

This may be explained by the order in which the DD is translated in the context of the fusion protein. When placed at the N-terminus, the DD will be translated before the GFP. When the protein is being produced in the absence of Shield1, it will not fold correctly and may already be targeted for degradation at this early stage, meaning that as soon as the remaining GFP portion of the fusion protein is produced it will also already be targeted for degradation. Conversely, when the DD is fused to the C-terminus, the GFP will be translated first and may fold correctly until the DD domain is released. GFP would therefore be present in the cell for longer before being degraded in the absence of Shield1. However, it

must also be noted that the difference in basal expression between N- and C-terminal DD fusions was considerably lessened when Luciferase is the fusion partner, and, in following chapters it will be seen that C-terminal fusions of other DDs out perform N terminal. This implies the environment surrounding the DD is important in determining the regulatory profile of the system.

Reporter proteins have been widely used in molecular biology for their stability and reliability promoting their utilisation in initial testing of this system. Here we have not evaluated the system using more complex proteins, however, this system has been used to regulate many other classes of proteins such as kinases, cell cycle regulatory proteins, GTPases, transmembrane proteins and secreted proteins (Banaszynski et al., 2006; 2008), suggesting that it may be of use for studying other GOI. We were able to use both HIV and EIAV lentiviral vectors to transduce the DD/GOI cassette in 293T cells and HIV viral vector to transduce cultured E18 cortical neurons and striatal neurons *in vivo*. Other cell types (Banaszynski et al., 2006) had been successfully transduced using other vector systems (Rodriguez and Wolfgang, 2012), suggesting that the DD system could be highly versatile.

The luciferase reporter was cloned not only to test the ability of the DD system to regulate a different reporter in our hands, but also to facilitate studies in the kinetics of activation and deactivation. Luciferase has a much shorter half-life (approximately 3h) (Thompson et al., 1991; Kafri et al., 1998) than GFP (26h) (Corish and Taylor-Smith, 1999) in mammalian cells, suggesting that luciferase levels may better reflect the changes in levels of activation (Wang et

al., 2002). Other studies have taken a similar approach, using the DD with a PEST tagged luciferase (Imanishi et al., 2011). The PEST peptide sequence (rich in proline, glutamic acid, serine, and threonine), acting as a signal for protein degradation (Rogers et al., 1986; Rechsteiner, 1990), reduced the half-life to under one hour (Leclerc et al., 2000), meaning accumulation of residual luciferase was at a minimum.

We hoped these properties could give insight into the deactivation kinetics of the DD system. However, an attempted on-off kinetic study was not been reported here, due to very high variability in the data obscuring any trend in Luciferase levels. Experimental procedure is mostly likely the cause of this variation. It was considered that a simply exchanging Shield1 media for Shield1-free media would not sufficiently remove Shield1 as media would remain in the cell layer, and Shield1 would remain bound to protein in the cell. We therefore replaced the media several times, resulting in cells being dislodged. Subsequent unpublished data from the original authors indicate that doping the media with unliganded FKBP12 would result in more reliable experimental data. However, producing the protein in house as they suggest was outside the time scale of this project. We reported an off-on time course (Figure 3-8) suggested that the system is fully activated within 24h after the addition of Shield1. Similar induction kinetics have been reported in other studies (Banaszynski et al., 2006; Schoeber et al., 2009)

We have shown that HIV lentiviral vectors can successfully transduce cultured cortical neurons with the DD system, and dose-dependently regulate levels of a

GFP reporter. Other groups have not reported this and it suggests the system maybe of great use for controlling levels of GOI in cultured neuronal cells.

At the time of study, one *in vivo* study had been performed, and no information regarding the pharmacokinetics of Shield1 passing the blood brain barrier (BBB) was available. In an unpublished communication, the original investigators suggested that Shield1 would not enter the brain after intravenous injection. Cost considerations regarding Shield1 - the *in vivo* study by Banaszynski *et al* used relatively large amounts (5-10mg/kg mouse) of Shield1 - meant it was not feasible to investigate this. We decided to test this regulatable system in the CNS *in vivo* by directly injecting the ligand into the environs of cells overexpressing the regulatable GFP fusion protein. While we saw strong GFP expression in the striatum infused with a constitutively expressing GFP control (confirming that our experiment procedures were efficacious), we could not stimulate GFP from the DD-GFP infused striatum, either when infusing Shield1 to the striatum or ventricles at a higher dose. At the current time we cannot deduce a reason for the lack of activation, however, it is unknown how long the Shield1 ligand will remain biologically active in the striatum. The brain is constantly washed by cerebrospinal fluid (CSF). It is formed in the ventricles at a rate of 3.7µl/min (Harnish and Samuel, 1988) to a total volume of CSF in rat of 300-400µl (Bergman et al., 1998), therefore turning CSF over 13-18 times per day. Small molecules injected into the ventricles are quickly cleared (Nagaraja et al., 2005), which may prevent them from entering the tissue and maintaining high local concentrations. The *in vitro* work suggested that the system could be fully induced after 24 hours of exposure to Shield1, however, if the Shield1 is being

cleared and diluted, there may not be sufficient concentration in the striatum to see a significant effect. Furthermore, injecting the brain will result in glial scarring around the injection site. Glia cells are highly metabolically active, and may increase the removal of Shield1 in the vicinity of the transduced neurons.

We sought to achieve longer-term stabilisation by delivering Shield1 twice a day via cannula permanently implanted into the lateral ventricles. Unfortunately we did still not observe a significant increase in GFP expression. While cannulation of the brain and microinjection of Shield1 may have improved the experimental design by potentially prolonging the availability of Shield1 to transduced neurons, the technique for actually inserting the infusion cannula into the guide cannula was very difficult and resulted in frequent breakages to the infusion apparatus. While the apparatus was always checked before re-attempting it is possible that due to the difficulties of performing the technique, that reliability may have been lost. Furthermore, it is possible that the permanently implanted guide cannula became blocked, preventing the Sheild1 from reaching the correct location.

By transducing HEK293T cells at a range of MOI (Figure 3-10), we may have provided some explanation for the existence of individual GFP positive cells present in mock treated DD-GFP rats. In some of the brain sections, we observed that these cells occur in the area surrounding the needle tract. These cells would be transduced at the highest MOI and therefore have the most potential for overwhelming the proteasome, thereby accumulating GFP in the absence of Shield1.

If Shield1 is unable to easily activate the system in the rat brain, the FKBP-Shield1 system has limited scope for future use in neuronal systems. The sensitivity of the brain to damage means that invasive surgery must be kept to a minimum, yet there is no long-term therapy using this system possible without either continuous reinjection, or cannulation. In contrast to these difficulties, a new system obtained from the Wandless research group (Iwamoto et al., 2010) offers a system with a ligand that is already well characterized *in vivo*, is more cost efficient, can cross the BBB, and can therefore potentially cheaply and non-invasively regulate GOI in the brain. This system will be investigated in the next chapter.

Chapter 4 DHFR Destabilisation Domain

4.1 Introduction

The FKBP12 derived destabilisation domain system (Chapter 3) had been successfully used to conditionally regulate the levels of transgenes *in vivo* (Banaszynski et al., 2008), but the poor predicted pharmacokinetics and expense of the ligand made it unsuitable for long term delivery to the CNS. The Wandless group identified the need to develop a second destabilisation domain (DD) system capable of regulating levels of transgenes in the central nervous system (CNS). The full-length *Escherichia coli* (*E. coli*) dihydrofolate reductase (DHFR) protein was chosen to be engineered into a DD with these properties.

DHFR is a ubiquitously expressed 159-residue enzyme that catalyses the production of tetrahydrofolate (THF) from dihydrofolate. THF derivatives are required for purine and thymidylate synthesis and therefore necessary for cell growth and proliferation (Schnell et al., 2004). As rapidly dividing cells such as bacteria or tumour cells require more of these molecules, DHFR has been targeted in the development of bacteriostatic antibiotics and chemotherapy agents, creating many high affinity ligands already optimised as therapies for humans (Schweitzer et al., 1990).

Trimethoprim (TMP) is an example of a DHFR inhibitor developed for use as an antibiotic in humans. It has properties that make it highly suitable to activating the DD system in the CNS. As TMP binds to *E. coli* DHFR 3000-fold more tightly than to vertebrate DFHR (Matthews et al., 1985), adverse effects due the inhibition of endogenous DHFR are minimized. It is commercially available, inexpensive, and its pharmacokinetics have been studied in rats, (Meshi and

Sato, 1972; Tu et al., 1989), lending insight to potential *in vivo* studies. Importantly, it can cross the blood brain barrier (Barling and Selkont, 1978), and is rapidly absorbed from the gastrointestinal tract (Meshi and Sato, 1972).

The parental DHFR gene isolated from *E. coli* K12 (*fol*A) already encoded two mutations (R12H/G67S) from the wild type sequence. To develop DDs, a library of clones with further random mutations was generated using error prone PCR. This library was fused to a yellow fluorescent protein (YFP) reporter so that flow cytometry could be used to identify clones that responded to TMP, by assessing YFP fluorescence. Previous work by the Wandless Lab (Banaszynski et al., 2006) suggested DDs have different efficiencies when used at the N- or C-terminus of YFP. Therefore, two fusion libraries were created - one fusing the DHFR DD library to the N-terminus of YFP, and another fusing the DD library to the C-terminus of YFP. We were supplied one DD from the N-terminal-DD screen, bearing the engineered mutations R12Y/Y100I, and one DD from the C-terminal screen, with mutations N18T/A19V. The N-terminal DD therefore has three mutations (hereafter 3mut) in total - R12Y/G67S/Y100I - while the C-terminal DD has four (hereafter 4mut) - R12H/N18T/A19V/G67S. At the initiation of our studies, detailed description of the properties of the DHFR DD system had not been published by the Wandless laboratory. We therefore tested both domains at both the N- and C-terminus of our genes of interest (GOI).

In this chapter, we will evaluate the DHFR destabilisation domains at both the N- or C-terminus of GFP, to find the best construct for further investigation. We will assess the versatility of the system by cloning a luciferase reporter, also enabling study of the induction kinetics once TMP has been supplied. To confirm the suitability of the system for regulating levels of GOI in neurons, further characterization of induction kinetics will be performed in cultured primary neurons. Finally, the system will be tested *in vivo* with the aim of optimizing the delivery, dose and timing of TMP administration, potentially providing a robust strategy for regulating therapeutic genes in the CNS.

4.2 Methods

4.2.1 Optimised DD-GOI/GOI-DD cassette used in combination with PCR strategy

Two constructs were obtained from the Wandless laboratory – pBMN-3mutDD-YFP and pBMN-YFP-4mutDD. The pBMN plasmid is a Moloney Murine Leukaemia Virus based vector, therefore cloning into a pRRL series backbone will be necessary so the constructs can be used with our HIV based lentiviral vector system (Dull et al., 1998). Restriction enzyme (RE) site optimised constructs had already been designed for investigating the FKBP12 DD system (See Chapter 3). A PCR based strategy would facilitate the exchange of the FKBP12 for the new DHFR destabilisation domains in constructs pRRL-DD-GFP and pRRL-GFP-DD.

4.2.1.1 Sequences of 3mut and 4mut DHFR DD

```
                                      12              18 19
FolA ATGATCAGTCTGATTGCGGCGTTAGCGGTAGATCGCGTTATCGGCATGGAAAACGCCATGCCGTGGAACCTGCCTGCCGATCTCGCCTGGTTTAAACGCAACACCTTAAATAAACCCGTG
3mut ---ATCAGTCTGATTGCGGCGTTAGCGGTAGATTACGTTATCGGCATGGAAAACGCCATGCCGTGGAACCTGCCTGCCGATCTCGCCTGGTTTAAACGCAACACCTTAAATAAACCCGTG
4mut ---ATCAGTCTGATTGCGGCGTTAGCGGTAGATCACGTTATCGGCATGGAAACCGTCATGCCGTGGAACCTGCCTGCCGATCTCGCCTGGTTTAAACGCAACACCTTAAATAAACCCGTG
        ****************************  **************** ** ************************************************************
                                                                                                    67
FolA ATTATGGGCCGCCATACCTGGGAATCAATCGGTCGTCCGTTGCCAGGACGCAAAAATATTATCCTCAGCAGTCAACCGGGTACGGACGATCGCGTAACGTGGGTGAAGTCGGTGGATGAA
3mut ATTATGGGCCGCCATACCTGGGAATCAATCGGTCGTCCGTTGCCAGGACGCAAAAATATTATCCTCAGCAGTCAACCGAGTACGGACGATCGCGTAACGTGGGTGAAGTCGGTGGATGAA
4mut ATTATGGGCCGCCATACCTGGGAATCAATCGGTCGTCCGTTGCCAGGACGCAAAAATATTATCCTCAGCAGTCAACCGAGTACGGACGATCGCGTAACGTGGGTGAAGTCGGTGGATGAA
     ************************************************************************** ****************************************
                                      93                  100
FolA GCCATCGCGGCGTGTGGTGACGTACCAGAAATCATGGTGATTGGCGGCGGTCGCGTTTATGAACAGTTCTTGCCAAAAGCGCAAAAACTGTATCTGACGCATATCGACGCAGAAGTGGAA
3mut GCCATCGCGGCGTGTGGTGACGTACCAGAAATCATGGTGATTGGCGGCGGTCGCGTTATTGAACAGTTCTTGCCAAAAGCGCAAAAACTGTATCTGACGCATATCGACGCAGAAGTGGAA
4mut GCCATCGCGGCGTGTGGTGACGTACCAGAAATCATGGTTATTGGCGGCGGTCGCGTTTATGAACAGTTCTTGCCAAAAGCGCAAAAACTGTATCTGACGCATATCGACGCAGAAGTGGAA
     ************************************ *****************  ************************************************************

FolA GGCGACACCCATTTCCCGGATTACGAGCCGGATGACTGGGAATCGGTATTCAGCGAATTCCACGATGCTGATGCGCAGAACTCTCACAGCTATTGCTTTGAGATTCTGGAGCGGCGGTAA
3mut GGCGACACCCATTTCCCGGATTACGAGCCGGATGACTGGGAATCGGTATTCAGCGAATTCCACGATGCTGATGCGCAGAACTCTCACAGCTATTGCTTTGAGATTCTGGAGCGGCGA---
4mut GGCGACACCCATTTCCCGGATTACGAGCCGGATGACTGGGAATCGGTATTCAGCGAATTCCACGATGCTGATGCGCAGAACTCTCACAGCTATTGCTTTGAGATTCTGGAGCGGCGA---
     ********************************************************************************************************************
```

Figure 4-1 Sequence of 3mut and 4mut DHFR DD compared to mutant-free folA
Numbers above text indicate the amino acid number in the native *fol*A sequence. Blue nucleotides indicate mutations present in the parental *E. coli* K12 *fol*A clone. Red nucleotides indicate mutations introduced using error-prone PCR. Green nucleotides indicate silent mutations. Stars indicate nucleotide complementarity in the alignment. Start and stop codons have been omitted, as only one is present, depending on the termini fused to GOI.

4.2.1.2 PCR amplification of DHFR DD from pBMN-3mutDD-YFP and pBMN-YFP-4mutDD

PCR was performed (Methods 2.1.1) using the primers listed in Table 4-1. The same primer pair could be used to amplify both 3mut and 4mut DD sequences. N-terminal form PCR products (for forming pRRL-3/4mutDD-GFP) were 505bp, C-terminal form products (for forming pRRL-GFP-3/4mutDD) were 501bp. Each primer has 6bp at the 5', to ensure subsequent RE digestion is not compromised.

Primer Name	*Primer Sequence (5'-3')*
N-terminal-form forward	*TATATT*AgeI *ACCGGT**GCCACCATG**ATCAGTCTGATTGCGGCG*
N-terminal-form reverse	*TAGGTT*PspOMI *GGGCCC**GCCGCTCCAGAATCTC*
C-terminal-form forward	*TAGCGT*NheI *GCTAGC**ATCAGTCTGATTGCGGCG*
C-terminal-form reverse	*TATCGT*SalI *GTCGAC**TCA**TCGCCGCTCCAGAATCTC*

Table 4-1 Primers designed for the amplification of DHFR DD domains from 3mutDD-YFP and YFP-4mutDD.
Annotated sequences indicate RE sites, sequences shown in bold represent regions of template complementarity.

4.2.1.3 Cloning pRRL-3mutDD-GFP, pRRL-4mutDD-GFP, pRRL-GFP-3mutDD and pRRL-GFP-4mutDD

PCR products were separated, typically in a 1% agarose gel, the correct band was excised and DNA recovered (Method 2.1). Backbone plasmid pRRL-DD-GFP and N-terminal form DDs were digested with the REs *AgeI*/*PspOMI*; pRRL-GFP-DD and C-terminal form DDs with the *NheI*/*SalI* pair. After agarose gel electrophoresis, band excision and DNA recovery, products were quantified, and backbone-insert pairs ligated, transformed and sequenced.

4.2.1.4 Cloning pRRL-Luciferase-3mutDD

A luciferase reporter gene had already been cloned into the RE optimised cassette for investigating the FKBP12 derived DD system (Chapter 3). The REs *AgeI*/*NheI* were used to extract the Luciferase fragment from pRRL-Luciferase-DD. GFP was removed from pRRL-GFP-3mutDD using the same enzyme pair. After gel purification and extraction, DNA fragments were ligated to form pRRL-Luciferase-3mutDD.

4.2.2 Preparation and use of HIV lentiviral vectors

Lentiviral vectors were produced and titred (Method 2.2). In all *in vitro* experiments in this chapter, vectors were used MOI1. HEK293T cells and E18 rat cortical neurons seeded and transduced as described in (Methods 2.5.3 and 2.6.4 respectively). TMP was supplied at a range of doses – 0, 0.5, 5, 50μM – to both cell types.

4.2.3 Titres of lentiviral vectors used in vivo

Titres: CMV-GFP-3mutDD, $3.06x10^9$tfu/ml; CMV-GFP, $1.64x10^9$tfu/ml. Titres were not matched for *in vivo* experiments.

4.2.4 Preparation of trimethoprim stock solutions

For use *in vitro*, TMP (Sigma) was dissolved in neat DMSO (Sigma) to make a 200mM solution, and typically used at dilutions below 50μM. *In vivo*, when directly infusing TMP into the striatum, 2μl of stock solution was used (116μg TMP). TMP was used as a powder and disseminated in powdered normal rat

chow before mixing with water and flavouring agents to make a mash - final concentration 0.2% TMP.

4.2.5 Stereotactic injection of HIV-GFP-3mutDD into the CNS of adult rats

In all *in vivo* experiments in this chapter, adult male Wistar rats (250-300g) received 2µl of HIV-GFP-3mutDD vector via stereotactic injection (0.2µl/min infusion rate) to the striatum of the right hemisphere at the coordinates (AP/ML/DV relative to bregma) 0/3.5/4.75 (Method 2.7). TMP dosing regimen commenced three weeks later. At the end of the feeding regimen, the animals were euthanized,

4.3 Results

4.3.1 Cloning the DHFR destabilisation domain into GFP reporter cassette.

To test the efficacy of the different domains to destabilize a GFP reporter, both the 3mut and 4mut DD had to be cloned at both N and C-terminus of GFP. We utilised the restriction enzyme (RE) optimized cassettes that were already being used to study the FKBP12 DD (See chapter 3). PCR primers containing the appropriate RE sites (See 4.2.1.2) were used to amplify the new DHFR DDs, facilitating cloning into the DD-fusion cassette in an HIV-based lentiviral vector. This strategy enabled the formation of two N-terminally fused constructs - pRRL-3mutDD-GFP, pRRL-4mutDD-GFP – and two C-terminally fused GFP-DD constructs - pRRL-GFP-3mutDD and pRRL-GFP. These plasmids could then be used to produce HIV lentiviral vectors.

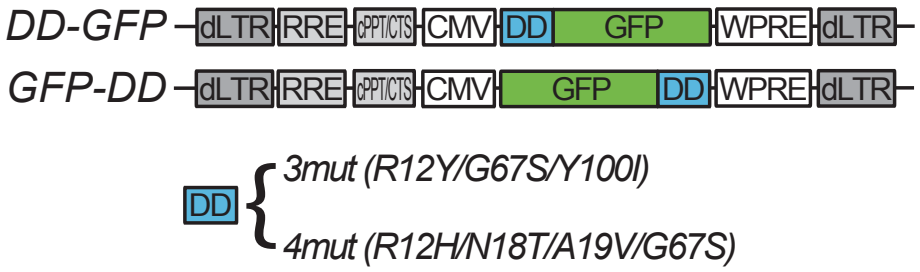

Figure 4-2 Schematic diagram of the viral insert of 3mutDD-GFP, 4mutDD-GFP, GFP-3mutDD and GFP-4mutDD constructs

4.3.2 HEK293 cells transduced with HIV lentiviral vectors expressing DHFR DD fusions to GFP accumulate GPF in the presence of TMP

HIV lentiviral vector preparations of the four constructs were made and used to transduce HEK293T cells. TMP doses ranging from 0 - 50μM were applied 48h prior to imaging, flow cytometry and Western blot analysis (Figure 4-3

[A/B/C/D]). All four constructs showed an accumulation of GFP when treated with TMP. The 4mutDD applied at either the N- or C-terminus achieved maximal levels of GFP at low doses of TMP, however, basal expression was high in the absence of TMP. The 3mutDD form (fused to either N or C-terminus of GFP) exhibited the most favourable characteristics, with low basal expression in the absence of TMP and dose dependent increase of GFP when treated with a range of TMP doses. Using flow cytometry techniques to assess mean fluorescence intensity, the 3mutDD-GFP construct showed a 16-fold induction upon exposure to 50μM TMP while the GFP-3mutDD construct showed a 42-fold induction, with maximal levels comparable to that of a constitutively expressed GFP control. This indicates that the 3mutDD used at the C-terminus is the most desirable construct, and this will therefore be used for further investigations. There was no change in fluorescence when the same range of TMP was applied to cells expressing a constitutive GFP reporter, indicating that TMP does not affect GFP fluorescence or CMV promoter activity.

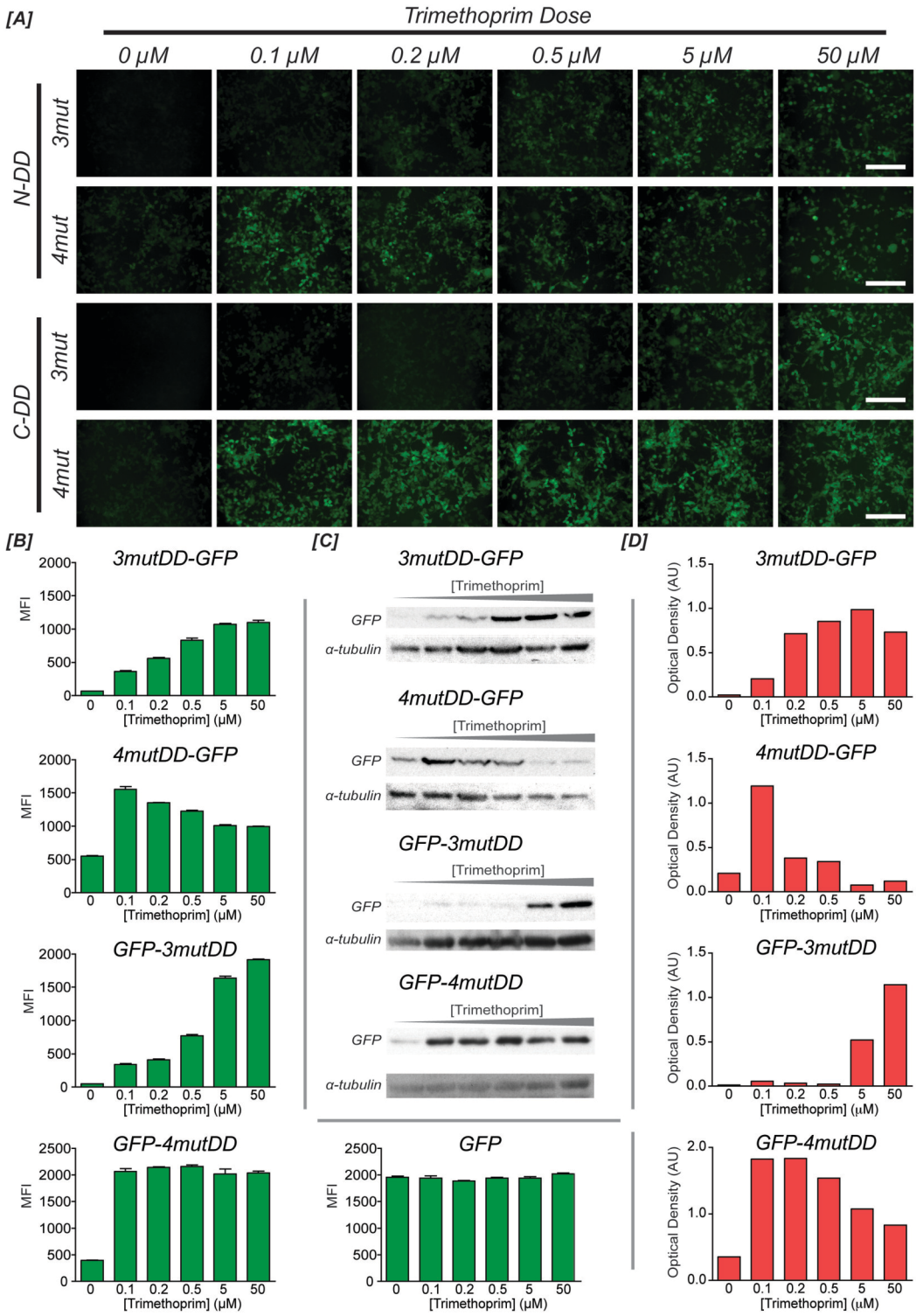

Figure 4-3 HEK293T cells transduced with DHFR DD constructs accumulate GFP in the presence of TMP.

[A] HEK293T cells transduced with unconcentrated HIV preparations of DHFR DD tagged GFP constructs, treated to a range of TMP doses 48h before imaging. Scale bar=400μm. ***[B]*** Analysis of GFP MFI (mean fluorescent intensity) by FACs analysis (n=3). ***[C]*** Western blot analysis of pooled samples, TMP doses (left to right): 0, 0.1, 0.2, 0.5, 5 and 50μM. Approximate molecular weight: 3/4mutDD-GFP, 45kDa; GFP-3/4mutDD, 45kDa; α-tubulin, 50kDa. ***[D]*** Densitometry of blots performed using ImageJ software.

4.3.3 HEK293T cells transduced with HIV-Luciferase-3mutDD accumulate luciferase in the presence of TMP, over time-course

To investigate the versatility and kinetics of the DD system, a firefly Luciferase reporter was employed. Luciferase has a much shorter half-life (≈3h) (Thompson et al., 1991) than GFP (≈26h) (Corish and Taylor-Smith, 1999), meaning that a DD tagged luciferase may better reflect the changes in levels of system activation in cells being treated with TMP (Wang et al., 2002). pRRL-Luciferase-3mutDD was developed as described (*See 4.2.1.4*). An unconcentrated HIV vector preparation was produced (*4.2.2*) and used to transduce HEK293T cells. TMP doses ranging from 0 - 50μM were applied 48h prior to cell lysis in preparation for luciferase assay (Figure 4-4 *[A]*). TMP caused a dose-dependent increase in luciferase activity, requiring a minimum dose of 0.25μM TMP to be significant (Dunnetts posthoc test). To assess the induction kinetics of the system, TMP (50μM) was supplied to HIV-Luciferase-3mutDD transduced HEK293T cells over a range of time points before harvesting (Figure 4-4 *[B]*). Luciferase activity increases significantly within the second hour after TMP addition Dunnetts posthoc test, reaching a maximal level within 24h.

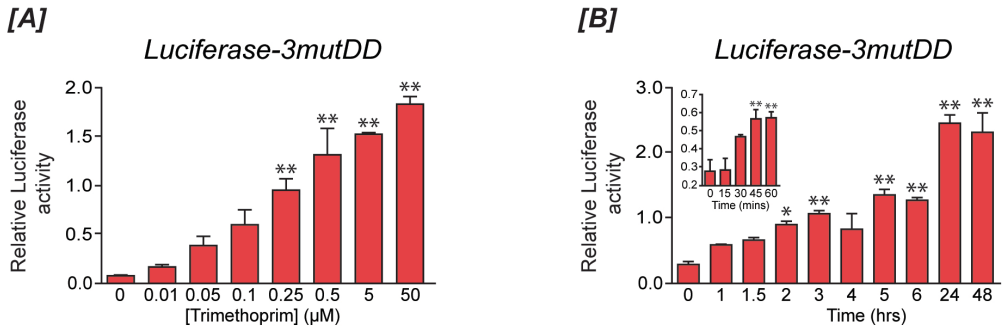

Figure 4-4 HIV-Luciferase-3mutDD transduced HEK293T cells accumulate luciferase activity over a range of TMP doses. Luciferase activity increases over time post TMP addition.
[A] HEK293T cells transduced with concentrated HIV vector of Luciferase-3mutDD, exposed to a range of TMP concentrations 48h before harvesting (n=3). A luciferase assay performed on cell lysates indicates significant increase in luciferase activity when analysed: One way ANOVA: *** p<0.0001, (f=26.35, R^2=0.9584); Stars indicate Dunnett posthoc test: 0vs0.25μM, ** p<0.01 (q=4.863) ***[B]*** HEK293T cells transduced with concentrated HIV vector of Luciferase-3mutDD were treated with TMP over a time course before harvesting (n=3). A luciferase assay performed on cell lysates indicates significant increase in luciferase activity, One way ANOVA: *** p<0.0001, (f=24.11, R^2=0.9156); Stars indicate Dunnett posthoc test: 0vs2hrs, * p<0.05 (q=2.997); 0vs3hrs ** p<0.01 (q=3.806). *[Inset]*: One way ANOVA: ** p=0.0028 (f=8.649, R^2=0.7758); Stars indicate Dunnett posthoc test: 0vs45mins, ** p<0.01 (q=4.121).

4.3.4 E18 rat cortical neurons transduced with HIV GFP-3mutDD treated with TMP accumulate GFP in the presence of TMP

When testing this system *in vivo*, successful transgene regulation in neural cells is essential if this system is to be used in the CNS *in vivo*. As we do not require the short half-life properties of luciferase, we will therefore use HIV-GFP-3mutDD vector. To test the efficacy of the system in neuronal cells, E18 rat cortical neurons were transduced *in vitro* with HIV-GFP-3mutDD, and treated with a range of TMP doses 96 hours before harvesting for immunocytochemistry. Photomicrographs indicate that neuronal cells accumulate GFP in a dose dependent manner, due to colocalisation of NeuN and GFP staining in higher TMP doses (Figure 4-5 *[A]*). To confirm that the system could be activated in neurons in a similar time scale to that seen in HEK293Ts cells, E18 rat cortical neurons transduced with HIV-GFP-3mutDD were treated with 50μM TMP at time points between 96h and 1h before harvesting (Figure 4-5 *[B]*). Immunofluorescent staining suggests that GFP accumulation reached a

maximum within 24h of exposure to TMP, and was maintained until at least 96h. Staining for NeuN (neurons) was not included in this experiment, as it has previously been established in our laboratory that E18 cortical cultures contain over 90% neurons (approximately 6% glia), and immunostaining in Figure 4-4 *[A]* already indicates that the system is functional in neurons.

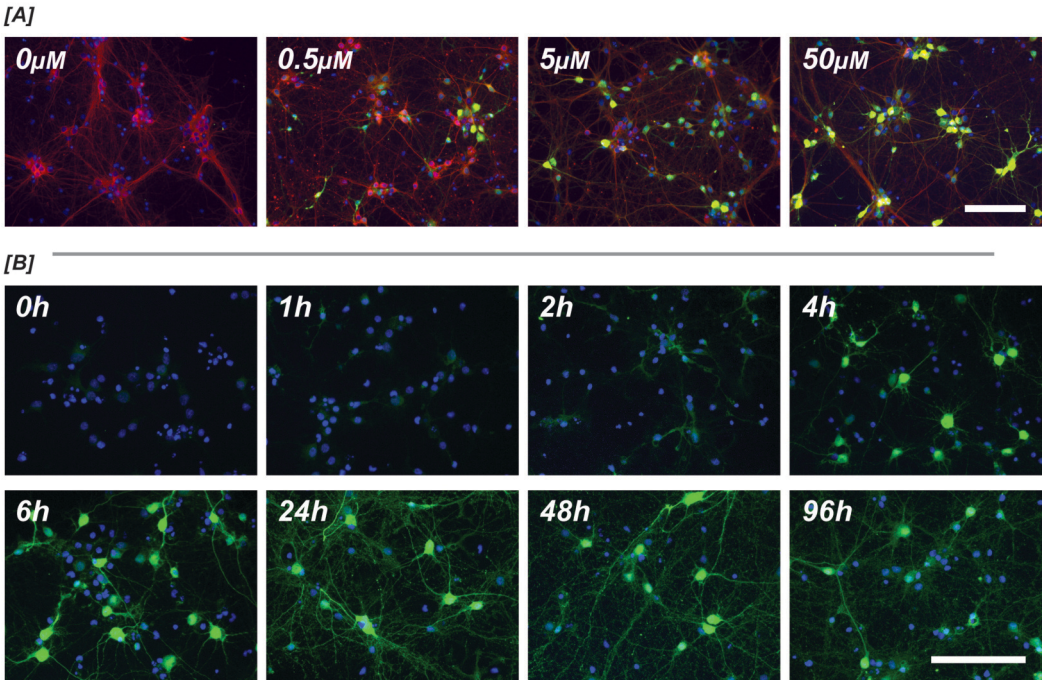

Figure 4-5 HIV-GFP-3mutDD transduced E18 rat cortical neurons accumulate GFP over a range of TMP doses. Accumulation occurs over time post TMP addition.
[A] E18 rat cortical neurons seeded at 10000 cells/well were transduced with HIV-GFP-3mutDD at day 5, then treated with 50μM TMP from day 8 (96h) to day 12 (0h) before harvesting for immunostaining. **βIII-Tubulin/GFP/DAPI**. Scale bar=100μm. ***[B]*** E18 rat cortical neurons seeded and transduced as before were treated with TMP over a time course ranging from 1 hour to 96 hours prior to harvesting for immunostaining. A control that did not have TMP added was included (0h). **GFP/DAPI**. Scale bar=100μm.

4.3.5 Testing the efficacy of HIV-GFP-3mutDD vector in adult rat CNS

Adult male Wistar rats received a stereotactic injection of pRRL-GFP-3mutDD in the striatum of the right hemisphere. Three weeks later, TMP solution (116μg TMP total) was infused into the striatum, 6h before the brain was harvested in preparation for cryosectioning and immunohistochemistry. Control rats did not

receive any injection of TMP, and consequently there was minimal GFP immunoreactivity in sections from these animals (Figure 4-6 *[A]*). However, rats that received TMP had a large area of cells positively stained for GFP in the striatum (Figure 4-6 *[B]*). Higher magnification images reveal that GFP and NeuN (neuronal marker) immunostaining is co-localised (Figure 4-6 *[D/E]*). This confirms that the HIV-GFP-3mutDD system can be regulated in neurons *in vivo*. However, in some of the sections, it was observed that the TMP infusion had led to damage in the striatum, possibly due to the high local concentration of DMSO or TMP, or both. Furthermore, this method of activation requires animals to undergo at least two rounds of invasive surgery, which should be kept to a minimum.

TMP is readily absorbed when orally ingested (Meshi and Sato, 1972). Administration of TMP via either the chow or drinking water of rats would be highly advantageous, as it would eliminate the need for invasive surgery, while providing a more constant supply that could be maintained over weeks if required. To investigate this possibility, adult male Wistar rats received a stereotactic injection of HIV-GFP-3mutDD vector in the striatum of the right hemisphere. After three weeks, normal chow was replaced with a mashed chow containing 0.2% TMP (On average 230mg/kg TMP eaten per day) for three days, before harvesting the brain for cryosection and immunostaining. Rats eating a control diet did not have an accumulation of GFP (as seen before - Figure 4-6 *[A]* is representative), while rats eating a TMP supplemented diet had a large area amount of positively GFP stained neurons in the striatum (Figure 4-6 *[C]*). Again, higher magnification images confirm that this method of

activating the system leads to increased levels of GFP in neurons (Figure 4-6 *[F/G]*), without the need for invasive surgery to deliver TMP.

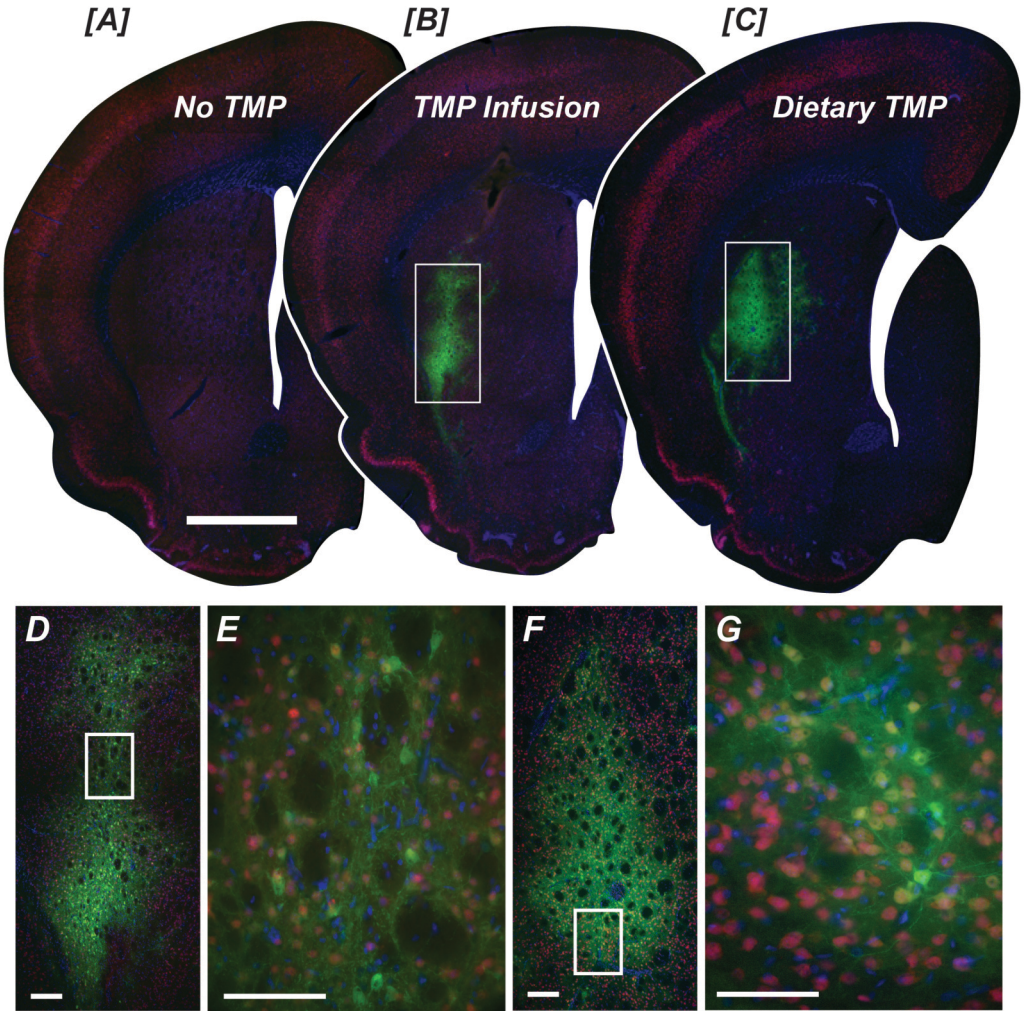

Figure 4-6 Two TMP delivery methods to adult rat CNS transduced with HIV-GFP-3mutDD vector leads to accumulation of GFP.
[A/B/C] HIV-GFP-3mutDD lentiviral vector was stereotactically injected in the striatum of adult male Wistar rats (n=3). ***[A]*** Control rats without TMP administration. ***[B]*** TMP was stereotactically delivered directly into the striatum 3 weeks post vector injection, brain harvested after 6h. ***[C]*** TMP was supplied at 0.2% of diet (≈250mg/kg/day) for 4d before harvesting. Scale bar=1mm. ***[D/E]*** Enlarged area outlines in ***[B/D]*** respectively. ***[F/G]*** Enlarged area outline in ***[C/F]*** respectively. **NeuN**/**GFP**/**DAPI**. Scale bar=50µm.

4.4 Discussion

When our study of the DHFR based DD system was commenced, data describing the system had yet to be published. The Wandless Lab supplied us with two constructs without clarification that they were the product of two independent library screens. Therefore, we cloned both domains at both N- and C-terminus of GFP to fully test which would be best at regulating GFP in our hands. As discussed in chapter 3, in our experience, the efficiency of the DD is altered by the GOI that it is fused to. Therefore, ideally, for each new GOI, all four possible constructs should be investigated. However, in the initial test of the four DD GFP fusions (Figure 4-3) the 4mutDD constructs did not exhibit desirable regulatory characteristics, so we did not use it for further experiments. GFP levels dose dependently increased when increasing TMP dose was supplied to cells transduced with HIV-GFP-3mutDD, and the maximum accumulation level was approximately double that shown by cells transduced with HIV-3mutDD-GFP. Basal expression in the absence of ligand was also lower when using GFP-3mutDD. Both properties are important when considering the potential of this system to regulate therapeutic genes *in vivo*. Higher levels of maximal induction will provide higher levels of therapeutic GOI when the system is activated. That this can be achieved over a large range of TMP doses may make it possible to tune the level of activation *in vivo*, where controlling the TMP dose precisely may be difficult. When the therapeutic window has passed, unwanted effects from the continued expression of the GOI will be abrogated as far as possible if basal expression (in the absence of ligand) is minimal. Bearing in mind that these properties would initially be assessed *in vivo* using a GFP

reporter, we decided to use the GOI-3mutDD form when investigating another GOI (Luciferase).

The HIV-Luciferease-3mutDD vector was produced to assess the ability of the system to regulate other GOI, as well as gain an understanding of the kinetics of the system activation/deactivation. Luciferase has a much shorter half than GFP, meaning that immediate changes in levels of activation in the DD system will be more accurately reported, particularly when looking at deactivation (or "turning off") kinetics. As we reported, luciferase activity increased dose dependently with increasing TMP concentration, and supplying TMP over a time course indicated that the system is fully activated within 24h, however, the deactivation kinetics were not assessed as intended. Removing the TMP ligand from the transduced cells proved to be technically challenging, as washing cells with new media in a 96 well plate format resulted in the removal of patches of cells, causing highly variable readings in luciferase activity (result not shown). It has subsequently been suggested in unpublished communication from the Wandless Lab, that doping cell culture media with unliganded DHFR would improve the experimental result, as this will sequester free TMP away from the cells. Reported deactivation times suggest that levels of GOI can be reduced to basal levels between 4h (Iwamoto et al., 2010) in cell lines (Muralidharan et al., 2011) to 17h in *P .falciparum* after withdrawal of TMP.

The *in vivo* efficacy of the DHFR DD system had not been published when our *in vivo* studies began. Therefore we had to optimise the procedure used to deliver TMP to the animals. The initial approach involved direct stereotactic

infusion of TMP into the CNS (Figure 4-6 *[B]*) and harvesting 6h later. This time point was chosen, first because it was apparent from the time course studies *in vitro* (Figure 4-4 *[B],* Figure 4-5 *[B]*) that the system could be activated within 6h, and second, that over time the TMP may be removed from the injection site by the clearing effects of cerebral spinal fluid (CSF), potentially deactivating the system again. We administered the maximal dosage (116µg TMP) permitted, which resulted in robust activation of the system. However, this procedure requires two rounds of invasive surgery into the CNS, and does not provide a method of long-term delivery of TMP. Also, damaged areas were observed in the striatum, possibly due to the double injection, or high DMSO or TMP concentration at that site. However, it did indicate that the system had efficacy to regulate GOI in the CNS.

In an intermediate study (not reported), two methods avoiding the need for direct delivery of delivered TMP into the CNS were tested: A twice-daily intraperitoneal (IP) injection of TMP for three days, and delivery via the drinking water for three days. Both aimed to deliver 50mg/kg/day TMP, chosen partly because dose had been used by others when studying TMP as an antibiotic in rats (Kluge et al., 1978). Both experimental procedures were suboptimal. First, twice-daily IP injection was distressing to the animals, and long-term delivery of TMP would lead to the abdominal skin becoming very sensitive due to multiple of injection sites. Secondly, rats did not accept the TMP doped drinking water. Supplementation with 5% sucrose and 5% Ribena was required before drinking would commence. This means that not only is the diet is supplemented with sugar, but the sugary water will encourage bacterial and

fungal growth, necessitating large wastage of TMP as it is replaced. However, over three days after drinking commenced rats consumed an average of approximately 55mg/kg/day, indicating that this may be a way of providing TMP non-invasively. However, both approaches failed to yield positive results - after immunohistochemistry on the brains, only very weakly GFP positive cells were observed in the striatum, indicating incomplete activation of the system. We hypothesised that the TMP dose supplied to the animals was too low, and as such increased the dose by supplying TMP in chow, where the taste would be better concealed. However, after this work was completed, the Wandless Lab published data showing TMP supplied in drinking water to rats at a dose of approximately 20mg/kg/day for three weeks, lead to activation of the system (Iwamoto et al., 2010). This is under half the dose our animals received, but it supplied for a much longer time, suggesting that the system may need prolonged exposure to activate at low doses. However, they did not report findings at intermediate time points, leaving the kinetics of activation of the system *in vivo* poorly elucidated. The lower dosing regimen is attractive in monetary terms, and would potentially require less flavouring agents to be palatable for animals. However, for our intended application of this system (in models of spinal cord injury and Parkinson's' disease - See Chapter 5/6) we may require that the system be activated quickly in a shorter timescale.

TMP supplied via chow leads to activation of the system within three days (Figure 4-6 *[C]*). On average rats ate a dose of 230mg/kg/day, when the TMP (0.2%) powder had been completely disseminated in flavoured powdered chow. This dose activated the system within 3 days, while still being well below a toxic

levels (Oral rat LD_{50}=5.7g/kg). This feeding procedure will be used when testing other therapeutic genes *in vivo* in the following chapters. In conclusion the work in this chapter indicates that the DHFR system has the potential to regulate levels of GOI in the brain.

Chapter 5 RARβ2

5.1 Introduction

The retinoic acid signalling pathway plays vital roles in development, patterning and regeneration in the mammalian central nervous system (CNS). Retinoic acid (RA) is a biologically active metabolite of vitamin A. It is obtained in the diet in the form of carotenoids (from plant material) or retinyl esters (in animal products), and stored in several sites in the body, including the kidneys, bone marrow and lungs. It is released into blood plasma as retinol and is transported by the plasma retinol-binding protein 4 (RBP4). Retinol can then be taken up into cells where it is then bound to the cellular retinol binding protein (CRBP), following which it can then be metabolized into all-trans RA by retinol and retinaldehyde dehydrogenases. Newly synthesized RA can be bound by cellular retinoic acid-binding proteins 1 and 2 (CRABP-1 and CRABP-2) (reviewed by Maden, 2007).

RA exerts physiological effects on cells by binding to nuclear receptors - retinoic acid receptor (RAR)/retinoic X receptors (RXR) heterodimers. There are three families of both RARs and RXRs - RARα/RARβ/RARγ and RXRα/RXRβ/RXRγ - all exhibiting several isoforms resulting from differential promoter usage and variable splicing (Leid et al., 1992; Chambon, 1994; reviewed by Chambon, 1996) alluding to the pleotropic effects of RA signalling. The structure of these receptors is modular and highly conserved across species, particularly in the ligand binding domain, suggesting that they play important roles in normal physiological and biological processes. Upon activation by the ligand, the RAR/RXR heterodimer complex is translocated to the nucleus and

with additional phosphorylation and recruitment of a range of cofactors (Taneja et al., 1997; Bastien and Rochette-Egly, 2004), it binds to DNA sequences called retinoic acid response elements (RAREs) in the promoter regions of genes. RA signalling in cells directly affects 27 genes, although more than 500 have been observed to be RA responsive, probably due to RARE independent mechanisms (Balmer and Blomhoff, 2002).

RA is classically involved in the development of the embryonic nervous system, namely in patterning and neuronal differentiation (reviewed by Maden, 2007). RA gradients, together with WNTs and fibroblast growth factors (FGFs), are necessary for the organizing the posterior hindbrain and the anterior spinal cord (Melton et al., 2004) while RA, in combination with sonic hedgehog (SHH), bone morphogenetic proteins (BMPs) and FGFs, is important for establishing dorsoventral patterning of the neural plate and neural tube (Novitch et al., 2003) (Wilson and Maden, 2005). RA also plays an extensive role in differentiation of various neuronal types and glia, through the activation of transcription factors, cell signalling molecules, structural proteins, enzymes and receptors. For example, RA is known to induce neuronal differentiation of embryonic carcinoma cell lines (Jones-Villeneuve et al., 1983) and has been used in embryonic neural progenitor cells to derive neurons/glia for transplantation in models of neurodegenerative disease (reviewed by Maden, 2007).

More recently roles for RA signalling have been described in the adult nervous system. The RA synthesizing enzymes, binding proteins and RAR/RXR are expressed in the adult nervous system. Particularly in the field of axonal

regeneration, there is growing evidence that RA signalling may contribute significantly to axonal growth processes, possible through the reactivation of developmental programs in the adult. For example, in peripheral nerves that regenerate (as opposed to central nerves that do not), RA signalling is induced upon nerve injury, as evidenced by increased activity in RARE-LacZ reporter mice, with peak activity being reported 7 days following injury (Zhelyaznik et al., 2003). By comparing the levels of all RAR isoforms in embryonic dorsal root ganglion (DRG) cultures extending neurites in response to RA (and isoform specific agonists), Corcoran et al. found that RARβ2 was the principal modulator of RA based neurite outgrowth (Corcoran et al., 2000). In confirmation, they observed a rise in RARβ2 expression when embryonic spinal cord explants were treated with RA and this was correlated with an increase in neurite outgrowth (Corcoran et al., 2002). However, treating adult spinal cord explants with RA did not result in the up-regulation in RARβ2 and neurite outgrowth was not induced. This suggested that the differences seen between the regenerative ability of the embryonic and peripheral nervous system (PNS) compared to the adult CNS were in part due to the lack of RARβ2 levels. Furthermore, neurotrophins such as nerve growth factor (NGF) that are important in the development of the nervous system have been shown to increase retinaldehyde dehydrogenase-2 (RALDH-2) and RARβ2 levels, resulting in increased neurite outgrowth from adult mouse DRG (Corcoran and Maden, 1999). Finally, So et al. (So et al., 2006) demonstrated that there was decreased peripheral nerve regeneration in adult RARβ null mice while Puttagunta et al. (Puttagunta et al., 2011) have demonstrated that postnatal

cerebellar granule neurons from RARβ null mice failed to extend neurites in response to RA.

The above evidence suggested that RARβ is the primary receptor through which RA acts to induce neurite outgrowth in embryonic and adult neurons. Corcoran et al. (Corcoran et al., 2002) showed that lentiviral vector-mediated overexpression of RARβ2, not RARβ4, induced neurite outgrowth in organotypic adult spinal cord preparations. This indicated that re-introducing endogenous signalling pathways back into adult tissue could provide a method of inducing local neurite outgrowth. Based on these and other observations, Wong et al. (Wong et al., 2006) investigated the utility of this lentiviral approach to exogenously express RARβ2 *in vivo* in order to increase axonal regeneration after nerve injury. Having confirmed that transducing DRG neurons with a lentiviral vector overexpressing RARβ2 induced neurite outgrowth on a nonpermissive substrate, adult rat DRGs were transduced *in vivo* in a dorsal root lesion model. The authors observed that lentiviral-mediated overexpression of RARβ2 promoted growth of injured DRG neurons into the non-permissive dorsal root entry zone (DREZ). Furthermore, improvements in motor deficits recorded after a dorsal root crush indicated regenerating sensory neurons could reconnect to appropriate targets (Wong et al., 2006). In another CNS lesion model, Yip et al. (2006) demonstrated that lentiviral overexpression of RARβ2 encouraged axonal outgrowth from adult cortical neurons *in vitro*, and transduction of the sensorimotor cortex prior to spinal cord lesion led to axonal and functional regeneration of the corticospinal tract (CST) in adult rats (Yip et

al., 2006). Finally, a RARβ specific agonist, CD2019, infused into the brain following a dorsal column lesion also increased regeneration of CST axons and functional forelimb recovery (Agudo et al., 2010). These studies, together with the *in vitro* data, confirm that the RA-RARβ2 signalling pathway is involved in promoting growth programs in injured neurons to facilitate functional regeneration.

The downstream targets of RA-RARβ2 signalling are not well studied. The study by Wong et al. (Wong et al., 2006) indicated that lentiviral overexpression of RARβ2 increased cAMP production and inhibition of cAMP production by an adenylate cyclase inhibitor, 2', 5'-dideoxyadenosine (DDA) attenuated RARβ2-induced neurite outgrowth from DRG neurons. However, Agudo et al. (Agudo et al., 2010) showed that the growth promoting effects of the RARβ agonist CD2019 was decreased by a PI3K (Phosphoinositide 3-kinase) inhibitor but not a PKA (Protein kinase A) inhibitor. More recently Puttagunta et al. (Puttagunta et al., 2011) demonstrated that the RA-RARβ-mediated neurite outgrowth acted via suppression of myelin-activated Nogo receptor (NgR) pathway, specifically through the transcriptional repression of the NgR complex member Lingo-1. The authors demonstrated that that RA treatment recruits binding of RARβ to a RARE element found in the Lingo-1 promoter, thereby inhibiting its expression in response to myelin. This is particularly relevant as the inhibitory myelin-associated molecules within the CNS are known to signal through the neuronal membrane-bound NgR complex to activate RhoA, which then triggers a chain of events that ultimately result in growth cone collapse (He and Koprivica, 2004).

So far, no other direct transcriptional targets of RARβ have been identified to be involved in mediating neurite outgrowth, although RARβ2 target genes have been described in RA-treated F9 wild-type teratocarcinoma cells (Zhuang et al., 2003).

The use of the lentiviral vector to deliver the transcription factor RARβ2 in *in vivo* models of central nerve injury suggested that this may be a relevant target to pursue further therapeutically. However, in order to improve the appeal of gene therapy for CNS injuries such as spinal cord injury, it would be desirable to engineer a system whereby exogenous gene expression from the vector can be regulated in a dose-dependent manner; making it more acceptable in the clinic. In this chapter, we will assess the ability of the DHFR destabilisation domain (DD) technology to regulate the levels of RARβ2 *in vitro* and *in vivo*. Initial testing of the DD at both the N or C terminus of RARβ2 will reveal the best construct for further investigation. To confirm the suitability of the system for regulating levels of RARβ2 in neurons, further characterization will be performed in cultured primary neurons harvested from the cortex and DRGs. Using an *in vitro* model of neurite outgrowth over inhibitory substrates, we will discover if the regulatable RARβ2 can induce greater outgrowth when activated. Finally, the system will be tested *in vivo* using a model of spinal cord injury.

5.2 Methods

5.2.1 Cloning DD-RARβ2 construct, a constitutively expressed RARβ2 construct, and a GFP control construct

To form a regulatable RARβ2 construct, the restriction site (RE) optimised constructs (pRRL-DD-GFP/pRRL-GFP-DD) that had already been designed for investigating the DHFR DD system (See Chapter 4) were used. A PCR based cloning strategy facilitated the replacement of the green fluorescent protein (GFP) gene with the RARβ2 gene. Two sets of primer pairs were used for this, one for cloning the RARβ2 so that it is N-terminally tagged by the DD, and one so that it is C-terminally tagged. The expression cassette from these constructs was then shuttled into a "dual promoter" construct - containing a GFP reporter driven by a spleen focus forming virus (SFFV) promoter upstream of the cytomegalovirus (CMV) driven DD/RARβ2 - to form pRRL-SFFV-GFP-CMV-DD-RARβ2, pRRL-SFFV-GFP-RARβ2-DD (hereafter DD-RARβ2 and RARβ2-DD respectively). This two-stage process was required, due to cloning sites in the DD cassette being non unique in the dual promoter vector.

To form a constitutively expressed RARβ2 construct, a PCR based strategy allowed RARβ2 to be inserted directly into the dual promoter vector, forming pRRL-SFFV-GFP-CMV-RARβ2 (hereafter RARβ2).

A control plasmid was made by removing the CMV promoter-driven gene from the dual promoter parental construct, leaving only the SFFV-driven GFP gene followed by the CMV promoter (pRRL-SSFV-GFP-CMV, hereafter GFP).

5.2.1.1 PCR amplification of mouse RARβ2 cDNA from pONYK-FLAGmRAR

PCR was performed (Method 2.1.1) using the primers listed in Table 5-1. PCR products for forming pRRL-DD-RARβ2 were 1388bp, those for forming pRRL-RARβ2-DD were 1386bp, while those for forming pRRL-RARβ2 were 1413bp long. Each primer has 6bp at the 5', to ensure subsequent RE digestion was not compromised.

Primer Name	*Primer Sequence (5'-3')*
DD-RARβ2 forward	*TAGCAT*PspOMI *GGGCCC TC**GACTACAAGGACGACGAT***
DD-RARβ2 reverse	*TATAAT*SalI *GTCGAC GGTACC**TCACTGCAGCAGTGGTG***
RARβ2-DD forward	*TAGCAT*AgeI *ACCGGT**GCCACCATGGACTACAAG***
RARβ2-DD reverse	*TATAAT*NheI *GCTAGC**CTGCAGCAGTGGTGACTG***
RARβ2 forward	*ACCGGT*XhoI *CTCGAG TCTAGA**GCCACCATGGACTACAAGG***
RARβ2 reverse	*GGTACC*SpeI *ACTAGT GTCGAC**TCACTGCAGCAGTGGTG***

Table 5-1 Primers designed for the amplification of RARβ2 for insertion into the destabilization domain cassette, and also into a constitutively expressing construct.
Annotated sequences indicate RE sites. Highlighted bold sequences indicate template complementarity.

5.2.1.2 Cloning pRRL-DD-RARβ2 and pRRL-RARβ2-DD

PCR products were separated, typically in a 1% agarose gel, the correct band was excised and DNA recovered (Method 2.1). Backbone plasmid pRRL-DD-GFP and RARβ2 (to be N-terminally tagged) were digested with the REs *PspOMI*/*SalI*; pRRL-GFP-DD and RARβ2 (to be C-terminally tagged) with the *AgeI*/*NheI* pair. After agarose gel electrophoresis, band excision and DNA recovery, products were quantified and backbone-insert pairs ligated, transformed and sequenced. To insert the expression cassette into the dual promoter construct, the parental dual reporter plasmid (pRRL-SFFV-GFP-CMV-

NCS1 – a gift from Dr Ping Yip, Kings College London) was digested with *XbaI* (NEB), before creating a blunt end using Klenow polymerase. After running the digested backbone through a PCR clean up column (Qiagen), the backbone was digested with *SalI* (NEB) and subsequently dephosphorylated using the rAPID dephosphorylation kit (Roche), before separating the products in an agarose gel. After band excision and DNA recovery, products were quantified, and backbone-insert pairs ligated, transformed and sequenced.

5.2.1.3 Cloning pRRL-RARβ2

Backbone plasmid pRRL-SSFV-GFP-CMV-NSC1 and RARβ2 PCR products were both digested using REs *XhoI* and *SpeI*. After agarose gel electrophoresis, band excision and DNA recovery, products were quantified, and backbone-insert pairs ligated, transformed and sequenced as described before (Method 2.1).

5.2.1.4 Cloning pRRL-SFFV-GFP-CMV

Backbone plasmid pRRL-SSFV-GFP-CMV-NSC1 was digested using REs *XhoI* and *SpeI*. Klenow DNA polymerase was used to create blunt ends, before separating the fragments in an agarose gel. After the correct band had been excised and purified, it was ligated (no dephosphorylation), transformed and sequenced as described before (Method 2.1).

5.2.2 Preparation and use of HIV-DD-RARβ2, HIV-RARβ2-DD, HIV-RARβ2 and HIV-GFP vectors

Lentiviral vectors were produced and titred (Method 2.2). HEK293T cells and E18 rat cortical neurons seeded and transduced as described in (Method 2.5.3 and 2.6.4 respectively).

5.2.3 Dorsal root ganglion (DRG) neuron culture

5.2.3.1 Preparation of Trimethoprim stock solutions

For use *in vitro*, TMP (Sigma) was dissolved in neat dimethyl sulphoxide (DMSO, Sigma) to make a 200mM solution, and typically used at concentrations below 50μM. For use *in vivo*, TMP was used as a powder and disseminated in powdered normal rat chow before mixing with water and flavouring agents to make a mash - final concentration 0.2% TMP.

5.2.3.2 Preparation of multi-well plates

Poly-L-lysine solution (0.01% solution (Sigma)) was added to each well of a 24-well plate (Nunc) containing flame-sterilised glass coverslips, followed by incubation at room temperature for at least 4 hours, or at 4°C over night. The solution was then removed and wells washed three times with sterile ddH_20, for 15 minutes per wash. After the final wash, the water was removed and the plates left open to dry in laminar flow hood for at least 1 hour, before adding 250μl of 10μg/ml laminin (Sigma) (for DRG neurite outgrowth assay, reduced laminin (0.1mg/ml) was used, see Method 5.2.3.5) and incubating at 37°C for at least 2 hours. The laminin solution was removed immediately before plating.

5.2.3.3 Dissection and plating of DRG neurons

All surgical instruments were cleaned and sterilised by autoclave. Adult male Wistar rats were obtained from Charles River, UK. The animal was swabbed with 100% ethanol and the head removed before exposing the spinal column. Hemisection of the vertebra allowed the DRGs to be removed into prewarmed Ham's F-12 basal media (Gibco), before the root sleeve membrane and dorsal

and ventral roots were carefully removed under a MZ6 dissection microscope (Leica, Switzerland) with a K1500 electronic light source (Schott, USA). Cleaned DRGs were incubated in 0.125% Collagense F-12 for 2 hours at 37^{o}C. Collagenase was removed by transferring the DRGs to 15ml of warm Hank's F-12, allowing them to sink before removing the media. DRGs were triturated by adding 1ml of Bottenstein and Sato's (BS) media (F-12 (Gibco), 1% N-2 Supplement (Gibco), 0.3% BSA (Sigma), 10,000U Penicillin/Streptomycin (Sigma)) and pipetting up and down using a Gilson P1000 pipette, allowing cell clumps to settle before collecting the cell suspension. Twice further triturating the non-individualised cells gave 3mls of cell suspension. Three 15% bovine serum albumin (BSA) cushions were prepared by mixing (without bubbles) 1ml 30% BSA solution (Sigma) with 1ml F-12. 1ml cell suspension was applied to the top of the cushions very carefully to avoid mixing. DRG neurons were spun through the cushion at 600 RCF for 8 minutes with the brake function turned off. After removal of the supernatant, the three pellets of DRG cells were resuspended in 100µl TID (CMF (1x Hanks Buffered Salt solution (HBSS Calcium- and magnesium-free, Gibco), 0.001% Phenol Red (Sigma), 0.0345% Sodium bicarbonate (Gibco), H_2O) 3mg/ml BSA (Sigma), 50µg/ml Deoxyribonuclease type I (Sigma), 250µg/ml Soybean trypsin inhibitor (Type II, Sigma), 0.038% Magnesium Sulphate (Gibco)). 8µl of cells was removed, 2µl of Trypan blue (Sigma) added and cells counted. The cell suspension could then be diluted in an appropriate volume of BS media in preparation for plating.

5.2.3.4 Culture of DRG neurons for protein lysates

DRG neurons were plated at a density of 3000 cells/well in 500µl BS media and incubated at 37°C 5% CO_2. On day 2, 200µl of the media was removed and lentiviral vectors (HIV-DD-RARβ2, HIV-RARβ2, and HIV-GFP – all at MOI10) were added. After 6 hours the wells were topped up using 250µl BS media. On day 3, 50µM TMP was supplied to some of the cells. On day 5, cell lysates were harvested in 50µl RIPA buffer (Method 2.4.1).

5.2.3.5 DRG neurite outgrowth assay

Plates were prepared as described above using reduced laminin (0.1µg/ml), before plating 1500 cells/well in 500µl BS media and incubating the cell at 37°C. On day 2, the DRGs were transduced as described above. On day 3, 50µM TMP was supplied to some of the cells. On day 5, the DRGs were gently washed with PBS, before fixing in 4% paraformaldehyde for 10 minutes. Fixed cells were stored in PBS at 4°C before immunocytochemistry. Primary antibodies were chicken-anti-GFP (1:1000), mouse-anti-βIII-tubulin (1:1000). Secondary antibodies were anti-chicken-ALEXA488 (Goat 1:500) and anti-mouse-Cy3 (Goat 1:500). DAPI was used to stain DNA (Table 2-5).

5.2.4 Stereotactic injection of HIV-DD-RARβ2 and HIV-RARβ2 to the CNS of adult rats

In all *in vivo* experiments in this chapter, adult male Wistar rats (250-300g) received infusions of lentiviral vector via stereotactic injection (0.2µl/min infusion rate) under anaesthesia detailed in Methods 2.7. Additional post-operative analgesia was not provided in accordance with PPL 30/2537.

However, it must be noted that there is substantial trauma to tissues when modeling spinal cord injuries *in vivo*, and that in the future we would seek to administer additional post-operative analgesia, continuing for several days after surgical intervention. This would be unlikely to confound behavioural findings if all animals received the same dose. It must also be noted that patients receiving surgery for spinal cord injuries are treated with analgesia, so this may help to improve the efficacy of potential therapies in the rat models of cord injury. At the end of experiments, the animals were terminated using 150mg/Kg pentobarbital (*Euthatal*) and transcardially perfused with PFA (Method 2.7.3) and the relevant tissue harvested.

5.2.4.1 Titres of lentiviral vectors used in vivo

Lentiviral preparations above $1x10^8$tfu/ml were considered sufficient to provide robust transduction *in vivo*. SFFV-GFP-CMV-RARβ2, $3.68x10^8$tfu/ml; SFFV-GFP-CMV-DD-RARβ2, $1.58x10^9$tfu/ml; SFFV-GFP-CMV, $6.18x10^9$tfu/ml. Titres were not matched for *in vivo* experiments.

5.2.4.2 Expression study

Six rats received infusions 2µl of HIV-DD-RARβ2 vector into the cortex of the right hemisphere at 4 co-ordinates (AP/ML/DV relative to bregma) -1.5/2.5/2, 0.5/3.5/2, -1/1.5/2 and 1.5/2.5/2. Three weeks later, 3 rats had normal chow replaced with a mashed diet containing 0.2% TMP, 3 rats received mashed chow that did not contain TMP. Once feeding began, this diet was continued for 3 days, recording the amounts consumed daily. The animals euthanized on day 4,

and following perfusion fixation with PFA the brains were harvested, and prepared for section via cryostat.

5.2.5 Cervical crush model spinal cord injury

5.2.5.1 Viral vector delivery to the sensorimotor cortex

To ensure that a maximal number of neurons in the corticospinal tract were transduced, 8 rats received 6 infusions of 2µl of HIV-DD-RARβ2 vector per hemisphere into the cortex at coordinates as determined from a microstimulation mapping study (Neafsey et al., 1986) (relative to bregma; AP/ML/DV): Left hemisphere: -1.5/2.5/2, -0.5/3.5/2, 0.5/3.5/2, -1/1.5/2, 1.5/2.5/2 and 2/3.5/2. Right hemisphere: -1.5/-2.5/2, -0.5/-3.5/2, 0.5/-3.5/2, -1/-1.5/2, 1.5/-2.5/2 and 2/-3.5/2. Rate of infusion: 0.2µl/minute. Wait one minute before slowly removing needle. 4 rats began to receive mashed chow containing 0.2% TMP, while 4 rats received mashed chow that did not contain TMP immediately after completion of surgery.

5.2.5.2 Dorsal crush of spinal cord

After three weeks, the animals were re-anaesthetised, the spinal column exposed at the level of C4 vertebra, and a bilateral dorsal column crush performed using fine forceps (2mm depth). Dr Liang Fong Wong performed this surgical technique. Rats were randomly selected to be prepared for surgery by Ben Houghton, to blind the surgical procedure.

5.2.5.3 Behavioural testing

Animals were trained on apparatus three times a week after recovery from viral vector infusions and data was collected once a week for 8 weeks after column

crush. Ladder apparatus consisted of 11 small rungs 10cm apart. Animals back legs were supported if necessary where motor deficits were severe.

5.2.5.4 BDA tracer injection

After 8 weeks post spinal cord lesion, rats were once again anaesthetised to inject biotinylated dextran amine (MW10000, Molecular Probes) (BDA). 2µl BDA was injected into six sites per hemisphere, using the coordinates listed in method 5.2.4.2.

5.2.5.5 Harvesting tissue

After animals were euthanized using 150mg/Kg pentobarbital (*Euthatal*) and perfusion-fixed with PFA (Method 2.7.3), the brains were harvested. The spinal cord was carefully exposed and the cord very carefully removed.

The brains were prepared for sectioning using a cryostat (Method 2.8.1). To section, the brain was cut in half down the midline. The right hemisphere was cut coronally, while the left hemisphere was cut sagittally.

A small section of lumbar cord was removed and prepared for coronal sectioning in the cryostat. A 2cm fragment encompassing lesion site in the cervical region was prepared for sectioning longitudinally using a vibratome by embedding into 10% gelatin (Method 2.8.2).

In all cases, 40µm sections were harvested and kept in PBS at 4^{o}C until immunohistological staining.

5.2.5.6 Immunohistochemistry

Refer to Table 2-5 for full details of antibodies. Brain sections were stained in two groups. Group 1 sections (1 section in every 5 slices of tissue) were prepared for antibody binding as (Method 2.9). Primary antibodies: anti-GFP (chicken 1:1000)/anti-RARβ2 (mouse, 1:50), Secondary antibodies: anti-chicken-ALEXA488/anti-mouse-ALEXA-568 (both mouse, 1:500) and DNA was visualized using DAPI. Sections in group 2 (containing another set of 1 in every 5 slices of tissue) were stained using primary antibody anti-GFP (chicken 1:1000), and secondary antibodies anti-chicken-ALEXA488. Neutr-avidin-TexasRed (without tyramide amplification step) was applied with the secondary antibodies, and DAPI used to visualize DNA.

Longitudinal sections of spinal cord encompassing the lesion site were washed 3x5 minutes in PBST (0.01M PBS, 0.1% TritonX-100). Sections were incubated in 0.3% H_2O_2 to inactivate endogenous peroxidases, before washing 3x5mins with PBST. Sections were then incubated in avidin-biotin peroxidase complex (Vectastain ABC Elite Kite, Vector Laboratories) for 30 minutes, washed 3x5 minutes with PBST, incubated in biotinyl tyramide (1:100, Molecular Probes) for 10 minutes and washed again 3x5 minutes PBST, before incubating with Neutr-avidin-TexasRed (1:400, Sigma) for 2 hours. Sections were mounted after a final wash step.

Protein Kinase γ (PKCγ) staining was performed to determine whether the column crush had completely lesioned the dorsolateral CST. The presence of

PKCγ staining in the dorsal funiculus would indicate incomplete lesion of the dorsolateral CST (Bradbury et al., 2002; Mori et al., 2004).

5.3 Results

5.3.1 Cloning DD-RARβ2, RARβ2 and GFP reporter constructs

We began our investigation into regulating RARβ2 expression using the DD technology by cloning the mouse RARβ2 gene into the RE optimized cassettes previously described (Chapter 4). We chose the '3mut' form of the DHFR based DD and applied to the N- and C-terminus of RARβ2. To facilitate experimental methodologies used in this chapter, the expression cassette of both regulatable and constitutive RARβ2 constructs was shuttled into a dual promoter vector (Yip et al., 2010) that constitutively expressed GFP under a SFFV promoter (Method 5.2.1). The resulting plasmids DD-RARβ2, RARβ2-DD, RARβ2 and GFP could then be used to produce HIV based lentiviral vectors.

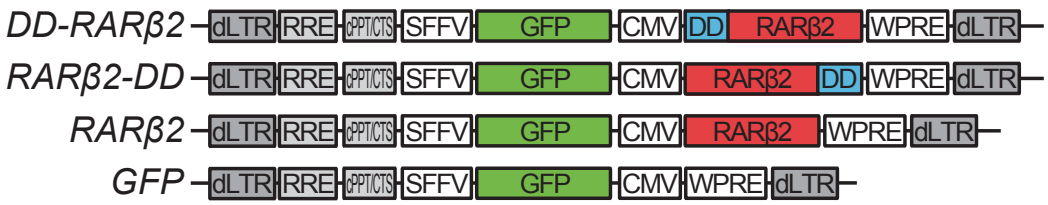

Figure 5-1 Schematic diagram of the viral insert of DD-RARβ2, RARβ2-DD, RARβ2 and GFP constructs

5.3.2 HEK203T cells transduced with HIV-DD-RARβ2 accumulate RARβ2 in the presence of TMP

HIV lentiviral preparations of DD-RARβ2, RARβ2-DD, HIV-RARβ2 and HIV-GFP were made and used to transduce HEK293T cells at an MOI1. TMP doses ranging from 0 - 50μM were applied 48 hours prior to harvesting the cells for either immunocytochemistry, or Western blot analysis (Figure 5-2 *[A/B]*). Cells transduced with HIV-DD-RARβ2 accumulated DD-RARβ2 in response to

increasing TMP dose, with maximal levels similar to RARβ2 levels seen in cells expressing RARβ2 constitutively. Basal levels of DD-RARβ2 in cells that had not been treated with TMP were as low as the levels of endogenously expressed RARβ2 in cells expressing GFP as a control. It can also been seen that increasing TMP had no effect on endogenous RARβ2 expression in HEK293T cells. RARβ2-DD could not be detected in lysates derived from cells transduced with HIV-RARβ2-DD.

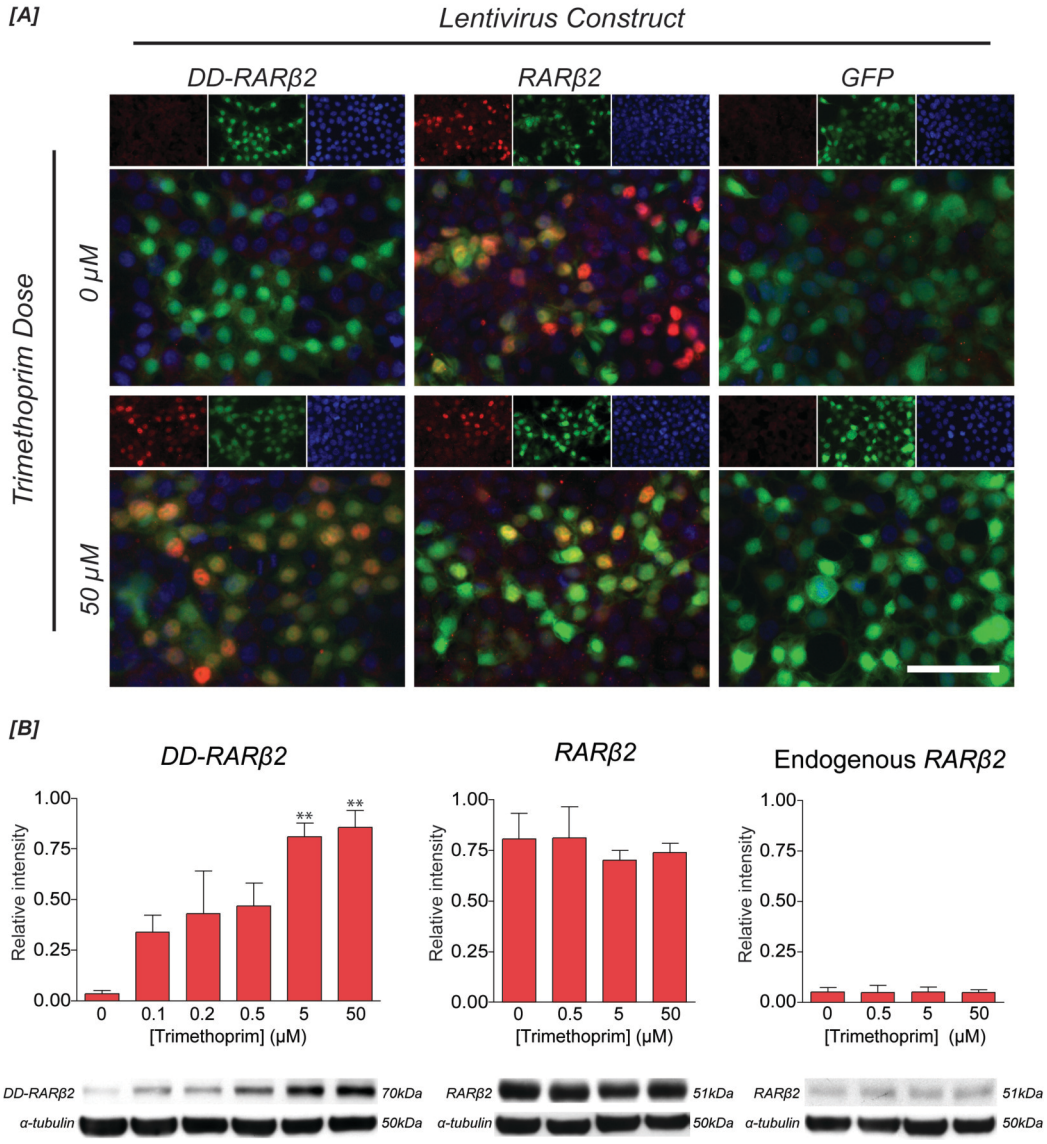

Figure 5-2 HEK293T cells transduced with HIV-DD-RARβ2 accumulate RARβ2 in the presence of TMP

[A] HEK293T cells transduced with HIV-DD-RARβ2, HIV-RARβ2 and HIV-GFP, treated to a range of TMP doses 48h before fixing and immunocytochemistry. **RARβ2/GFP/DAPI**. Scale bar=50μm. ***[B]*** Western blot analysis of pooled samples (n=3) with representative blots illustrated below. Densitometry of blots performed using ImageJ software. Significant increase in DD-RARβ2 levels with TMP dose. DD-RARβ2: One way ANOVA: ** p=0.0025 (f=7.180, R^2=0.7496); Stars indicate Dunnett posthoc test: 0vs0.5μM, ** p<0.01 (q=4.769). TMP dose does not affect constitutive RARβ2 over-expression. One way ANOVA: ns (p=0.8524). TMP does not affect endogenous RARβ2 expression. One way ANOVA: ns (p=0.9985).

5.3.3 E18 rat cortical neurons and adult DRG neurons transduced with HIV-DD-RARβ2 accumulate RARβ2 in the presence of TMP

Anticipated experimental methodologies would require the DD-RARβ2 construct to be efficacious in both cortical neurons *in vivo* and DRG neurons *in*

vitro. To begin testing the efficacy of DD-RARβ2 regulation in a neural cell type, E18 rat cortical neuron cultures were transduced *in vitro* with HIV-DD-RARβ2 at an MOI1. These cultures have been established in our laboratory to contain a high percentage of neurons – between 80-90%. TMP doses were applied 96 hours before harvesting for Western blot analysis (Figure 5-3). Again, maximal levels of DD-RARβ2 activation are similar to that of constitutively expressed RARβ2. Higher basal levels of activation in the absence of TMP suggest that regulation may not be as tight in embryonic cortical neural cells as in HEK293T cells. There is a 4-fold increase when TMP is supplied to E18 cortical cells expressing DD-RARβ2.

To see if these regulatory characteristics would also be seen in DRG neurons, HIV-DD-RARβ2 (and the control vectors) were used to transduce DRG neurons growing *in vitro* (Figure 5-4) at an MOI10. Again, there are higher levels of basal expression. Levels of DD-RARβ2 do not reach those of the constitutive RARβ2 control when TMP is supplied at 50μM. There is a 1.8-fold increase when TMP is supplied to E19 cortical neurons expressing DD-RARβ2.

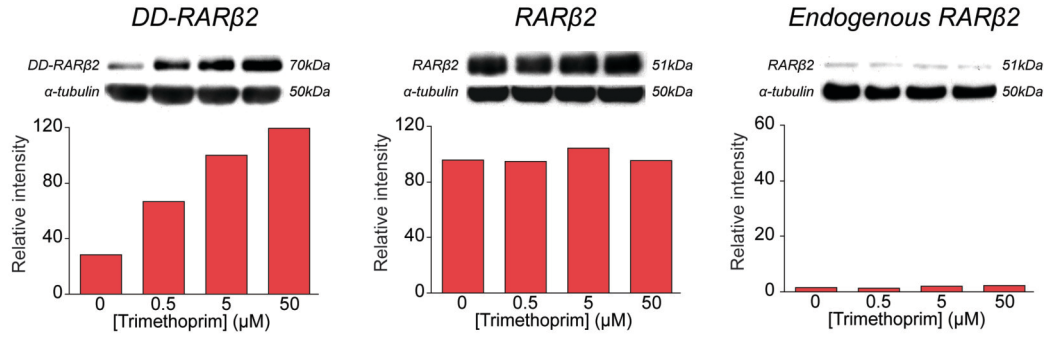

Figure 5-3 Rat E18 cortical neurons transduced with HIV-DD-RARβ2 accumulate RARβ2 in the presence of TMP

HEK293T cells transduced with HIV-DD-RARβ2, HIV-RARβ2 and HIV-GFP, treated to a range of TMP doses 96h before harvesting for Western blot analysis. Blots illustrated above graphs including predicted

molecular weight. Densitometry of blots performed using ImageJ software; all data normalised to endogenous RARβ2 untreated with TMP (n=1, samples pooled from at least 3 separate transductions).

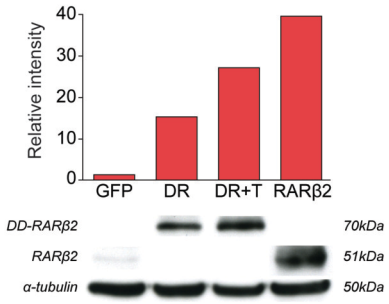

Figure 5-4 Adult rat DRG neurons transduced with HIV-DD-RARβ2 accumulate RARβ2 in the presence of TMP
DRG neurons were transduced with HIV-DD-RARβ2 (DR), HIV-RARβ2 and HIV-GFP on day 2 *in vitro*. On day 3, 50μM TMP was supplied to half of the neurons expressing DD-RARβ2 (DR+T), 48h before harvesting for Western blot analysis. Blots illustrated below graphs including predicted molecular weight. Densitometry of blots performed using ImageJ software; all data normalised to endogenous RARβ2 untreated with TMP (n=1, samples pooled from 3 separate transductions).

5.3.4 DRG neurite outgrowth assay

RARβ2 has already been show to encourage neurite outgrowth from DRG neurons grown on inhibitory surfaces (Wong et al., 2006). To test if DRGs expressing the regulatable RARβ2 construct could have a similar physiological effect in the presence of TMP, adult rat DRGs sparsely plated (1500-2000 cells/well in a 24-well plate) on a reduced laminin substrate (0.1μg/ml) were transduced with HIV-RARβ2, HIV-DD-RARβ2, HIV-DD-RARβ2 and HIV-GFP vectors at an MOI10. The mean length of the longest neurite, total neurite length and number of neurites of individual neurons were analysed from pictomicrographs (Figure 5-5). The data indicates that there is a trend of increased neurite outgrowth in DRGs accumulating more RARβ2. However, while there is significant increase in the total length of neurites and in neurite

number, the physiological differences between the different groups is small, particularly between DD-RARβ2 in the absence or presence of TMP.

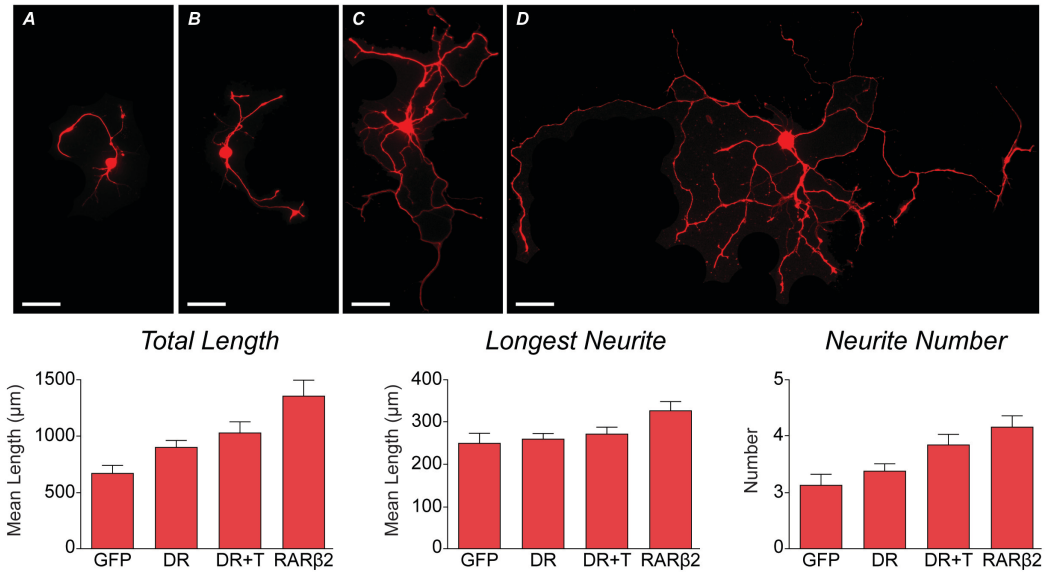

Figure 5-5 Analysis of neurites sprouting from adult rat DRG neurons growing on a non-permissive substrate.
Fixed DRG cultures were stained using mouse anti-βIII-tubulin and chicken anti-GFP primary antibodies. Secondary antibodies anti-mouse-Cy3 and anti-chicken-ALEXA488 allowed selection of transduced neurons for analysis. ***[A/B/C/D]*** Representative pictomicrographs of neurites, scale bar=100µm. Pictomicrographs of between 50-100 individual DRG neurons transduced with ***[A]*** HIV-GFP (GFP) ***[B]*** HIV-DD-RARβ2 (DR), ***[C]*** HIV-DD-RARβ2+TMP (DR+T), ***[D]*** HIV-RARβ2 (RARβ2) were analysed using the NeuronJ plugin for ImageJ Software. All following statistical analysis: One-way Anova. ***[Total length]*** *** *(p=0.0004)* ***[Longest Neurite]*** *ns* ***[Neurite Number]*** ** *(p=0.0035).*

5.3.5 Testing the efficacy of HIV-DD-RARβ2 and HIV-RARβ2 vector in adult rat CNS

Adult male Wistar rats received stereotactic injections of HIV-DD-RARβ2 in the cortex of the right hemisphere. As described in method 5.2.4.2 of this chapter, four stereotactic coordinates were used, rather than six that would be used in models of spinal cord injury. Some rats received stereotactic injections of HIV-RARβ2 or HIV-GFP to the cortex of the left hemisphere as controls. Three weeks later, normal chow was replaced with a mashed chow containing 0.2% TMP (On average 185mg/kg TMP eaten per day) for four days before harvesting

the brain for cryosection and immunostaining (Figure 5-6). In the cortex of rats fed a TMP containing diet, immunohistochemistry revealed greater amounts of RARβ2 compared to animals that have not received TMP in the diet.

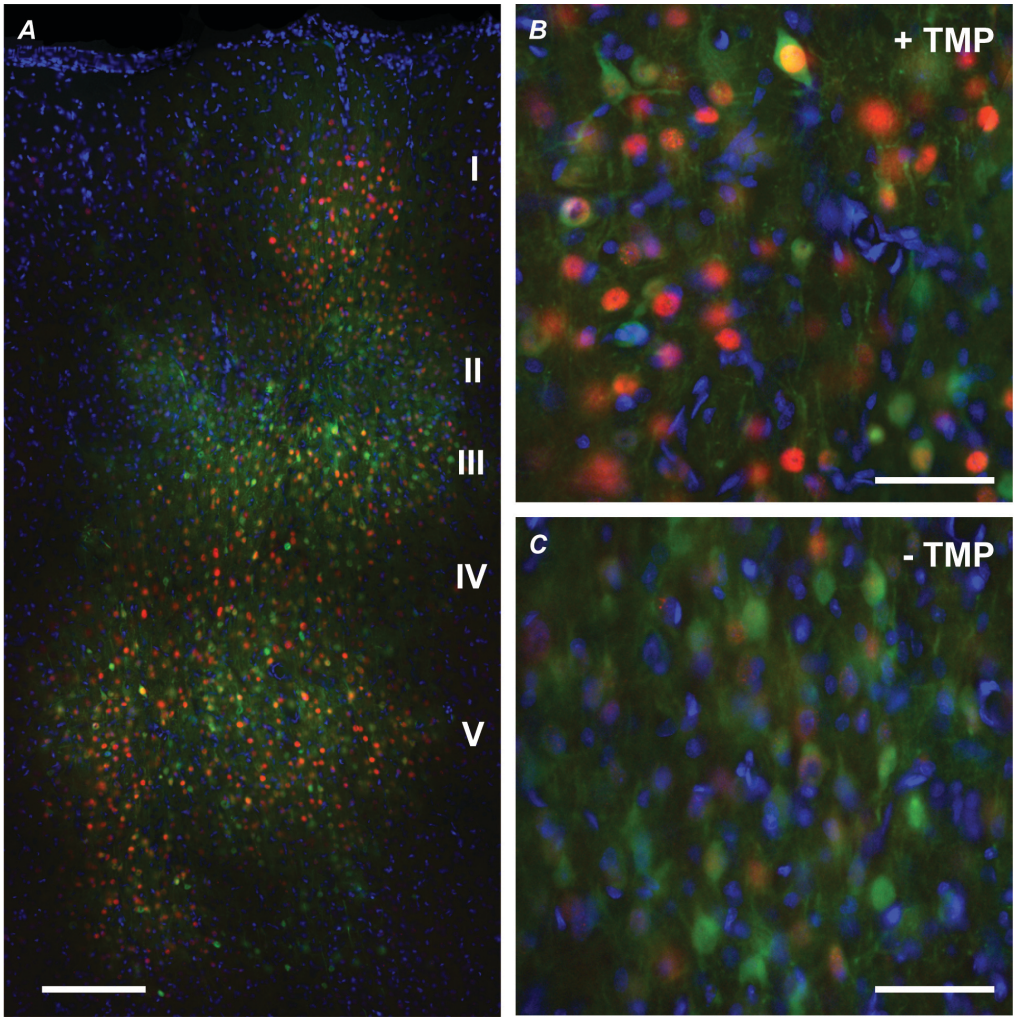

Figure 5-6 Adult rat cortex transduced with HIV-DD-RARβ2 accumulates RARβ2 when diet contains TMP

[A] Adult male Wistar rats received stereotactic infusions of HIV-DD-RARβ2 into the cortex. After three weeks, TMP was supplied at 0.2% of diet for 4 days before harvesting the brain for cryosection (40μm sections) and immunohistological staining. **RARβ2/GFP/DAPI**. Scale bar=100μm. ***[B]*** Higher magnification of layer V pyramidal neurons in animals eating TMP chow. ***[C]*** Higher magnification of layer V pyramidal neurons in animals eating control chow. **RARβ2/GFP/DAPI**. Scale bar=25μm.

5.3.6 Evaluating DD-RARβ2 in a dorsal column crush model of spinal cord injury

This marked difference suggested that the DD-RARβ2 vectors had the potential to regulate the timing and dose of RARβ2 *in vivo* models of spinal cord injury with oral administration of TMP. To begin investigating the use of these vectors in a spinal cord injury model, 8 adult male Wistar rats received stereotactic injection of HIV-DD-RARβ2 vector to the cortex of both hemispheres. Infusions took place at six stereotactic coordinates per hemisphere, determined in a microstimulation mapping study (Neafsey et al., 1986) to cover as large an area of the sensory motor complex as possible. TMP supplementation of the diet began immediately for four rats, while the remaining four ate a control diet that did not contain TMP. After spinal cord lesion, behavioural testing, BDA tracer infusion and subsequent harvesting of tissue (as described in methods 5.2.5.2 to 5.2.5.5), immunohistochemical analysis was performed. Two rats had to be euthanized during the course of the experiment, leaving three rats in each group.

PKCγ immunohistochemical staining of lumbar spinal cord sections revealed that the dorsolateral CST of all the animals in the study had been completely lesioned, as indicated by the lack of PKCγ immunoreactivity in the dorsal funicular of the lumbar spinal cord (Figure 5-7). Therefore, all animals can be included in further analysis.

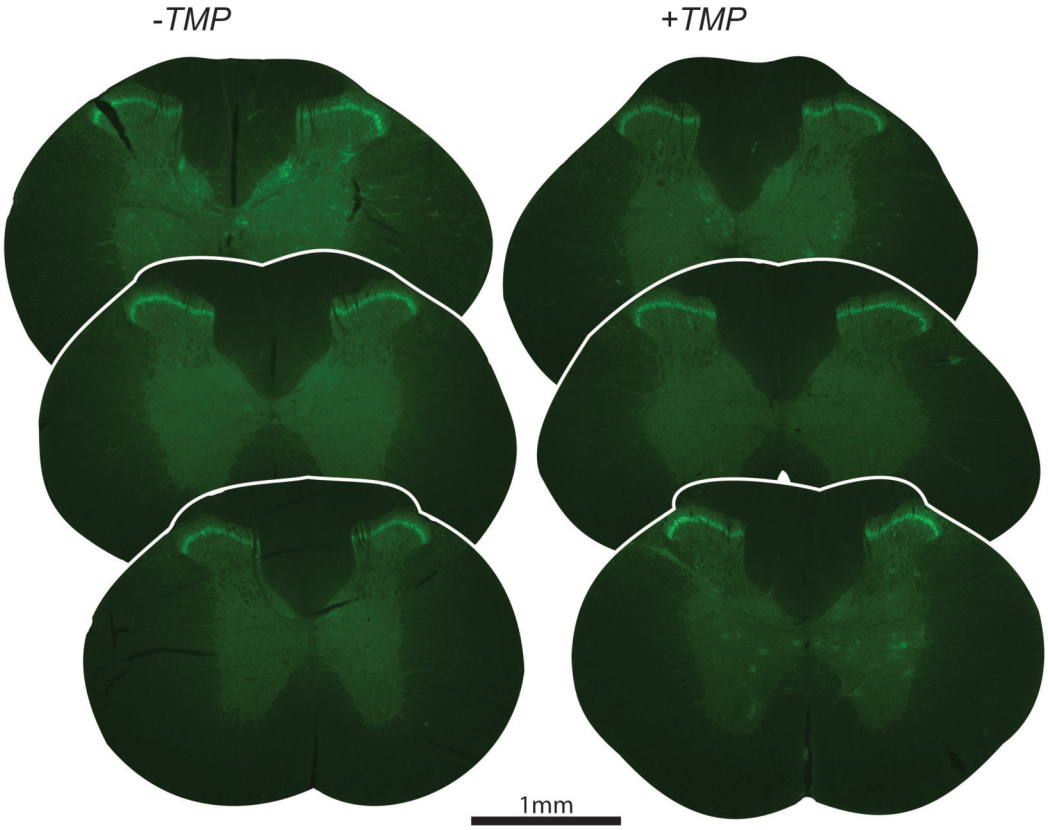

Figure 5-7 Absence of PKCγ in the dorsal funicular of lumbar spinal cord indicates complete lesion of CST fibres.
Pictomicrographs of lumbar spinal cord sections probed for PKCγ. Lack of signal in the dorsal funiculus indicates complete lesion of CST fibres. **PKCγ**.

To confirm that anterograde BDA tracer labelling of CST in the cortex had been achieved, 40μm sections of the brains were probed with Neutr-avidin-TexasRed. BDA staining could be found in abundance in the cortex around needle tracts. Furthermore, BDA labelled fibres could be seen descending through the parenchyma from the BDA infusion site in the cortex (Figure 5-8 *[A/B/C/D]*). To confirm that the HIV-DD-RARβ2 vectors had transduced the cortex and that transduced neurons were also labelled with BDA tracer, 40μm brain sections were probed with anti-bodies against the GFP reporter, neurons and BDA (Figure 5-8 *[E]*).

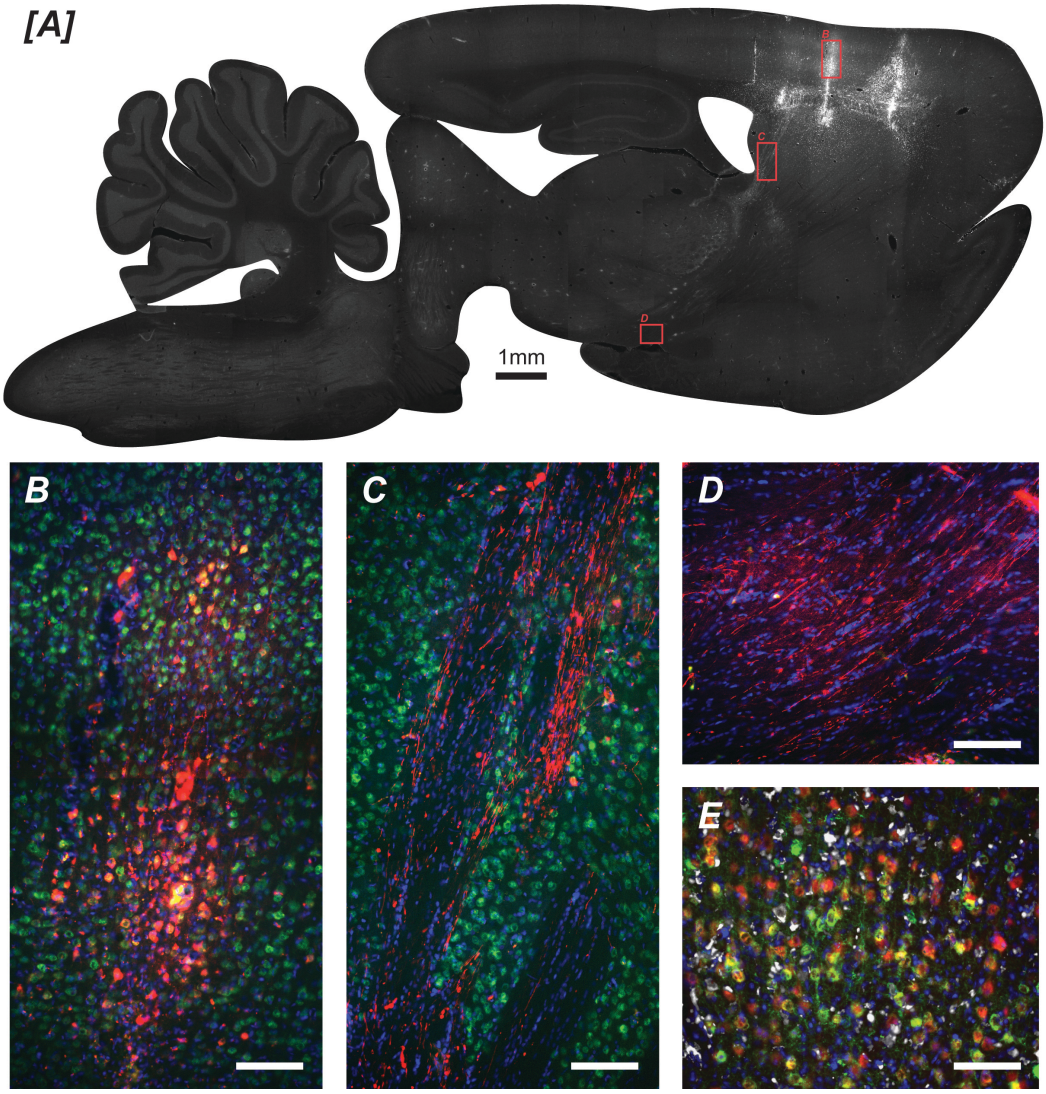

Figure 5-8 BDA staining in the brain of adult rats colocalises with GFP immunoreactivity
[A] Sagittal brain section showing BDA labelled fibres descending from the BDA infusion site in cortex. ***[B/C/D]*** close up images corresponding to boxes indicated in ***[A]***. **BDA**/**NeuN**/**DAPI**. Scale bar=100μm. ***[E]*** GFP immunoreactivity colocalising with both neurons and BDA tracer labelling in the striatum. **GFP**/**NeuN**/**DAPI**/**BDA** Scale bar=200μm.

BDA labelled CST fibres were visualized using immunohistochemistry in the spinal cord both rostral and caudal to the lesion site. After pictomicrographs were taken at 0.5mm intervals, the fibres were counted (Figure 5-9 *[A/B]*).

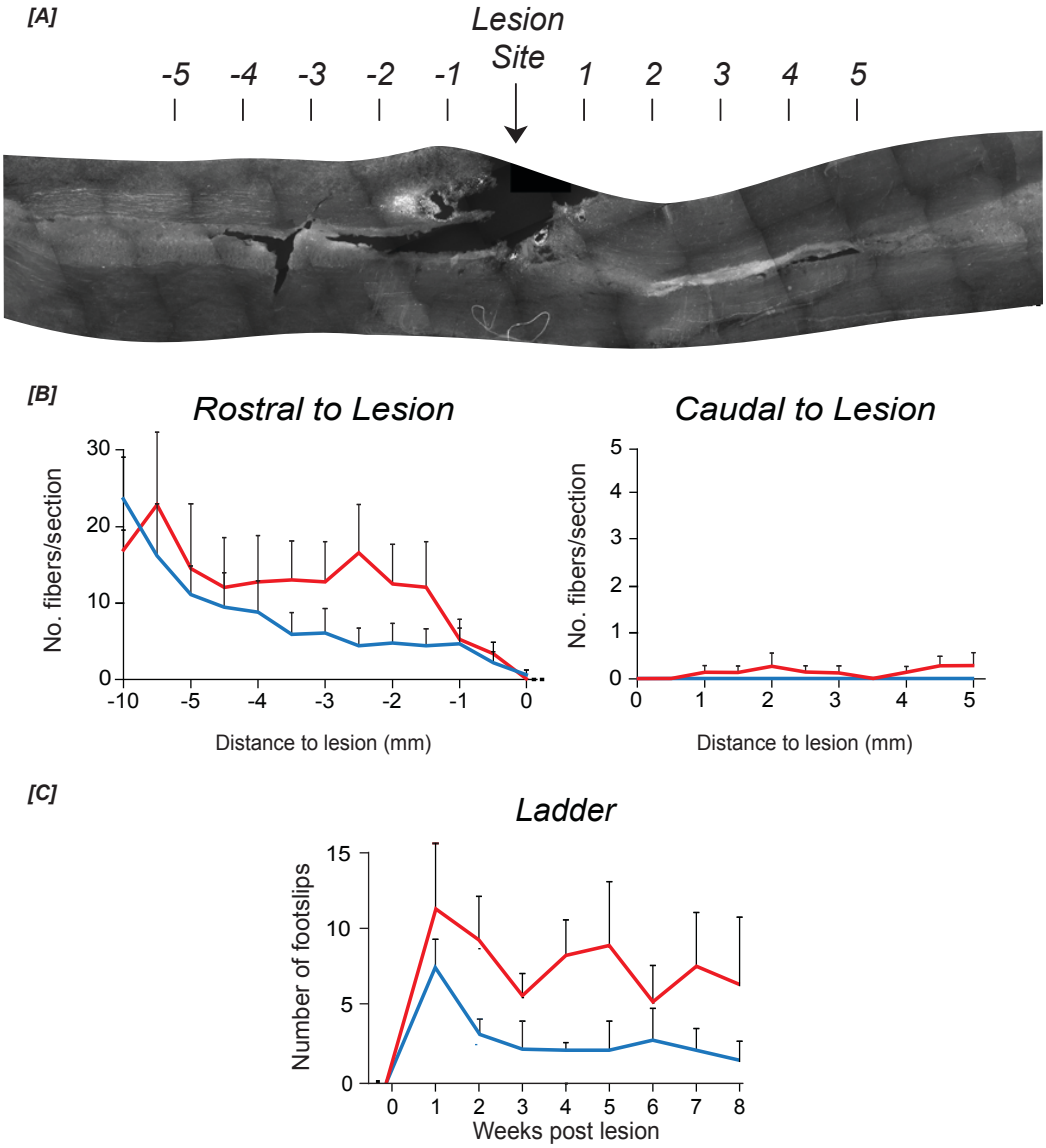

Figure 5-9 Quantification of BDA labelled CST neurons in the spinal cord of adult rats 8 weeks after bilateral dorsal column crush
[A] Pictomicrograph shows representative spinal cord section, after immunohistochemical staining to visualize BDA tracer. Distances in mm. ***[B]*** Counts of BDA positive fibres at specified distances rostral and caudal to the lesion. **+TMP**/**-TMP**. ***[C]*** Behavioural analysis of animals crossing ladder apparatus, average of total foot slips by both front paws. **+TMP**/**-TMP**.

There was no significant difference in the numbers of fibres found rostral to the lesion site in the dorsal CST between the two groups of animals. There was also no significant difference between fibres were found in the dorsal CST caudal to the lesion in animals receiving TMP, to animals receiving a control diet. Low

numbers of BDA labelled fibres could also be found in the ventral CST (data not shown).

Neurons of the CST are responsible for the fine motor control of limbs. Deficits in motor control exhibited by the CST lesioned animals were assessed over an 8-week period. Pre-lesioned animals were trained to cross a ladder apparatus that was suspended above the ground. In the weeks following CST lesion, changes in the ability of the rats to cross this apparatus was monitored by recording the number of misplaced foot 'slips'. A baseline test taken before lesion indicated all rats could cross the ladder without any slips. In the first week post lesion, all rats showed deficits in motor function (Figure 5-9 *[C]*). In the following weeks, no significant differences in motor function appeared between rats eating control or TMP diet.

5.4 Discussion

In this study, we began by testing the ability the DHFR DD system to regulate levels of the nuclear receptor RARβ2. The DHFR DD technology was supplied by the Wandless laboratory. As previously described, (Chapter 3), two different domains were supplied: one that had been developed to be used at the N-terminus of a gene of interest (GOI), and one developed to be used a the C-terminus of a GOI. In previous work using the DD domains to regulate GFP levels, we found that only the '3mut' form imparted desirable regulatory characteristics, and that applying that domain to the C-terminus of GFP was most favourable. As the 4mut domain had not imparted desirable characteristics on GFP (and in the absence of supporting literature available at the time of study) only the 3mut domains were tested in this study. With consideration to previous observations that the domains' regulatory properties were dependent on the protein they were destabilising, we tested the 3mut DD at both the N- and C-terminus of RARβ2, expressed from a dual promoter construct. We chose to use a dual promoter reporter to provide a robust reporter of cell transduction for cells growing *in vitro*. Furthermore the RARβ2 antibodies that were used in this study were not very specific and not suitable for detecting the relatively low levels of RARβ2 expression in DRG neurons in immunohistochemistry, therefore a more robust reporter of transduction was required. A two-step cloning strategy was required due to RE sequences in the DD cassette being non unique in the dual promoter vector.

When HEK293T cells transduced with lentiviral vectors made from these constructs were supplied a range of TMP, only the N-terminally tagged form (DD-RARβ2) gave rise to RARβ2 accumulation. The C-terminally tagged form failed to express any detectable RARβ2. Cells that were transduced with these vectors expressed GFP, (confirming transduction) Furthermore, the experiment was repeated several times to confirm the result. The reason for the lack of RARβ2 expression from this construct is unclear. It is possible that there could be mutations in the CMV promoter that drives RARβ2-DD expression. Although the constructs were sequenced prior to lentiviral production, the sequencing primers were not designed to cover the promoter, meaning that there could be mutations would remain undetected. This might explain why GFP expression was still seen, as the SFFV promoter would not necessarily have been affected. It may be that this fusion protein is non permissive in the cell, either due to interaction between two domains (DD and RARβ2) on one polypeptide chain, or interaction with other molecules in the cells. Or perhaps the fusion mRNA forms structures that block translation at the ribosome. Although this finding is interesting and highlights the importance of testing DD at both termini, we also found that DD-RARβ2 accumulates RARβ2 in a dose responsive manner to TMP in HEK293T cells and neurons *in vitro*, indicating that this construct is suitable for use *in vivo*. Therefore, the reason for the lack of expression was not investigated further.

When testing the efficacy of DD-RARβ2 in neural cells, we found more basal activation of the system than had been seen in HEK293T cells. The process through which the DD tagged proteins are degraded is not fully understood, but

it is at least in part mediated by the proteasome, as indicated by the Wandless studies that described the accumulation of DD fusions in cells in the absence of stabilising ligand when proteasome inhibitors were applied (Banaszynski et al., 2006; Maynard-Smith et al., 2007) and DD-tagged proteins co-localising with subunits of the proteasome (Leong et al., 2012). Proteins destined for degradation by the proteasome are usually tagged with multiple ubiquitin moieties, and this was recently found to be the case for FKBP12-based DD fusion, only minutes after the removal of Shield1. It may be that neurons are particularly sensitive to overloading of the ubiquitin-proteasome system (UPS). For example, in diseases such as Huntingdon's disease, Parkinson's disease and ALS (Amyotrophic lateral sclerosis), the proteinaceous inclusions that form are comprised of aggregated proteins and among these is ubiquitin. The presence of these aggregates reduces the efficiency of the UPS in these cells, so aggregated proteins do not get removed and build up. It may be that by overexpressing an unstable protein (in the absence of TMP) in neurons, the proteasome becomes overloaded and therefore DD-RARβ2 levels increase, giving rise to basal expression in the absence of TMP.

E18 cortical neural cultures have been shown in our lab to contain a high percentrage of neurons. Although there are glia present in the culture and they will also be transduced with the lentiviral vectors, the low numbers (approximately 10%) mean that our result will be

Overexpressing RARβ2 in adult DRG neurons had been previously shown to increase neurite outgrowth (Wong et al., 2006). In our study, while the group of

DRG neurons constitutively expressing RARβ2 do support this finding, a similarly convincing result could not be observed in the group of DRG neurons that expressed DD-RARβ2 in the presence of TMP. The trend in the extent of neurite outgrowth from these neurons mirrors the levels of DD-RARβ2 found in DD-RARβ2 transduced DRGs when analysing protein levels by Western Blot (Figure 5-4). That is, the levels of DD-RARβ2 in DRG neurons overexpressing DD-RARβ2 upon exposure to 50μM TMP did not reach the levels of RARβ2 observed in DRG neurons overexpressing the constitutive RARβ2 construct. Therefore, the lack of extensive neurite outgrowth from the DRG neurons expressing the DD-RARβ2 construct may be attributed to the lower levels of RARβ2 observed in these neurons, and it may be possible that a certain threshold level of RARβ2 is required in order to mediate significant neurite outgrowth effects.

To investigate the ability of the DD system to regulate RARβ2 in the cortex of the CNS, an *in vivo* expression study was performed. This study indicated that we could transduce a large area of the cortex and all cortical layers. Furthermore, there was a noticeable difference in the levels of DD-RARβ2 between animals that were fed TMP and those that were fed a control diet when the sections of the respective brains were probed via immunohistochemistry, though this technique precludes quantitative analysis. To provide a quantitative assessment of transgene levels, a Western blot could be performed. However, Western blot analysis of lysates prepared from brain explants had been attempted when investigating regulating GFP levels. Even though the anti-GFP antibody had

proven highly specific when probing blots of lysates derived from cell lines, we could not detect GFP in this way. We concluded that the amount of GPF from transduced cells was being diluted beyond the limit of detection. As the anti-RARβ antibody is less specific and the area of cortex that would need to be harvested large, this would not be a robust method to determine DD-RARβ2 levels.

Lentiviral vectors constitutively expressing RARβ2 had previously been shown to stimulate axon outgrowth and reduce motor function deficits in adult rats in the same lesion model of spinal cord injury (Yip et al., 2006). Here we attempted to replicate this study using the lentiviral vector overexpressing DD-RARβ2 in order to demonstrate that a regulatable lentiviral vector could be utilized in a gene therapy for spinal cord injury. Although we found a wide area of BDA-labelled cell bodies in the cortex and labelled axons could be traced through the parenchyma to the brain stem and found in large numbers rostral to the lesion site, few were found caudal to the lesion. We did not observe any significant differences axonal regeneration between animals that received TMP in their diet and those that did not, and this was correlated with the lack of significant improvement in the behavioural measurement of motor function (such as the ladder crossing test). Yip and Wong et al found much higher numbers of CST axons in the caudal spinal cord, correlating with significant reductions in motor deficits. This suggests that it is the lack of sufficient outgrowth of CST axons from the DD-RARβ2 neurons that led to the poor improvement in motor tasks. The small amount of improvement seen could be accounted by the presence of BDA labelled fibres in the ventral CST. Ventral CST fibres are not lesioned in a

dorsal CST crush and although the ventral CST holds less than 5% of the total fibres found in the dorsal CST they can sprout to provide compensation for the lost pathway (Niikura et al., 2000; Weidner et al., 2001; Lapenna et al., 2009).

The main restriction on drawing conclusions from the CST lesioned rats is the lack of appropriate numbers of animals and groups in the experiment. Indeed, although all rats appear to have the same degree of lesion indicated by PKCγ staining, there were very noticeable differences in the motor deficits seen within groups. Furthermore, given that the DD-RARβ2 appeared to have higher levels of basal RARβ2 expression in the cortical and DRG neuron *in vitro* in the absence of TMP, it would have been advisable to include two further groups of animals: one, a negative control group that will receive control GFP lentiviral vector; and two, a positive control group that will receive the constitutive RARβ2 lentiviral vector. In addition, group numbers of at least 8-10 in each group will be required to obtain statistically meaningful immunohistochemical and behavioural data. Therefore, to fully determine the efficacy of the DD-RARβ2 vector, further experiments would have to be performed but this was not pursued due to time constraints.

Our data suggest that DD-RARβ2 may not be able to confer the same degree of axonal outgrowth as that observed from a constitutively expressed RARβ2. One possibility is that the translocation of RARβ2 to the nucleus in order to act as a transcription factor could be affected by the addition of the DD, either due to the increased size or changes in protein conformation. While we see DD-RARβ2 colocalising with DAPI immunostaining in many transduced cells treated with

TMP *in vitro* and *in vivo* indicating that DD-RARβ2 is able to reach the nucleus, this may not be occurring to the same extent as native RARβ2. A further possibility is that the DD inhibits, in some part, the biological function of RARβ2. The N-terminus of RARβ2 harbours a ligand-independent transcription activation function (AF-1) (Bastien and Rochette-Egly, 2004) the function of which is not fully understood, although it has been established that it can cooperate with similar domains on the same or different isotypes of RARs and other coactivators (Bommer et al., 2002), leading to cell type- and promoter context dependent activation (Nagpal et al., 1992; 1993; Taneja et al., 1997). As the method by which RARβ2 stimulates neurite outgrowth is not completely elucidated, it is possible that the activity of this domain is affected by the DD.

In order to further investigate if this is indeed the case, further experiments will have to be carried out using a reporter system, formed by placing RARβ2 responsive promoter upstream of a luciferase gene (de The et al., 1990; Sucov et al., 1990) . The efficacy of the DD-RARβ2 activation function can then be tested on this RARβ2 responsive element and compared to that of the endogenous RARβ2 protein, allowing one to assess if the DD domain indeed does affect the biological activity of RARβ2. These studies will be critical for evaluating the utility of these DDs in viral vector systems for use in gene therapy.

Chapter 6 CDNF

6.1 Introduction

Parkinson's disease is a progressive neurodegenerative disorder that affects over 6 million people worldwide. The severity of the disease is correlated with the loss of dopaminergic neurons in the substantia nigra pars compacta (SNPC) of the midbrain. This leads to the motor deficits that characterize the disease: tremor, bradykinesia, ridigity and postural instability. At this time there is no cure for the disease and current treatments serve to alleviate symptoms, for example the use of dopamine agonists or L-DOPA to substitute dopamine deficits or deep brain stimulation to decrease neuronal activity in the subthalamic nucleus. While L-DOPA is the current gold standard treatment, long term administration often leads to reduced efficiency and side effects such as on/off oscillations and dyskinesias (Obeso et al., 2000; Lees et al., 2009). A better treatment that can combat the cause, or halt the progression of the disease is required.

One possible therapeutic intervention to slow or halt the progressive degenerative process occurring in Parkinson's disease to protect the dopamine neurons from further degeneration and promote their survival, for example through application of neurotrophic factors (NTFs). NTFs are secreted proteins that function as growth factors in the developing nervous system, and promote survival, formation and maintenance of neuronal connections (Huang and Reichardt, 2001; Airaksinen and Saarma, 2002). Thus far, Glial cell line-derived neurotrophic factor (GDNF) (Lin et al., 1993) has been found to be the most potent NTF to protect and restore the dopaminergic system in rodent and primate

models (reviewed by Kirik et al., 1998; Evans and Barker, 2008) and has entered clinical trials to treat human patients. However, these trials have proven controversial. Infusions of GDNF into the putamen of PD patients showed clinical benefits in two open-label studies (Gill et al., 2003; Patel et al., 2005; Slevin et al., 2005) however another randomized, double-blind study showed no clinical benefit (Lang et al., 2006) while another trial suggested that there were potential serious side effects after GDNF infusion (Nutt et al., 2003). Therefore, the identification of novel neuroprotective (and neurorestorative) factors was desired.

Human conserved dopamine neurotrophic factor (hCDNF) is a secreted 18kD glycosylated protein and is the second member of the MANF/CDNF family to be discovered. A few years previous to this discovery, the founding member of this family - Mesencephalic-astrocyte-derived neurotrophic factor (MANF) – was identified from the culture medium of rat mesencephalic type-1 astrocyte cell line 1 (VMCL1) and was found to promote survival of dopaminergic neurons *in vitro* (Petrova et al., 2003). CDNF is widely expressed throughout the nervous system and is up-regulated in adult mice brain after induction of pathological conditions such as status epilepticus and global forebrain ischemia (Lindholm et al., 2008), leading to the suggestion that this family could present a potential therapy for other neurological disorders.

CDNF was identified using bioinformatics and found to be 59% homologous to its human MANF paralogue (Lindholm et al., 2007). Analysis of the crystal structure revealed CDNF and MANF are both composed of two domains: an N-

terminal domain that is structurally saposin-like and may interact with lipids or membranes, and a C-terminal domain that may protect cells against endoplasmic reticulum (ER) stress, or be involved with protein folding in the ER (Parkash et al., 2009; Lindholm and Saarma, 2010). Both CDNF and MANF have 8 cysteine residues, conserved across vertebrate species, and a secondary structure dominated by α-helices (Sun et al., 2011).

CDNF mRNA and protein was detected throughout development in the midbrain and also in the adult striatum and substantia nigra (Lindholm et al., 2007), suggesting a neurotrophic role for CDNF in dopaminergic neurons. To determine if CDNF could promote the survival of dopaminergic neurons in an *in vivo* model of Parkinson's disease, Lindholm and colleagues administered a single pre-lesion treatment of CDNF (10ug) to the striatum of 6OHDA-lesion model rats (Lindholm et al., 2007). Indeed, pre-lesion treatment with CDNF was protective to dopaminergic neurons in the SNPC in this lesion model; the same group went on to show that CDNF treatment 4 weeks after lesion led to partial restoration of dopaminergic neurons after lesioning (Lindholm et al., 2007). Subsequent to this study, Voutilainen et al. (2011) found that chronic infusion of CDNF protein starting two weeks post-lesion inhibited the 6-OHDA induced loss of dopaminergic neurons in the SNPC and tyrosine hydroxylase (TH)-positive fibres in the striatum (Voutilainen et al., 2011), suggesting that CDNF can provide a real alternative to GDNF as a neuroprotective, or even neurorestorative, therapy for PD.

Providing a chronic infusion of CDNF protein to the striatum requires invasive surgery to implant the cannulae; furthermore, continuous administration of CDNF over an extended period of time may be costly and the implanted cannulae may be prone to infection, indicating taht this would not be ideal as a therapeutic strategy for PD patients. To provide long-term neurotrophic support, a gene therapy approach to deliver CDNF to the brain would be advantageous. As neurotrophic factors clearly play important roles in the control of neural cell fate, it seems likely that prolonged viral expression may not be desirable in order to avoid potential side effects from developing, especially in the peripheral nervous system. It will also be important to find the correct dosing and timing of delivery of CDNF, in order to maximize the efficacy of neurotrophic support to the dopaminergic neurons, whilst minimizing potential side effects.

Gene therapy approaches to treat PD has been extensively explored and many studies have described the use of various viral vectors including adenoviral vectors, adeno-associated viral vectors and lentiviral vectors. A number of research papers have demonstrated that viral vector mediated delivery of GDNF is efficacious in rodent and primate PD models (for example Kordower et al., 2000; Azzouz et al., 2004a; Dowd et al., 2005; reviewed by Hong et al., 2008). Other gene therapy strategies for treating PD include: 1) an AAV vector overexpressing neurturin, another neurotrophic factor to protect dopaminergic neurons in the SN (Marks et al., 2008); 2) an AAV vector overexpressing glutamic acid decarboxylase (GAD) to modulate GABA production in the subthalamic nucleus in order to improve basal ganglia function in PD patients (LeWitt et al., 2011); 3) AAV vector overexpressing AADC (Aromatic L-amino

acid decarboxylase) to increase dopamine synthesizing enzymes in dopaminergic neurons (Muramatsu et al., 2010; Mittermeyer et al., 2012) 4) EIAV-based lentiviral vector overexpressing AADC, tyrosine hydroxylase (TH) and GTP cyclohydrolase I (GCH) in a single transcriptional unit, in order to replacing lost dopamine by inducing local production of dopamine with dopamine-synthesizing enzymes (Azzouz et al., 2002), or 5) Using three AAV2-based vectors separately expressing these factors (Shen et al., 2000; Muramatsu et al., 2002) .

In this chapter we will apply the DFHR regulatory system to the novel neurotrophic factor CDNF and test the therapeutic approach of delivering CDNF in a regulatable manner in an *in vivo* model of PD. The system will be initially tested *in vitro* in HEK293T cells and E18 rat cortical neuron cultures, where we will determine if TMP can lead to dose dependent secretion of CDNF. We will then assess CDNF regulation *in vivo*, before using the regulatable CDNF vector in the 6OHDA lesion model of Parkinson's disease.

6.2 Methods

6.2.1 Cloning a DD-CDNF construct

To form a regulatable CDNF construct, the restriction site (RE) optimised construct (pRRL-GFP-DD) that had already been designed for investigating the DHFR DD system (See Chapter 4) was used. A PCR strategy was used to amplify a CDNF fragment flanked by the appropriate RE sites to replace GFP. In order to provide a GFP reporter, the expression cassette was then shuttled into a dual promoter construct. This gave the final construct pRRL-SFFV-GPP-CMV-CDNF-DD (hereafter CDNF-DD).

6.2.2 cDNA clone of CDNF

cDNA clones of human CDNF were purchased from Gene Service, in the form of a bacterial culture transformed with the gene-bearing plasmid, selectable via kanamycin resistance. The bacteria were streaked onto LB agar containing Kanamycin (100μg/ml, Sigma) and grown at 37^{o}C overnight. An individual colony was picked into LB-Kanamycin media, grown overnight, and miniprepped (Methods 2.1). Plasmids were stored at -20^{o}C.

6.2.3 PCR amplification of human CDNF cDNA from

PCR was performed (Method 2.1.1) using the primers listed in Table 6-1. PCR products for forming pRRL-DD-CDNF were 587bp, while those for forming pRRL-CDNF-DD were 594bp.

Primer Name	*Primer Sequence (5'-3')*
CDNF-DD forward	*TAGCATACCGGTGCCACC**ATGTGGTGCGCGAGCCC***
CDNF-DD reverse	*TATAATGCTAGC**GAGCTCTGTTTTGGGGTG***

Table 6-1 PCR primers designed to amplify CDNF for insertion into destabilisation domain cassette
Annotated sequences indicate RE sites. Highlighted bold sequences indicate template complementarity.

6.2.3.1 Cloning pRRL-CDNF-DD

PCR products were separated, typically in a 1% agarose gel, the correct band was excised and DNA recovered (Methods 2.1.2). Backbone plasmid pRRL-DD-GFP and CDNF PCR products (to be N-terminally tagged) were digested with the REs *PspOMI*/*SalI*; pRRL-GFP-DD and CDNF PCR products (to be C-terminally tagged) with *AgeI*/*NheI*. After agarose gel electrophoresis, band excision and DNA recovery, products were quantified, and backbone-insert pairs ligated, transformed and sequenced as described before (Method 2.1). To insert the expression cassette into the dual promoter construct, the parental dual reporter plasmid (pRRL-SFFV-GFP-CMV-NCS1 – a gift from Dr Ping Yip, Kings College London) was digested with *XbaI* (NEB), before creating a blunt end using Klenow polymerase. After running the digested backbone through a PCR clean up column (Qiagen), the backbone was digested with *SalI* (NEB) and subsequently dephosphorylated using the rAPID dephosphorylation kit (Roche), before separating the products in an agarose gel. After band excision and DNA recovery, products were quantified, and backbone-insert pairs ligated, transformed and sequenced (Method 2.1).

6.2.4 Preparation and use of HIV-DD-CDNF and HIV-CDNF-DD

Lentiviral vectors were produced and titred (Method 2.2). In all *in vitro* experiments in this chapter, vectors were used at MOI1. HEK293T cells and E18 rat cortical neurons seeded and transduced (methods 2.5.3 and 2.6.4 respectively). TMP was supplied at a range of doses – 0, 0.5, 5, 50μM – to both cell types. To harvest the culture supernatant to analyse secreted CDNF-DD, the media was aspirated and centrifuged at 17,900 RCF for 5 minutes, before removing supernatant to a fresh tube and storing at -20^{o}C. To prepare for loading into an 8% SDS-PAGE gel, 20μl supernatant was mixed with 20μl 2x loading dye (Method 2.4.1) before boiling. Cells were prepared as described in Method 2.4.1.

6.2.5 Preparation of trimethoprim stock solutions

For use *in vitro*, TMP (Sigma) was dissolved in neat DMSO (Sigma) to make a 200mM solution, and typically used at dilutions below 50μM. For use *in vivo*, TMP was used as a powder and disseminated in powdered normal rat chow before mixing with water and flavouring agents to make a mash - final concentration either 0.2% TMP, or 0.05% TMP.

6.2.6 Stereotactic injection of HIV-CDNF-DD to the CNS of adult rats

In all *in vivo* experiments in this chapter, adult male Wistar rats (250-300g) received infusions of lentiviral vector via stereotactic injection (0.2nl/min infusion rate). Additional post-operative analgesia was not used, however, it must be noted that there is trauma to tissues when forming *in vivo* models of PD and that in the future we would seek to administer additional post-operative

analgesia, continuing for several days after surgical intervention. This would be unlikely to confound behavioural findings if all animals received the same dose. It must also be noted that patients receiving surgery for PD are treated with analgesia, so this may help to improve the efficacy of potential therapies when using the rat PD model. At the end of experiments, the animals were terminated using 150mg/Kg pentobarbital (*Euthatal*) and the brain harvested (Method 2.7).

6.2.6.1 Titres of lentiviral vectors used in vivo

Lentiviral preparations above $1x10^8$tfu/ml were considered sufficient to provide robust transduction *in vivo*. SFFV-GFP-CMV-CDNF, $3.68x10^8$tfu/ml; SFFV-GFP-CMV-CDNF-DD, $1.82x10^8$tfu/ml; SFFV-GFP-CMV, $6.18x10^9$tfu/ml; Rabise pseudotyped SFFV-GFP-CMV, $2.73x10^8$tfu/ml (This virus was prepared in collaboration with Dr Oscar Cordero Llana, Plasmid containing rabies coat is described by Mazarakis et al, 2001) Titres were not matched for *in vivo* experiments.

6.2.6.2 Expression study

5 rats received a 2µl infusion of HIV-CDNF-DD vector into the striatum of the right hemisphere at the co-ordinate (AP/ML/DV relative to bregma) 0/3.5/4.75. Three weeks later, 3 rats had normal chow replaced with a mashed diet containing 0.2% TMP, 3 rats received mashed chow that did not contain TMP. Once feeding began, this diet was continued for 3 days, recording the amounts consumed daily. The animals euthanized using 150mg/Kg pentobarbital (*Euthatal*) on day 4, and following perfusion fixation (Method 2.7.3) the brain was harvested, and prepared for section via cryostat (Method 2.8.1).

6.2.6.3 Intranigral infusion of VSV-G pseudotyped vectors

To directly transduce cells in the SNPC, 2μl VSV-G pseudotyped HIV-GFP vector was infused at the coordinate (AP/ML/DV relative to bregma): -5.3/-2.2/7.2.

6.2.6.4 Intrastriatal infusion of Rabies-G pseudotyped vectors

Rabies-G pseudotyped HIV-GFP was infused at two coordinates in the striatum (AP/ML/DV relative to bregma): 0/3.5/4.8 and 1/3.5/4.8.

6.2.7 6-hydroxy dopamine lesion model of Parkinson's disease

6.2.7.1 Nigro-Striatal lesions

6-Hydroxydopamine (6OHDA, Sigma) was made up to 5g/L in deoxygenated water (bubbled with N_2 for 5 minutes) and aliquoted under sterile conditions and stored at -80^{o}C. To prevent the rapid oxidation of 6OHDA, a new aliquot was used for every animal. Adult male Wistar rats received two unilateral stereotactic injections of 6OHDA (2μl each site, 20μg total 6OHDA at a rate of 400nl/minute) to induce a pre-terminal lesion in the striatum, as described by Kirik and colleagues (Kirik et al., 1998). Coordinates (AP/ML/DV relative to bregma): 0/-2.6/5.0 and -1.2/-3.9/5.0. Infusion of 6OHDA into these sites in striatum should lead to approximately 70% loss of TH positive neurons in the SNPC in the lesion hemisphere three weeks after lesion (Kirik et al., 1998). A total of 34 rats were used in this study. In all surgeries, viral group injections were randomised by distributing animals in each group between surgeons (Ben Houghton and Oscar Cordero Llana) and over the course of the day.

6.2.7.2 Behavioural measurements

In order to assess the functional integrity of the nigro-striatal dopaminergic system, rotation behaviour is triggered by the injection of either apomorphine (a dopamine receptor agonist) or amphetamine (a dopamine releasing compound). The number of rotations, due to the imbalance of striatal dopamine signalling between lesioned and non-lesioned hemispheres, correlates with the magnitude of the SNPC lesion and DA neuron loss. Apomorphine typically induces contralateral rotations, while amphetamine typically induces ipsilateral rotations. Animals were injected IP with 2.5mg/kg D-amphetamine sulphate (Sigma) or subcutaneously with 0.25mg/kg R-apomorphine hydrochloride hemihydrate (Sigma). Amphetamine solutions were made up fresh on the day of turning whereas for apomorphine, a 10X stock (apomorphine 2.5g/L 0.1% [w/v] ascorbic acid) was made up in deoxygenated-sterile ddH_2O and kept at -80ºC. Immediately after injection of the drugs, animals were placed inside 30-cm rotometer bowls (loaned from Oxford Biomedica) and attached to the revolution counter using an elastic harness. Ipsilateral and contralateral rotations were recorded every 5min using the rotarod software (purposely-designed in Oxford-Biomedica). Animals were monitored for up to 60 minutes in apomorphine-induced rotations or up to 90 minutes in amphetamine-induced rotations and returned to their cages.

6.2.8 Tissue preparation and immunohistochemistry

Brains were cryoprotected in sucrose and frozen in preparation for sectioning to 40μm slices via cryostat (Method 2.8.1). Typically the brain was sequentially dived into 5 and one fifth of the brain used for immunohistochememistry

(Methods 2.9, see Table 2-5 for detail of antibodies). Anti-CDNF and Anti-TH antibodies were a kindly supplied by the Caldwell laboratory.

6.3 Results

6.3.1 Cloning a CDNF-DD construct

CDNF is a secreted protein, and we anticipated that a DD cloned to the N-terminus would be removed with the secretion signal (Lindholm et al., 2007). We chose the '3mut' form of the DHFR DD (Chapter 4) and applied it to the C-terminus of CDNF using a PCR based strategy. We then shuttled the expression cassette in to a dual promoter vector (Yip et al., 2010) that constitutively expressed GFP under a spleen focus forming virus (SFFV) promoter. The resulting CDNF-DD plasmid could then be used to make lentiviral vectors.

Figure 6-1 Schematic diagram of the viral insert of CDNF-DD

6.3.2 HEK293T cells and E18 rat cortical neurons dose dependently secrete CDNF when treated with TMP

A HIV lentiviral preparation of CDNF-DD was made and used to transduce HEK293T cells, alongside a HIV-GFP control (Chapter 5). TMP was supplied over a range of doses - 0 - 50μM - 48h prior to harvesting the culture supernatant and cell pellets in preparation for Western blot analysis. Blots revealed that there was a dose-dependent increase in the levels of CDNF in the culture supernatant from both HEK293T and E18 cortical neurons cells expressing the CDNF-DD construct (Figure 6-2 *[A/B]*). There was a small accumulation of CDNF within

the cells expressing CDNF-DD, some of which remained when cells were treated with TMP. This effect appears slightly enhanced in E18 cortical neurons.

6.3.3 CDNF accumulates in the striatum of adult rats transduced with HIV-CDNF-DD when TMP is supplied in the diet

Six adult male Wistar rats received stereotactic infusions of HIV-CDNF-DD to the striatum of the right hemisphere (Method 5.2.4.2) Three weeks later, the diet of three of the rats was exchanged for chow containing 0.2% TMP (On average 260mg/kg TMP eaten per day), while the remaining three rats received a control diet. Three days later, the brains were harvested, sectioned and immunohistologically probed before visualizing the CDNF either by DAB staining, or using fluorophore conjugated antibodies (Figure 6-2 *[C]*). Both DAB and fluorescent staining revealed the presence of more CDNF in the striatum of rats that had received TMP in their diet. This suggests that the DD system can be used to regulate the levels of CDNF in the brain and can therefore be tested in the 6OHDA lesion model for Parkinson's disease.

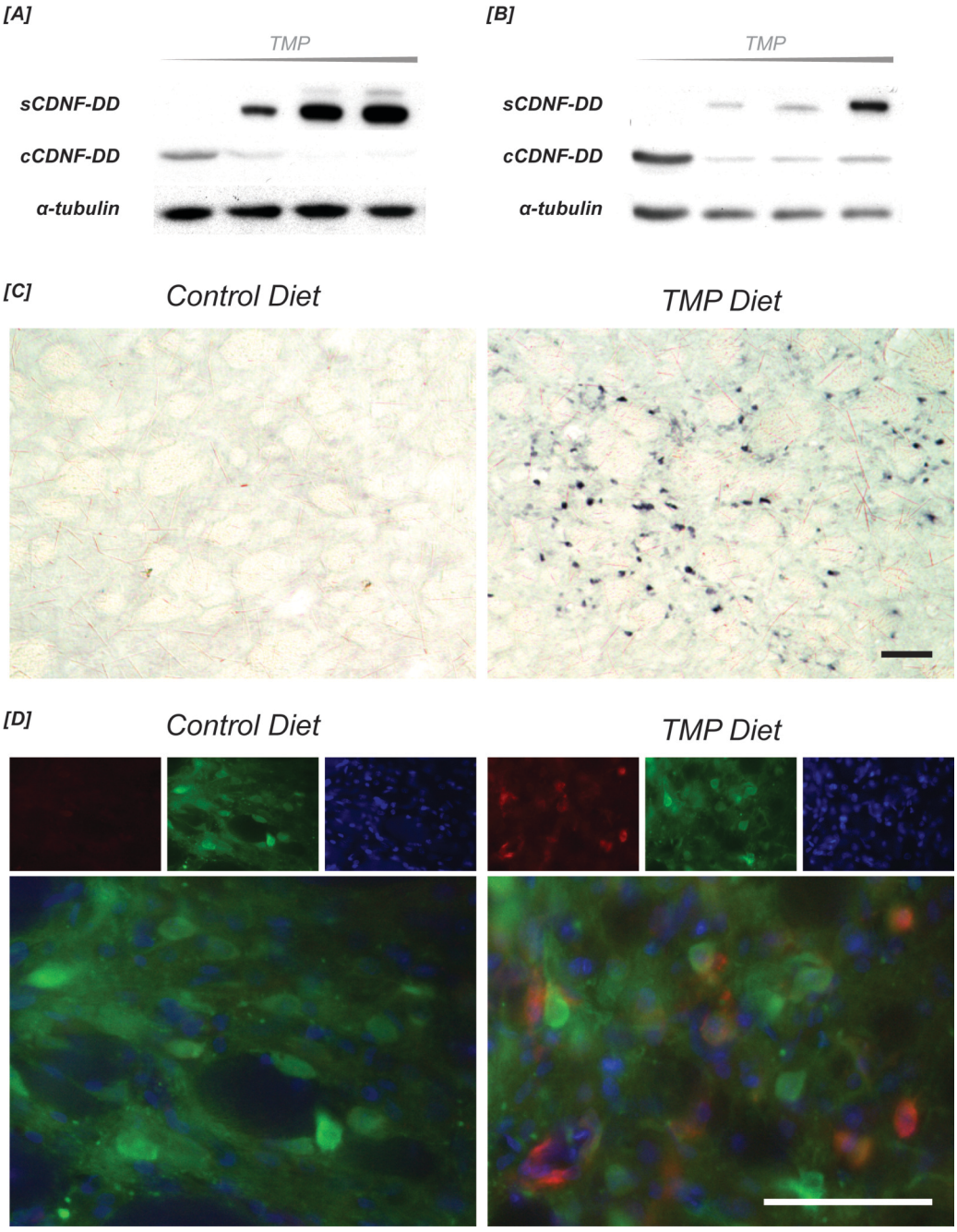

Figure 6-2 Validation of HIV-CDNF-DD in HEK293T cells, E18 rat cortical neurons and adult male rats

[A] HEK293T cells transduced with HIV-CDNF-DD were treated to a range of TMP concentrations (left to right: 0, 0.5, 5 and 50μM) 48h prior to harvesting the media supernatant (sCDNF-D) and cell pellets (cCDNF-DD). Supernatants were centrifuged to remove cell debris, before mixing 1:1 with sample loading buffer in preparation for Western blot analysis. Approximate molecular weight of CDNF-DD is 37kDa. ***[B]*** Similarly, E18 rat cortical neurons were transduced and received the same range of TMP doses 96h prior to harvesting, before preparing in the same way. ***[C]*** Adult male Wistar rats received stereotactic injections of HIV-CDNF-DD into the striatum of the right hemisphere. After three weeks, some rats received mashed chow containing 0.2% TMP for three days prior to perfusion fixation and harvesting of the brain. After cryoprotection, brains were sectioned into 40μm sections in a cryostat. ***[C]*** Some sections were DAB stained for CDNF (light microscope images) Scale bar=50μm. ***[D]*** Other sections were stained using ALEXA-conjugated secondary antibodies. **CDNF**/**GFP**/**DAPI**. Scale bar=50μm.

6.3.4 Optimising the viral delivery method of CDNF expressing vectors to the SNPC of adult rats

In order to transduce as much of the SNPC as possible, while not physically damaging the area, two different methods of viral delivery were considered. As implemented in our previous studies, VSV-G-pseudotyped vectors can be used to transduce cell bodies at the site of injection. These vectors require precise targeting of the SNPC in stereotactic surgery. Rabies-G-pseudotyped vectors have the ability to retrogradely transport along the processes projecting into the striatum from cells in the SNPC. By avoiding direct infusion to the SNPC, this may avoid damaging the SNPC with infusion needles, and be more reliable in targeting this small area. Preparations of Rabies-G-pseudotyped HIV-CDNF were made and infused into striatum of adult male Wistar rats at two sites (Method 6.2.6.4). To assess our ability to accurately target the SNPC, preparations of VSV-G-pseudotyped HIV-CDNF were infused directly to the SNPC (Method 6.2.6.3). Three week post-infusion, the animals were transcardially perfused and the brains collected. After cryoprotection and section via cryostat, the brains were probed for CDNF and visualized using fluorescent antibodies. Tyrosine hydroxylase (TH) was also probed to reveal the SNPC. Animals that had received Rabies-G-pseudotyped vector had very few transduced neurons in the SNPC (located by staining for tyrosine hydroxylase positive cells) (Figure 6-3 [*A/B/E*]. In contrast, animals that had received infusions of VSV-G-pseudotyped vectors directly to the SNPC had many transduced neurons in the SNPC (Figure 6-3 [*C/F*]. This suggests that while there is slight danger of damaging the SNPC by infusing viral vectors directly to

the SNPC, this method is preferable as it leads to many more cells being transduced.

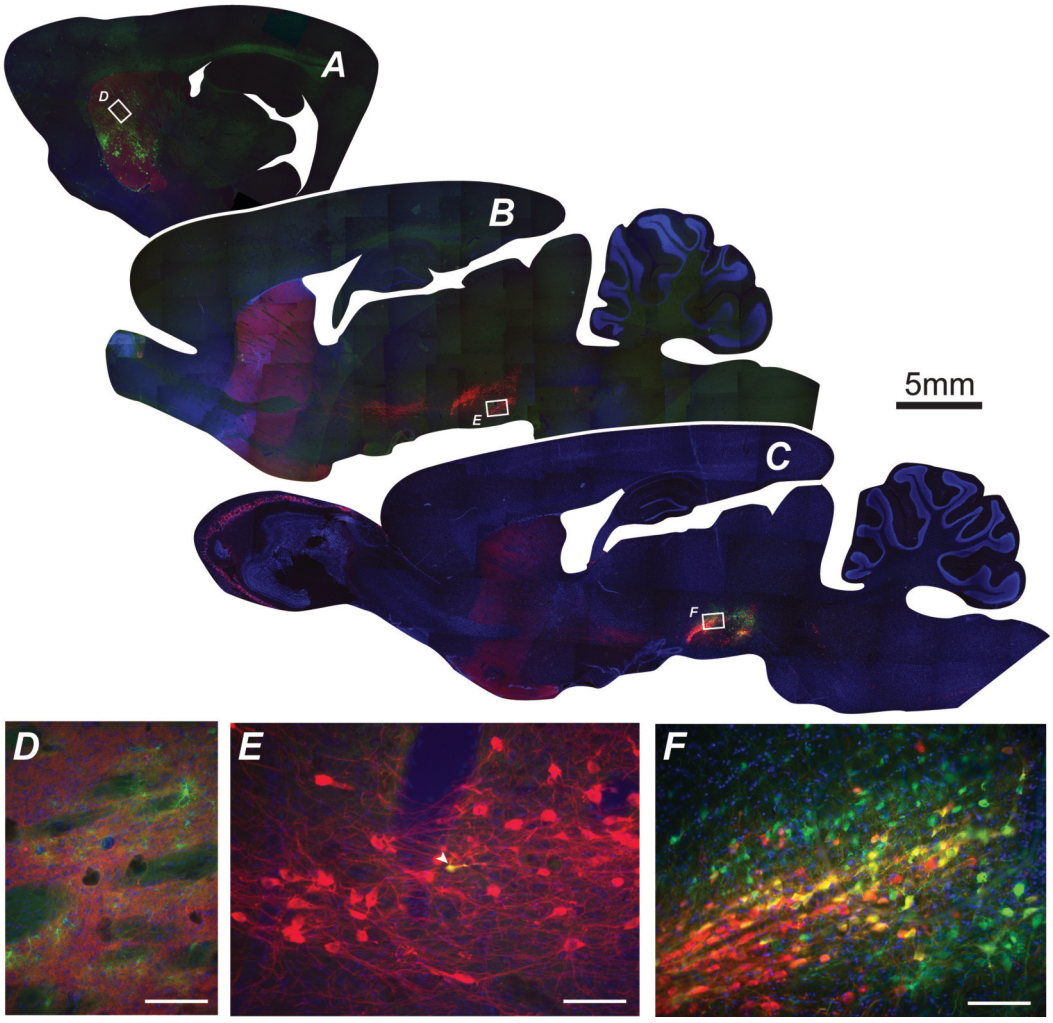

Figure 6-3 HIV-CDNF pseudotyped with Rabies-G or VSV-G delivered to the striatum or SNPC
[A/B] Rabies-G-pseudotyped HIV-GFP delivered to the striatum. Labelled boxes indicate close-up photos below showing ***[D]*** GFP in the striatum and ***[E]*** presence of one transduced TH+ neuron in the SNPC. ***[C]*** VSV-G-pseudotyped HIV-GFP delivered to the SNPC. ***[F]*** Close-up of SNPC indicated in ***[C]*** shows many TH+ neurons. **GFP**/**TH**/**DAPI**. Scale bar=200μm.

6.3.5 Testing HIV-CDNF-DD in the 6OHDA lesion rat model of Parkinson's disease

Adult male Wistar rats received infusions of VSV-G-pseudotyped HIV-CDNF-DD, HIV-CDNF (constitutive expression of CDNF) or HIV-GFP directly into the SNPC (for coordinates, see 6.2.6.3). In the same surgery, they received two

further infusions of 6OHDA in the striatum. This meant that the rats were lesioned at the same time as CDNF viral vector delivery. One day after surgery, some CDNF-DD rats were supplied chow that contained 0.2% TMP, while the remaining received a control diet. Two weeks later, apomorphine induced rotation behaviour was stimulated in the rats restrained in rotometer bowls (Method 6.2.7.2). Rotation data was also collected on weeks 3, 4, 6 and 8 post-lesion (Figure 6-4 *[A]*).

CDNF rats showed significantly lower number of turns over time compared to the control GFP rats. CDNF-DD rats not eating TMP also showed considerably reduced turning behaviour. These data suggested that the animals that received CDNF had a reduced dopaminergic deficit in the striatum that was induced by the 6-OHDA lesion, that is, CDNF protected dopamine neurons from degeneration. Unexpectedly, CDNF-DD rats maintained on a diet containing TMP immediately after surgery rotated substantially more than those that did not eat TMP. Rats that had been lesioned without viral vector infusion and maintained on a TMP diet also showed a similar increase in turning behaviour. CDNF-DD rats that had started eating TMP two weeks after surgery did not show an increase in turning behaviour (Figure 6-4 *[A]*).

To investigate the difference between CDNF-DD rats maintained on a TMP or a control diet, amphetamine was used to induce rotation behaviour. Rats that had been maintained on a TMP diet exhibited 8 fold more turning behaviour than rats eating a control diet (Figure 6-4 *[B]*).

These data indicate that TMP was affecting the drug-induced behaviour of the 6OHDA lesioned animals. Because animals that were not injected with vectors but were eating a TMP diet also increased in turns, we hypothesised that the effect was not due to problems caused by the overexpression of CDNF-DD, but rather that TMP was directly affecting the dopamine signalling pathway in these lesioned animals.

6.3.6 Testing the effects of TMP on rats with 6OHDA lesion

We considered that feeding the rats TMP immediately after surgery could be exacerbating the formation of the 6OHDA lesion. To investigate if delaying feeding abrogated this behaviour, rats lesioned as before were fed a normal diet for three weeks, before commencing on a TMP diet. During the three weeks, the apomorphine-induced turning behaviour was monitored to establish baseline readings. This data enabled distribution of the animals into groups, such that there was no difference in cumulative rotations between the groups. The lesioned rats were divided into 3 groups maintained on a diet of 0.2% TMP chow, a reduced 0.05% TMP chow or a control chow that did not contain TMP. Apomorphine-induced rotation behaviour was to be monitored over the following 8 weeks. However, during this experiment, rats developed self-mutilation behaviour and in order to prevent this the dose of apomorphine used to induce rotations was lowered. Furthermore, the harnesses for restraining the rats in the rotometer bowls were changed. These changes during the experiment made it difficult to draw firm conclusions from this part of the experiment. However, at 8 weeks post-lesion, amphetamine was used to induce rotation

behaviour. Rats that had been eating 0.2% and 0.05% TMP diet showed a 2.5 and 2.7 fold increase in rotation behaviour respectively (Figure 6-4 *[C]*).

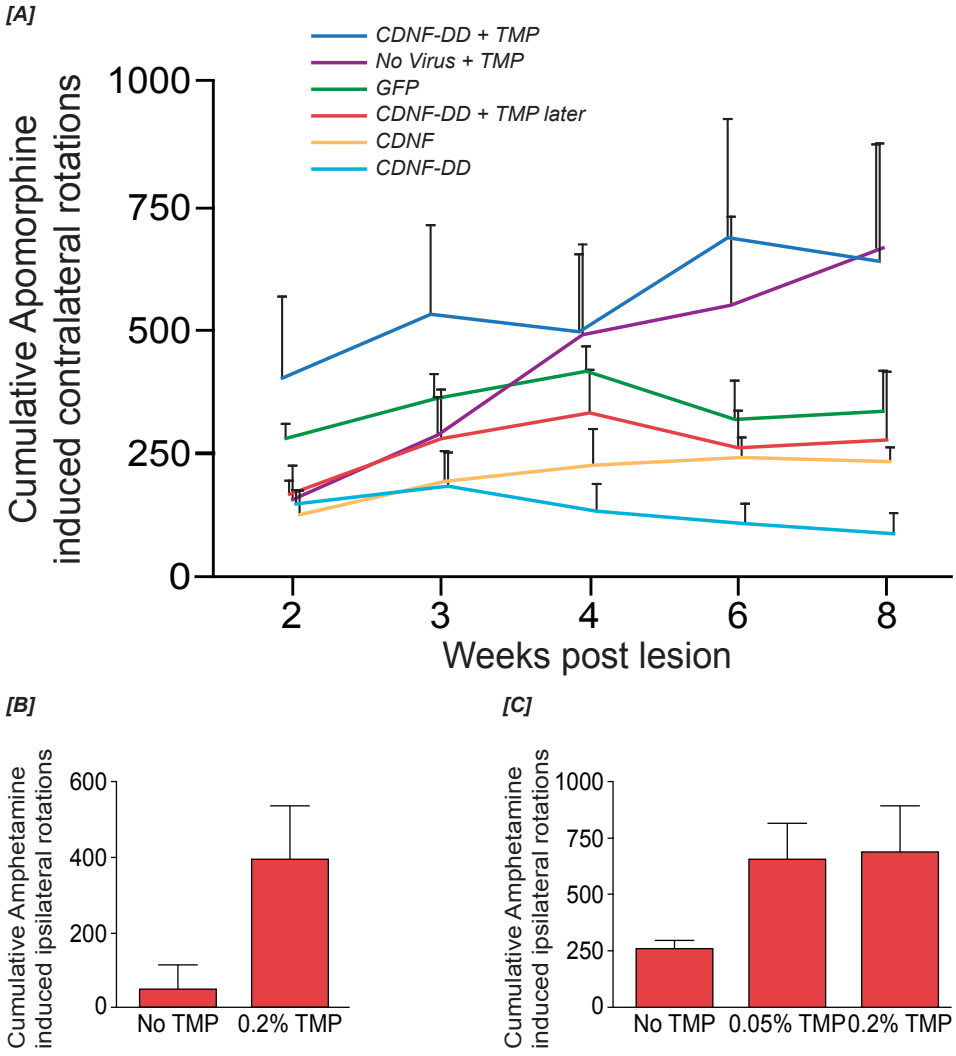

Figure 6-4 Rotation data of 6OHDA lesion rats
[A] Adult male Wistar rats lesioned with 6OHDA and expressing either CDNF, CDNF-DD, GFP or no virus and eating mashed chow containing 0.2% TMP as indicated in the graph key. Turning behaviour was induced by apomorphine and data collected over 90 minutes (n=3-6). ***[B]*** Cumulative amphetamine-induced rotations of CDNF-DD rats eating TMP or control diet (n=3). ***[C]*** Cumulative amphetamine-induced rotation of adult male Wistar rats lesioned with 6OHDA, commencing either a diet containing 0.05% TMP, 0.2%TMP or a control diet, three weeks post lesion (n=4).

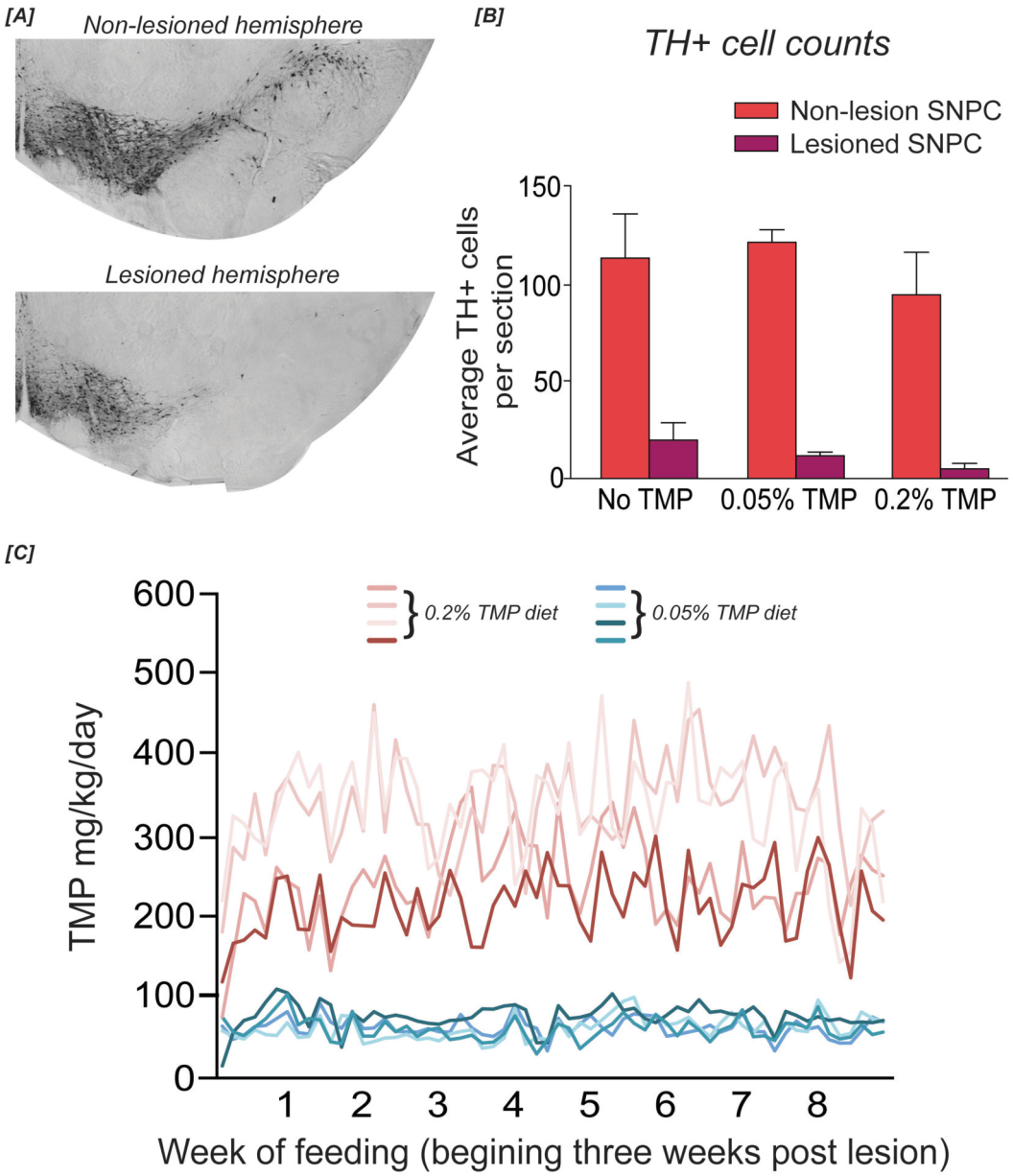

Figure 6-5 Counts of TH$^+$ cells in the SNPC
[A] Brains of 6OHDA lesion rats eating either 0.05% TMP, 0.2% TMP or a control diet were sectioned coronally. One fifth of the brain was immunohistochemically stained for tyrosine hydroxylase (TH) to reveal the neurons in the SNPC, substantia nigra pars reticulata, and VTA (ventral tegmental area). Neurons of the SNPC were counted over at least 7 sections per animal, an average was taken, before taking another average for each group ***[B]***. ***[C]*** TMP feeding data for rats on a diet of 0.2% TMP or 0.05% TMP over an 8 week period, commencing 3 three weeks after 6OHDA lesion. Rats receiving a 0.2% TMP diet ate an average 270mg/kg per day. Rats receiving a 0.05% TMP diet ate an average 70mg/kg per day.

6.4 Discussion

In this chapter, we aimed to fuse the DHFR destabilization domain to the CDNF protein in order to obtain regulatable secretion of CDNF in dopaminergic neurons in an *in vivo* model of Parkinson's disease. Fusion of the DHFR destabilization domain to the C-terminus of the CDNF protein resulted in TMP-responsive secretion of CDNF from neurons *in vitro* and *in vivo*. When we tested the efficacy of this regulatable CDNF in the 6-OHDA lesion rat model, we unexpectedly found that rats that received the CDNF-DD viral vector and maintained on a TMP diet showed an increase in dopaminergic deficit as assessed by drug-induced rotational behaviour.

CDNF is a secreted protein and the protein sequence of CDNF indicates that there is a 26 amino acid secretory signal at the N-terminus of the peptide (Lindholm et al., 2007). This means that any moiety placed at the N-terminus should be removed as the secretion signal is cleaved off upon entry into the endoplasmic reticulum. Therefore, we only developed a C-terminally tagged form of CDNF, using the DD domain that had given the best regulatory characteristics in earlier work (Chapter 4). When HEK293T cells expressing CDNF-DD were treated with TMP, there was a dose dependent increase in the levels of CDNF in the supernatant. While the transduced cells did not secret a detectable amount of CDNF in the absence of TMP, a small amount accumulated within the transduced cells which was partially removed in the presence of TMP. A similar trend was observed in E18 cortical neurons. It is currently unclear why accumulation of CDNF in the transduced cells in the

absence of TMP was observed. It is possible that the degradation of the fusion CDNF protein in the proteasome occurs at low efficiencies leading to accumulation of the protein in the cell, or that TMP on its own can affect the secretion of the CDNF protein.

As hCDNF is only 161 residues long after the removal of the 26-residue pro-sequence, it is encouraging that the 159-residue DHFR DD can regulate the levels of secreted CDNF. Not only is the DD nearly doubling the size of the small protein, but the C-terminus has an important role in CDNF secretion. The recent study by Sun et al explained that CDNF secondary structure is dominated by 8 α-helices. Using mutagenesis they inserted proline (α-helix blocker) between each one. When the proline was between the penultimate and final α-helices, CDNF was not efficiently sorted to secretory granules destined for the regulatory secretory pathway (Sun et al., 2011). While the DD may potentially be interfering with the folding of the C-terminus of the CDNF, we still saw dose dependent secretion when TMP was applied, suggesting constitutive secretion at least was still occurring.

To investigate the efficacy of using the CDNF-DD construct in an *in vivo* model of Parkinson's disease, we performed an expression study. We found that when TMP was added to the diet of rats that had received an infusion of HIV-CDNF-DD, there was markedly more CDNF present when we probed brain sections using immunohistochemistry. There was also very little CDNF present in animals receiving a control diet. Using a DAB staining protocol, we hoped that secreted CDNF could be visualized in a similar way to how the Björklund lab

recently visualised GDNF secretion (Decressac et al., 2011). We cannot be sure if the lack of the 'dark halo' of staining is due the CDNF-DD not being secreted as we see *in vitro*, or due to the antibody used in staining or methodologies used when harvesting or staining the brain. It is unlikely that this is due to insufficient viral transduction in the striatum, as viruses of similar titre have produced robust transduction in the striatum, as previously shown in this thesis (See chapters 3 and 4).

In unilaterally 6OHDA-lesioned rats, we had hoped that when HIV-CDNF-DD was used to transduce the SNPC of rats that also received a diet containing TMP, we would see a reduction in induced turning behaviour thus demonstrating that regulated CDNF expression is neuroprotective in this lesion model. However, in our experiments, we found that these animals exhibited increased turning behaviour compared to CDNF-DD rats on a TMP-absent diet, or animals that had received a control GFP vector.

High doses of TMP can lead to inhibition of protein and purine synthesis by inhibiting endogenous DHFR in mammalian cells. This could lead to the exacerbation of the effects of the 6OHDA, as cells fail to cope with the added burden. However, our data suggest that it was not TMP exacerbating the 6OHDA lesion that led to the increase in turning behaviour. When TMP diet was withheld until three weeks after lesion, the same effect was also seen. Cell degeneration and death induced by 6-OHDA in the lesion model occurs between one to four weeks and is usually complete within 4 weeks of administration of 6OHDA. The fact that the same effects were observed when TMP was

administered after the 6-OHDA lesion had stabilized suggested that TMP was not affecting the lesion size or characteristics per se. Furthermore, TH^+ cell counts in the SNPC reveal that there were no significant differences in TH+ cell counts between groups eating TMP eating a control diet (Figure 6-5*)*, suggesting that the effect of TMP on turning behaviour is not due increased death of DA neurons. This indicated that the behavioural read-out from these animals reflected differences in the levels of DA in rats eating TMP or a control diet. There are several documented cases of humans receiving high dose Trimethoprim-Sulphamexazole (TMP-SMX) medication developing tremors and movement disorders as side effects. Many of these are adult patients with AIDS (Borucki et al., 1988; Van Gerpen, 1988; Aboulafia, 1996; Salkind, 2000) while some were immunocompetent (Patterson and Couchenour, 1999; Dakin, 2009), including a child (Bua et al., 2005). Indeed, horses receiving high dose TMP medication also developed abnormal gait and erratic behaviour (Stack and Schott, 2011), suggesting this effect is not specific to humans. The one juvenile human reporting an adverse reaction had a deficiency in dihydropteridine reductase – an essential enzyme in the regeneration of tetra-hydrobiopterin (Woody and Brewster, 2008). This suggests a mechanism by which TMP fed to unilaterally 6OHDA lesioned rats can lead to increased turning behaviour.

Although mammalian DHFR (mDHFR) binds TMP 3000-fold less tightly than the *E. coli* DHFR (Matthews et al., 1985), off target effects will be seen when animals are consuming a particularly high TMP diet over long periods. mDHFR reduces 7,8-dihydropterin to tetrahydrobioperin, a cofactor required for the production of dopamine (Figure 6-6). Inhibition of mDHFR through TMP

binding could lead to a reduction in tetrahydrobiopterin synthesis, thereby leading to lowered DA levels. In unilaterally lesioned rats, TMP will also lead to an overall reduction in DA. However, the lesioned hemisphere will already have a dopamine deficit due to the loss of dopaminergic neurons, leading to an even greater differential between intact and lesioned hemispheres. We suggest that this increased fold difference between the hemisphere leads to the greater turning behaviour seen in rats eating a TMP diet. Further experiments will be required to confirm this hypothesis.

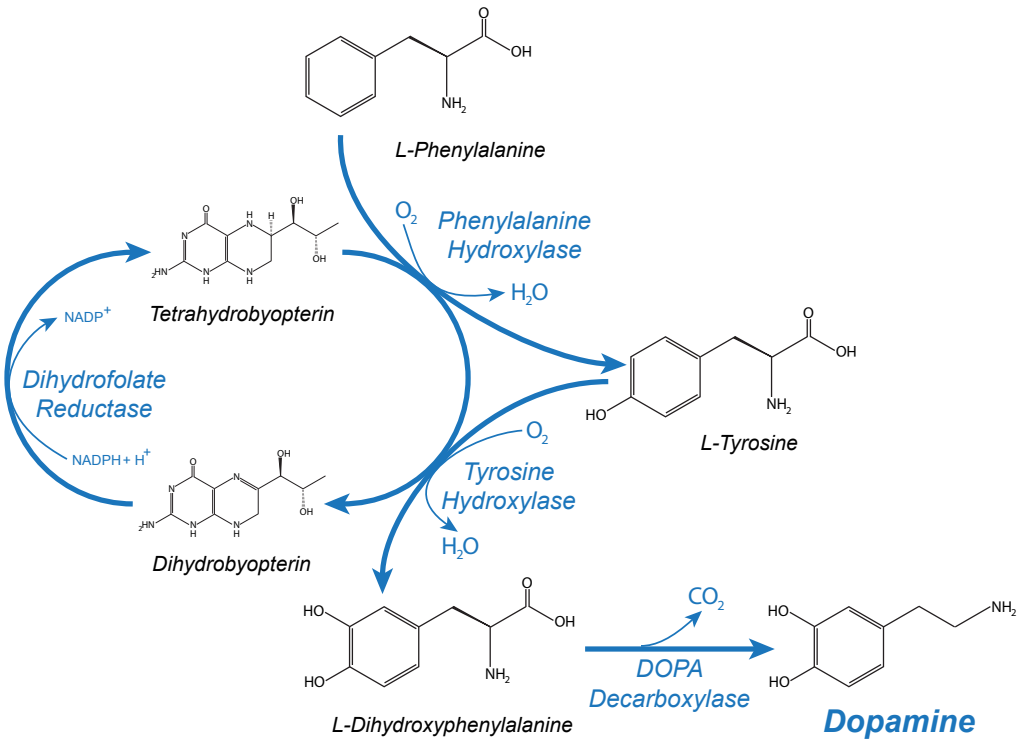

Figure 6-6 Dopamine synthesis schematic diagram

In patients, reducing or ceasing the TMP medication completely halted the side effects of tremor and movement disorders. Accordingly, we included a lower

TMP diet group in our experiment. Rats eating 0.2% TMP diet ate an average of 280mg/kg per day over the experiment, while those eating 0.05% TMP ate 70 mg/kg per day on average (Figure 6-5 *[C]*). However, we did not see a difference in the rotation behaviour of these animals. Further work must be carried out in order to find a dose of TMP that can be used *in vivo* to both activate a DHFR DD tagged GOI, yet not induce rotation behaviour. Since the start of these experiments, the Wandless lab have published their data on the DHFR DD system (Iwamoto et al., 2010). To activate the system in rat CNS, they used TMP supplied in the drinking water. The rats consumed approximately 20mg/kg per day and they saw activation of the system after three weeks. This suggests that a much lower dose of TMP could be used when investigating DD-tagged therapeutic genes, potentially abrogating the TMP-dependent turning behaviour we observed. However, in some cases it may be desirable to activate the system in a shorter time scale. Further studies are needed to fully elucidate the kinetics of the system *in vivo* when different feeding or dosing regimes are employed.

We observed that rats that received an infusion of CDNF-DD that ate a control diet actually exhibited the least amount of turning behaviour out of all the experimental groups. *In vitro* we saw low levels of CDNF-DD accumulating in cell bodies in the absence of TMP and although this basal activity was not detectable in immunostaining on brain sections from rats that had been maintained on a TMP-free diet, we suggest that low levels below the detection limit are present. Voutilainen et al noticed a dose dependent effect of CDNF when chronically infusing CDNF into lesioned rats, such that the highest dose

was not the best for protecting the DA neurons in the SNPC (Voutilainen et al., 2011). While further experiments would be needed to confirm this finding, it is possible that low levels of CDNF-DD can have a greater therapeutic effect than high levels.

CDNF-DD rats that commenced on a TMP diet two weeks later than other rats did not show an increase in rotation behaviour when TMP feeding began, suggesting that they had been made resistant to the effects of TMP by protection of DA neurons. Furthermore, animals infused with CDNF-DD (eating TMP or control diet) exhibited reduced amphetamine induced turning behaviour at 8 weeks post-lesion overall compared to control lesioned animals (eating TMP or control, respectively). Overall, this suggests that CDNF-DD can cause some degree of protection in the SNPC irrespective of TMP administration. Again, we would need to carry out more experiments with bigger group numbers to confirm these ideas.

Chapter 7 Discussion

7.1 Investigating the FKBP12-derived destabilisation (DD) regulatory system

In this study we set out to investigate a novel method of regulating the expression of therapeutic agents delivered via lentiviral vectors for the treatment of neurological disorders. We chose to assess the destabilisation domain technology developed by Thomas Wandless and colleagues (Banaszynski et al., 2006). This system consists of a mutated protein (FKBP12) domain that is unstable when expressed and immediately degraded, unless rescued by a stabilising ligand called Shield1. Fusion of this domain to a gene of interest (GOI) confers conditional instability onto the fusion partner. We designed two restriction enzyme-optimised cassettes: one with the destabilisation domain fused N-terminally to GFP, the other C-terminally to GFP. When Shield1 was supplied to HEK293T or E18 rat cortical neurons that had been transduced with lentiviral vectors expressing these cassettes, the N-terminally fused DD-GFP construct exhibited the lowest basal expression. Assessment of the kinetics of activation of the system indicated that maximal levels of induction are reached within 24 hours, although increases in GOI levels were seen almost immediately after addition of Shield1. This concurs with other studies using the FKBP12 DD system (Dolan et al., 2011; Skafte-Pedersen et al., 2012). Due to our experimental techniques, we were unable to determine the inactivation kinetics of the system, as this may be dependent on the GOI, which may influence the rate of degradation of the fusion protein in the absence of Shield1. However, reports have suggested that the half life of degradation is between 2.5 hours (Schoeber et al., 2009) and 4 hours (Banaszynski et al., 2006).

The means by which the DD leads to protein degradation was not completely resolved, although it has been observed that applying proteasome blockers in the absence of Shield1 lead to DD-fusions accumulating and these fusions co-localise with subunits of the proteasome (Banaszynski et al., 2006; Maynard-Smith et al., 2007). Recently, the Wandless laboratory discovered that FKBP-derived DD domains become ubiquitinated within minutes after removal of Shield1 (Egeler et al., 2011), indicating not only the involvement of the ubiquitin-proteasome system (UPS), but also the rapidity of the induction of degradation. Doxycycline or ecdysone regulated systems will not consistently match this speed for gene silencing, as they are dependent on the endogenous stability of the GOI. However, substrate recognition by the UPS is not well defined and therefore DD fusion proteins, especially DD fusion reporter proteins, could be useful as model substrates to help elucidate molecular mechanisms responsible for recognising and degrading misfolded cellular proteins.

We used the lentiviral vectors to transduce cells in the striatum of living rats. In animals that received a vector constitutively expressing GFP we observed abundant GFP expression in neurons. As Shield1 is not expected to cross the blood-brain-barrier (BBB), animals that had received a vector expressing DD-GFP received a second stereotactic intracranial injection to deliver Shield1. When the brains from these animals were analysed, only very weak GFP signal could be detected in the area surrounding the injection site. Investigation of the effects of increasing the multiplicity of infection (MOI) of the vectors in HEK293T cells indicated that the low level of expression seen at the injection

site in the animals was due to high MOI at the site of injection, not weak activation of the system. Investigation into the ability of Shield1 to cross the BBB is hindered by the significant cost of the ligand. Alternative regulatory systems, such as TetOn, and indeed the DFHR-based DD system, utilize a cheap, widely available activating ligand (Doxycycline and Trimethoprim respectively) that also crosses the BBB. This may explain why the FKBP12 DD system has been extensively utilised for *in vitro* studies, yet none of these are looking to regulate protein levels in either neurons or the CNS.

There have been three studies that utilize the FKBP12 DD system in living mice, all reporting the ability to regulate GOI satisfactorily and in two cases, tunably so. Maximal expression levels were reached in 12 hours after intravenous treatment with Shield1, and returned to baseline within 48 hours (Banaszynski et al., 2008; Rodriguez and Wolfgang, 2012). This is fast induction, most likely due to there being plentiful mRNA and protein already being produced at the time of Shield1 addition. Transcriptionally regulated systems take longer to reach maximal induction, as mRNA must be built up from very low levels. The inactivation kinetics are most likely related to the rate of clearance of Shield1 from the body. There are already several ligands in the Shield1 family and it is possible that looking for further derivatives may yield a ligand with more desirable pharmacokinetic properties.

While the reversibility of the DD system does allow for pulsatile expression of GOI (Kwan et al., 2011), this is restricted to pulses with a time course of approximately three days. For experiments investigating pulsatile expression of

GOI, defining the dose of Shield1 to give predictable levels of transgene over time is necessary; yet obtaining data such as this may be difficult for a therapeutic GOI. Wandless and colleagues used a DD-luciferase reporter expressed in tumourgenic xenografts in mice, providing them with quantifiable expression levels *in vivo* after delivery of Shield1. This approach could be adopted to allow quantifiable GOI expression by fusing luciferase to the DD-GOI fusion using a 2a self-cleaving peptide (Szymczak et al., 2004). As the both the DD-GOI and Luciferase are co-transcribed, the levels of luciferase could be used to approximate of the GOI. However, the presumed inability of Shield1 to cross the BBB makes it an unattractive candidate for further development of *in vivo* methodologies using the FKBP12 DD system. In addition, delivery of the ligand in this system *in vivo*, especially via an oral route, may be hampered by the significant cost of Shield1.

7.2 Investigating the DHFR-derived DD regulatory system

During the course of our study using the FKBP12 DD system, a second DD system was developed, comprising a mutated *E. coli* dihydrofolate reductase (DHFR) protein that is stabilized by trimethoprim (TMP) (Iwamoto et al., 2010). The Wandless laboratory selected two Ds, designed to be optimal for applying to either the N- or C-terminus of GOIs. The DD for applying to the N-terminus had three mutations ("3mut") while the C-terminal form had four ("4mut"). In the absence of published data at this time, we produced four DD/GOI constructs: both the "3mut" and "4mut" forms of DD were applied to both the N- and C-terminals of GFP. Lentiviral vectors of these constructs were used to transduce HEK293T cells and E18 cortical neurons. The "3mut" domain cloned to the C-terminus of GFP (GFP-3mutDD) was found to be the most destabilizing to GFP in the absence of TMP, yet exhibited a dose-dependent increase GPF levels in the presence of TMP.

In vivo, adult rats that had received a stereotactic injection of GFP-3mutDD into the striatum accumulated GFP after a stereotactic infusion of TMP into the same location three weeks later. However, TMP is highly absorbed from the gut and can cross the BBB, presenting a non-invasive method of activating the system. When the experiment was repeated and rats were fed a diet containing TMP, GFP accumulated in rats eating TMP, but not in animals eating a control diet.

Only three other studies have been reported since the system was first described. Interestingly, one of these was looking at regulating levels of GOI in neurons (Cohen et al., 2012). Cohen and colleagues used the DHFR DD system to

conditionally and spatially regulate the levels of both a small GTPase (RhoA) and the Wallerian degeneration slow protein (Wld^S) within neurons using a microfluidic culture platform. In the microfluidic devices, neuronal processes extend through narrow channels to a separate compartment that fluidically isolates them from the cell bodies of the neurons. This means TMP can be applied to the cell bodies alone, or to both cell bodies and axons, thereby potentially revealing the subcellular site of action of protein in neurons. Using this approach, they found that both RhoA and Wld^S exert their function (reducing NGF mediate neuron outgrowth, and protection of degenerating axons, respectively) primarily through their axonal pool.

A poster communication at the ESGCT conference (2011) reported regulation of glial-derived neurotrophic factor in the rat CNS, but this has not yet been published. The final study was based in *P. falciparum* and reported the ability of the system to dose dependently regulate the levels of the proteasome lid subunit Rpn6 in living parasites (Muralidharan et al., 2011). Prior to the development of the DFHR system, the FKBP12-DD system was one of the few methodologies available to conditionally proteins in this species and has received a lot of interest, despite Shield1 being toxic to the parasite (Russo et al., 2009).

In comparison to the FKBP12-based DD system, where Shield1 must be injected to animals, the DFHR-based system is advantageous, as TMP is rapidly absorbed from the gut and can therefore be supplied in the drinking water (Iwamoto et al., 2010) or in the diet. While this provides a non-invasive means to provide TMP, there will be fluctuations in dosage as animals do not eat

consistently throughout the day and night. It is also unclear at the present time, what proportion of the circulating TMP enters the central nervous system in rodents and more importantly in humans. While some pharmacokinetic data on TMP administration to rats has been reported and suggests TMP in the brain is about 10% that of the lung, kidneys and spleen, these focus of intravenous delivery of TMP (Tu et al., 1989). Information on the circulating levels of orally delivered TMP and its clearance rates by the liver in humans will probably be more readily available, as TMP is a commonly prescribed antibiotic for urinary tract infections, or used in combination with other drugs to treat pneumonia. Further studies would be needed to determine the impact of fluctuations in consumption of TMP have on the levels of TMP in circulation in the body and therefore on levels of DD GOI fusion proteins. Fluctuations in the levels of proteins in the CNS can be highly important in the context of gene therapy. For example, in the clinical trial of AADC therapy for Parkinson's disease, fluctuations in the oral dosing regime of L-DOPA can lead to L-DOPA-induced dyskinesia (Cress, 2008). If this form of regulatable gene therapy is applied to humans, it is quite likely that we will be able to control for fluctuations in TMP dosage by ensuring that regular doses of TMP are administered to patients.

In our experiments using the DFHR-based DD, we noticed some cells exhibited basal expression in the absence of TMP. One way to combat the 'leakiness' of the system would be to place the DD/GOI fusion cassette under the control of another form of regulatory system, such as a tetON system. In the off state (Dox and TMP absent), very little mRNA would be transcribed, and therefore very low amounts of destabilized proteins will be produced, which should be easily

degraded by the proteasome. While this may provide the tight regulation required for use in a clinical setting, compound systems are more complex, require more optimization to achieve correct dosage and present more safety risks. Also, the inclusion of another layer of regulation may affect the rate at which the system can be turned on, thereby negating the advantage of the quick tunability of the DHFR DD system.

It is clear that the site of the fusion of the DDs to the GOI should be optimized and rigorously tested for individual genes before selecting a configuration for use *in vivo*. We and others have found that the DDs should be tested at both the N- and C-terminals of the proteins, as the GOI may have effects of the efficiency of the DD system and vive versa (Ma et al., 2012). Interestingly, Sellmyer and colleagues (Sellmyer et al., 2012) showed that DD fusion proteins that were localised in the cytoplasm or nucleus can be efficiently degraded in mammalian cells; however, if the fusion proteins were targeted to the mitochondrial matrix or ER lumen, accumulation of the protein occurs even in the absence of ligand due to limited activation of the ubiquitin-proteasome system (UPS) and subsequent degradation of the DD. This suggests that specific cellular compartments such as the ER are tolerant of high DD levels in the absence of the ligand and that the DD is quite sensitive to local, compartment-specific protein quality control. This aspect of the DD technology should be considered when applied to different genes or proteins, for example tunability of mitochondrial or ER proteins may not be as readily achieved compared to nuclear or cytoplasmic proteins.

When looking at using the DD systems as potential tools for a clinical gene therapy, it is clear that more studies are required to determine the effects of high levels of DD fusion proteins in the targeted cells. As evidenced by diseases such as Parkinson's disease and Huntington's disease, neurons are particularly sensitive to accumulations of misfolded proteins. Therefore, safety concerns relating to the long-term overexpression of misfolding proteins must be raised. Furthermore, although TMP has been used for many years as a drug for human use and has very suitable pharmacokinetic properties, the interaction with the dopaminergic system is another serious concern, particularly after long periods of high trimethoprim consumption. There are, as yet, no other studies using the DFHR system *in vivo* (beyond proof of concept investigations).

As a tool to perturb the timing and levels of proteins of interest, DDs are powerful, offering a means to allow rapid, reversible and tunable of a wide range of different GOI. The DFHR-based DD is still very much in it infancy, yet it has advantages over the FKBP12-based system, particularly for use in the CNS, due to the desirable pharmacokinetic properties of the TMP ligand. As mentioned above, one potential application is to use the DD system to regulate protein levels in different subcompartments of an individual cell. The microfluidic devices that facilitate these studies will be described in more detail in the next section. Development of technologies not directly related to gene regulation may also prove useful. The Cornish lab at the University of Columbia were interested in developing a means to fluorescently label genes of interest, other than creating a GFP fusion protein. They initially demonstrated the feasibility of conjugating fluorophores to antifolates such as methotrexate and TMP and using these

molecules to visualise DHFR-GOI fusion proteins in cells (Miller et al., 2004) (Miller et al., 2005). Therefore, the chemistry has already been developed to visualize and stabilize DFHR-DD fusion proteins simultaneously, potentially allowing observation of the subcellular distribution of newly stabilized fusion proteins. Fluorophore-TMP binding to DHFR-DD is reversible, potentially allowing the DD system to be activated and inactivated (Calloway et al., 2007) in a dose dependent manner.

7.3 Developing a regulatable RARβ2 vector for use in nerve injury models

Yip and Wong et al. (Yip et al., 2006) had previously shown that a lentiviral vector overexpressing RARβ2 in the sensorimotor complex led to increased sprouting of corticospinal tract (CST) neurons and improvement in behavioural deficits in a rodent model of spinal cord injury. In this study, we aimed to capitulate this finding using a RARβ2 regulated the DFHR-based DD domain.

In vitro, we found that accumulation of RARβ2 could be dose dependently induced by TMP and reach high maximal levels. In neuronal cells, we found a higher degree of basal activity than observed in HEK293T cells but inducibility was maintained. Levels of DD-RARβ2 were increased in response to TMP in DRG cells, and this resulted in increased neurite outgrowth from DRGs This indicated the ability of DD-RARβ2 to induce TMP-dependent neurite outgrowth. When we assessed the efficacy of the DD-RARβ2 vector *in vivo*, we failed to see significant differences in behavioural tasks or numbers of newly sprouted axons between animals eating TMP or rats eating a control diet. The most likely reason for the lack of functional improvement observed in this study is the low group numbers in the experiments and the study will have to be repeated to confirm this finding. However, we cannot discount the possibility that fusing the DD to RARβ2 may have led to a partial loss of biological activity of RARβ2. To investigate this further, we proposed to develop a direct RARβ2 functional assay by cloning a luciferase reporter downstream of an RARβ2 responsive promoter.

The efficacy of the DD-RARβ2 to drive luciferase expression could then be compared to that of endogenous or constituently expressed RARβ2. Due to time constraints we were unable to complete these latter experiments.

Developing a regulatable form of RARβ2 therapy would have enabled us to investigate the effects of inducing or silencing RARβ2 overexpression at different time points after spinal cord injury, allowing us to determine if there is a therapeutic window for RARβ2 expression. Existing methodologies exploring the efficacy of RARβ2 expression has thus far required delivering the RARβ2 vector in advance of creating a spinal cord lesion. This does not allow us to determine if RARβ2 is a potential therapeutic agent for human spinal cord injury that will work after the injury has occurred. We had hoped to be able to inject the vector prior to lesion, yet induce RARβ2 levels at different time points after lesion. However, due to the outcome of the *in vivo* experiments and time constraints, we have not been able to perform such studies and therefore unable to determine if RARβ2 overexpression would be suitable as therapeutic intervention for spinal cord injury.

The mechanisms by which RARβ2 induces outgrowth of neurites from DRG or CST neurons is as yet unknown, but it is thought that RARβ2 can transcriptionally activate target genes and/or activate cAMP/Akt signalling pathways to stimulate growth from injured neurons. In cultured DRG neurons, RARβ2 overexpression leads to an increase in cytosolic cAMP (Wong et al., 2006), while in cerebellar granule neurons, RARβ induced phosphorylation of

Akt (Agudo et al., 2010). More recently it has been shown that RARβ2 can transcriptionally repress the expression of Lingo-1, a component of the Nogo receptor complex through which the myelin-derived inhibitory molecules signal to induce growth cone collapse (Puttagunta et al., 2011). Further studies such as microarray profiling to identify direct transcriptional targets of RARβ signalling following spinal cord injury and exploration of the interaction of RA- RARβ pathways with other pro-regenerative signals will yield insight into the complex molecular pathways that are involved during axonal regeneration.

Many of the interventions currently being explored are combination therapies, where two factors shown to have an effect on recovery after injury synergize to create a more efficacious treatment. As discussed in the introduction to this thesis, chondroitinase ABC (ChABC) is receiving a lot of interest as a potential therapy for spinal cord outgrowth after injury. Recently, lentiviral vectors have been used to deliver ChABC in a rat model of spinal cord injury (Zhao et al., 2011a). The extensive secretion of ChABC, both locally (spinal cord transduction) and from long-distance axon projections (striatal CST cell body transduction), reduced axonal recession and promoted sprouting and short-range regeneration of CST axons. Chondroitinase and RARβ2 therapies may work synergistically in a combination approach. This may be particularly useful, as ChABC will alleviate inhibition by chondroitin sulphate proteoglycans while RARβ2 can suppress myelin signalling through transcriptional repression of LINGO-1. A bicistronic vector could be used to deliver ChABC and RARβ2 together into the sensorimotor cortex. Alternatively the bicistronic lentiviral vector could be pseudotyped with a Rabies-G envelope glycoprotein which will

facilitate retrograde transport of the vector to the cell bodies of corticospinal neurons following injection into the lesion site (Wong et al., 2004). The advantages of using a Rabies-G pseudotyped lentiviral vector are two-fold: first, local expression of chondroitinase and RARβ2 will modify the inhibitory environment at the site of injury and second, retrograde transport of the vector in the injured corticospinal neurons and subsequent expression of RARβ2 and chondroitinase in these neurons can stimulate growth pathways and/or prevent atrophy. The combinatorial effects of RARβ2 and chondroitinase may have significant synergistic effects on axonal growth and plasticity, thereby facilitating repair and restoring spinal cord function.

When investigating DD-RARβ2 in DRG neurons we used methodology as described by Wong et al (Wong et al., 2006). However, recently developed microfluidic devices (Taylor et al., 2005) may provide an alternative methodology that is of particular interest when combined with the DHFR system. The devices consist of two media reservoirs separated by channels ("microgrooves") 10μm wide x 3μm high. Cells such as DRGs, plated into one reservoir will extend process through the microgrooves into the other reservoir, allowing separation of cell bodies from axon/dendrite material. By using slightly more media in one reservoir, a hydrostatic gradient can be produced, meaning that the compartments are fluidically isolated. Cohen and colleagues used this in combination with the DFHR system (Cohen et al., 2012). They found that they could stabilize DD-fusion proteins in the cell body compartment with TMP, yet the fluidic isolation prevents TMP penetrating the axonal compartment, thus preventing DD-fusion protein stabilization. Axonal stabilisation could be

rescued by addition of TMP to that compartment. Many proteins are translated locally at the synapse, therefore addition of TMP in the axonal fraction would stabilize molecules produced in the processes but not near the cell body. This tool could be of potential interest for studying factors that induce neurite outgrowth, by determining the location of both translation and biological action.

7.4 Developing a regulatable CDNF vector to test in models of Parkinson's disease

During the course of the study, the DHFR-based DD domain was also applied to regulate CDNF (conserved dopamine neurotrophic factor), a recently discovered neurotrophic factor that has been shown to mediate neuroprotection of dopaminergic neurons in rodent models of Parkinson's disease.

The DHFR-based DD was fused to the C-terminus of CDNF and by varying TMP concentrations we were able to regulate the levels of secreted CDNF produced by both cell lines and primary E18 rat cortical neurons transduced with HIV-CDNF-DD vector. When we injected this vector into rat striatum, we found that more CDNF accumulated in rats that had received a diet containing TMP compared to control rats. This suggested that CDNF levels in the brain can be regulated by TMP administration and therefore we proceeded to test this vector in the 6OHDA rat model of PD.

Infusion of the CDNF protein has previously been shown to protect neurons in the substantia nigra pars compacta (SNPC) from 6OHDA induced neurodegeneration (Lindholm et al., 2007). Here we used a lentiviral vector to overexpress CDNF or the CDNF-DD fusion protein in 6OHDA lesioned rats and assessed apomorphine/amphetamine-induced rotation behaviour. Animals that received the constitutively expressed CDNF showed a reduction in turning behaviour, however, we found that CDNF-DD rats that were maintained on a

TMP diet showed the opposite effect, that is, apomorphine/amphetamine rotation behaviour was increased.

This result was unexpected and upon closer examination of literature describing the use of TMP, we found reports that suggest that TMP treatment has also been responsible for Parkinsonian symptoms in human patients (Bua et al., 2005). Although the parental *E. coli* DHFR binds TMP at a much higher affinity compared to mammalian DHFR (approximately 3000-fold (Dauber-Osguthorpe et al., 1988)), it is possible that the high doses of TMP that were administered to the rats led to inhibition of endogenous DHFR which is required for the synthesis of the essential cofactor tetrahydrobiopterin (BH4). BH4 is an essential cofactor for tyrosine hydroxylase, the main enzyme responsible for catalysing the conversion of L-tyrosine into L-DOPA, and low levels of BH4 may have a significant impact on dopamine synthesis leading to lowered dopamine levels in the rats. The persistently low levels of dopamine in rats that were maintained on TMP diet may have led to heightened dopamine receptor sensitivity and upon injection of apomorphine/amphetamine, these receptors were hyper-activated resulting in an increased number of rotations during the behavioural assessment. The implications that this has on using the DHFR DD system in the CNS must be considered. In the paper published by Iwamoto et al. (2010) TMP was supplied to rats at a much lower dose and it is possible that using a lowered dose of TMP may not inhibit endogenous DFHR. At the moment, this is our working hypothesis and a number of future experiments may help clarify this unexpected result.

Dopamine is produced by both SHSY5Y cells and rodent ventral mesencephalon (VM) cultures. By exposing these cells or cultures to TMP, we can investigate if the concentrations of TMP that we used in our studies affect dopamine production by analysing dopamine levels in the culture supernatant using high-performance liquid chromatography (HPLC). Additionally, Western blotting could be used to investigate the levels of dopamine synthesis enzymes in the presence of TMP. *In vivo*, we could analyse cerebro-spinal-fluid (CSF) harvested from the striatum by microdialysis, to confirm that TMP causes changes in the levels of striatal dopamine.

The unexpected finding that long-term administration of TMP may lead to decreased dopamine levels in this study suggests that the use of this regulatable gene therapy system in PD should be approached with caution. A continuous supply of growth factors over a long period of time may lead to adverse effects and whilst it is desirable to be able to regulate levels of CDNF in a gene therapy approach for PD, more studies will have to be conducted to assess the off-target effects of TMP on endogenous dopamine production in the CNS.

7.5 Summary

Gene therapy approaches for neurodegenerative diseases would clearly benefit from novel vectors that allow for transient transgene delivery, for example by using gene promoters that automatically shut off after several weeks to months, or promoters that can respond to a changing environment by turning gene expression off once the transgene is no longer required. The ability to regulate the levels of the proteins that are produced from gene therapy vectors will greatly enhance their efficacy and safety thus increasing the appeal of genetic medicines in the clinic.

Here we have shown for the first time the use of the DFHR-based system in lentiviral vectors to regulate levels of two proteins – RARβ2 and CDNF – and have explored the use of these regulatable systems in a nerve injury model and PD model respectively. This system has now been used to regulate cytosolic proteins (GFP, YFP, Luciferase, RhoA, Rpn6 (Iwamoto et al., 2010; Muralidharan et al., 2011; Cohen et al., 2012)) predominantly nuclear proteins (Wld^s (Cohen et al., 2012)), nuclear receptors (RARβ2), transmembrane proteins (CD8α, β_2AR (Iwamoto et al., 2010)) and secreted proteins (CDNF), indicating the versatility of the system. While the use of DHFR-based regulatable gene therapy vectors is still in its infancy and more refinement will be required before further applications, it will be interesting to see how other studies develop this technology in the future. The ultimate goal of gene therapy will be to deliver genetic medicines in a regulatable, safe and efficacious manner.

Chapter 8 References

Aboulafia DM (1996) Tremors associated with trimethoprim-sulfamethoxazole therapy in a patient with AIDS: case report and review. Clinical Infectious Diseases 22:598–600.

Abremski K, Hoess R, Sternberg N (1983) Studies on the properties of P1 site-specific recombination: Evidence for topologically unlinked products following recombination. Cell 32:1301–1311.

Agudo M, Yip P, Davies M, Bradbury E, Doherty P, McMahon S, Maden M, Corcoran JPT (2010) A retinoic acid receptor beta agonist (CD2019) overcomes inhibition of axonal outgrowth via phosphoinositide 3-kinase signalling in the injured adult spinal cord. Neurobiology of Disease 37:147–155.

Agwuh KN, MacGowan A (2006) Pharmacokinetics and pharmacodynamics of the tetracyclines including glycylcyclines. Journal of Antimicrobial Chemotherapy 58:256–265.

Airaksinen MS, Saarma M (2002) The GDNF family: signalling, biological functions and therapeutic value. Nat Rev Neurosci 3:383–394.

Aiuti A, Slavin S, Aker M, Ficara F, Deola S, Mortellaro A, Morecki S, Andolfi G, Tabucchi A, Carlucci F, Marinello E, Cattaneo F, Vai S, Servida P, Miniero R, Roncarolo MG, Bordignon C (2002) Correction of ADA-SCID by stem cell gene therapy combined with nonmyeloablative conditioning. Science 296:2410–2413.

Albanese C, Reutens AT, Bouzahzah B, Fu M, D'Amico M, Link T, Nicholson R, Depinho RA, Pestell RG (2000) Sustained mammary gland-directed, ponasterone A-inducible expression in transgenic mice. FASEB J 14:877–884.

Ali RR (2012) Gene therapy for retinal dystrophies: twenty years in the making. Human Gene Therapy 23:337–339.

Anon (1996) A double-blind placebo-controlled clinical trial of subcutaneous recombinant human ciliary neurotrophic factor (rHCNTF) in amyotrophic lateral sclerosis. ALS CNTF Treatment Study Group. Neurology 46:1244–1249.

Arakaki AK, Tian W, Skolnick J (2006) High precision multi-genome scale reannotation of enzyme function by EFICAz. BMC Genomics 7:315.

Asokan A, Schaffer DV, Jude Samulski R (2012) The AAV Vector Toolkit: Poised at the Clinical Crossroads. Mol Ther 20:699–708.

Azzouz M, Le T, Ralph GS, Walmsley L, Monani UR, Lee DCP, Wilkes F, Mitrophanous KA, Kingsman SM, Burghes AHM, Mazarakis ND (2004a) Lentivector-mediated SMN replacement in a mouse model of spinal muscular atrophy. The Journal of Clinical Investigation 114:1726–1731.

Azzouz M, Martin-Rendon E, Barber RD, Mitrophanous KA, Carter EE, Rohll JB, Kingsman SM, Kingsman AJ, Mazarakis ND (2002) Multicistronic lentiviral vector-mediated striatal gene transfer of aromatic L-amino acid decarboxylase, tyrosine hydroxylase, and GTP cyclohydrolase I induces sustained transgene expression, dopamine production, and functional improvement in a rat model of Parkinson's disease. The Journal of Neuroscience 22:10302–10312.

Azzouz M, Ralph GS, Storkebaum E, Walmsley LE, Mitrophanous KA, Kingsman SM, Carmeliet P, Mazarakis ND (2004b) VEGF delivery with retrogradely transported lentivector prolongs survival in a mouse ALS model. Nature 429:413–417.

Bachmair A, Finley D, Varshavsky A (1986) In vivo half-life of a protein is a function of its amino-terminal residue. Science 234:179–186.

Bachmair A, Varshavsky A (1989) The degradation signal in a short-lived protein. Cell 56:1019–1032.

Bain J, McLauchlan H, Elliott M, Cohen P (2003) The specificities of protein kinase inhibitors: an update. Biochemical Journal 371:199–204.

Balabaskaran Nina P, Morrisey JM, Ganesan SM, Ke H, Pershing AM, Mather MW, Vaidya AB (2011) ATP synthase complex of Plasmodium falciparum: dimeric assembly in mitochondrial membranes and resistance to genetic disruption. The Journal of Biological Chemistry 286:41312–41322.

Balmer JE, Blomhoff R (2002) Gene expression regulation by retinoic acid. Journal of lipid research 43:1773–1808.

Banaszynski L, Chen L, Maynard-Smith L, Lisa Ooi A, Wandless T (2006) A Rapid, Reversible, and Tunable Method to Regulate Protein Function in Living Cells Using Synthetic Small Molecules. Cell 126:995–1004.

Banaszynski LA, Sellmyer MA, Contag CH, Wandless TJ, Thorne SH (2008) Chemical control of protein stability and function in living mice. Nature Medicine 14:1123–1127.

Bankiewicz KS, Forsayeth J, Eberling JL, Sanchez-Pernaute R, Pivirotto P, Bringas J, Herscovitch P, Carson RE, Eckelman W, Reutter B, Cunningham J (2006) Long-term clinical improvement in MPTP-lesioned primates after gene therapy with AAV-hAADC. Mol Ther 14:564–570.

Barcia C, Jimenez-Dalmaroni M, Kroeger KM, Puntel M, Rapaport AJ, Larocque D, King GD, Johnson SA, Liu C, Xiong W, Candolfi M, Mondkar S, Ng P, Palmer D, Castro MG, Lowenstein PR (2007) One-year expression from high-capacity adenoviral vectors in the brains of animals with pre-existing anti-adenoviral immunity: clinical implications. Mol Ther 15:2154–2163.

Barling RWA, Selkont JB (1978) The penetration of antibiotics into cerebrospinal fluid and brain tissue. Journal of Antimicrobial Chemotherapy 4:203–227.

Baron U, Bujard H (2000) Tet repressor-based system for regulated gene expression in eukaryotic cells: Principles and advances. Methods in Enzymology 327:401–421.

Bartel MA, Weinstein JR, Schaffer DV (2012) Directed evolution of novel adeno-associated viruses for therapeutic gene delivery. Gene Therapy 19:694–700.

Bartlett JS, Samulski RJ, McCown TJ (1998) Selective and rapid uptake of adeno-associated virus type 2 in brain. Human Gene Therapy 9:1181–1186.

Bartus RT, Herzog CD, Chu Y, Wilson A, Brown L, Siffert J, Johnson EM, Olanow CW, Mufson EJ, Kordower JH (2011) Bioactivity of AAV2-neurturin gene therapy (CERE-120): Differences between Parkinson's disease and nonhuman primate brains. Movement Disorders 26:27–36.

Bastien J, Rochette-Egly C (2004) Nuclear retinoid receptors and the transcription of retinoid-target genes. Gene 328:1–16.

Bathori M, Toth N, Hunyadi A, Marki A, Zador E (2008) Phytoecdysteroids and Anabolic-Androgenic Steroids - Structure and Effects on Humans. Current Medicinal Chemistry 15:75–91.

Batshaw ML, Wilson JM, Raper S, Yudkoff M, Robinson MB (1999) Recombinant adenovirus gene transfer in adults with partial ornithine transcarbamylase deficiency (OTCD). Human Gene Therapy 10:2419–2437.

Bayle JH, Grimley JS, Stankunas K, Gestwicki JE, Wandless TJ, Crabtree GR (2006) Rapamycin Analogs with Differential Binding Specificity Permit Orthogonal Control of Protein Activity. Chemistry & Biology 13:99–107.

Beattie MS, Farooqui AA, Bresnahan JC (2000) Review of current evidence for apoptosis after spinal cord injury. J Neurotrauma 17:915–925.

Bellefroid EJ, Poncelet DA, Lecocq PJ, Revelant O, Martial JA (1991) The evolutionarily conserved Krüppel-associated box domain defines a subfamily of eukaryotic multifingered proteins. PNAS 88:3608–3612.

Bergman I, Burckart G, Pohl C, Venkataramanan R, Barmada MA, Griffin JA,

Cheung N-KV (1998) Pharmacokinetics of IgG and IgM Anti-Ganglioside Antibodies in Rats and Monkeys after Intrathecal Administration. Journal of Pharmacology and Experimental Therapeutics 284:111–115.

Bianco Lo C, Déglon N, Pralong W, Aebischer P (2004) Lentiviral nigral delivery of GDNF does not prevent neurodegeneration in a genetic rat model of Parkinson's disease. Neurobiology of Disease 17:283–289.

Björklund A, Rosenblad C, Winkler C, Kirik D (1997) Studies on neuroprotective and regenerative effects of GDNF in a partial lesion model of Parkinson's disease. Neurobiology of Disease 4:186–200.

Blaese RM, Culver KW, Miller AD, Carter CS, Fleisher T, Clerici M, Shearer G, Chang L, Chiang Y, Tolstoshev P, Greenblatt JJ, Rosenberg SA, Klein H, Berger M, Mullen CA, Ramsey WJ, Muul L, Morgan RA, Anderson WF (1995) T Lymphocyte-Directed Gene Therapy for ADA- SCID: Initial Trial Results After 4 Years. Science 270:475–480.

Bommer M, Benecke A, Gronemeyer H, Rochette-Egly C (2002) TIF2 Mediates the Synergy between RARα1 Activation Functions AF-1 and AF-2. The Journal of Biological Chemistry 277:37961–37966.

Borucki MJ, Matzke DS, Pollard RB (1988) Tremor Induced by Trimethoprim-Sulfamethoxazole in Patients with the Acquired Immunodeficiency Syndrome (AIDS). Ann Intern Med 109:77–78.

Boudreau RL, McBride JL, Martins I, Shen S, Xing Y, Carter BJ, Davidson BL (2009) Nonallele-specific silencing of mutant and wild-type huntingtin demonstrates therapeutic efficacy in Huntington's disease mice. Mol Ther 17:1053–1063.

Bradbury EJ, Carter LM (2011) Manipulating the glial scar: chondroitinase ABC as a therapy for spinal cord injury. Brain Research Bulletin 84:306–316.

Bradbury EJ, Moon LDF, Popat RJ, King VR, Bennett GS, Patel PN, Fawcett JW, McMahon SB (2002) Chondroitinase ABC promotes functional recovery after spinal cord injury. Nature 416:636–640.

Bregman BS, McAtee M, Dai HN, Kuhn PL (1997) Neurotrophic factors increase axonal growth after spinal cord injury and transplantation in the adult rat. Experimental Neurology 148:475–494.

Brocard J, Warot X, Wendling O, Messaddeq N, Vonesch JL, Chambon P, Metzger D (1997) Spatio-temporally controlled site-specific somatic mutagenesis in the mouse. PNAS 94:14559–14563.

Broekman MLD, Comer LA, Hyman BT, Sena-Esteves M (2006) Adeno-associated virus vectors serotyped with AAV8 capsid are more efficient than AAV-1 or -2 serotypes for widespread gene delivery to the neonatal mouse brain. Neuroscience 138:501–510.

Brooks CF, Johnsen H, van Dooren GG, Muthalagi M, Lin SS, Bohne W, Fischer K, Striepen B (2010) The toxoplasma apicoplast phosphate translocator links cytosolic and apicoplast metabolism and is essential for parasite survival. Cell Host Microbe 7:62–73.

Bua J, Marchetti F, Barbi E, Sarti A, Ventura A (2005) Tremors and chorea induced by trimethoprim-sulfamethoxazole in a child with Pneumocystis pneumonia. Pediatr Infect Dis J 24:934–935.

Buckley RH (2002) Gene therapy for SCID—a complication after remarkable progress. The Lancet 360:1185–1186.

Burger C, Nash K, Mandel RJ (2005) Recombinant Adeno-Associated Viral Vectors in the Nervous System. Human Gene Therapy 16:781–791.

Calloway NT, Choob M, Sanz A, Sheetz MP, Miller LW, Cornish VW (2007) Optimized Fluorescent Trimethoprim Derivatives for in vivo Protein Labeling. Chembiochem 8:767–774.

Canonica L, Danieli B, Weisz-Vincze I (1972) Structure of muristerone A, a new phytoecdysone. JCS Chem Comm:1060–1061.

Carlson S, Parrish M, Springer J, Doty K, Dosset L (1998) Acute Inflammatory Response in Spinal Cord Following Impact Injury. Experimental Neurology 151:77–88.

Cavazzana-Calvo M, Hacein-Bey S, de Saint Basile G, Gross F, Yvon E, Nusbaum P, Selz F, Hue C, Certain S, Casanova JL, Bousso P, Deist FL, Fischer A (2000) Gene therapy of human severe combined immunodeficiency (SCID)-X1 disease. Science 288:669–672.

Chambon P (1994) The retinoid signaling pathway: molecular and genetic analyses. Seminars in Cell Biology 5:115–125.

Chambon P (1996) A decade of molecular biology of retinoic acid receptors. FASEB J 10:940–954.

Chau CH, Shum DKY, Li H, Pei J, Lui YY, Wirthlin L, Chan YS, Xu XM (2004) Chondroitinase ABC enhances axonal regrowth through Schwann cell-seeded guidance channels after spinal cord injury. FASEB J 18:194–196.

Chen KH, Wu CH, Tseng CC, Shiau JM, Lee CT, Lin CRL (2008) Intrathecal coelectrotransfer of a tetracycline-inducible, three-plasmid-based system to achieve tightly regulated antinociceptive gene therapy for mononeuropathic rats. The Journal of Gene Medicine 10:208–216.

Cheng H, Cao Y, Olson L (1996) Spinal cord repair in adult paraplegic rats: partial restoration of hind limb function. Science 273:510–513.

Cheng H, Liao K-K, Liao S-F, Chuang T-Y, Shih Y-H (2004) Spinal Cord Repair With Acidic Fibroblast Growth Factor as a Treatment for a Patient With Chronic Paraplegia. Spine 29:E284–E288.

Chenuaud P (2004) Optimal Design of a Single Recombinant Adeno-associated Virus Derived from Serotypes 1 and 2 to Achieve More Tightly Regulated Transgene Expression from Nonhuman Primate Muscle. Molecular Therapy 9:410–418.

Clackson T, Yang W, Rozamus LW, Hatada M, Amara JF, Rollins CT, Stevenson LF, Magari SR, Wood SA, Courage NL, Lu X, Cerasoli F, Gilman M, Holt DA (1998) Redesigning an FKBP-ligand interface to generate chemical dimerizers with novel specificity. PNAS 95:10437–10442.

Cohen MS, Ghosh AK, Kim HJ, Jeon NL, Jaffrey SR (2012) Chemical genetic-mediated spatial regulation of protein expression in neurons reveals an axonal function for wld(s). Chemistry & Biology 19:179–187.

Corcoran J, Maden M (1999) Nerve growth factor acts via retinoic acid synthesis to stimulate neurite outgrowth. Nature Neuroscience 2:307–308.

Corcoran J, Shroot B, Pizzey J, Maden M (2000) The role of retinoic acid receptors in neurite outgrowth from different populations of embryonic mouse dorsal root ganglia. J Cell Sci 113 :2567–2574.

Corcoran J, So P-L, Barber RD, Vincent KJ, Mazarakis ND, Mitrophanous KA, Kingsman SM, Maden M (2002) Retinoic acid receptor beta2 and neurite outgrowth in the adult mouse spinal cord in vitro. J Cell Sci 115:3779–3786.

Corish P, Taylor-Smith C (1999) Attenuation of green fluorescent protein half-life in mammalian cells. Protein Engineering 12:1035–1040.

Coughlan L, Alba R, Parker AL, Bradshaw AC, McNeish IA, Nicklin SA, Baker AH (2010) Tropism-modification strategies for targeted gene delivery using adenoviral vectors. Viruses 2:2290–2355.

Cress DE (2008) The need for regulatable vectors for gene therapy for Parkinson's disease. Experimental Neurology 209:30–33.

Cronin J, Zhang X-Y, Reiser J (2005) Altering the tropism of lentiviral vectors through pseudotyping. Current Gene Therapy 5:387–398.

Crowe MJ, Bresnahan JC, Shuman SL, Masters JN, Crowe MS (1997) Apoptosis and delayed degeneration after spinal cord injury in rats and monkeys. Nature Medicine 3:73–76.

Cummings BJ, Uchida N, Tamaki SJ, Salazar DL, Hooshmand M, Summers R, Gage FH, Anderson AJ (2005) Human neural stem cells differentiate and promote locomotor recovery in spinal cord-injured mice. PNAS 102:14069–

14074.

Dakin LE (2009) Probable trimethoprim/sulfamethoxazole-induced higher-level gait disorder and nocturnal delirium in an elderly man. The Annals 43:129–133.

Danielian PS, Muccino D, Rowitch DH, Michael SK, McMahon AP (1998) Modification of gene activity in mouse embryos in utero by a tamoxifen-inducible form of Cre recombinase. Current biology 8:1323–1326.

Danthinne X, Imperiale MJ (2000) Production of first generation adenovirus vectors: a review. Gene Therapy 7:1707–1714.

Dauber-Osguthorpe P, Roberts VA, Osguthorpe DJ, Wolff J, Genest M, Hagler AT (1988) Structure and energetics of ligand binding to proteins:Escherichia coli dihydrofolate reductase-trimethoprim, a drug-receptor system. Proteins 4:31–47.

Dauer W, Przedborski S (2003) Parkinson's Disease: Mechanisms andn Models. Neuron 39:889–909.

Davies SP, Reddy H, Caivano M, Cohen P (2000) Specificity and mechanism of action of some commonly used protein kinase inhibitors. Biochemical Journal 351:95–105.

Davis GC, Williams AC, Markey SP, Ebert MH, Caine ED, Reichert CM, Kopin IJ (1979) Chronic Parkinsonism secondary to intravenous injection of meperidine analogues. Psychiatry Res 1:249–254.

Dawson TM, Ko HS, Dawson VL (2010) Genetic Animal Models of Parkinson's Disease. Neuron 66:646–661.

Dawson VL, Dawson TM (1996) Free radicals and neuronal cell death. Cell Death Differ 3:71–78.

de Azevedo MF, Gilson PR, Gabriel HB, Simões RF, Angrisano F, Baum J, Crabb BS, Wunderlich G (2012) Systematic analysis of FKBP inducible degradation domain tagging strategies for the human malaria parasite Plasmodium falciparum. PLoS ONE 7:e40981.

de The H, del Mar Vivanco-Ruiz M, Tiollais P, Stunnenberg H, Dejean A (1990) Identification of a retinoic acid responsive element in the retinoic acid receptor beta gene. Nature 343:177–180.

Decressac M, Ulusoy A, Mattsson B, Georgievska B, Romero-Ramos M, Kirik D, Björklund A (2011) GDNF fails to exert neuroprotection in a rat α-synuclein model of Parkinson's disease. Brain 134:2302–2311.

Deuschle U, Meyer WK, Thiesen HJ (1995) Tetracycline-reversible silencing of eukaryotic promoters. Molecular and Cellular Biology 15:1907–1914.

Dinan L, Lafont R (2006) Effects and applications of arthropod steroid hormones (ecdysteroids) in mammals. Journal of Endocrinology 191:1–8.

Dinan L, Savchenko T, Whiting P (2001) On the distribution of phytoecdysteroids in plants. Cellular and Molecular Life Sciences 58:1121–1132.

Dodge JC, Treleaven CM, Fidler JA, Hester M, Haidet A, Handy C, Rao M, Eagle A, Matthews JC, Taksir TV, Cheng SH, Shihabuddin LS, Kaspar BK (2010) AAV4-mediated expression of IGF-1 and VEGF within cellular components of the ventricular system improves survival outcome in familial ALS mice. Mol Ther 18:2075–2084.

Dohmen R, Wu P, Varshavsky A (1994) Heat-inducible degron: a method for constructing temperature-sensitive mutants. Science 263:1273–1276.

Dolan BP, Li L, Velez L, Ireland CM, Bennink JR, Yewdell JW (2011) Distinct pathways generate peptides from defective ribosomal products for CD8+ T cell immunosurveillance. J Immunol 186:2065–2072.

Dominguez E, Marais T, Chatauret N, Benkhelifa-Ziyyat S, Duque S, Ravassard P, Carcenac R, Astord S, Pereira de Moura A, Voit T, Barkats M (2011) Intravenous scAAV9 delivery of a codon-optimized SMN1 sequence rescues SMA mice. Hum Mol Genet 20:681–693.

Dowd E, Monville C, Torres EM, Wong L-F, Azzouz M, Mazarakis ND, Dunnett SB (2005) Lentivector-mediated delivery of GDNF protects complex motor functions relevant to human Parkinsonism in a rat lesion model. Eur J Neurosci 22:2587–2595.

Drouet V, Perrin V, Hassig R, Dufour N, Auregan G, Alves S, Bonvento G, Brouillet E, Luthi-Carter R, Hantraye P, Déglon N (2009) Sustained effects of nonallele-specific Huntingtin silencing. Annals of Neurology 65:276–285.

Duan D, Yue Y, Yan Z, Engelhardt JF (2002) Trans-splicing vectors expand the packaging limits of adeno-associated virus for gene therapy applications. Methods in Molecular Medicine.

Dull T, Zufferey R, Kelly M, Mandel RJ, Nguyen M, Trono D, Naldini L (1998) A third-generation lentivirus vector with a conditional packaging system. Journal of Virology 72:8463–8471.

Dumont RJ, Okonkwo DO, Verma S, Hurlbert RJ, Boulos PT, Ellegala DB, Dumont AS (2001) Acute Spinal Cord Injury, Part I: Pathophysiologic Mechanisms. Clinical Neuropharmacology 24:254–264.

Egeler EL, Urner LM, Rakhit R, Liu CW, Wandless TJ (2011) Ligand-switchable substrates for a ubiquitin-proteasome system. The Journal of Biological Chemistry 286:31328–31336.

Eger K et al. (2004) 4-Epidoxycycline: an alternative to doxycycline to control gene expression in conditional mouse models. Biochem Biophys Res Commun 323:979–986.

Elsworth JD, Roth RH (1997) Dopamine synthesis, uptake, metabolism, and receptors: relevance to gene therapy of Parkinson's disease. Experimental Neurology 144:4–9.

Erles K, Sebökovà P, Schlehofer JR (1999) Update on the prevalence of serum antibodies (IgG and IgM) to adeno-associated virus (AAV). Journal of Medical Virology 59:406–411.

Evans JR, Barker RA (2008) Neurotrophic factors as a therapeutic target for Parkinson's disease. Expert Opin Ther Targets 12:437–447.

Farrell A, Thirugnanam S, Lorestani A, Dvorin JD, Eidell KP, Ferguson DJP, Anderson-White BR, Duraisingh MT, Marth GT, Gubbels M-J (2012) A DOC2 protein identified by mutational profiling is essential for apicomplexan parasite exocytosis. Science 335:218–221.

Faull RL, Laverty R (1969) Changes in dopamine levels in the corpus striatum following lesions in the substantia nigra. Experimental Neurology 23:332–340.

Favre D, Blouin V, Provost N, Spisek R, Porrot F, Bohl D, Marmé F, Chérel Y, Salvetti A, Hurtrel B, Heard J-M, Rivière Y, Moullier P (2002) Lack of an Immune Response against the Tetracycline-Dependent Transactivator Correlates with Long-Term Doxycycline-Regulated Transgene Expression in Nonhuman Primates after Intramuscular Injection of Recombinant Adeno-Associated Virus. Journal of Virology 76:11605–11611.

Fawcett JW, Asher RA (1999) The glial scar and central nervous system repair. Brain Research Bulletin 49:377–391.

Feil R, Brocard J, Mascrez B, LeMeur M, Metzger D, Chambon P (1996) Ligand-activated site-specific recombination in mice. PNAS 93:10887–10890.

Ferrari FK, Samulski T, Shenk T, Samulski RJ (1996) Second-strand synthesis is a rate-limiting step for efficient transduction by recombinant adeno-associated virus vectors. Journal of Virology 70:3227–3234.

Ferrari FK, Xiao X, Mccarty D, Samulski RJ (1997) New developments in the generation of Ad-free, high-titer rAAV gene therapy vectors. Nature Medicine 3:1295–1297.

Follenzi A, Ailles LE, Bakovic S, Geuna M, Naldini L (2000) Gene transfer by lentiviral vectors is limited by nuclear translocation and rescued by HIV-1 pol sequences. Nat Genet 25:217–222.

Fornai F, Schlüter OM, Lenzi P, Gesi M, Ruffoli R, Ferrucci M, Lazzeri G, Busceti CL, Pontarelli F, Battaglia G, Pellegrini A, Nicoletti F, Ruggieri S, Paparelli A, Südhof TC (2005) Parkinson-like syndrome induced by continuous MPTP infusion: convergent roles of the ubiquitin-proteasome system and alpha-synuclein. Proc Natl Acad Sci USA 102:3413–3418.

Forno LS (1996) Neuropathology of Parkinson's Disease. J Neuropathol Exp Neurol 55:259.

Forsayeth J, Eberling J, Sanftner L, Zhen Z, Bringas J, Cunningham J, Bankiewicz K (2006) A Dose-Ranging Study of AAV-hAADC Therapy in Parkinsonian Monkeys. Molecular Therapy 14:571–577.

Foust KD, Wang X, McGovern VL, Braun L, Bevan AK, Haidet AM, Le TT, Morales PR, Rich MM, Burghes AHM, Kaspar BK (2010) Rescue of the spinal muscular atrophy phenotype in a mouse model by early postnatal delivery of SMN. Nat Biotechnol 28:271–274.

Frampton AR, Goins WF, Nakano K, Burton EA, Glorioso JC (2005) HSV trafficking and development of gene therapy vectors with applications in the nervous system. Gene Therapy 12:891–901.

Franz S, Weidner N, Blesch A (2012) Gene therapy approaches to enhancing plasticity and regeneration after spinal cord injury. Experimental Neurology 235:62–69.

Freundlieb S, Müller CS, Bujard H (1999) A tetracycline controlled activation/repression system with increased potential for gene transfer into mammalian cells. The Journal of Gene Medicine 1:4–12.

Galimi F, Saez E, Gall J, Hoong N, Cho G, Evans RM, Verma M (2005) Development of Ecdysone-Regulated Lentiviral Vectors. Molecular Therapy 11:142–148.

Gao Y, Deng K, Hou J, Bryson JB, Barco A, Nikulina E, Spencer T, Mellado W, Kandel ER, Filbin MT (2004) Activated CREB is sufficient to overcome inhibitors in myelin and promote spinal axon regeneration in vivo. Neuron 44:609–621.

Gardaneh M, O'Malley KL (2004) Rat tyrosine hydroxylase promoter directs tetracycline-inducible foreign gene expression in dopaminergic cell types. Molecular Brain Research 126:173–180.

Gash DM, Zhang Z, Ovadia A, Cass WA, Yi A, Simmerman L, Russell D, Martin D, Lapchak PA, Collins F, Hoffer BJ, Gerhardt GA (1996) Functional recovery in parkinsonian monkeys treated with GDNF. Nature 380:252–255.

Gasic GP, Hollmann M (1992) Molecular Neurobiology of Glutamate Receptors. Annu Rev Physiol 54:507–536.

Gasser T (2009) Molecular pathogenesis of Parkinson disease: insights from genetic studies. Expert Rev Mol Med 11:e22.

Georgievska B, Jakobsson J, Persson E, Ericson C, Kirik D, Lundberg C (2004a) Regulated delivery of glial cell line-derived neurotrophic factor into rat striatum, using a tetracycline-dependent lentiviral vector. Human Gene Therapy 15:934–944.

Georgievska B, Kirik D, Björklund A (2002) Aberrant sprouting and downregulation of tyrosine hydroxylase in lesioned nigrostriatal dopamine neurons induced by long-lasting overexpression of glial cell line derived neurotrophic factor in the striatum by lentiviral gene transfer. Experimental Neurology 177:461–474.

Georgievska B, Kirik D, Björklund A (2004b) Overexpression of Glial Cell Line-Derived Neurotrophic Factor Using a Lentiviral Vector Induces Time- and Dose-Dependent Downregulation of Tyrosine Hydroxylase in the Intact Nigrostriatal Dopamine System. The Journal of Neuroscience 24:6437–6445.

Gharami K, Xie Y, An JJ, Tonegawa S, Xu B (2008) Brain-derived neurotrophic factor over-expression in the forebrain ameliorates Huntington's disease phenotypes in mice. Journal of Neurochemistry 105:369–379.

Gill SS, Patel NK, Hotton GR, O'Sullivan K, McCarter R, Bunnage M, Brooks DJ, Svendsen CN, Heywood P (2003) Direct brain infusion of glial cell line-derived neurotrophic factor in Parkinson disease. Nature Medicine 9:589–595.

Ginhoux F, Turbant S, Gross DA, Poupiot J, Marais T, Lone Y, Lemonnier FA, Firat H, Perez N, Danos O, Davoust J (2004) HLA-A*0201-restricted cytolytic responses to the rtTA transactivator dominant and cryptic epitopes compromise transgene expression induced by the tetracycline on system. Molecular Therapy 10:279–289.

Gore A et al. (2011) Somatic coding mutations in human induced pluripotent stem cells. Nat Cell Biol 471:63–67.

Gossen M, Bujard H (1992) Tight control of gene expression in mammalian cells by tetracycline-responsive promoters. PNAS 89:5547–5551.

Gossen M, Freundlieb S, Bender G, Muller G, Hillen W (1995) Transcriptional activation by tetracyclines in mammalian cells. Science 268:1766–1769.

Gould DJ, Berenstein M, Dreja H, Ledda F, Podhajcer OL, Chernajovsky Y (2000) A novel doxycycline inducible autoregulatory plasmid which displays "on"/“off” regulation suited to gene therapy applications. Gene Therapy 7:2061–2070.

Goverdhana S, Puntel M, Xiong W, Zirger JM, Barcia C, Curtin JF, Soffer EB,

Mondkar S, King GD, Hu J, Sciascia SA, Candolfi M, Greengold DS, Lowenstein PR, castro MG (2005) Regulatable gene expression systems for gene therapy applications: progress and future challenges. Mol Ther 12:189–211.

Graham DG (1978) Oxidative pathways for catecholamines in the genesis of neuromelanin and cytotoxic quinones. Mol Pharmacol 14:633–643.

Grimpe B, Silver J (2002) The extracellular matrix in axon regeneration. Elsevier.

Gu H, Marth JD, Orban PC, Mossmann H, Rajewsky K (1994) Deletion of a DNA polymerase beta gene segment in T cells using cell type-specific gene targeting. Science 265:103–106.

Guest JD, Hiester ED, Bunge RP (2005) Demyelination and Schwann cell responses adjacent to injury epicenter cavities following chronic human spinal cord injury. Experimental Neurology 192:384–393.

Guiner CL, Stieger K, Snyder RO, Rolling F, Moullier P (2007) Immune Responses to Gene Product of Inducible Promoters. Current Gene Therapy 7:334–346.

Gwendalyn D King JFCMCKKPRLMGC (2005) Gene Therapy and Targeted Toxins for Glioma. Current Gene Therapy 5:535.

Hacein-Bey-Abina S, Kalle von C, Schmidt M, Le Deist F, Wulffraat N, McIntyre E, Radford I, Villeval J-L, Fraser CC, Cavazzana-Calvo M, Fischer A (2003) A serious adverse event after successful gene therapy for X-linked severe combined immunodeficiency. N Engl J Med 348:255–256.

Hameyer D, Loonstra A, Eshkind L, Schmitt S, Antunes C, Groen A, Bindels E, Jonkers J, Krimpenfort P, Meuwissen R, Rijswijk L, Bex A, Berns A, Bockamp E (2007) Toxicity of ligand-dependent Cre recombinases and generation of a conditional Cre deleter mouse allowing mosaic recombination in peripheral tissues. Physiol Genomics 31:32–41.

Hamilton DL, Abremski K (1984) Site-specific recombination by the bacteriophage P1 lox-Cre system. Cre-mediated synapsis of two lox sites. J Mol Biol 178:481–486.

Han Y, Chang QA, Virag T, West NC, George D, castro MG, Bohn MC (2010) Lack of humoral immune response to the tetracycline (Tet) activator in rats injected intracranially with Tet-off rAAV vectors. Gene Therapy 17:616–625.

Hanks M, Wurst W, Anson-Cartwright L, Auerbach AB, Joyner AL (1995) Rescue of the En-1 mutant phenotype by replacement of En-1 with En-2. Science 269:679–682.

Harding TC, Geddes BJ, Murphy D, Knight D, Uney JB (1998) Switching transgene expression in the brain using an adenoviral tetracycline-regulatable system. Nat Biotechnol 16:553–555.

Harnish PP, Samuel K (1988) Reduced Cerebrospinal Fluid Production in the Rat and Rabbit by Diatrizoate Ventriculocisternal Perfusion. Investigative Radiology 23:534–636.

Harper SQ, Staber PD, He X, Eliason SL, Martins IH, Mao Q, Yang L, Kotin RM, Paulson HL, Davidson BL (2005) RNA interference improves motor and neuropathological abnormalities in a Huntington's disease mouse model. Proc Natl Acad Sci USA 102:5820–5825.

Harrow S, Papanastassiou V, Harland J, Mabbs R, Petty R, Fraser M, Hadley D, Patterson J, Brown SM, Rampling R (2004) HSV1716 injection into the brain adjacent to tumour following surgical resection of high-grade glioma: safety data and long-term survival. Gene Therapy 11:1648–1658.

He Z, Koprivica V (2004) The Nogo signaling pathway for regeneration block. Annu Rev Neurosci 27:341–368.

Hermens WTJMC, Verhaagen J (1997) Adenoviral Vector-Mediated Gene Expression in the Nervous System of Immunocompetent Wistar and T Cell-Deficient nude Rats: Preferential Survival of Transduced Astroglial Cells in nude Rats. Human Gene Therapy 8:1049–1063.

Herzog CD, Dass B, Gasmi M, Bakay R, Stansell JE, Tuszynski M, Bankiewicz KS, Chen EY, Chu Y, Bishop K, Kordower JH, Bartus RT (2008) Transgene Expression, Bioactivity, and Safety of CERE-120 (AAV2-Neurturin) Following Delivery to the Monkey Striatum. Molecular Therapy 16:1737–1744.

Herzog CD, Dass B, Holden JE, Stansell J III, Gasmi M, Tuszynski M, Bartus RT, Kordower JH (2007) Striatal delivery of CERE-120, an AAV2 vector encoding human neurturin, enhances activity of the dopaminergic nigrostriatal system in aged monkeys. Movement Disorders 22:1124–1132.

Hirsch EC, Hunot S (2009) Neuroinflammation in Parkinson's disease: a target for neuroprotection? Lancet Neurol 8:382–397.

Hoess RH, Ziese M, Sternberg N (1982) P1 site-specific recombination: nucleotide sequence of the recombining sites. PNAS 79:3398–3402.

Hong M, Mukhida K, Mendez I (2008) GDNF therapy for Parkinson’s disease. Expert Rev Neurotherapeutics 8:1125–1139.

Hoppe UC, Marbán E, Johns DC (2000) Adenovirus-mediated inducible gene expression in vivo by a hybrid ecdysone receptor. Mol Ther 1:159–164.

Horger BA, Nishimura MC, Armanini MP, Wang L-C, Poulsen KT, Rosenblad

C, Kirik D, Moffat B, Simmons L, Johnson E, Milbrandt J, Rosenthal A, Björklund A, Vandlen RA, Hynes MA, Phillips HS (1998) Neurturin Exerts Potent Actions on Survival and Function of Midbrain Dopaminergic Neurons. The Journal of Neuroscience 18:4929–4937.

Huang EJ, Reichardt LF (2001) Neurotrophins: roles in neuronal development and function. Annu Rev Neurosci 24:677–736.

Hutson TH, Verhaagen J, Yanez-Muñoz RJ, Moon LDF (2011) Corticospinal tract transduction: a comparison of seven adeno-associated viral vector serotypes and a non-integrating lentiviral vector. Gene Therapy 19:49–60.

Imanishi M, Nakamura A, Doi M, Futaki S, Okamura H (2011) Control of Circadian Phase by an Artificial Zinc Finger Transcription Regulator. Angew Chem Int Ed 50:9396–9399.

Iuliucci JD, Oliver SD, Morley S, Ward C, Ward J, Dalgarno D, Clackson T, Berger HJ (2001) Intravenous safety and pharmacokinetics of a novel dimerizer drug, AP1903, in healthy volunteers. J Clin Pharmacol 41:870–879.

Iwamoto M, Björklund T, Lundberg C, Kirik D, Wandless TJ (2010) A General Chemical Method to Regulate Protein Stability in the Mammalian Central Nervous System. Chemistry & Biology 17:981–988.

Iwanami A, Kaneko S, Nakamura M, Kanemura Y, Morillon E, Kobayashi S, Yamasaki M, Momoshima S, Ishii H, Ando K, Tanioka Y, Tamaoki N, Nomura T, Toyama Y, Okano H (2005) Transplantation of human neural stem cells for spinal cord injury in primates. Journal of Neuroscience Research 80:182–190.

Jakeman LB, Reier PJ (1991) Axonal projections between fetal spinal cord transplants and the adult rat spinal cord: a neuroanatomical tracing study of local interactions. J Comp Neurol 307:311–334.

Jarraya B, Boulet S, Ralph GS, Jan C, Bonvento G, Azzouz M, Miskin JE, Shin M, Delzescaux T, Drouot X, Hérard A-S, Day DM, Brouillet E, Kingsman SM, Hantraye P, Mitrophanous KA, Mazarakis ND, Palfi S (2009) Dopamine gene therapy for Parkinson's disease in a nonhuman primate without associated dyskinesia. Sci Transl Med 1:2ra4.

Jeon BS, Jackson-Lewis V, Burke RE (1995) 6-Hydroxydopamine lesion of the rat substantia nigra: time course and morphology of cell death. Neurodegeneration 4:131–137.

Jones LL, Margolis RU, Tuszynski MH (2003) The chondroitin sulfate proteoglycans neurocan, brevican, phosphacan, and versican are differentially regulated following spinal cord injury. Experimental Neurology 182:399–411.

Jones LL, Yamaguchi Y, Stallcup WB (2002) NG2 is a major chondroitin sulfate proteoglycan produced after spinal cord injury and is expressed by macrophages and oligodendrocyte progenitors. The Journal of Neuroscience 22:2792–2803.

Jones TB, McDaniel EE, Popovich PG (2005) Inflammatory-Mediated Injury and Repair in the Traumatically Injured Spinal Cord. curr pharm des 11:1223–1236.

Jones-Villeneuve EM, Rudnicki MA, Harris JF, McBurney MW (1983) Retinoic acid-induced neural differentiation of embryonal carcinoma cells. Molecular and Cellular Biology 3:2271–2279.

Kadoya K, Tsukada S, Lu P, Coppola G, Geschwind D, Filbin MT, Blesch A, Tuszynski MH (2009) Combined intrinsic and extrinsic neuronal mechanisms facilitate bridging axonal regeneration one year after spinal cord injury. Neuron 64:165–172.

Kafri T, Morgan D, Krahl T, Sarvetnick N, Sherman L, Verma I (1998) Cellular immune response to adenoviral vector infected cells does not require de novo viral gene expression: Implications for gene therapy. PNAS 95:11377–11382.

Kanemaki M, Sanchez-Diaz A, Gambus A, Labib K (2003) Functional proteomic identification of DNA replication proteins by induced proteolysis in vivo. Nature 423:720–724.

Kaplitt MG, Feigin A, Tang C, Fitzsimons HL, Mattis P, Lawlor PA, Bland RJ, Young D, Strybing K, Eidelberg D, During MJ (2007) Safety and tolerability of gene therapy with an adeno-associated virus (AAV) borne GAD gene for Parkinson's disease: an open label, phase I trial. Lancet 369:2097–2105.

Karimi-Abdolrezaee S, Eftekharpour E, Wang J, Morshead CM, Fehlings MG (2006) Delayed Transplantation of Adult Neural Precursor Cells Promotes Remyelination and Functional Neurological Recovery after Spinal Cord Injury. The Journal of Neuroscience 26:3377–3389.

Kaspar BK, Lladó J, Sherkat N, Rothstein JD, Gage FH (2003) Retrograde viral delivery of IGF-1 prolongs survival in a mouse ALS model. Science 301:839–842.

Keirstead HS, Nistor G, Bernal G, Totoiu M, Cloutier F, Sharp K, Steward O (2005) Human embryonic stem cell-derived oligodendrocyte progenitor cell transplants remyelinate and restore locomotion after spinal cord injury. J Neurosci 25:4694–4705.

Kellendonk C, Tronche F, Casanova E, Anlag K, Opherk C, Schütz G (1999) Inducible site-specific recombination in the brain. J Mol Biol 285:175–182.

Kellendonk C, Tronche F, Monaghan AP, Angrand PO, Stewart F, Schütz G (1996) Regulation of Cre recombinase activity by the synthetic steroid RU 486. Nucleic Acids Res 24:1404–1411.

Kells AP, Henry RA, Connor B (2008) AAV-BDNF mediated attenuation of quinolinic acid-induced neuropathology and motor function impairment. Gene Therapy 15:966–977.

Kirik D, Georgievska B, Björklund A (2004) Localized striatal delivery of GDNF as a treatment for Parkinson disease. Nature Neuroscience 7:105–110.

Kirik D, Rosenblad C, Björklund A (1998) Characterization of behavioral and neurodegenerative changes following partial lesions of the nigrostriatal dopamine system induced by intrastriatal 6-hydroxydopamine in the rat. Experimental Neurology 152:259–277.

Kistner A, Gossen M, Zimmermann F, Jerecic J, Ullmer C, Lübbert H, Bujard H (1996) Doxycycline-mediated quantitative and tissue-specific control of gene expression in transgenic mice. PNAS 93:10933–10938.

Kluge RM, Spaulding DM, Spain AJ (1978) Combination of Pentamidine and Trimethoprim-Sulfamethoxazole in the Therapy of Pneumocystis carinii Pneumonia in Rats. Antimicrobial Agents and Chemotherapy 13:975–978.

Kochanek S, Clemens PR, Mitani K, Chen HH, Chan S, Caskey CT (1996) A new adenoviral vector: Replacement of all viral coding sequences with 28 kb of DNA independently expressing both full-length dystrophin and beta-galactosidase. PNAS 93:5731–5736.

Koda M, Okada S, Nakayama T, Koshizuka S, Kamada T, Nishio Y, Someya Y, Yoshinaga K, Okawa A, Moriya H, Yamazaki M (2005) Hematopoietic stem cell and marrow stromal cell for spinal cord injury in mice. NeuroReport 16:1763–1767.

Kohn DB, Sadelain M, Glorioso JC (2003) Occurrence of leukaemia following gene therapy of X-linked SCID. Nat Rev Cancer 3:477–488.

Kordower JH et al. (2000) Neurodegeneration prevented by lentiviral vector delivery of GDNF in primate models of Parkinson's disease. Science 290:767–773.

Kordower JH, Herzog CD, Dass B, Bakay RAE, Stansell J III, Gasmi M, Bartus RT (2006) Delivery of neurturin by AAV2 (CERE-120)-mediated gene transfer provides structural and functional neuroprotection and neurorestoration in MPTP-treated monkeys. Annals of Neurology 60:706–715.

Kordower JH, Palfi S, Chen EY, Ma SY, Sendera T, Cochran EJ, Mufson EJ, Penn R, Goetz CG, Comella CD (1999) Clinicopathological findings

following intraventricular glial-derived neurotrophic factor treatment in a patient with Parkinson's disease. Annals of Neurology 46:419–424.

Koshizuka S, Okada S, Okawa A, Koda M, Murasawa M, Hashimoto M, Kamada T, Yoshinaga K, Murakami M, Moriya H, Yamazaki M (2004) Transplanted Hematopoietic Stem Cells from Bone Marrow Differentiate into Neural Lineage Cells and Promote Functional Recovery after Spinal Cord Injury in Mice. J Neuropathol Exp Neurol 63:64–72.

Kotin RM, Linden RM, Berns KI (1992) Characterization of a preferred site on human chromosome 19q for integration of adeno-associated virus DNA by non-homologous recombination. The EMBO Journal 11:5071.

Kotzbauer PT, Lampe PA, Heuckeroth RO, Golden JP, Creedon DJ, Johnson EM Jr, Milbrandt J (1996) Neurturin, a relative of glial-cell-line-derived neurotrophic factor. Nature 384:467–470.

Kubo I, Klocke J (1983) Plant Resistance to Insects. J Am Chem Soc 83:329–346.

Kumer SC, Vrana KE (1996) Intricate regulation of tyrosine hydroxylase activity and gene expression. Journal of Neurochemistry 67:443–462.

Kwan MD, Sellmyer MA, Quarto N, Ho AM, Wandless TJ, Longaker MT (2011) Chemical control of FGF-2 release for promoting calvarial healing with adipose stem cells. The Journal of Biological Chemistry 286:11307–11313.

Lakso M, Sauer B, Mosinger B, Lee EJ, Manning RW, Yu SH, Mulder KL, Westphal H (1992) Targeted oncogene activation by site-specific recombination in transgenic mice. PNAS 89:6232–6236.

Lamartina S, Roscilli G, Rinaudo CD, Sporeno E, Silvi L, Hillen W, Bujard H, Cortese R, Ciliberto G, Toniatti C (2002) Stringent Control of Gene Expression In Vivo by Using Novel Doxycycline-Dependent Trans-Activators. Human Gene Therapy 13:199–210.

Lamartina S, Silvi L, Roscilli G, Casimiro D, Simon AJ, Davies M-E, Shiver JW, Rinaudo CD, Zampaglione I, Fattori E, Colloca S, Paz OG, Laufer R, Bujard H, Cortese R, Ciliberto G, Toniatti C (2003) Construction of an rtTA2s-m2/ttskid-Based transcription regulatory switch that displays no basal activity, good inducibility, and high responsiveness to doxycycline in mice and Non-Human primates. Molecular Therapy 7:271–280.

Lang AE et al. (2006) Randomized controlled trial of intraputamenal glial cell line-derived neurotrophic factor infusion in Parkinson disease. Annals of Neurology 59:459–466.

Langston JW, Ballard P, Tetrud JW, Irwin I (1983) Chronic Parkinsonism in humans due to a product of meperidine-analog synthesis. Science 219:979–

980.

Langston JW, Forno LS, Tetrud J, Reeves AG, Kaplan JA, Karluk D (1999) Evidence of active nerve cell degeneration in the substantia nigra of humans years after 1-methyl-4-phenyl-1,2,3,6-tetrahydropyridine exposure. Annals of Neurology 46:598–605.

Lapenna S, Dinan L, Friz J, Hopfinger AJ, Liu J, Hormann RE (2009) Semi-Synthetic Ecdysteroids as Gene-Switch Actuators: Synthesis, Structure-Activity Relationships, and Prospective ADME Properties. ChemMedChem 4:55–68.

Latta-Mahieu M, Rolland M, Caillet C, Wang M, Kennel P, Mahfouz I, Loquet I, Dedieu J-F, Mahfoudi A, Trannoy E, Thuillier V (2002) Gene transfer of a chimeric trans-activator is immunogenic and results in short-lived transgene expression. Human Gene Therapy 13:1611–1620.

Law LK, Davidson BL (2005) What does it take to bind CAR? Mol Ther 12:599–609.

Leclerc G, Boockfor F, Faught W, Frawley LS (2000) Development of a Destabilized Firefly Luciferase Enzymes for Measurement of Gene Expression. Biotechniques 29:590–601.

Lee H, Puppala D, Choi E-Y, Swanson H, Kim K-B (2007) Targeted degradation of the aryl hydrocarbon receptor by the PROTAC approach: a useful chemical genetic tool. Chembiochem 8:2058–2062.

Lee Y-S, Lin C-Y, Robertson RT, Hsiao I, Lin VW (2004) Motor recovery and anatomical evidence of axonal regrowth in spinal cord-repaired adult rats. J Neuropathol Exp Neurol 63:233–245.

Lees AJ, Hardy J, Revesz T (2009) Parkinson's disease. Lancet 373:2055–2066.

Leff SE, Spratt SK, Snyder RO, Mandel RJ (1999) Long-term restoration of striatal L-aromatic amino acid decarboxylase activity using recombinant adeno-associated viral vector gene transfer in a rodent model of Parkinson's disease. Neuroscience 92:185–196.

Lehrman S (1999) Virus treatment questioned after gene therapy death. Nature 401:517–518.

Leid M, Kastner P, Chambon P (1992) Multiplicity generates diversity in the retinoic acid signalling pathways. Trends in Biochemical Sciences 17:427–433.

Lemons ML, Howland DR, Anderson DK (1999) Chondroitin Sulfate Proteoglycan Immunoreactivity Increases Following Spinal Cord Injury and Transplantation. Experimental Neurology 160:51–65.

Leong HS, Lizardo MM, Ablack A, McPherson VA, Wandless TJ, Chambers AF, Lewis JD (2012) Imaging the Impact of Chemically Inducible Proteins on Cellular Dynamics In Vivo. PLoS ONE 7:e30177.

Levi ADO, Dancausse H, Li X, Duncan S, Horkey L, Oliviera M (2002) Peripheral nerve grafts promoting central nervous system regeneration after spinal cord injury in the primate. J Neurosurg 96:197–205.

LeWitt PA, Rezai AR, Leehey MA, Ojemann SG, Flaherty AW, Eskandar EN, Kostyk SK, Thomas K, Sarkar A, Siddiqui MS, Tatter SB, Schwalb JM, Poston KL, Henderson JM, Kurlan RM, Richard IH, Meter LV, Sapan CV, During MJ, Kaplitt MG, Feigin A (2011) AAV2-GAD gene therapy for advanced Parkinson's disease: a double-blind, sham-surgery controlled, randomised trial. Lancet Neurol 10:309–319.

Li H, He Z, Su T, Ma Y, Lu S, Dai C, Sun M (2003) Protective action of recombinant neurturin on dopaminergic neurons in substantia nigra in a rhesus monkey model of Parkinson's disease. Neurol Res 25:263–267.

Liberles SD, Diver ST, Austin DJ, Schreiber SL (1997) Inducible gene expression and protein translocation using nontoxic ligands identified by a mammalian three-hybrid screen. PNAS 94:7825–7830.

Limenitakis J, Soldati-Favre D (2011) Functional genetics in Apicomplexa: potentials and limits. FEBS Lett 585:1579–1588.

Lin L, Doherty D, Lile J, Bektesh S, Collins F (1993) GDNF: a glial cell line-derived neurotrophic factor for midbrain dopaminergic neurons. Science 260:1130–1132.

Lindholm P, Peränen J, Andressoo J-O, Kalkkinen N, Kokaia Z, Lindvall O, Timmusk T, Saarma M (2008) MANF is widely expressed in mammalian tissues and differently regulated after ischemic and epileptic insults in rodent brain. Mol Cell Neurosci 39:356–371.

Lindholm P, Saarma M (2010) Novel CDNF/MANF family of neurotrophic factors Chao MV, Ip NY, eds. Dev Neurobiol 70:360–371.

Lindholm P, Voutilainen MH, Laurén J, Peränen J, Leppänen V-M, Andressoo J-O, Lindahl M, Janhunen S, Kalkkinen N, Timmusk T, Tuominen RK, Saarma M (2007) Novel neurotrophic factor CDNF protects and rescues midbrain dopamine neurons in vivo. Nature 448:73–77.

Liu G, Martins IH, Chiorini JA, Davidson BL (2005) Adeno-associated virus type 4 (AAV4) targets ependyma and astrocytes in the subventricular zone and RMS. Gene Therapy 12:1503–1508.

Liu XZ, Xu XM, Hu R, Du C, Zhang SX, McDonald JW, Dong HX, Wu YJ, Fan GS, Jacquin MF, Hsu CY, Choi DW (1997) Neuronal and glial apoptosis after traumatic spinal cord injury. The Journal of Neuroscience

17:5395–5406.

Livet J, Weissman TA, Kang H, Draft RW, Lu J, Bennis RA, SAnes JR, Lichtman JW (2007) Transgenic strategies for combinatorial expression of fluorescent proteins in the nervous system. Nature 450:56–63.

Lloyd KG, Davidson L, Hornykiewicz O (1975) The neurochemistry of Parkinson's disease: effect of L-dopa therapy. Journal of Pharmacology and Experimental Therapeutics 195:453–464.

Long M, Gollapalli DR, Hedstrom L (2012) Inhibitor Mediated Protein Degradation. Chemistry & Biology 19:629–637.

Lu P, Wang Y, Graham L, McHale K, Gao M, Wu D, Brock J, Blesch A, Rosenzweig ES, Havton LA, Zheng B, Conner JM, Marsala M, Tuszynski MH (2012) Long-distance growth and connectivity of neural stem cells after severe spinal cord injury. Cell 150:1264–1273.

Luthman J, Fredriksson A, Sundström E, Jonsson G, Archer T (1989) Selective lesion of central dopamine or noradrenaline neuron systems in the neonatal rat: motor behavior and monoamine alterations at adult stage. Behavioural Brain Research 33:267–277.

Ma C, Rosenzweig J, Zhang P, Johns DC, LaMotte RH (2010) Expression of inwardly rectifying potassium channels by an inducible adenoviral vector reduced the neuronal hyperexcitability and hyperalgesia produced by chronic compression of the spinal ganglion. Mol Pain 6:65.

Ma YF, Weiss LM, Huang H (2012) A method for rapid regulation of protein expression in Trypanosoma cruzi. Int J Parasitol 42:33–37.

Madeira da Silva L, Owens KL, Murta SMF, Beverley SM (2009) Regulated expression of the Leishmania major surface virulence factor lipophosphoglycan using conditionally destabilized fusion proteins. PNAS 106:7583–7588.

Maden M (2007) Retinoic acid in the development, regeneration and maintenance of the nervous system. Nat Rev Neurosci 8:755–765.

Margolin JF, Friedman JR, Meyer WK, Vissing H, Thiesen HJ, Rauscher FJ (1994) Krüppel-associated boxes are potent transcriptional repression domains. PNAS 91:409–4513.

Marks WJ, Ostrem JL, Verhagen L, Starr PA, Larson PS, Bakay RA, Taylor R, Cahn-Weiner DA, Stoessl AJ, Olanow CW, Bartus RT (2008) Safety and tolerability of intraputaminal delivery of CERE-120 (adeno-associated virus serotype 2-neurturin) to patients with idiopathic Parkinson's disease: an open-label, phase I trial. Lancet Neurol 7:400–408.

Markusic D (2005) Comparison of single regulated lentiviral vectors with rtTA

expression driven by an autoregulatory loop or a constitutive promoter. Nucleic Acids Res 33:e63–e63.

Markusic DM, de Waart DR, Seppen J (2010) Separating Lentiviral Vector Injection and Induction of Gene Expression in Time, Does Not Prevent an Immune Response to rtTA in Rats. PLoS ONE 5:e9974.

Matthews DA, Bolin JT, Burridge JM, Filman DJ, Volz KW, Kaufman BT, Beddell CR, Champness JN, Stammers DK, Kraut J (1985) Refined crystal structures of Escherichia coli and chicken liver dihydrofolate reductase containing bound trimethoprim. Journal of Biological Chemistry 260:381–391.

Maynard-Smith LA, Chen L-C, Banaszynski LA, Ooi AGL, Wandless TJ (2007) A Directed Approach for Engineering Conditional Protein Stability Using Biologically Silent Small Molecules. Journal of Biological Chemistry 282:24866–24872.

Mazarakis N, Azzouz M, Rohll JB, Ellard FM, Wilkes FJ, Olsen AL, Carter EE, Barber ED, Baban DF, Kingsman SM, Kingsman AJ, O'Malley K, Mitrophanous KA (2001) Rabies virus glycoprotein pseudotyping of lentiviral vectors enables retrograde axonal transport and access to the nervous system after peripheral delivery. Human Molecular Genetics 10:2109-2121

McAdoo DJ, Xu GY, Robak G, Hughes MG (1999) Changes in Amino Acid Concentrations over Time and Space around an Impact Injury and Their Diffusion Through the Rat Spinal Cord. Experimental Neurology 159:538–544.

McBride JL, During MJ, Wuu J, Chen EY, Leurgans SE, Kordower JH (2003) Structural and functional neuroprotection in a rat model of Huntington's disease by viral gene transfer of GDNF. Experimental Neurology 181:213–223.

McBride JL, Ramaswamy S, Gasmi M, Bartus RT, Herzog CD, Brandon EP, Zhou L, Pitzer MR, Berry-Kravis EM, Kordower JH (2006) Viral delivery of glial cell line-derived neurotrophic factor improves behavior and protects striatal neurons in a mouse model of Huntington's disease. Proc Natl Acad Sci USA 103:9345–9350.

McCaffrey AP, Fawcett P, Nakai H, McCaffrey RL, Ehrhardt A, Pham T-TT, Pandey K, Xu H, Feuss S, Storm TA, Kay MA (2008) The Host Response to Adenovirus, Helper-dependent Adenovirus, and Adeno-associated Virus in Mouse Liver. Mol Ther 16:931–941.

McCormack MP, Rabbitts TH (2004) Activation of the T-Cell Oncogene LMO2 after Gene Therapy for X-Linked Severe Combined Immunodeficiency. New England Journal of Medicine 350:913–922.

McCown TJ (2005) Adeno-Associated Virus (AAV) Vectors in the CNS. Current Gene Therapy 5:333–338.

McDonald JW, Liu XZ, Qu Y, Liu S, Mickey SK, Turetsky D, Gottlieb DI, Choi DW (1999) Transplanted embryonic stem cells survive, differentiate and promote recovery in injured rat spinal cord. Nature Medicine 5:1410–1412.

McFarland NR, Lee J-S, Hyman BT, McLean PJ (2009) Comparison of transduction efficiency of recombinant AAV serotypes 1, 2, 5, and 8 in the rat nigrostriatal system. Journal of Neurochemistry 109:838–845.

McTigue DM (2008) Potential Therapeutic Targets for PPARgamma after Spinal Cord Injury. PPAR Res 2008:517162.

Melton KR, Iulianella A, Trainor PA (2004) Gene expression and regulation of hindbrain and spinal cord development. Front Biosci 9:117–138.

Meshi T, Sato Y (1972) Studies on Sulfamethoxazole/Trimethoprim. Absorption, Distribution, Excretion and Metabolism of Trimethoprim in Rat. Chemical & Pharmaceutical Bulletin 20:2079–2090.

Metzger D, Clifford J, Chiba H, Chambon P (1995) Conditional site-specific recombination in mammalian cells using a ligand-dependent chimeric Cre recombinase. PNAS 92:6991–6995.

Mezzina M, Merten O-W (2011) Adeno-associated viruses. Methods Mol Biol 737:211–234.

Miller AD (1990) Retrovirus Packaging Cells. Human Gene Therapy 1:5–14.

Miller AD (1992) Retroviral vectors. Current Topics in Microbiology and Immunology 158:1–24.

Miller LW, Cai Y, Sheetz MP, Cornish VW (2005) In vivo protein labeling with trimethoprim conjugates: a flexible chemical tag. Nat Methods 2:255–257.

Miller LW, Sable J, Goelet P, Sheetz MP, Cornish VW (2004) Methotrexate conjugates: a molecular in vivo protein tag. Angew Chem Int Ed Engl 43:1672–1675.

Mingozzi F, A High K (2011) Immune Responses to AAV in Clinical Trials. Current Gene Therapy 11:321–330.

Mittermeyer G, Christine CW, Rosenbluth KH, Baker SL, Starr P, Larson P, Kaplan PL, Forsayeth J, Aminoff MJ, Bankiewicz KS (2012) Long-Term Evaluation of a Phase 1 Study of AADC Gene Therapy for Parkinson's Disease. Human Gene Therapy 23:377–381.

Mittoux V, Ouary S, Monville C, Lisovoski F, Poyot T, Conde F, Escartin C, Robichon R, Brouillet E, Peschanski M, Hantraye P (2002) Corticostriatopallidal neuroprotection by adenovirus-mediated ciliary

neurotrophic factor gene transfer in a rat model of progressive striatal degeneration. J Neurosci 22:4478–4486.

Miura K, Okada Y, Aoi T, Okada A, Takahashi K, Okita K, Nakagawa M, Koyanagi M, Tanabe K, Ohnuki M, Ogawa D, Ikeda E, Okano H, Yamanaka S (2009) Variation in the safety of induced pluripotent stem cell lines. Nat Biotechnol 27:743–745.

Miyazaki Y, Imoto H, Chen L-C, Wandless TJ (2012) Destabilizing Domains Derived from the Human Estrogen Receptor. J Am Chem Soc 134:3942–3945.

Mizuno Y, Sone N, Saitoh T (1987) Effects of 1-Methyl-4-Phenyl-1,2,3,6-Tetrahydropyridine and 1-Methyl-4-Phenylpyridinium Ion on Activities of the Enzymes in the Electron Transport System in Mouse Brain. Journal of Neurochemistry 48:1787–1793.

Mohyeldin A, Chiocca EA (2012) Gene and Viral Therapy for Glioblastoma. The Cancer Journal 18:82–88.

Mori M, Kose A, Tsujino T, Tanaka C (2004) Immunocytochemical localization of protein kinase C subspecies in the rat spinal cord: Light and electron microscopic study. J Comp Neurol 299:167–177.

Muir EM, Fyfe I, Gardiner S, Li L, Warren P, Fawcett JW, Keynes RJ, Rogers JH (2010) Modification of N-glycosylation sites allows secretion of bacterial chondroitinase ABC from mammalian cells. J Biotechnol 145:103–110.

Muralidharan V, Oksman A, Iwamoto M, Wandless TJ, Goldberg DE (2011) Asparagine repeat function in a Plasmodium falciparum protein assessed via a regulatable fluorescent affinity tag. PNAS 108:4411–4416.

Muramatsu S-I, Fujimoto K-I, Ikeguchi K, Shizuma N, Kawasaki K, Ono F, Shen Y, Wang L, Mizukami H, Kume A, Matsumura M, Nagatsu I, Urano F, Ichinose H, Nagatsu T, Terao K, Nakano I, Ozawa K (2002) Behavioral recovery in a primate model of Parkinson's disease by triple transduction of striatal cells with adeno-associated viral vectors expressing dopamine-synthesizing enzymes. Human Gene Therapy 13:345–354.

Muramatsu S-I, Fujimoto K-I, Kato S, Mizukami H, Asari S, Ikeguchi K, Kawakami T, Urabe M, Kume A, Sato T, Watanabe E, Ozawa K, Nakano I (2010) A phase I study of aromatic L-amino acid decarboxylase gene therapy for Parkinson's disease. Mol Ther 18:1731–1735.

Nagaraja TN, Patel P, Gorski M, Gorevic PD, Patlak CS, Fenstermacher JD (2005) In normal rat, intraventricularly administered insulin-like growth factor-1 is rapidly cleared from CSF with limited distribution into brain. Cerebrospinal Fluid Research 2.

Nagatsu T, Ichinose H (1997) GTP cyclohydrolase I gene, dystonia, juvenile

parkinsonism, and Parkinson's disease. J Neural Transm Suppl 49:203–209.

Nagatsu T, Sawada M (2007) Biochemistry of postmortem brains in Parkinson's disease: historical overview and future prospects (Gerlach M, Deckert J, Double K, Koutsilieri E, eds). Journal of Neural Transmission.

Nagpal S, Friant S, Nakshatri H, Chambon P (1993) RARs and RXRs: evidence for two autonomous transactivation functions (AF-1 and AF-2) and heterodimerization in vivo. The EMBO Journal 12:2349–2360.

Nagpal S, Saunders M, Kastner P, Durand B, Nakshatri H, Chambon P (1992) Promoter context- and response element-dependent specificity of the transcriptional activation and modulating functions of retinoic acid receptors. Cell 70:1007–1019.

Nakai H, Storm TA, Kay MA (2000) Increasing the size of rAAV-mediated expression cassettes in vivo by intermolecular joining of two complementary vectors. Nat Biotechnol 18:527–532.

Naldini L (2001) Viral vectors for gene therapy: the art of turning infectious agents into vehicles of therapeutics. Nature Medicine 7:33–40.

Nayak S, Herzog RW (2010) Progress and prospects: immune responses to viral vectors. Gene Therapy 17:295–304.

Neafsey EJ, Bold EL, Haas G, Hurley-Gius KM, Quirk G, Sievert CF, Terreberry RR (1986) The organization of the rat motor cortex: a microstimulation mapping study. Brain Res 396:77–96.

Neumann S, Bradke F, Tessier-Lavigne M, Basbaum AI (2002) Regeneration of sensory axons within the injured spinal cord induced by intraganglionic cAMP elevation. Neuron 34:885–893.

Nicklas WJ, Vyas I, Heikkila RE (1985) Inhibition of NADH-linked oxidation in brain mitochondria by 1-methyl-4-phenyl-pyridine, a metabolite of the neurotoxin, 1-methyl-4-phenyl-1,2,5,6-tetrahydropyridine. Life Sci 36:2503–2508.

Niikura T, Murayama N, Hashimoto Y, Ito Y, Yamagishi Y, Matsuoka M, Takeuchi Y, Aiso S, Nishimoto I (2000) V642I APP-inducible neuronal cells: a model system for investigating Alzheimer's disorders. Biochem Biophys Res Commun 274:445–454.

No D, Yao TP, Evans RM (1996) Ecdysone-inducible gene expression in mammalian cells and transgenic mice. PNAS 93:3346–3350.

Nori S, Okada Y, Yasuda A, Tsuji O, Takahashi Y, Kobayashi Y, Fujiyoshi K, Koike M, Uchiyama Y, Ikeda E, Toyama Y, Yamanaka S, Nakamura M, Okano H (2011) Grafted human-induced pluripotent stem-cell-derived neurospheres promote motor functional recovery after spinal cord injury in

mice. PNAS 108:16825–16830.

Novitch BG, Wichterle H, Jessell TM, Sockanathan S (2003) A requirement for retinoic acid-mediated transcriptional activation in ventral neural patterning and motor neuron specification. Neuron 40:81–95.

Nutt JG, Burchiel KJ, Comella CL, Jankovic J, Lang AE, Laws ER, Lozano AM, Penn RD, Simpson RK, Stacy M, Wooten GF (2003) Randomized, double-blind trial of glial cell line-derived neurotrophic factor (GDNF) in PD. Neurology 60:69–73.

Obeso JA, Olanow CW, Nutt JG (2000) Levodopa motor complications in Parkinson's disease. Trends Neurosci 23:S2–S7.

Ogawa Y, Sawamoto K, Miyata T, Miyao S, Watanabe M, Nakamura M, Bregman BS, Koike M, Uchiyama Y, Toyama Y, Okano H (2002) Transplantation of in vitro-expanded fetal neural progenitor cells results in neurogenesis and functional recovery after spinal cord contusion injury in adult rats. Journal of Neuroscience Research 69:925–933.

Oiwa Y, Yoshimura R, Nakai K, Itakura T (2002) Dopaminergic neuroprotection and regeneration by neurturin assessed by using behavioral, biochemical and histochemical measurements in a model of progressive Parkinson's disease. Brain Res 947:271–283.

Olanow CW, Obeso JA (2000) Preventing levodopa-induced dyskinesias. Annals of Neurology 47:S167–76–discussionS176–8.

Orban PC, Chui D, Marth JD (1992) Tissue- and site-specific DNA recombination in transgenic mice. In, pp 6861–6865.

Ott MG et al. (2006) Correction of X-linked chronic granulomatous disease by gene therapy, augmented by insertional activation of MDS1-EVI1, PRDM16 or SETBP1. Nature Medicine 12:401–409.

Oyinbo CA (2011) Secondary injury mechanisms in traumatic spinal cord injury: a nugget of this multiply cascade. Acta Neurobiol Exp (Wars) 71:281–299.

Park EC, Finley D, Szostak JW (1992) A strategy for the generation of conditional mutations by protein destabilization. PNAS 89:1249–1252.

Parkash V, Lindholm P, Peränen J, Kalkkinen N, Oksanen E, Saarma M, Leppanen VM, Goldman A (2009) The structure of the conserved neurotrophic factors MANF and CDNF explains why they are bifunctional. Protein Engineering Design and Selection 22:233–241.

Parks RJ, Chen L, Anton M, Sankar U, Rudnicki MA, Graham FL (1996) A helper-dependent adenovirus vector system: Removal of helper virus by Cre-mediated excision of the viral packaging signal. PNAS 93:13565–

13570.

Patel NK, Bunnage M, Plaha P, Svendsen CN, Heywood P, Gill SS (2005) Intraputamenal infusion of glial cell line-derived neurotrophic factor in PD: A two-year outcome study. Annals of Neurology 57:298–302.

Paterna J-C, Feldon J, Büeler H (2004) Transduction profiles of recombinant adeno-associated virus vectors derived from serotypes 2 and 5 in the nigrostriatal system of rats. Journal of Virology 78:6808–6817.

Patterson RG, Couchenour RL (1999) Trimethoprim-Sulfamethoxazole-Induced Tremor in an Immunocompetent Patient. Pharmacotherapy 19:1456–1458.

Pelleymounter MA, Cullen MJ, Wellman CL (1995) Characteristics of BDNF-induced weight loss. Experimental Neurology 131:229–238.

Perry VH, Gordon S (1991) International Review of Cytology. Elsevier.

Petrova PS, Raibekas A, Pevsner J, Vigo N, Anafi M, Moore MK, Peaire AE, Shridhar V, Smith DI, Kelly J, Durocher Y, Commissiong JW (2003) MANF: A New Mesencephalic, Astrocyte-Derived Neurotrophic Factor with Selectivity for Dopaminergic Neurons. Journal of Molecular Neuroscience 20:173–187.

Pollock R, Clackson T (2002) Dimerizer-regulated gene expression. Curr Opin Biotechnol 13:459–467.

Pratt MR, Schwartz EC, Muir TW (2007) Small-molecule-mediated rescue of protein function by an inducible proteolytic shunt. PNAS 104:11209–11214.

Puttagunta R, Schmandke A, Floriddia E, Gaub P, Fomin N, Ghyselinck NB, Di Giovanni (2011) RA–RAR-β counteracts myelin-dependent inhibition of neurite outgrowth via Lingo-1 repression. The Journal of Cell Biology 193:1147–1156.

Qiu J, Cai D, Dai H, McAtee M, Hoffman PN, Bregman BS, Filbin MT (2002) Spinal axon regeneration induced by elevation of cyclic AMP. Neuron 34:895–903.

Radtke C, Sasaki M, Lankford KL, Vogt PM, Kocsis JD (2008) Potential of olfactory ensheathing cells for cell-based therapy in spinal cord injury. J Rehabil Res Dev 45:141–151.

Ralph GS, Radcliffe PA, Day DM, Carthy JM, Leroux MA, Lee DCP, Wong L-F, Bilsland LG, Greensmith L, Kingsman SM, Mitrophanous KA, Mazarakis ND, Azzouz M (2005) Silencing mutant SOD1 using RNAi protects against neurodegeneration and extends survival in an ALS model. Nature Medicine 11:429–433.

Ramaswamy S, McBride JL, Han I, Berry-Kravis EM, Zhou L, Herzog CD,

Gasmi M, Bartus RT, Kordower JH (2009) Intrastriatal CERE-120 (AAV-Neurturin) protects striatal and cortical neurons and delays motor deficits in a transgenic mouse model of Huntington's disease. Neurobiology of Disease 34:40–50.

Ramezani A, Hawley TS, Hawley RG (2000) Lentiviral vectors for enhanced gene expression in human hematopoietic cells. Molecular Therapy 2:458–469.

Ramirez-Solis R, Liu P, Bradley A (1995) Chromosome engineering in mice. Nature 378:720–724.

Raoul C, Abbas-Terki T, Bensadoun J-C, Guillot S, Haase G, Szulc J, Henderson CE, Aebischer P (2005) Lentiviral-mediated silencing of SOD1 through RNA interference retards disease onset and progression in a mouse model of ALS. Nature Medicine 11:423–428.

Rechsteiner M (1990) PEST sequences are signals for rapid intracellular proteolysis. Seminars in Cell Biology 1:433–440.

Reynolds B, Weiss S (1992) Generation of neurons and astrocytes from isolated cells of the adult mammalian central nervous system. Science 255:1707–1710.

Richardson PM, McGuinness UM, Aguayo AJ (1980) Axons from CNS neurones regenerate into PNS grafts. Nature 284:264–265.

Riddiford L, Cherbas P, Truman J (2000) Ecdysone receptors and their biological actions. Vitamins and Hormones.

Rodriguez S, Wolfgang MJ (2012) Targeted chemical-genetic regulation of protein stability in vivo. Chemistry & Biology 19:391–398.

Rogers S, Wells R, Rechsteiner M (1986) Amino acid sequences common to rapidly degraded proteins: the PEST hypothesis. Science 234:364–368.

Rosenblad C, Grønborg M, Hansen C, Blom N, Meyer M, Johansen J, Dagø L, Kirik D, Patel UA, Lundberg C, Trono D, Björklund A, Johansen TE (2000) In vivo protection of nigral dopamine neurons by lentiviral gene transfer of the novel GDNF-family member neublastin/artemin. Mol Cell Neurosci 15:199–214.

Rosenblad C, Kirik D, Devaux B, Moffat B, Phillips HS, Björklund A (1999) Protection and regeneration of nigral dopaminergic neurons by neurturin or GDNF in a partial lesion model of Parkinson's disease after administration into the striatum or the lateral ventricle. Eur J Neurosci 11:1554–1566.

Rosenblad C, Martinez-Serrano A, Björklund A (1998) Intrastriatal glial cell line-derived neurotrophic factor promotes sprouting of spared nigrostriatal dopaminergic afferents and induces recovery of function in a rat model of

Parkinson's disease. Neuroscience 82:129–137.

Russo I, Oksman A, Vaupel B, Goldberg DE (2009) A calpain unique to alveolates is essential in Plasmodium falciparum and its knockdown reveals an involvement in pre-S-phase development. PNAS 106:1554–1559.

Saez E, Nelson MC, Eshelman B, Banayo E, Koder A, Cho GJ, Evans RM (2000) Identification of ligands and coligands for the ecdysone-regulated gene switch. PNAS 97:14512–14517.

Sakamoto KM, Kim KB, Kumagai A, Mercurio F, Crews CM, Deshaies RJ (2001) Protacs: Chimeric molecules that target proteins to the Skp1–Cullin–F box complex for ubiquitination and degradation. PNAS 98:8554–8559.

Salkind AR (2000) Acute delirium induced by intravenous trimethoprim–sulfamethoxazole therapy in a patient with the Acquired Immunodeficiency Syndrome. Human & Experimental Toxicology 19:149–151.

Sandner B, Prang P, Rivera FJ, Aigner L, Blesch A, Weidner N (2012) Neural stem cells for spinal cord repair. Cell Tissue Res 349:349–362.

Saner A, Thoenen H (1971) Model Experiments on the Molecular Mechanism of Action of 6-Hydroxydopamine. Mol Pharmacol 7:147–154.

Satake K, Matsuyama Y, Kamiya M, Kawakami H, Iwata H, Adachi K, Kiuchi K (2000) Nitric oxide via macrophage iNOS induces apoptosis following traumatic spinal cord injury. Molecular Brain Research 85:114–122.

Sauer B, Henderson N (1990) Targeted insertion of exogenous DNA into the eukaryotic genome by the Cre recombinase. New Biol 2:441–449.

Sauer H, Oertel WH (1994) Progressive degeneration of nigrostriatal dopamine neurons following intrastriatal terminal lesions with 6-hydroxydopamine: a combined retrograde tracing and immunocytochemical study in the rat. Neuroscience 59:401–415.

Schanne F, Kane A, Young E, Farber J (1979) Calcium dependence of toxic cell death: a final common pathway. Science 206:700–702.

Schneekloth JS, Fonseca FN, Koldobskiy M, Mandal A, Deshaies R, Sakamoto K, Crews CM (2004) Chemical Genetic Control of Protein Levels: Selective in Vivo Targeted Degradation. J Am Chem Soc 126:3748–3754.

Schnell J, Dyson H, Wright PE (2004) Structure, dynamics, and catalytic function of dihydrofolate reductase. Annu Rev Biophys Biomol Struct 33:119–140.

Schnell L, Schwab ME (1990) Axonal regeneration in the rat spinal cord produced by an antibody against myelin-associated neurite growth

inhibitors. Nature 343:269–272.

Schoeber JPH, van de Graaf SFJ, Lee KP, Wittgen HGM, Hoenderop JGJ, Bindels RJM (2009) Conditional fast expression and function of multimeric TRPV5 channels using Shield-1. Am J Physiol Renal Physiol 296:F204–F211.

Schweitzer BI, Dicker AP, Bertino JR (1990) Dihydrofolate reductase as a therapeutic target. The FASEB journal 4:2441–2452.

Schwenk F, Kuhn R, Angrand PO, Rajewsky K, Stewart AF (1998) Temporally and spatially regulated somatic mutagenesis in mice. Nucleic Acids Res 26:1427–1432.

Seijffers R, Allchorne AJ, Woolf CJ (2006) The transcription factor ATF-3 promotes neurite outgrowth. Mol Cell Neurosci 32:143–154.

Sellmyer MA, Chen L-C, Egeler EL, Rakhit R, Wandless TJ (2012) Intracellular context affects levels of a chemically dependent destabilizing domain. PLoS ONE 7:e43297.

Shen Y, Muramatsu SI, Ikeguchi K, Fujimoto KI, Fan DS, Ogawa M, Mizukami H, Urabe M, Kume A, Nagatsu I, Urano F, Suzuki T, Ichinose H, Nagatsu T, Monahan J, Nakano I, Ozawa K (2000) Triple transduction with adeno-associated virus vectors expressing tyrosine hydroxylase, aromatic-L-amino-acid decarboxylase, and GTP cyclohydrolase I for gene therapy of Parkinson's disease. Human Gene Therapy 11:1509–1519.

Shults CW, Kimber T, Martin D (1996) Intrastriatal injection of GDNF attenuates the effects of 6-hydroxydopamine. NeuroReport 7:627–631.

Shuman SL, Bresnahan JC, Beattie MS (1997) Apoptosis of microglia and oligodendrocytes after spinal cord contusion in rats. Journal of Neuroscience Research 50:798–808.

Silver J, Miller JH (2004) Regeneration beyond the glial scar. Nat Rev Neurosci 5:146–156.

Singleton AB (2005) Altered alpha-synuclein homeostasis causing Parkinson's disease: the potential roles of dardarin. Trends Neurosci 28:416–421.

Singleton AB et al. (2003) alpha-Synuclein locus triplication causes Parkinson's disease. Science 302:841.

Sinn PL, Sauter SL, McCray PB (2005) Gene therapy progress and prospects: development of improved lentiviral and retroviral vectors - design, biosafety, and production. Gene Therapy 12:1089–1098.

Skafte-Pedersen P, Hemmingsen M, Sabourin D, Blaga FS, Bruus H, Dufva M (2012) A self-contained, programmable microfluidic cell culture system

with real-time microscopy access. Biomed Microdevices 14:385–399.

Slevin JT, Gerhardt GA, Smith CD, Gash DM, Kryscio R, Young B (2005) Improvement of bilateral motor functions in patients with Parkinson disease through the unilateral intraputaminal infusion of glial cell line-derived neurotrophic factor. J Neurosurg 102:216–222.

Smith RH (2008) Adeno-associated virus integration: virus versus vector. Gene Therapy 15:817–822.

So P-L, Yip PK, Bunting S, Wong L-F, Mazarakis ND, Hall S, McMahon S, Maden M, Corcoran JPT (2006) Interactions between retinoic acid, nerve growth factor and sonic hedgehog signalling pathways in neurite outgrowth. Developmental Biology 298:167–175.

Spencer D, Wandless T, Schreiber S, Crabtree G (1993) Controlling signal transduction with synthetic ligands. Science 262:1019–1024.

Stack A, Schott HC II (2011) Suspect novel adverse drug reactions to trimethoprim-sulphonamide combinations in horses: A case series. Equine Veterinary Journal 43:117–120.

Stankunas K, Bayle JH, Gestwicki JE, Lin Y-M, Wandless TJ, Crabtree GR (2003) Conditional Protein Alleles Using Knockin Mice and a Chemical Inducer of Dimerization. Molecular Cell 12:1615–1624.

Stankunas K, Bayle JH, Havranek JJ, Wandless TJ, Baker D, Crabtree GR, Gestwicki JE (2007) Rescue of degradation-prone mutants of the FK506-rapamycin binding (FRB) protein with chemical ligands. Chembiochem 8:1162–1169.

Steeves J, Fawcett J, Tuszynski M (2004) Report of International Clinical Trials Workshop on Spinal Cord Injury February 20–21, 2004, Vancouver, Canada. Spinal Cord 42:591–597.

Sternberg N, Hamilton D (1981) Bacteriophage P1 site-specific recombination. I. Recombination between loxP sites. The Journal of Biological Chemistry 150:467–486.

Stieger K, Belbellaa B, Le Guiner C, Moullier P, Rolling F (2009) In vivo gene regulation using tetracycline-regulatable systems. Adv Drug Deliv Rev 61:527–541.

Stieger K, Le Meur G, Lasne F, Weber M, Deschamps J-Y, Nivard D, Mendes-Madeira A, Provost N, Martin L, Moullier P, Rolling F (2006) Long-term Doxycycline-regulated Transgene Expression in the Retina of Nonhuman Primates Following Subretinal Injection of Recombinant AAV Vectors. Molecular … 13:967–975.

Strathdee CA, McLeod MR, Hall JR (1999) Efficient control of tetracycline-

responsive gene expression from an autoregulated bi-directional expression vector. Gene 229:21–29.

Sucov HM, Murakami KK, Evans RM (1990) Characterization of an autoregulated response element in the mouse retinoic acid receptor type beta gene. PNAS 87:5392–5396.

Suhr ST, Gil EB, Senut MC, Gage FH (1998) High level transactivation by a modified Bombyx ecdysone receptor in mammalian cells without exogenous retinoid X receptor. PNAS 95:7999–8004.

Sullivan PGP, Krishnamurthy SS, Patel SPS, Pandya JDJ, Rabchevsky AGA (2007) Temporal characterization of mitochondrial bioenergetics after spinal cord injury. J Neurotrauma 24:991–999.

Sun Z-P, Gong L, Huang S-H, Geng Z, Cheng L, Chen Z-Y (2011) Intracellular trafficking and secretion of cerebral dopamine neurotrophic factor in neurosecretory cells. Journal of Neurochemistry 117:121–132.

Szymczak AL, Workman CJ, Wang Y, Vignali KM, Dilioglou S, Vanin EF, Vignali DAA (2004) Correction of multi-gene deficiency in vivo using a single "self-cleaving" 2A peptide-based retroviral vector. Nat Biotechnol 22:589–594.

Takahashi K, Yamanaka S (2006) Induction of Pluripotent Stem Cells from Mouse Embryonic and Adult Fibroblast Cultures by Defined Factors. Cell 126:663–676.

Taneja R, Rochette-Egly C, Plassat J-L, Penna L, Gaub M-P, Chambon P (1997) Phosphorylation of activation functions AF-1 and AF-2 of RARalpha and RARgamma is indispensable for differentiation of F9 cells upon retinoic acid and cAMP treatment. The EMBO Journal 16:6452–6465.

Taoka Y, Okajima K, Uchiba M, Murakami K, Kushimoto S, Johno M, Naruo M, Okabe H, Takatsuki K (1997) Role of neutrophils in spinal cord injury in the rat. Neuroscience 79:1177–1182.

Taylor AM, Blurton-Jones M, Rhee SW, Cribbs DH, Cotman CW, Jeon NL (2005) A microfluidic culture platform for CNS axonal injury, regeneration and transport. Nat Methods 2:599–605.

Tenenbaum L, Lehtonen E, Monahan PE (2003) Evaluation of Risks Related to the Use of Adeno-Associated Virus-Based Vectors. Current Gene Therapy 3:545–565.

Tetzlaff W, Okon EB, Karimi-Abdolrezaee S, Hill CE, Sparling JS, Plemel JR, Plunet WT, Tsai EC, Baptiste D, Smithson LJ, Kawaja MD, Fehlings MG, Kwon BK (2011) A systematic review of cellular transplantation therapies for spinal cord injury. J Neurotrauma 28:1611–1682.

Thanos A, Morizane Y, Murakami Y, Giani A, Mantopoulos D, Kayama M, Roh MI, Michaud N, Pawlyk B, Sandberg M, Young LH, Miller JW, Vavvas DG (2012) Evidence for baseline retinal pigment epithelium pathology in the Trp1-Cre mouse. Am J Pathol 180:1917–1927.

Thomas CE, Schiedner G, Kochanek S, castro MG, Lowenstein PR (2000) Peripheral infection with adenovirus causes unexpected long-term brain inflammation in animals injected intracranially with first-generation, but not with high-capacity, adenovirus vectors: Toward realistic long-term neurological gene therapy for chronic diseases. PNAS 97:7482–7487.

Thomas HE, Stunnenberg HG, Stewart AF (1993) Heterodimerization of the Drosophila ecdysone receptor with retinoid X receptor and ultraspiracle. Nature 362:471–475.

Thompson JF, Hayes LS, Lloyd DB (1991) Modulation of firefly luciferase stability and impact on studies of gene regulation. Gene 103:171–177.

Tsuji O et al. (2010) Therapeutic potential of appropriately evaluated safe-induced pluripotent stem cells for spinal cord injury. PNAS 107:12704–12709.

Tu YH, Allen LV, Fiorica VM, Albers DD (1989) Pharmacokinetics of trimethoprim in the rat. J Pharm Sci 78:556–560.

Tuszynski MH, Thal L, Pay M, Salmon DP, U HS, Bakay R, Patel P, Blesch A, Vahlsing HL, Ho G, Tong G, Potkin SG, Fallon J, Hansen L, Mufson EJ, Kordower JH, Gall C, Conner J (2005) A phase 1 clinical trial of nerve growth factor gene therapy for Alzheimer disease. Nature Medicine 11:551–555.

Ungerstedt U (1968) 6-hydroxy-dopamine induced degeneration of central monoamine neurons. European Journal of Pharmacology 5:107–110.

Ungerstedt U, Arbuthnott GW (1970) Quantitative recording of rotational behavior in rats after 6-hydroxy-dopamine lesions of the nigrostriatal dopamine system. Brain Res 24:485–493.

Urlinger S, Baron U, Thellmann M, Hasan MT, Bujard H, Hillen W (2000) Exploring the sequence space for tetracycline-dependent transcriptional activators: Novel mutations yield expanded range and sensitivity. PNAS 97:7963–7968.

Valori CF, Ning K, Wyles M, Azzouz M (2008) Development and applications of non-HIV-based lentiviral vectors in neurological disorders. Current Gene Therapy 8:406–418.

Van Gerpen JA (1988) Tremor caused by trimethoprim-sulfamethoxazole in a patient with AIDS. Neurology 48:537–538.

van Kesteren RE, Mason MRJ, Macgillavry HD, Smit AB, Verhaagen J (2011) A gene network perspective on axonal regeneration. Front Mol Neurosci 4:46.

Voutilainen MH, Bäck S, Peränen J, Lindholm P, Raasmaja A, Mannisto PT, Saarma M, Tuominen RK (2011) Chronic infusion of CDNF prevents 6-OHDA-induced deficits in a rat model of Parkinson's disease. Experimental Neurology 228:99–108.

Voutilainen MH, Bäck S, Pörsti E, Toppinen L, Lindgren L, Lindholm P, Peränen J, Saarma M, Tuominen RK (2009) Mesencephalic Astrocyte-Derived Neurotrophic Factor Is Neurorestorative in Rat Model of Parkinson's Disease. The Journal of Neuroscience 29:9651–9659.

Wakeman DR, Dodiya HB, Kordower JH (2011) Cell transplantation and gene therapy in Parkinson's disease. Mt Sinai J Med 78:126–158.

Wang Q, Finer MH (1996) Second–generation adenovirus vectors. Nature Medicine 2:714–716.

Wang Y, Yu Y, Shabahang S, Wang G, Szalay AA (2002) Renilla luciferase-Aequorea GFP (Ruc-GFP) fusion protein, a novel dual reporter for real-time imaging of gene expression in cell cultures and in live animals. Molecular Genetics Genomics 268:160–168.

Watson DJ, Kobinger GP, Passini MA, Wilson JM, Wolfe JH (2002) Targeted Transduction Patterns in the Mouse Brain by Lentivirus Vectors Pseudotyped with VSV, Ebola, Mokola, LCMV, or MuLV Envelope Proteins. Molecular Therapy 5:528–537.

Weidner N, Ner A, Salimi N, Tuszynski MH (2001) Spontaneous corticospinal axonal plasticity and functional recovery after adult central nervous system injury. PNAS 98:3513–3518.

Weinberg MS, Samulski RJ, McCown TJ (2012) Adeno-associated virus (AAV) gene therapy for neurological disease. Neuropharmacology 1.

Wilcox JT, Cadotte D, Fehlings MG (2012) Spinal cord clinical trials and the role for bioengineering. Neuroscience Letters 519:93–102.

Wilson L, Maden M (2005) The mechanisms of dorsoventral patterning in the vertebrate neural tube. Developmental Biology 282:1–13.

Wissmann A, Meier I, Wray LV, Geissendörfer M, Hillen W (1986) Tn10 tet operator mutations affecting Tet repressor recognition. Nucleic Acids Res 14:4253–4266.

Witzgall R, O'Leary E, Leaf A, Onaldi D, Bonventre JV (1994a) The Krüppel-associated box-A (KRAB-A) domain of zinc finger proteins mediates transcriptional repression. PNAS 91:4514–4518.

Witzgall R, Volk R, Yeung RS, Bonventre JV (1994b) Genomic Structure and Chromosomal Location of the Rat Gene Encoding the Zinc Finger Transcription Factor Kid-1. Genomics 20:203–209.

Wolfe D, Mata M, Fink DJ (2009) A human trial of HSV-mediated gene transfer for the treatment of chronic pain. Gene Therapy 16:455–460.

Wong L-F, Azzouz M, Walmsley LE, Askham Z, Wilkes FJ, Mitrophanous KA, Kingsman SM, Mazarakis ND (2004) Transduction patterns of pseudotyped lentiviral vectors in the nervous system. Mol Ther 9:101–111.

Wong L-F, Yip PK, Battaglia A, Grist J, Corcoran J, Maden M, Azzouz M, Kingsman SM, Kingsman AJ, Mazarakis ND, McMahon SB (2006) Retinoic acid receptor beta2 promotes functional regeneration of sensory axons in the spinal cord. Nature Neuroscience 9:243–250.

Woody RC, Brewster MA (2008) Adeverse Effects of Trimethoprim-sulfamethoxazole in a Child with Dihydropteridine Reductase Deficiency. Developmental Medicine & Child Neurology 32:639–642.

Wu S, Suzuki Y, Ejiri Y, Noda T, Bai H, Kitada M, Kataoka K, Ohta M, Chou H, Ide C (2003) Bone marrow stromal cells enhance differentiation of cocultured neurosphere cells and promote regeneration of injured spinal cord. Journal of Neuroscience Research 72:343–351.

Wu Z, Asokan A, Samulski RJ (2006) Adeno-associated virus serotypes: vector toolkit for human gene therapy. Molecular Therapy 14:316–327.

Xia X, Zhou H, Huang Y, Xu Z (2006) Allele-specific RNAi selectively silences mutant SOD1 and achieves significant therapeutic benefit in vivo. Neurobiology of Disease 23:578–586.

Xiong W, Goverdhana S, Sciascia SA, Candolfi M, Zirger JM, Barcia C, Curtin JF, King GD, Jaita G, Liu C, Kroeger K, Agadjanian H, Medina-Kauwe L, Palmer D, Ng P, Lowenstein PR, Castro MG (2006) Regulatable Gutless Adenovirus Vectors Sustain Inducible Transgene Expression in the Brain in the Presence of an Immune Response against Adenoviruses. Journal of Virology 80:27–37.

Xiong Y, Rabchevsky AG, Hall ED (2007) Role of peroxynitrite in secondary oxidative damage after spinal cord injury. Journal of Neurochemistry 100:639–649.

Xu GY, Hughes MG, Zhang L, Cain L, McAdoo DJ (2005) Administration of glutamate into the spinal cord at extracellular concentrations reached post-injury causes functional impairments. Neuroscience Letters 384:271–276.

Yamagata T, Saito H, Habuchi O, Suzuki S (1968) Purification and properties of bacterial chondroitinases and chondrosulfatases. Journal of Biological Chemistry 243:1523–1535.

Yang W, Rozamus LW, Narula S, Rollins CT, Yuan R, Andrade LJ, Ram MK, Phillips TB, van Schravendijk MR, Dalgarno D, Clackson T, Holt DA (2000) Investigating protein-ligand interactions with a mutant FKBP possessing a designed specificity pocket. J Med Chem 43:1135–1142.

Yao T-P, Forman BM, Jiang Z, Cherbas L, Chen JD, McKeown M, Cherbas P, Evans RM (1993) Functional ecdysone receptor is the product of EcR and Ultraspiracle genes. Nature 366:476–479.

Yao TP, Segraves WA, Oro AE, McKeown M, Evans RM (1992) Drosophila ultraspiracle modulates ecdysone receptor function via heterodimer formation. Cell 71:63–72.

Yick LW, Wu W, So KF, Yip HK, Shum DK (2000) Chondroitinase ABC promotes axonal regeneration of Clarke's neurons after spinal cord injury. NeuroReport 11:1063–1067.

Yip PK, Wong L-F, Pattinson D, Battaglia A, Grist J, Bradbury EJ, Maden M, McMahon SB, Mazarakis ND (2006) Lentiviral vector expressing retinoic acid receptor beta2 promotes recovery of function after corticospinal tract injury in the adult rat spinal cord. Hum Mol Genet 15:3107–3118.

Yip PK, Wong L-F, Sears TA, Yáñez-Muñoz RJ, McMahon SB (2010) Cortical overexpression of neuronal calcium sensor-1 induces functional plasticity in spinal cord following unilateral pyramidal tract injury in rat. PLoS Biol 8:e1000399.

Yu SF, Rüden von T, Kantoff PW, Garber C, Seiberg M, Rüther U, Anderson WF, Wagner EF, Gilboa E (1986) Self-inactivating retroviral vectors designed for transfer of whole genes into mammalian cells. PNAS 83:3194–3198.

Zala D, Bensadoun J-C, Pereira de Almeida L, Leavitt BR, Gutekunst C-A, Aebischer P, Hayden MR, Déglon N (2004) Long-term lentiviral-mediated expression of ciliary neurotrophic factor in the striatum of Huntington's disease transgenic mice. Experimental Neurology 185:26–35.

Zaldumbide A, Weening S, Cramer SJ, Rabelink MJWE, Hoeben RC (2010) A potentailly immunologically inert derivative of the reverse tetracycline-controlled transactivator. Biotechnology Letters 32:749–754.

Zennou V, Petit C, Guetard D, Nerhbass U, Montagnier L, Charneau P (2000) HIV-1 genome nuclear import is mediated by a central DNA flap. Cell 101:173–185.

Zhang Z, Miyoshi Y, Lapchak PA, Collins F, Hilt D, Lebel C, Kryscio R, Gash DM (1997) Dose response to intraventricular glial cell line-derived neurotrophic factor administration in parkinsonian monkeys. J Pharmacol Exp Ther 282:1396–1401.

Zhao R-R, Muir EM, Alves JN, Rickman H, Allan AY, Kwok JC, Roet KCD, Verhaagen J, Schneider BL, Bensadoun J-C, Ahmed SG, Yáñez-Muñoz RJ, Keynes RJ, Fawcett JW, Rogers JH (2011a) Lentiviral vectors express chondroitinase ABC in cortical projections and promote sprouting of injured corticospinal axons. Journal of Neuroscience Methods 201:228–238.

Zhao T, Zhang Z-N, Rong Z, Xu Y (2011b) Immunogenicity of induced pluripotent stem cells. Nature 474:212–216.

Zhelyaznik N, Schrage K, McCaffery P, Mey J (2003) Activation of retinoic acid signalling after sciatic nerve injury: up-regulation of cellular retinoid binding proteins. Eur J Neurosci 18:1033–1040.

Zhou X, Vink M, Klaver B, Berkhout B, Das AT (2006) Optimization of the Tet-On system for regulated gene expression through viral evolution. Gene Therapy 13:1382–1390.

Zhuang Y, Faria TN, Chambon P, Gudas LJ (2003) Identification and characterization of retinoic acid receptor beta2 target genes in F9 teratocarcinoma cells. Mol Cancer Res 1:619–630.

Zörner B, Schwab ME (2010) Anti-Nogo on the go: from animal models to a clinical trial. Ann N Y Acad Sci 1198 Suppl 1:E22–E34.

Zufferey R, Nagy D, Mandel RJ, Naldini L, Trono D (1997) Multiply attenuated lentiviral vector achieves efficient gene delivery in vivo. Nature 15:871–874.

List of Abbreviations

6OHDA	*6-hydroxy dopamine*
AACD	*Aromatic L-amino Acid Decarboxylase*
AAV	*Adeno associated virus*
AD	*Alzheimer's disease*
AdV	*Adenovirus*
AIDS	*Acquired immunodeficiency disease*
ALS	*Amyotrophic lateral sclerosis*
AP/ML/DV	*Anterior-Posterior/Medial-Lateral/Dorsal-Ventricular*
ATF3	*Activating transcription factor 3*
ATP	*Adenosine triphosphate*
BBB	*Blood-brain-barrier*
BDNF	*Brain derived neurotrophic factor*
BH4	*Tetrahydrobiopterin*
BMP	*Bone morphogenetic proteins*
BMSC	*Bone marrow stromal cells*
bp	*Base pair*
BS	*Bottenstein and Sato's medium*
BSA	*Bovine serum albumin*
cAMP	*Cyclic adenosine monophosphate*
CAR	*Coxsackie adenovirus*
CDNF	*Conserved dopamine neurotrophic factor*
ChABC	*Chondroitinase ABC*
CNS	*Central nervous system*
CNTF	*Ciliary derived neurotrophic factor*
cPPT/CTS	*Central polypurine tract*
CsCl	*Caesium chloride*
CSF	*Cerebro-spinal fluid*
CSPGS	*Chondroitinase sulphate proteoglycan*
CST	*Corticospinal tract*
DA	*Dopaminergic*
DD	*Destabilisation domain*
DHFR	*Dihydrofolate reductase*
DMEM	*Dulbecco's Modified Eagle Medium*
DMSO	*Dimethyl sulphoxide*
DNA	*Deoxyribosenucleic acid*
Dox	*Doxcycline*
DRG	*Dorsal root ganglion*
E. coli	*Escherichia coli*
EcR	*Ecdysone receptor*
EDTA	*Ethylenediaminetetraacetic acid*
EIAV	*Equine infectious anaemia virus*
ERE	*Ecdysone responsive element*
ESGCT	*European society of gene and cell therapy*
EtBr	*Ethidium bromide*
FACS	*Fluorescence-activated cell sorting*

FGF	*Fibroblast growth factor*
FKBP12	*FK506-binding protein, 12kDa*
FRAB	*Krupple-associated box*
*FRB**	*FKBP-rapamycin binding domain*
GABA	*Gamma-aminobutyric acid*
GAD	*Glutamic decarboxylase*
GCH-1	*GTP cyclohydrolase*
GDNF	*Glial derived neurotrophic factor*
GFP	*Green fluorescent protein*
GOI	*Gene of interest*
HBS	*HEPES-buffered saline*
HBSS	*Hanks Balanced Salt Solution*
HD	*Huntington's disease*
HEK	*Human embryonic kidney*
HIV-1	*Human immunodeficiency virus*
HSPG	*Heparin sulphate proteoglycan*
HSV	*Herpes simplex virus*
IGF1	*Insulin-like growth factor*
IP	*Intraperitoneal*
iPSC	*Induced pluripotent stem cells*
IRES	*Internal ribosome entry site*
ITR	*Inverted terminal repeat*
L-DOPA	*L-3,4-dihydroxyphenylalanine*
LB	*Luria Broth*
LHS	*Left-hand side*
LRRK2	*Leucine rich repeat kinase 2*
LTR	*Long terminal repeat*
LV	*Lentivirus*
MAG	*Myelin associated glycoprotein*
MANF	*Mesenchymal-astrocyte neurotrophic factor*
MFBB	*Medial forebrain bundle*
MOI	*Multiplicity of infection*
MoMLV	*Moloney-murine leukaemia virus*
MPTP	*1-methyl-4-phenyl-1,2,3,6-tetrahydropyridine*
mRNA	*Messenger ribonucleic acid*
NaBu	*Sodium butyrate*
NGF	*Nerve growth factor*
NGS	*Normal goat serum*
NPC	*Neural progenitor cell*
NTF	*Neurotrophic factor*
OEC	*Olfactory ensheathing cells*
PCR	*Polymerase chain reaction*
PD	*Parkinson's disease*
PFA	*Paraformaldehyde*
PI3K	*Phosphoinositide 3-kinase*
PINK1	*PTEN-induced novel kinase 1*
PKA	*Protein kinase A*
PKCγ	*Protein Kinase C gamma*
PROTACs	*Proteolysis targeting chimeric protein*

PTEN	*Phosphatase and tensin homolog*
RA	*Retinoic acid*
RAG	*Regeneration-associated genes*
RALDH2	*Retinaldehyde dehydrogenase 2*
RAR	*Retinoic acid receptor*
RARE	*Retinoic acid response element*
RBP4	*Retinol binding protein 4*
RE	*Restriction enzyme*
RHS	*Right-hand side*
RRE	*Rev-responsive element*
RXR	*Retinoid X receptor*
SCI	*Spinal cord injury*
SCID	*Severe combined immunodeficiency disease*
SFFV	*Spleen focus forming virus*
SLF	*Synthetic ligand for FKBP*
SMA	*Spinal muscular atrophy*
SMN1	*Survival of motor neuron gene*
SN	*Subthalamic nucleus*
SNPC	*Substantia nigra pars compacta*
SURF	*Split ubiquitin for the rescue of function*
SVZ	*Subventricular zone*
Tet	*Tetracycline*
TH	*Tyrosine hydroxylase*
THF	*Tetrahydrofolate*
TMP	*Trimethoprim*
TRE	*Tet responsive element*
TS	*Temperature sensitive*
tTA	*Tet-controlled transcription activator*
UPS	*Ubiquitin-proteasome system*
USP	*Ultraspiracle Protein*
VEGF	*Vascular endothelial growth factor*
VSV-G	*Vesicular Stromal Virus G-protein*
VTA	*Ventral tegmental area*
Wld^S	*Wallerian slow degradation protein*
WPRE	*Woodchuck post transcription regulatory element*
YFP	*Yellow fluorescent protein*